

CYCLIC SHEAR LOADING RESPONSE OF FRASER RIVER DELTA SILT

By

Maria Victoria Sanín

B.Sc. Universidad Nacional De Colombia, 1999

A THESIS SUBMITTED IN PARTIAL FULFILLMENT OF
THE REQUIREMENTS FOR THE DEGREE OF

MASTER OF APPLIED SCIENCE

In

THE FACULTY OF GRADUATE STUDIES
CIVIL ENGINEERING

The University of British Columbia

May 2005

© Maria Victoria Sanín 2005

ABSTRACT

The cyclic shear response of silt obtained from a natural channel-fill soil deposit in the Fraser River Delta of British Columbia, Canada, was investigated using the direct simple shear (DSS) test apparatus. Constant volume cyclic DSS tests conducted on undisturbed silt specimens consolidated to a vertical stress similar to, or above, the in situ effective overburden stress exhibited cyclic mobility type progressive strain development and equivalent pore water pressure rise. The observations are similar to the behaviour observed for dense sand by others. The cyclic resistance ratio (CRR) of the tested material indicated no significant sensitivity to the initial confining stress level for stress levels below 200 kPa, suggesting that the response is similar to that of normally consolidated clay. The cyclic resistance ratio of the silt increased with increasing overconsolidation ratio (OCR) for OCR greater than 1.3. The silt specimens that developed high equivalent pore water pressures during cyclic loading, suffered significant volumetric strains during post-cyclic reconsolidation, indicating considerable changes in the particle fabric under cyclic loading. Repeated cyclic loading (re-liquefaction) tests conducted after post-cyclic reconsolidation displayed a reduction in CRR in comparison to that noted under first cyclic loading. The decrease in CRR due to the degradation of particle fabric as a result of previous shearing appears to have overshadowed any gain in CRR that would have

taken place due to the reduction of void ratio during re-consolidation. The commonly used empirical liquefaction criteria displayed limitations in describing the cyclic response of the tested silt. Laboratory element testing that allows capturing the effect of most controlling parameters seems to remain as the more reliable approach for estimating liquefaction susceptibility of fine-grained soils.

TABLE OF CONTENTS

ABSTRACT	ii
TABLE OF CONTENTS	iv
LIST OF TABLES	viii
LIST OF FIGURES	ix
ACKNOWLEDGEMENTS	xvi
1 INTRODUCTION	1
2 LITERATURE REVIEW	4
2.1 Mechanical Response of Sand	5
2.1.1 Monotonic Loading	5
2.1.2 Cyclic Loading Response	8
2.1.3 Post-Cyclic Shear Resistance	13
2.2 CYCLIC LOADING RESPONSE OF SILTY SANDS	15
2.3 LIQUEFACTION SUSCEPTIBILITY OF FINE-GRAINED SOILS	16
2.3.1 Evidence of Liquefaction in Fine-grained Soils During Past Earthquakes	16
2.3.2 Empirically Based Liquefaction Criteria	17
2.3.3 Effects of Pre-loading	20
2.3.4 Liquefaction Susceptibility of Fine-grained Mine Tailings	21
2.4 Proposed Research Program	24

3 EXPERIMENTAL ASPECTS	26
3.1 MATERIAL TESTED	27
3.2 DIRECT SIMPLE SHEAR (DSS) TESTING	31
3.2.1 UBC Direct Simple Shear Test Device	31
3.2.2 DSS Loading System	35
3.2.3 Data Acquisition, Control System and Measurement Resolution	36
3.2.4 DSS Test Procedure	37
3.2.4.1 Specimen Extrusion and Setup	37
3.2.4.2 Consolidation Phase	39
3.2.4.3 Shear Loading Phase	39
3.2.4.4 Post-cyclic Reconsolidation and Repeated Cyclic Loading	40
3.3 TRIAXIAL TESTING	41
3.4 OTHER TESTING	42
3.4.1 Consolidation Tests	42
3.4.2 Index Tests	43
3.5 UNDISTURBED SOIL SPECIMEN HOLDER FOR PREPARATION OF TRIAXIAL SPECIMENS	43
3.5.1 Description of the Undisturbed Soil Sample Holder	48
3.5.1.1 Principle of Operation of the USSH	52
3.5.1.2 Basic Steps in Sample Preparation	54
3.5.2 Assessment of the Effectiveness of the USSH	58
3.5.2.1 Specimen Deformations Immediately After Extrusion through Sample Set up	59
3.5.2.2 Volumetric Strains Experienced During Reconsolidation	62
3.5.2.3 Undrained Response to Monotonic Shear Loading	62
3.6 TEST PROGRAM	65

4	CYCLIC LOADING RESPONSE OF CHANNEL-FILL FRASER RIVER SILT	67
4.1	CONSOLIDATION CHARACTERISTICS	67
4.2	ASSESSMENT OF SAMPLE DISTURBANCE	70
4.3	UNDRAINED RESPONSE OF FRASER RIVER DELTA SILT	72
4.3.1	Monotonic Shear Response	72
4.3.2	Cyclic Shear Response of Normally Consolidated Silt	74
4.3.2.1	Definition of Liquefaction in Laboratory Specimens Subject to Cyclic Shear Loading	74
4.3.2.2	General Stress-Strain and Pore Water Pressure Response	79
4.3.2.3	General Stress-Strain and Pore Water Pressure Response at Other Stress Levels	89
4.3.2.4	Degradation of Shear Stiffness During Cyclic Loading	99
4.3.2.5	Cyclic Resistance Ratio	103
4.3.2.6	Post-cyclic Re-consolidation Response	105
4.3.2.7	Effects of Repeated Cyclic Loading (Re-liquefaction)	105
4.3.2.8	Post-cyclic Consolidation Response after Re-Liquefaction	119
4.3.3	Cyclic Loading Response of Overconsolidated Specimens	119
4.3.3.1	Degradation of Shear Stiffness During Cyclic Loading	131
4.3.3.2	Cyclic Resistance Ratio (CRR)	139
4.3.3.3	Post-cyclic Consolidation Response	139
4.4	APPLICABILITY OF EMPIRICALLY BASED CRITERIA FOR LIQUEFACTION ASSESSMENT	143
5	CYCLIC LOADING RESPONSE OF FINE-GRAINED MINE TAILINGS	151
5.1	INTRODUCTION	151
5.2	MINE TAILINGS MATERIALS OF THE DATABASE	152
5.3	TEST PROGRAM	155

5.4	CYCLIC SHEAR RESISTANCE OF FINE-GRAINED MINE TAILINGS	157
5.4.1	Cyclic Stress Ratio	157
5.4.2	Post-Cyclic Shear Resistance	167
5.4.3	Applicability of Empirically Based Liquefaction Criteria	172
6	SUMMARY AND CONCLUSIONS	177
6.1	Undrained Monotonic Response of Channel-Fill Fraser River silt	177
6.2	Undrained Cyclic Loading Response of Normally Consolidated Silt	178
6.3	Undrained Cyclic Loading Response of Overconsolidated Silt	178
6.4	Repeated Cyclic Loading Response of Silt	179
6.5	Post-cyclic Consolidation Response of Channel-fill Fraser River Silt	179
6.6	Applicability of Empirically Based Criteria for Liquefaction Assessment	180
6.7	Cyclic Loading Response of Fine-grained Mine Tailings	181
6.8	Sample Disturbance	182
7	REFERENCES	183

LIST OF TABLES

Table 3.1. Index parameters of Fraser River delta silt	28
Table 3.2. Measurement resolution of UBC-DSS device	37
Table 3.3. Measurement resolution of triaxial device	42
Table 3.4. Summary of consolidation tests	66
Table 3.5. Summary of undrained triaxial and constant volume DSS tests	66
Table 3.6. Summary of constant volume cyclic DSS tests	66
Table 4.1. Summary of results from consolidation tests performed in Fraser River silt	68
Table 4.2. Sample quality classification according to Lunne et al. (1997) for channel-fill Fraser River silt samples of this study	71
Table 4.3. Summary of results of constant volume cyclic DSS tests performed on channel-fill Fraser River silt.	87
Table 4.4. Factors controlling the response of soils to cyclic loading and their consideration by different empirical criteria for liquefaction assessment	150
Table 5.1. Characteristics and properties of the tailings included in this study	153

LIST OF FIGURES

- Figure 2.1. Typical shear response of loose and dense sand observed during drained monotonic loading in the direct shear apparatus (Modified from Schofield and Wroth, 1968) 6
- Figure 2.2. Typical undrained monotonic loading response of sand. a) Stress-strain response. b) Stress path (after Vaid and Chern, 1985). 7
- Figure 2.3. Typical “liquefaction” response during undrained cyclic loading. a) Stress-Strain response. b) Stress Path. c) Shear strain development (after Vaid and Chern, 1985). 9
- Figure 2.4. Typical “cyclic mobility” type of response during undrained cyclic loading. a) Stress-Strain response. b) Stress Path. c) Shear strain development (after Vaid and Chern, 1985). 10
- Figure 2.5. Typical “limited liquefaction due to cyclic loading” type of response during undrained cyclic loading. a) Stress-Strain response. b) Stress Path. c) Shear strain development (after Vaid and Chern, 1985). 11
- Figure 2.6. Summary of cyclic resistance of different tailings material presented by various authors. 23
- Figure 3.1. Cone penetration test profile of the site 29
- Figure 3.2. Grain size analysis of different samples of Fraser River silt 30
- Figure 3.3. Stress conditions under seismic loading (a) Field and laboratory model cases and (b) stress conditions for an element of soil. 32
- Figure 3.4. Comparison of stress conditions in (a) Simple Shear testing – DSS and (b) Triaxial testing – CTX (After Sriskandakumer, 2004). 33
- Figure 3.5. Schematic diagram of UBC simple shear test device (Modified from Sriskandakumar, 2004) 34
- Figure 3.6. Hypothetical stress path during tube sampling and specimen preparation of fine-

grained soils for laboratory element testing (After Ladd and DeGroot 2003)	45
Figure 3.7. Typical mechanisms of sample disturbance in soft fine-grained soils due to self-weight during the free-standing period. (a) vertical deformation and lateral bulging; (b) tilting. [Samples extruded from a 76-mm diameter sample tube]	47
Figure 3.8. The Undisturbed Soil Sample Holder (USSH) - Assembly for tube sample extrusion.	49
Figure 3.9. The Undisturbed Soil Sample Holder (USSH) - Side view and dimensions. (see 3.10 for Section X-X details).	50
Figure 3.10. The Undisturbed Soil Sample Holder (USSH) - Section X-X (see Figure 3.9 for location of section X-X).	51
Figure 3.11. Variation of internal diameter of the USSH in response to applied vacuum (p) through suction port.	53
Figure 3.12. The USSH assembled in the triaxial pedestal during specimen preparation.	56
Figure 3.13. Plan view of lateral confinement provided by the USSH immediately after extrusion of a soil specimen.	60
Figure 3.14. Timeline of axial strains during sample preparation - with and without the use of USSH.	61
Figure 3.15. Volumetric strains during isotropic consolidation - with and without the use of USSH.	63
Figure 3.16. Mechanical response during consolidated-undrained triaxial compression testing - with and without the use of USSH. - a) Stress-strain response, b) Excess pore water pressure response and c) Stress path	64
Figure 4.1. Consolidation tests performed on Fraser River delta silt	69
Figure 4.2. Results of consolidated undrained tests performed on Fraser River silt. a) Stress-strain, b) pore water pressure development, c) stress-path	73
Figure 4.3. Results of constant volume monotonic direct simple shear tests performed on Fraser River silt. a) Stress-strain, b) pore water pressure development, c) stress-path	75
Figure 4.4. Results of constant volume monotonic direct simple shear tests performed on Fraser River silt. on normally and overconsolidated samples a) Stress-strain, b) pore water pressure development, c) stress-path	76
Figure 4.5. Typical contractive response observed for loose Fraser River sand (after Wijewickreme et al., <i>In print</i>)	78
Figure 4.6. Constant volume DSS test results on normally consolidated sample - Tests series	

NC-1 (CSR = 0.10, σ'_{vo} = 100 kPa). a) Stress-strain response. b) Stress-path.	80
Figure 4.7. Constant volume DSS test results on normally consolidated sample – Tests series NC-1 (CSR = 0.15, σ'_{vo} = 100 kPa). a) Stress-strain response. b) Stress-path.	81
Figure 4.8. Constant volume DSS test results on normally consolidated sample – Tests series NC-1 (CSR = 0.18, σ'_{vo} = 100 kPa). a) Stress-strain response. b) Stress-path.	82
Figure 4.9. Constant volume DSS test results on normally consolidated sample – Tests series NC-1 (CSR = 0.20, σ'_{vo} = 100 kPa). a) Stress-strain response. b) Stress-path.	83
Figure 4.10. Constant volume DSS test results on normally consolidated sample – Tests series NC-1 (CSR = 0.30, σ'_{vo} = 100 kPa). a) Stress-strain response. b) Stress-path.	84
Figure 4.11. Cumulative pore water pressure during constant volume DSS test on normally consolidated sample – Tests series NC-1 (σ'_{vo} = 100 kPa).	85
Figure 4.12. Constant volume DSS test results on normally consolidated sample – Tests series NC-2 (CSR = 0.10, σ'_{vo} = 85 kPa). a) Stress-strain response. b) Stress-path.	90
Figure 4.13. Constant volume DSS test results on normally consolidated sample – Tests series NC-2 (CSR = 0.15, σ'_{vo} = 85 kPa). a) Stress-strain response. b) Stress-path.	91
Figure 4.14. Constant volume DSS test results on normally consolidated sample – Tests series NC-2 (CSR = 0.25, σ'_{vo} = 85 kPa). a) Stress-strain response. b) Stress-path.	92
Figure 4.15. Constant volume DSS test results on normally consolidated sample – Tests series NC-2 (CSR = 0.30, σ'_{vo} = 85 kPa). a) Stress-strain response. b) Stress-path.	93
Figure 4.16. Cumulative pore water pressure during constant volume DSS test on normally consolidated sample – Tests series NC-2 (σ'_{vo} = 85 kPa).	94
Figure 4.17. Constant volume DSS test results on normally consolidated sample – Tests series NC-3 (CSR = 0.11, σ'_{vo} = 200 kPa). a) Stress-strain response. b) Stress-path.	95
Figure 4.18. Constant volume DSS test results on normally consolidated sample – Tests series NC-3 (CSR = 0.15, σ'_{vo} = 200 kPa). a) Stress-strain response. b) Stress-path.	96
Figure 4.19. Constant volume DSS test results on normally consolidated sample – Tests series NC-3 (CSR = 0.20, σ'_{vo} = 200 kPa). a) Stress-strain response. b) Stress-path.	97
Figure 4.20. Cumulative pore water pressure during constant volume DSS test on normally consolidated sample – Tests series NC-3 (σ'_{vo} = 200 kPa).	98
Figure 4.21. Schematic representation of degradation of shear stiffness during cyclic loading.	100
Figure 4.22. Modulus degradation for samples tested in the DSS on normally consolidated state.	101

- Figure 4.23. Cyclic resistant ratio versus number of cycles to reach liquefaction for specimens tested on the DSS on normally consolidated conditions. 102
- Figure 4.24. Post-cyclic volumetric strain vs. maximum pore water pressure ratio developed during cyclic loading. Test series NC-1, NC-2 and NC-3 104
- Figure 4.25. Constant volume DSS test results on normally consolidated sample – Tests series NC-2 (CSR = 0.10, $\sigma'_{vo} = 85$ kPa) – Second cyclic loading. a) Stress-strain response. b) Stress-path. 106
- Figure 4.26. Constant volume DSS test results on normally consolidated sample – Tests series NC-2 (CSR = 0.15, $\sigma'_{vo} = 85$ kPa) – Second cyclic loading. a) Stress-strain response. b) Stress-path. 107
- Figure 4.27. Constant volume DSS test results on normally consolidated sample – Tests series NC-2 (CSR = 0.25, $\sigma'_{vo} = 85$ kPa) – Second cyclic loading. a) Stress-strain response. b) Stress-path. 108
- Figure 4.28. Constant volume DSS test results on normally consolidated sample – Tests series NC-2 (CSR = 0.29, $\sigma'_{vo} = 85$ kPa) – Second cyclic loading. a) Stress-strain response. b) Stress-path. 109
- Figure 4.29. Cumulative pore water pressure during constant volume DSS test on normally consolidated sample – Tests series NC-1 ($\sigma'_{vo} = 85$ kPa) – Second cyclic loading. 110
- Figure 4.30. Constant volume DSS test results on normally consolidated sample – Tests series NC-1 (CSR = 0.15, $\sigma'_{vo} = 100$ kPa) – Second cyclic loading. a) Stress-strain response. b) Stress-path. 113
- Figure 4.31. Constant volume DSS test results on normally consolidated sample – Tests series NC-1 (CSR = 0.18, $\sigma'_{vo} = 100$ kPa) – Second cyclic loading. a) Stress-strain response. b) Stress-path. 114
- Figure 4.32. Constant volume DSS test results on normally consolidated sample – Tests series NC-1 (CSR = 0.21, $\sigma'_{vo} = 100$ kPa) – Second cyclic loading. a) Stress-strain response. b) Stress-path. 115
- Figure 4.33. Constant volume DSS test results on normally consolidated sample – Tests series NC-1 (CSR = 0.29, $\sigma'_{vo} = 100$ kPa) – Second cyclic loading. a) Stress-strain response. b) Stress-path. 116
- Figure 4.34. Cumulative pore water pressure during constant volume DSS test on normally consolidated sample – Tests series NC-1 ($\sigma'_{vo} = 100$ kPa) – Second cyclic loading. 117
- Figure 4.35. Cyclic resistant ratio versus number of cycles to reach liquefaction for samples tested on the DSS on normally consolidated state. Effects of repeated cyclic loading. a) Test Series NC-1. b) Test Series NC-2. 118
- Figure 4.36. Post-cyclic volumetric strain vs. maximum pore water pressure ratio developed

during first and second cyclic loading. Test series NC-1 and NC-2.	120
Figure 4.37. Constant volume DSS test results on overconsolidated sample – Tests series OC-1 (OCR = 1.2). a) Stress-strain response. b) Stress-path.	121
Figure 4.38. Constant volume DSS test results on overconsolidated sample – Tests series OC-1 (OCR = 1.5). a) Stress-strain response. b) Stress-path.	122
Figure 4.39. Cumulative pore water pressure during constant volume DSS test on overconsolidated samples – Tests series OC-1 (CSR = 0.15).	123
Figure 4.40. Constant volume DSS test results on overconsolidated sample – Tests series OC-2 (OCR = 1.3). a) Stress-strain response. b) Stress-path.	125
Figure 4.41. Constant volume DSS test results on overconsolidated sample – Tests series OC-2 (OCR = 1.4). a) Stress-strain response. b) Stress-path.	126
Figure 4.42. Constant volume DSS test results on overconsolidated sample – Tests series OC-2 (OCR = 1.5). a) Stress-strain response. b) Stress-path.	127
Figure 4.43. Constant volume DSS test results on overconsolidated sample – Tests series OC-2 (OCR = 1.7). a) Stress-strain response. b) Stress-path.	128
Figure 4.44. Constant volume DSS test results on overconsolidated sample – Tests series OC-2 (OCR = 1.9). a) Stress-strain response. b) Stress-path.	129
Figure 4.45. Constant volume DSS test results on overconsolidated sample – Tests series OC-2 (OCR = 2.1). a) Stress-strain response. b) Stress-path.	130
Figure 4.46. Cumulative pore water pressure during constant volume DSS test on overconsolidated samples – Tests series OC-2 (CSR = 0.20).	132
Figure 4.47. Constant volume DSS test results on overconsolidated sample – Tests series OC-3 (OCR = 1.2). a) Stress-strain response. b) Stress-path.	133
Figure 4.48. Constant volume DSS test results on overconsolidated sample – Tests series OC-3 (OCR = 1.4). a) Stress-strain response. b) Stress-path.	134
Figure 4.49. Constant volume DSS test results on overconsolidated sample – Tests series OC-3 (OCR = 1.6). a) Stress-strain response. b) Stress-path.	135
Figure 4.50. Constant volume DSS test results on overconsolidated sample – Tests series OC-3 (OCR = 1.9). a) Stress-strain response. b) Stress-path.	136
Figure 4.51. Cumulative pore water pressure during constant volume DSS test on overconsolidated samples – Tests series OC-2 (CSR = 0.20).	137
Figure 4.52. Modulus degradation for samples tested in the DSS on overconsolidated state.	138

Figure 4.53. Cyclic resistant ratio versus number of cycles to reach liquefaction for samples tested on the DSS: influence of overconsolidation ratio.	140
Figure 4.54. Variation of OCR with No. of cycles to reach $\gamma = 3.75\%$ for constant cyclic stress ratio.	141
Figure 4.55. Post-cyclic volumetric strain for overconsolidated samples.	142
Figure 4.56. Applicability of the Chinese criteria for liquefaction assessment for Fraser River silt.	144
Figure 4.57. Applicability of Andrews and Martin (2000) criteria for liquefaction assessment on Fraser River silt.	145
Figure 4.58. Applicability of Polito (2001) criteria for liquefaction assessment on Fraser River silt.	146
Figure 4.59. Applicability of Bray et al. (2004b) criteria for liquefaction assessment on Fraser River silt.	148
Figure 5.1. Typical response of laterite tailings in constant volume cyclic DSS loading (sample L-100-02: $\sigma'_{vo} = 100$ kPa, CSR = 0.225). a) Stress strain, b) stress path response, and c) pore water pressure ratio versus number of cycles.	158
Figure 5.2. Typical response of copper-gold tailings in constant volume cyclic DSS loading (sample CG-03: $\sigma'_{vo} = 100$ kPa, CSR = 0.190). a) Stress strain, b) stress path response, and c) pore water pressure ratio versus number of cycles.	159
Figure 5.3. Typical response of copper-gold-zinc tailings in constant volume cyclic DSS loading (sample CGZ-20: $\sigma'_{vo} = 314$ kPa, CSR = 0.129). a) Stress strain, b) stress path response, and c) pore water pressure ratio versus number of cycles.	160
Figure 5.4. Cyclic stress ratio versus number of cycles to trigger liquefaction for samples of laterite tailings tested at two confining stress levels.	161
Figure 5.5. Cyclic stress ratio versus number of cycles to trigger liquefaction for samples of copper-gold-zinc tailings tested at different confining stress levels.	163
Figure 5.6. Comparison of cyclic stress ratio versus number of cycles to trigger liquefaction for laterite, copper-gold, and copper-gold-zinc tailings.	165
Figure 5.7. Cyclic shear resistance to liquefaction of samples included in this study compared with data from literature.	166
Figure 5.8. Post cyclic monotonic DSS tests on samples of a) laterite – sample L-100-02, b) copper-gold – sample CG-03 and c) copper-gold zinc – sample CGZ-20. Definition of post-cyclic maximum undrained shear strength (S_{u-PC}) is also shown.	168
Figure 5.9. Variation of post-cyclic maximum shear strength ratio with void ratio.	170

Figure 5.10. Applicability of Chinese criteria for the tailings considered in this study (modified from Marcuson et al. 1990). 173

Figure 5.11. Applicability of the liquefaction susceptibility criteria proposed by Bray et al. (2004b) for the tailings considered in this study. 175

AKNOWLEDGEMENTS

The author wishes to express her most sincere gratitude to her supervisor, Dr. Dharma Wijewickreme, for his constant guidance, support and encouragement throughout this research. The author is also grateful to Dr. P. M. Byrne for his lessons, input and valuable comments during this research.

The author also wishes to thank her professors during the pursuit of the Master of Applied Science Degree, Drs. R. J. Fannin, J. A. Howie, D. Shuttle and C. Ventura. The author is also grateful to Dr. W.D.L. Finn for his support and valuable discussions along this research program.

Especially thanks to Dr. Pat Monahan for facilitating access to the field sampling program and for his valuable comments and thoughts throughout this research. The author also wishes to express her gratitude to Graham Greenaway from Knight Piésold Ltd. for the contribution of the fine-grained mine tailings database used in this study and for valuable discussions.

The author is also grateful to her colleagues in the geotechnical group; Alex, Kumar, Hamid, Ali, Megan, Ricardo, Pascale and Maoxin for interesting, critical and enjoyable conversations regarding this research, laboratory techniques and extracurricular activities. Also, the author is

grateful to the undergrad students, Jennifer Scott and Andrew Chand for their assistance during this research.

The undisturbed soil samples were obtained as a result of a field testing program supported by the British Columbia Geological Survey, the City of Richmond, and the Joint Emergency Preparedness Program (Province of British Columbia, Canada), for which the author is grateful. Technical assistance of Messrs Harald Schremp, Bill Leung, Scott Jackson and John Wong of the Department of Civil Engineering Workshop is also acknowledged with deep regard.

Financial support provided by the National Research Council of Canada (NSERC), the University of British Columbia and the Vancouver Geotechnical Society is deeply appreciated.

Finally, the author would like to express her gratitude to her husband, Jose Roberto, for his constant support, encouragement and understanding, which helped to keep her focused and to enjoy every moment throughout this journey.

1 INTRODUCTION

Earthquake-induced ground displacements and associated geotechnical hazards are one of the main concerns in areas with moderate to high seismicity with loose/soft soils such as those found in the Fraser River Delta of British Columbia, Canada. Liquefaction of saturated sands has been the topic of extensive research during the past 30 years, while the behaviour of silty sands and silts has been studied only on a very limited scale. It has been found that certain fine-grained soils can be as susceptible to liquefaction as relatively clean sands, and there is a significant controversy and confusion regarding the liquefaction potential of silts including clayey silts (Youd et al., 2001; Seed et al., 2001).

Silty soils are found in most earthquake-prone soft soils areas, are common in river deposits with high levels of saturation and are also the product of crushed rock waste in the mining industry. The current approach to evaluate the liquefaction susceptibility of fine-grained soils depends mainly on empirical criteria based on soil index parameters (Wang, 1979; Finn et al., 1994; Koester, 1992; Andrews and Martin, 2000; Polito, 2001; Bray et al., 2004b) with no direct consideration of many fundamental parameters that govern the seismic response of soils such as intensity and duration of the loading conditions. Recent evidence of ground failure in fine-grained soils during strong earthquakes have emphasized the need for a fundamental

understanding of their earthquake-induced behaviour that can lead to more appropriate engineering procedures for the evaluation of seismic performance.

The response of a given soil to cyclic loading is controlled by many parameters such as packing density, microstructure, fabric, level and duration of cyclic loading, confining stress, initial static bias, etc. These parameters would contribute to gradual strain development (or strength loss) and increase of pore water pressures, that may lead to instability during the occurrence of an earthquake. The current empirical criteria for liquefaction assessment of fine-grained soils do not consider most of these parameters, and limit the liquefaction analyses to simple "yes/no" classification. A more fundamental approach, such as laboratory testing, that includes more of the above described parameters would provide a better understanding of the liquefaction susceptibility of fine-grained soils, similar to those that have been developed in the past 30 years for sands.

Considering the above, there is a strong need to undertake research that leads to a fundamental understanding of the earthquake response of fine-grained soils. In recognition of this, a laboratory element testing program was undertaken focusing on the cyclic loading response of natural silt obtained from a channel-fill in the Fraser River Delta of British Columbia, Canada. The research program also examined the applicability of the empirically based liquefaction criteria for the silt, and investigated the cyclic response of fine-grained mine tailings from available data from constant volume direct simple shear tests.

The mechanical response of Fraser River silt was investigated including the following components:

- consolidation characteristics,

- undrained monotonic response of normally consolidated and overconsolidated silt, and
- undrained cyclic loading response of normally and overconsolidated silt.

The NGI-type (Bjerrum and Landva, 1966) cyclic direct simple shear (DSS) test device at UBC was used for the main component of the present study. The DSS loading mode has been considered to be more effective in simulating seismic loading than the triaxial loading mode. Particular emphasis was made on sample disturbance considering that undisturbed silt samples were used for this research.

2 LITERATURE REVIEW

Understanding the mechanical behaviour of soils is fundamental in engineering design particularly with respect to the development of meaningful constitutive models for numerical modeling and laboratory element testing plays an essential role in developing this understanding. While the use of undisturbed samples obtained from the field would be preferable for element testing, laboratory studies on coarse grained soils (i.e., sands, gravels) are often undertaken using reconstituted samples because of difficulties in obtaining good quality samples. Evidence from recent earthquakes indicate that deposits composed of silts are as much susceptible to liquefaction as sand deposits, thus, emphasizing the strong need to obtain fundamental understanding in the cyclic shear response of natural silt deposits. In spite of this, not much research has been conducted on silts. This is primarily due to the difficulties in obtaining high quality undisturbed samples as well as in reconstituting samples in the laboratory that may be representative of field conditions.

The present study is mainly related to investigating the response of a natural silt under cyclic conditions. Nevertheless, an overview of the current understanding of the mechanical response of sands warranted considering that most of the understanding of liquefaction has been based on tests conducted on sands. In consideration of this, the general stress-strain response of sand with some general definitions used in the study of liquefaction is presented. A discussion on

some of the parameters that govern the liquefaction susceptibility of soils, with particular reference to fine-grained soils is then presented. Because of the intimate linkage with laboratory testing of natural soils, aspects related to sampling and sampling disturbance are discussed. The proposed research program, which forms the core component of this thesis, is also described.

2.1 MECHANICAL RESPONSE OF SAND

2.1.1 Monotonic Loading

Drained and undrained static behaviour of sands has been studied by several researchers (Casagrande, 1936a; Roscoe et al., 1963; Castro, 1969, Vaid and Chern, 1985; Vaid and Thomas, 1995). Typical response of sand observed during drained monotonic loading in the direct shear apparatus is shown in Figure 2.1. Volumetric response has been observed as contractive (compression) or dilative (expansion). At large strains, the angle of friction at which the soil deforms at constant void ratio is called the constant volume friction angle (ϕ_{cv}).

Typical undrained monotonic loading response of sand is presented in Figure 2.2. The behaviour has been interpreted in three types of response: Type 1 response is characterized by reaching a maximum shear strength followed by continuous strain softening. This has been defined as liquefaction by Castro (1969), Casagrande (1975) and Seed (1979) and as true liquefaction by Chern (1985). This type of response is considered to result in flow failure under field conditions. Type 2 response shows maximum peak of shear strength followed by initial strain-softening and immediate strain-hardening (dilation). This typical behaviour was named

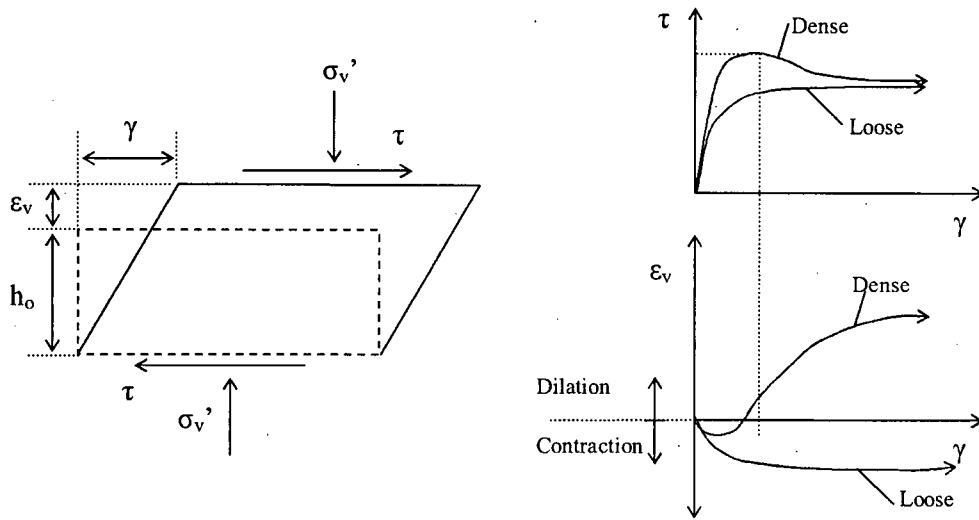


Figure 2.1. Typical shear response of loose and dense sand observed during drained monotonic loading in the direct shear apparatus (Modified from Schofield and Wroth, 1968)

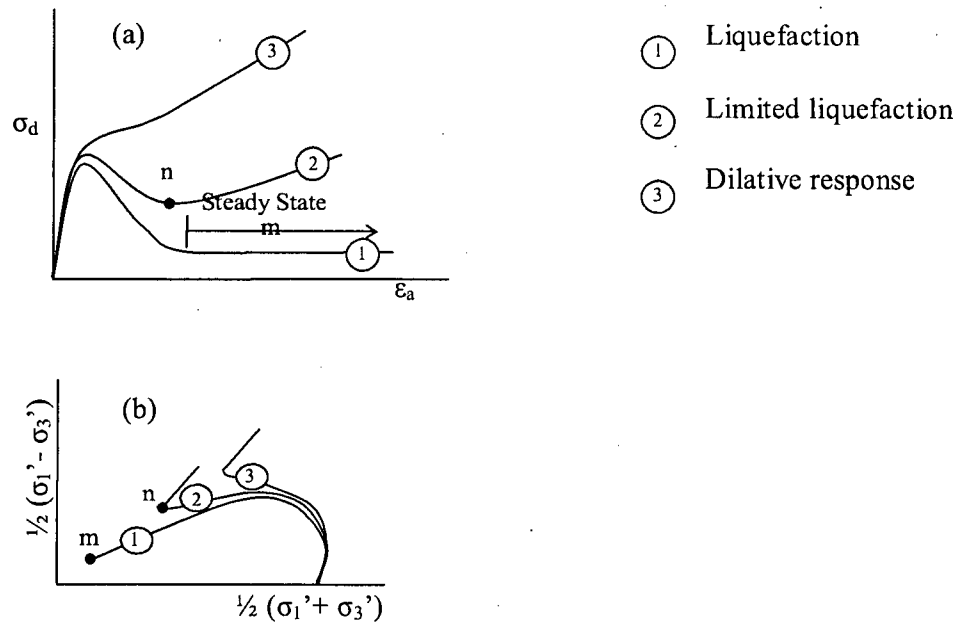


Figure 2.2. Typical undrained monotonic loading response of sand. a) Stress-strain response. b) Stress path (after Vaid and Chern, 1985).

as limited liquefaction by Castro (1969). After reaching the CSR the soil start to strain soften and followed by deformation at constant stress ratio and subsequent dilative response. The deformation at constant stress ratio has been called quasi-steady-state (QSS) by Ishihara et al. (1975). In terms of stress path (see Figure 2.2), the term phase transformation (PT) is the point at which the soil changes its behaviour from contractive to dilative (point of maximum excess pore water pressure). The mobilized friction angle at PT, ϕ_{PT} , has been noted to be unique for a given sand (Ishihara, 1975; Vaid and Chern, 1985; Kuerbis et al., 1988). It has been also found that the friction angle at phase transformation (ϕ_{pt}) is essentially the same as the constant volume friction angle (ϕ_{cv}) for a given sand (Chern, 1985; Neguessy et al., 1988).

In Type 3 response the soil exhibits increasing shear resistance with increasing deformation with no strain-softening. The excess pore water pressure initially shows an increase (contractive response), then followed by a decrease (dilative response), with increasing strain.

2.1.2 Cyclic Loading Response

While cyclic loading can induce significant volumetric strains in unsaturated sands, most of the research focus has been on the performance of saturated sands because of their noted potential for generation of excess pore water pressures and associated strength and stiffness degradation under cyclic loading. In this regard, behaviour of saturated sands has been typically simulated using laboratory undrained cyclic tests. As in the case of monotonic undrained loading, three types of response have been identified (Castro, 1969, Vaid and Chern, 1985), and they are schematically presented in Figure 2.3 through Figure 2.5. In the “liquefaction” type of response, as per Figure 2.3, the soil experiences continuous contractive deformation. The

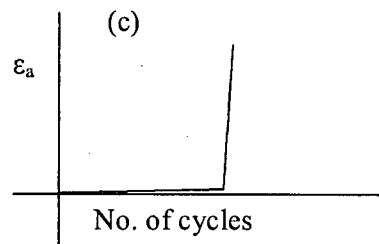
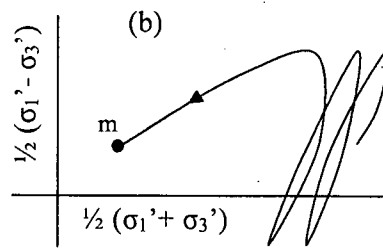
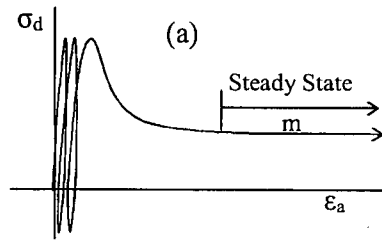


Figure 2.3. Typical “liquefaction” response during undrained cyclic loading. a) Stress-Strain response. b) Stress Path. c) Shear strain development (after Vaid and Chern, 1985).

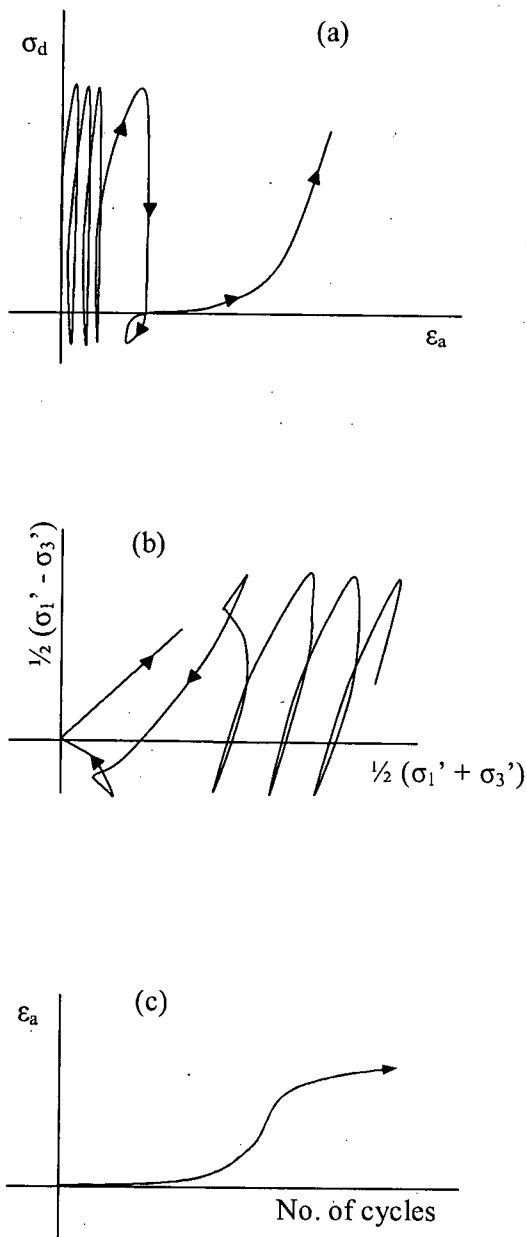


Figure 2.4. Typical "cyclic mobility" type of response during undrained cyclic loading. a) Stress-Strain response. b) Stress Path. c) Shear strain development (after Vaid and Chern, 1985).

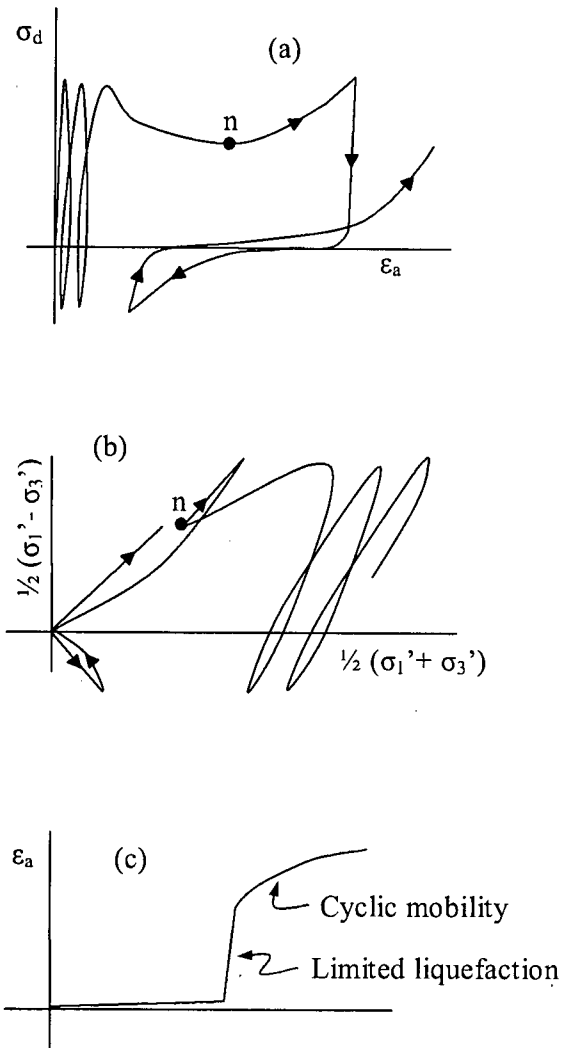


Figure 2.5. Typical "limited liquefaction due to cyclic loading" type of response during undrained cyclic loading. a) Stress-Strain response. b) Stress Path. c) Shear strain development (after Vaid and Chern, 1985).

second type of response is called cyclic mobility with limited liquefaction (see Figure 2.4). Herein, once the stress ratio has reached PT , the soil starts to behave in a dilative manner. Following the unloading part of the cycle, larger excess pore water pressure are developed producing a state of zero effective stress. The cycles that follow would cause a dilative response leading to strain-hardening tendency. In the third type of response, called cyclic mobility without limited liquefaction, as presented in Figure 2.5, the shear strains increase gradually with increasing number of load cycles although there is no strain-softening.

Earthquake geotechnical problems generally involve level ground as well as slope configurations. For level ground conditions “no static shear bias” is commonly used to indicate that there are not initial shear stresses on the horizontal plane prior to earthquake loading (Seed and Peacock, 1971; Vaid and Finn, 1979). To replicate these conditions on the laboratory the samples are consolidated without initial applied static shear stress. To simulate field conditions with configuration of sloping ground, samples are consolidated with an applied static shear stress prior to cyclic loading, and these tests are typically referred to as cyclic shear tests with “initial static shear stress bias”. It has been found that the presence of initial static shear have a profound influence on the cyclic resistance of sands. While some researchers have found that the presence of initial static shear increases the cyclic resistance to liquefaction (Lee and Seed, 1967; Seed et al., 1975), others have observed that the increase in static shear stress would decrease the cyclic resistance to liquefaction (Castro, 1969; Casagrande, 1975; Castro et al., 1982). Vaid and Finn (1979), Vaid and Chern (1985), Seed and Harder (1990), Vaid et al. (2001) and Sriskandakumar (2004) have found that the effect of static shear stress on the cyclic resistance of sands is influenced by the initial density; thus, loose sands would experience reduction in the cyclic resistance with the presence of static shear, while the cyclic resistance of

dense (dilative) sands would increase if applied initial static shear. If the deformation mechanism of a given sand is of the “cyclic mobility” type, the cyclic resistance to liquefaction would increase with increasing initial static shear (Vaid and Chern, 1985).

Cyclic resistance of sands has also been noted to be significantly affected by past liquefaction or pre-shearing (Finn et al., 1970; Seed et al., 1977; Isihara and Okada, 1978; Suzuki and Toki, 1984; Vaid et al., 1989; Sriskandakumar, 2004). Finn et al. (1970) found that previously liquefied samples exhibited significantly less cyclic shear resistance than virgin samples, despite a significant increase in density following consolidation after the first liquefaction stage. Similar results were found by Sriskandakumar (2004) based on tests conducted on loose Fraser River Sand in the direct simple shear. Small pre-shearing improves the soil fabric and increase the cyclic resistance of sand to liquefaction during a second cyclic loading phase, while large pre-shearing weakens the soil fabric and decreases the cyclic resistance to liquefaction in the following cyclic loading.

2.1.3 Post-Cyclic Shear Resistance

As described by Finn et al. (1994), there are three fundamental questions in seismic evaluations of earth structures, including tailings dams: (i) Will liquefaction be triggered in significant zones of the structure for the design earthquake? (ii) What are the expected consequences of liquefaction? and (iii) What remedial measures are practical and cost-effective. The procedures in the current state-of-practice address the first two questions with three separate analyses (Byrne et al. 2004): (i) triggering analysis to compute the cyclic stress ratios (CSR) for comparison with the cyclic resistance ratios (CRR) to identify zones that will liquefy; (ii) conventional limit equilibrium analysis to assess post-liquefaction stability (flow slide

analysis); and (iii) if no flow slide is predicted, then undertaking simple dynamic analysis using the strength of the soil to assess permanent displacements induced by shaking. It is however important to note that such analyses are not fundamental and are not likely to improve our basic understanding of the liquefaction process because they do not directly consider pore pressures in the prediction of liquefaction (Byrne et al. 2004). Instead, coupled effective stress analysis procedures that allow capturing of the full stress strain response are more suitable to solve the boundary value problems (Byrne et al. 2004; Finn and Yogendrakumar 1989).

One of the key parameters required in limit equilibrium analysis to assess post-liquefaction stability is the post-cyclic undrained shear strength of potentially liquefiable soil zones. Seed and Harder (1990), Stark and Mesri (1992) and Olson and Stark (2002) have developed correlations between liquefied strength $S_u(\text{LIQ})$, or liquefied strength ratio $S_u(\text{LIQ})/\sigma'_{vc}$, and in-situ standard penetration values computed by back-analyses of field case histories. Such back-analysis for estimation of $S_u(\text{LIQ})$ has been considered more suitable, since laboratory testing is not able to simulate the water film effects, that take place after liquefaction, particularly in layered deposits with contrasting permeability (Kokusho 2003). Kokusho showed that sand deposits containing sublayers of different permeability are susceptible to the development of water films at the sublayer boundaries that, in turn, may lead to flow failure during or after earthquake loading. In particular, this is a very important issue for tailings deposits that can be highly stratified. Nevertheless, the evaluation of laboratory data provides important information to understanding the soil response in a fundamental manner as well as to support and confirm field-based approaches. The recent evaluation of data from laboratory triaxial compression tests by Olson and Stark (2003) to confirm liquefied strength ratio concepts for clean and silty sands is a good example in this regard. Moreover, from the point of view of

understanding element response, constant volume DSS tests are considered to provide the best estimate of post-cyclic strength, as the test corresponds to the predominant mode of deformation in the field.

2.2 CYCLIC LOADING RESPONSE OF SILTY SANDS

In the past decade, several investigations have been undertaken to understand the cyclic behaviour of sand containing fines. Kuerbis et al. (1988) showed that increasing silt content up to 20% in sand, makes compression behaviour slightly more dilative and extension behaviour less contractive. This small change is attributed to the fact that the sand skeleton remains invariable and that the fines are “just” filling the voids within the sand.

Contrary to the above, Lade and Yamamuro (1997) observed that increasing the non-plastic silt content in Nevada sand increased the contractive tendency of a specimen in spite of the net increase in overall relative density of the granular matrix. Polito and Martin (2001) also studied the effects of non-plastic fines in the liquefaction resistance of sands. They found that for silts contents below a limiting silt content, that corresponds to the largest amount of silt that can be accommodated in the voids of the sand skeleton, the cyclic resistance is controlled by the relative density of the specimen, where the relative density is computed based on the void ratio of the specimen and the maximum and minimum void ratio of the sand and silt mixture, and increasing the relative density increases the liquefaction resistance. For silt contents higher than the limiting silt content, the liquefaction susceptibility is lower than that of soils below the limiting silt content at similar relative densities.

Thevanayagam et al. (2002) observed that inter-granular void ratio is a better index to characterize the mechanical response of granular mixtures than the global void ratio. These quantities are related to the distribution of fine and coarse material and not only to the volume of solids and voids. At low fine contents, the behaviour of a silty sand was noted to be similar to clean sands since the friction between the coarse grains serves as the dominant mechanism for providing shear resistance. At higher silt contents, the "inter-fine" contact density and friction appear to govern the response; however, the strength of sandy silt was observed to be higher than that of pure silt at the same inter-granular void ratio.

2.3 LIQUEFACTION SUSCEPTIBILITY OF FINE-GRAINED SOILS

The following section summarizes the evidence of liquefaction in fine-grained soils from past earthquakes and the approaches that have been proposed to evaluate liquefaction of fine-grained soils. A review on the liquefaction susceptibility of fine-grained mine tailings is also presented to provide background for the evaluation of laboratory data on this subject undertaken as part of this thesis.

2.3.1 Evidence of Liquefaction in Fine-grained Soils During Past Earthquakes

Wang (1979) summarized the events in which liquefaction was evident in past earthquakes in China. Based on this database, he proposed some empirical criteria to identify potentially liquefiable fine-grained soils as described in Section 2.3.2. Tohno and Yasuda (1981) presented information supporting liquefaction of fine-grained soils from observations made during the 1968 Tokachi-Oki earthquake in Japan. They found that soils with fine contents up

to 90% have liquefied during this seismic event. Boulanger et al. (1998) also found evidence of liquefaction of fine-grained soils during the 1989 Loma Prieta earthquake. Using laboratory testing, it was shown that silty clay developed high excess pore water pressure and significant shear strains. They also noted that the use of traditional approaches for liquefaction assessment would characterize this material as non-liquefiable. Similar findings were presented by Atukorala et al. (2000).

Bray et al. (2004a) presented the results of a complete study of soil performance after the 1999 Kocaeli (Turkey) earthquake. It was found that buildings that were supported on low plasticity silts at shallow depths, suffered significant damage during this earthquake. The observed damage was attributed to softening of these foundation soils due to cyclic mobility, and the gradual “working” of buildings into the softened soils. Based on the index tests of the liquefied soils, Bray et al (2004b) also proposed some criteria for the liquefaction susceptibility assessment of fine-grained soils, which are also discussed in the next section.

2.3.2 Empirically Based Liquefaction Criteria

As presented by Wang (1979), the Chinese Criteria was developed on the basis of observed field performance under earthquake loading to evaluate the liquefaction susceptibility of fine-grained soils. The criteria stipulate that soils that satisfy the following conditions would be vulnerable to liquefaction: i) Percent of particles finer than 0.005 mm < 15%; ii) liquid limit (LL) < 35% iii) ratio of water content (w_c) to liquid limit (w_c/LL) > 0.9 and iv) liquidity index (I_w) ≤ 0.75. If soils that fulfill these conditions plot above the A line in the plasticity chart, the soils may be considered as potentially liquefiable; otherwise, they may be considered non-vulnerable to liquefaction. Finn et al. (1994), after considering the changes due to uncertainties

in the measurement of index parameters, proposed the following modifications to the measured properties before applying the criteria: i) decrease fines content by 5%; ii) decrease LL by 2%; and iii) increase w_c by 2%. Considering the differences between the devices used in China and the United States to determine the liquid limit, Koester (1992) also proposed slight changes to the measured values by decreasing the fines contents by 5%, increasing the LL by 1% and decreasing the w_c by 2%. These modified criteria essentially suggest that soils with relatively small fines content are liquefiable, and they call for a narrow range of LL between 33 and 36 as the threshold for liquefaction susceptibility.

Andrews and Martin (2000) have proposed new empirical criteria based on percent of particles finer than 0.002 mm and liquid limit. They emphasize the importance of the origin of the fine-grained soils, noting that soils such as mine tailings may be susceptible to liquefaction in spite of possessing relatively high clay-size particle content. Andrews and Martin (2000) propose that soils having less than 10% of particles finer than 0.002 mm and $LL < 32$ (LL determined using the Casagrande device) are liquefiable. Soils that do not satisfy both the criteria above would be considered non-liquefiable.. On the other hand, only if one of the criteria is satisfied, such soils should be further tested to understand the liquefaction susceptibility.

Based on a series of cyclic triaxial tests on sandy soils with different amounts of plastic fines up to 37%, Polito (2001) presented recommendations for a simplified plasticity-based liquefaction criteria. It was denoted that soils with $LL < 25$ and plasticity index $PI < 7$ are “liquefiable”, soils with liquid limit between 25 and 35 and PI between 7 and 10 are “potentially liquefiable”, and soils outside this boundary in the plasticity chart are “susceptible to cyclic mobility”.

Based on the observations following the Kocaeli earthquake (Turkey) and thorough laboratory work, Bray et al. (2004b) have shown that it is the plasticity characteristics, and not the amount

of clay-size particles, that best describe the liquefaction susceptibility of fine-grained soils. Bray et al. proposed that soils are liquefiable if the plasticity index (PI) is less than 12 and the ratio w_c/LL is greater than 0.85, and that they are not susceptible to liquefaction if PI is greater than 20 and w_c/LL ratio is less than 0.8. Soils within these two boundaries are considered to have moderate susceptibility to liquefaction, and they recommended that laboratory testing be undertaken to clearly determine the liquefaction potential of such soils.

As an alternative to the above empirical criteria, Boulanger and Idriss (2004) have recently recommended that fine-grained soils be classified as “sand-like” (susceptible to liquefaction) if $PI < 7$ and “clay like” if $PI \geq 7$. They also indicate that this criterion may be adjusted on a site-specific basis if justified by the results of detailed in-situ and laboratory testing.

In general terms, all of the above criteria consider liquid limit as key controlling parameter of liquefaction susceptibility. The Chinese criteria and its later modifications (Wang 1979, Finn et al. 1994 and Koester 1992) as well as Andrews and Martin (2000) criteria consider the amount of clay size particles (percentage smaller than 0.005 mm or 0.002 mm) as an added parameter. Polito (2001) and Bray et al. (2004b) criteria, both based on laboratory element testing, suggest that the amount of clay size particles does not play a significant role in the liquefaction susceptibility of fine-grained soils. Chinese criteria and Bray et al. (2004b) criteria both suggest that the natural water content (in-situ state) of the soil is also of great importance for the liquefaction assessment while Andrews and Martin (2000) and Polito (2001) consider that it only depends on the mineralogy of the soil in terms of liquid limit, plasticity index, and clay size particles.

2.3.3 Effects of Pre-loading

Pre-loading is a method commonly used in engineering practice to reduce post-construction settlements. Soil deposits are “pre-loaded” by placing fills in the site where a given structure is to be built. Settlements occur due to this added load, and once the fill is removed, an overconsolidated soil would be available to found the intended structure. Soil improvement herein basically involves reduction of void ratio (or increase in density) of the soil mass, in turn leading to a foundation with increased strength and stiffness.

Ishihara et al. (1977) presented a study on reconstituted samples of sandy silt and silty sand. Cyclic triaxial tests were performed on samples that were previously loaded and unloaded to obtain overconsolidation ratios (OCR) between 1.0 and 2.0. The test results showed that in reconstituted samples, OCR value of 2.0 could increase the cyclic strength by up to 70% compared to the normally consolidated samples, and that the strength increase became less pronounced as the percent of fines in the sample decreased (Ishihara et al., 1977).

Based on cyclic triaxial tests, Campanella and Lim(1981) also presented the influence of OCR in the cyclic resistance of undisturbed samples of clayey silt and silty clay. The increase in liquefaction resistance was of 75% and 150% for OCR values of 2 and 4 respectively. Stamatopoulos et al. (1995) reported similar results for reconstituted samples of silty sand. Comparisons made with some of the results of previous investigations were compared and in agreement with the effects observed by Stamatopoulos et al. (1995).

2.3.4 Liquefaction Susceptibility of Fine-grained Mine Tailings

Tailings essentially comprise the waste crushed rock particles derived from the processing of ore. Tailings are commonly transported and placed hydraulically in slurry form during the process of storage. Because of the nature of deposition, combined with the resulting high degree of saturation and relatively loose densities, the “as-placed” tailings is generally considered susceptible to liquefaction. Liquefaction of tailings can lead to instability and failure of tailings impoundments, with potentially severe consequences including loss of life and multi-faceted environmental, social, and economic impacts.

While static liquefaction is noted as the contributory mechanism in most tailings dam failures (Davies 2002), liquefaction due to earthquake loading is still a concern, particularly for many tailings dams that are built using the upstream method of construction. The physical characteristics of mine tailings vary significantly, depending on many factors, including ore-type, mill process and deposition method. Generally, tailings may be classified as coarse-grained or fine-grained. Some tailings types can be considered as predominantly coarse-grained in nature (e.g., uranium tailings) or fine-grained (e.g., phosphatic clays). However, there are many tailings types that contain both coarse and fine fractions (e.g., copper, gold). In many tailings facilities, the coarse and fine fractions are often separated to some degree by segregation of the tailings particles after slurry discharge into the storage facility. This can result in coarser sandy tailings deposited close to slurry discharge points and fine tailings deposited in areas further from the discharge points. Some mixing and interlayering of the coarse and fine tailings is also typical, depending on the type of tailings discharge strategy. Some tailings facilities may contain only fine-grained tailings due to mechanical separation

(cycloning) of the coarse and fine fractions, with the coarse fraction typically being used for embankment construction or underground backfill.

The available published information on the cyclic shear response of fine-grained mine tailings is limited. Vick (1983) published a compilation of cyclic resistance ratio (CRR) curves from different mine tailings. A number of studies on silty tailings originating from different mineral extractions report data from conventional characterization and index tests, cyclic shear tests, and undrained monotonic post-cyclic behaviour of undisturbed and reconstituted samples of tailings. Moriwaki et al. (1982) presented results of field and laboratory tests on tailings slimes from copper mines. The study indicated that the tailings slimes exhibit contractive behaviour under static undrained shearing, and the cyclic response of the tailings were examined based on triaxial and direct simple shear (DSS) testing.

Ishihara et al. (1980) examined the cyclic resistance of reconstituted silty tailings of several different minerals, including the influence of the consistency characteristics and plasticity. In a second study, Ishihara et al. (1981) presented the results of cyclic triaxial tests on undisturbed samples of tailings obtained from several tailings dams located in Japan. Other authors (McKee et al. 1978; Poulos et al. 1985) have also presented studies of cyclic strength characteristics of silty tailings. Based on triaxial tests, Peters and Verdugo (2003) have shown that the cyclic shear resistance would decrease with increasing fines content, when comparisons are made at the same void ratio. The conclusions from these published data demonstrate the potentially high susceptibility of tailings to liquefaction, and the need to further understand the fundamental response of tailings to cyclic loading. Figure 2.6 shows a summary of the cyclic resistance ratio versus number of cycles of the mentioned previous works on mine tailings.

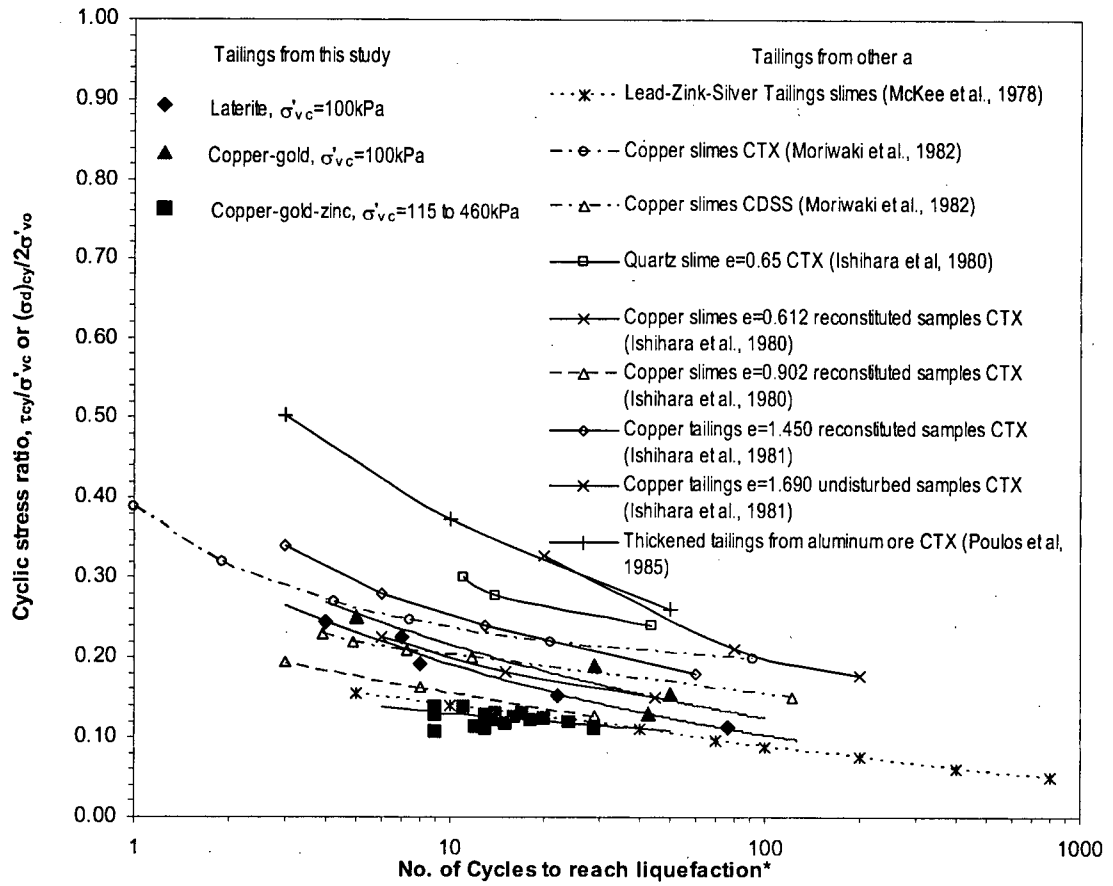


Figure 2.6. Summary of cyclic resistance of different tailings material presented by various authors.

2.4 PROPOSED RESEARCH PROGRAM

It is clear that despite major advances in the knowledge of the shear loading response of sands, our understanding of the mechanical response of fine-grained soils is still very limited. It is also important to note that certain fine-grained soils can be as much susceptible to liquefaction as relatively clean sands, and there is a significant controversy and confusion regarding the liquefaction potential of silts including clayey silts (Youd et al., 2001; Seed et al., 2001).

In recognition of the above, a detailed laboratory element testing research program was undertaken at the University of British Columbia concentrated on the cyclic shear response of “undisturbed” samples of Fraser River Delta silt. The testing was mainly focused on results provided by the NGI type cyclic direct simple shear device (Bjerrum and Landva, 1966), which has been considered more effective in simulating effects of earthquake loading. In order to characterize the monotonic response of this material a limited number of triaxial tests were also conducted.

The experimental procedures and description of apparatus and material tested are presented in Chapter 3 of this study. In recognition of the severe influence that sampling and sample disturbance may have in the results of testing fine-grained materials, an overview of sample disturbance and details related to the development of a soil sample holder intended to minimize the effects of disturbance during and after sample extrusion are also part of Chapter 3. Chapter 4 presents the experimental results from the main testing program and discussion of the relevant findings. In particular laboratory observations made on the following aspects of the mechanical response are presented and discussed: (i) monotonic loading response, (ii) cyclic

loading response (iii) effects of overconsolidation, and (iv) effects of repeated cyclic loading. Effects of static shear stress were not included in the scope of this study. As part of the investigation of the cyclic loading response of silts, it was considered appropriate to evaluate already available data from a series of cyclic DSS tests, conducted as a part of geotechnical studies at three mine sites, to further understand the seismic response of fine-grained tailings. This work is summarized in Chapter No. 5. While enhancing the current publicly available knowledge, the evaluation also provides insight into the cyclic resistance ratio with respect to liquefaction triggering and post-cyclic shear strength for tailings of different mineralogy. The applicability of the commonly used empirical approaches for the assessment of liquefaction susceptibility of silty tailings is also examined. The cyclic shear resistance values reported by others are also compiled as a part of the effort. Finally, summary and conclusion derived from this investigation are presented in Chapter 6.

3 EXPERIMENTAL ASPECTS

This chapter presents the experimental aspects related to the present study. Several important considerations including field sampling and laboratory specimen preparation procedures and the selection of a test device, are carefully addressed with respect to understanding the cyclic loading response of Fraser River Delta silt. Initially, a description of the test material is provided along with the field sampling techniques adopted. A description of the UBC direct simple shear (DSS) apparatus that includes the loading system, instrumentation, and data acquisition system is then presented. Disturbance during sample extrusion and setup is a major consideration particularly with respect to the preparation of triaxial specimens of silt. In recognition of this, a new sample holder concept that had been developed to minimize specimen-disturbance was implemented as part of the research presented herein. The work included finalization of the design concept, fabrication of the device, and proof testing prior to its use in the preparation of specimens for triaxial testing. Only a limited number of triaxial tests were conducted within the scope of the present program; however, the implementation of the use of this device was still considered essential in minimizing disturbance during specimen preparation in the testing herein as well as in future planned research works conducted on silts at UBC. Finally, the experimental program is outlined.

3.1 MATERIAL TESTED

The mechanical response of soils is dependant on a multitude of factors including particle fabric, microstructure, density, and age. As pointed out by Lerouil and Hight (2003), testing of undisturbed samples of soils is critically important in representing soil conditions in-situ, and, in turn, in understanding the field response of natural soils. Significant differences in the response of soils have been observed between undisturbed and reconstituted samples of sands (Vaid et al. 1999) and silt and sandy silt (Høeg et al., 2000). These differences are mainly attributed to the differences in fabric between the undisturbed and reconstituted specimens.

A channel-fill silt obtained from the Fraser River Delta of British Columbia, Canada, was selected for the investigation of the cyclic response of silts. The choice of silt from this area is considered relevant since it is located in one of the most seismically active regions in Canada (NBCC, 1995) and the area is experiencing rapid urban and industrial growth. The general ground surface elevation in the area is below the high-tide level; as such, the area is now protected by dikes. In addition, deltaic silts are compressible and susceptible to settlements under building loads (Crawford ad Morrison, 1996).

Deposits of the delta are Holocene in age and have a maximum known thickness of 305 m (Clague et al., 1996). The deltaic deposits can be subdivided into topset, foreset and bottomset units (Monahan et al., 1997), and the upper part of the topset comprises flood-plain silts and peat (Monahan et al., 2000).

The subject site is located in immediately north of the South Arm of the Fraser River, at the southern foot of No. 3 Road in Richmond, B.C. A channel-fill silt deposit is underlain by about 3.5 m thickness of dyke-fill materials at the site. Available data from in situ cone penetration

testing, CPT (see Figure 3.1), suggested that the upper part of this channel fill silt between depths of 5.6 m and 9.3 m below the ground surface is relatively uniform, and, therefore, this deposit was considered suitable as the source of test material for the present study.

A fixed-piston tube sampling conducted in a conventional mud-rotary drill hole was used to obtain a number of undisturbed samples from the silt deposit. A specially fabricated ~75-mm diameter, 0.9-m long tubes (with no inside clearance, a 5-degree cutting edge, and 1.5 mm wall thickness) were used for this purpose. As noted by Leroueil and Hight (2003), piston sampling using thin, sharp-edged tubes offers a suitable and acceptable means of obtaining relatively undisturbed samples of fine-grained soils. Figure 3.2 show the gradation curves for several samples obtained from the silt deposit. As may be noted, the generally homogeneous samples have an average clay content of 10% and sand content of 13%. Parameters obtained from index tests at different depths are presented in Table 3.1. These observations also confirm the uniformity of the deposit previously noted based on field cone penetration test data.

Table 3.1. Index parameters of Fraser River delta silt

Depth (m)	w_c [*] (%)	Sand (%)	Silt (%)	Clay (%)	LL (%)	PL (%)	PI (%)
5.4 - 5.5		13.1	75.9	11	30	25	5
5.6 - 6.2	37.14	9.8	81.5	8.7	30.5	27.3	3.2
6.2 - 6.8	37.60						
6.8 - 7.4	38.68						
7.7 - 7.8		8.9	81.7	9.4	30	27	3
7.9 - 8.0		5.5	84.6	9.9	31	26	5
8.7 - 9.3	40.82	10	80	10	39.2	36.3	2.9
Specific Gravity, G_s		2.69					

* Average natural water content from several samples of the depth shown

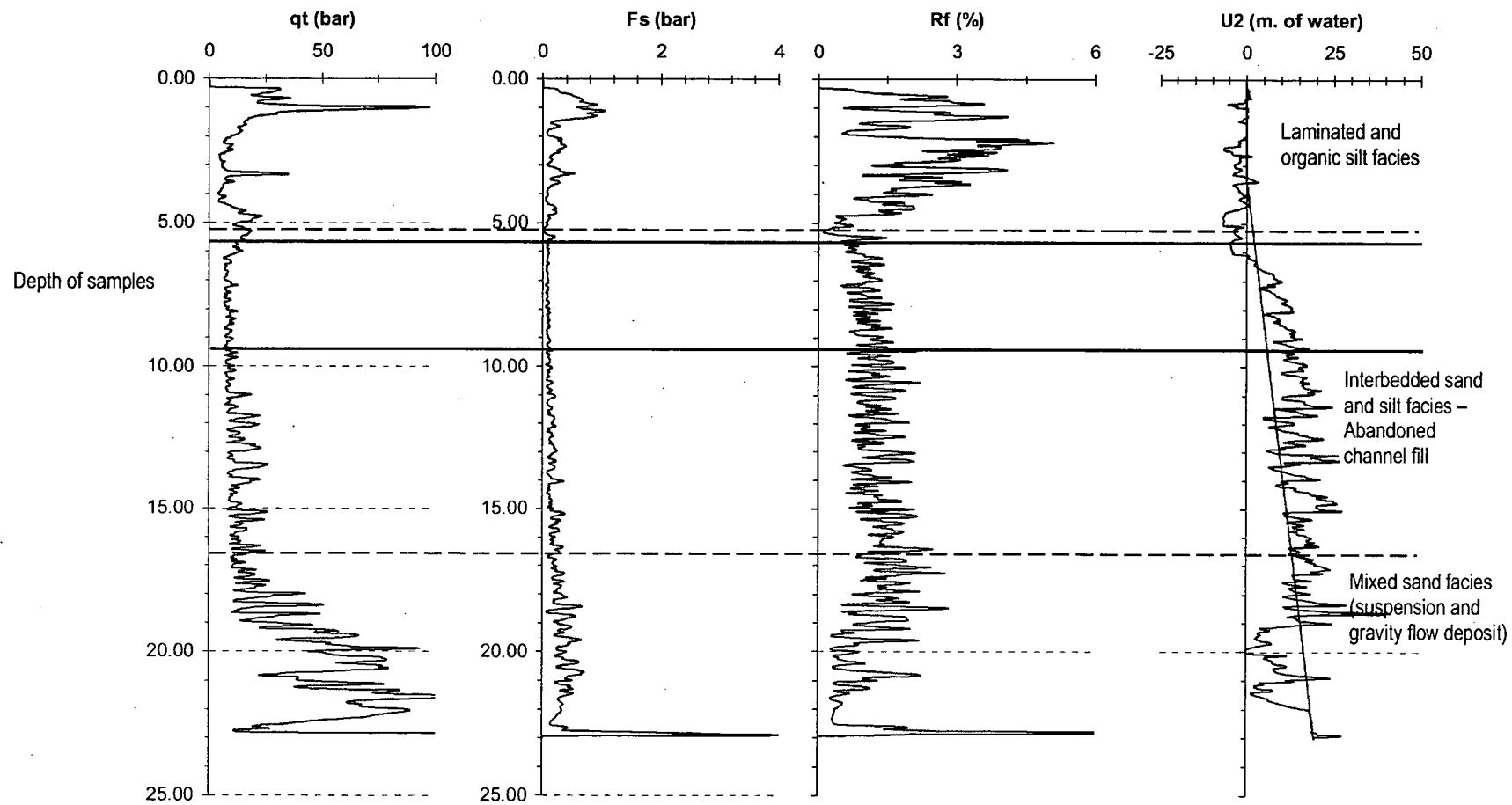


Figure 3.1. Cone penetration test profile of the site

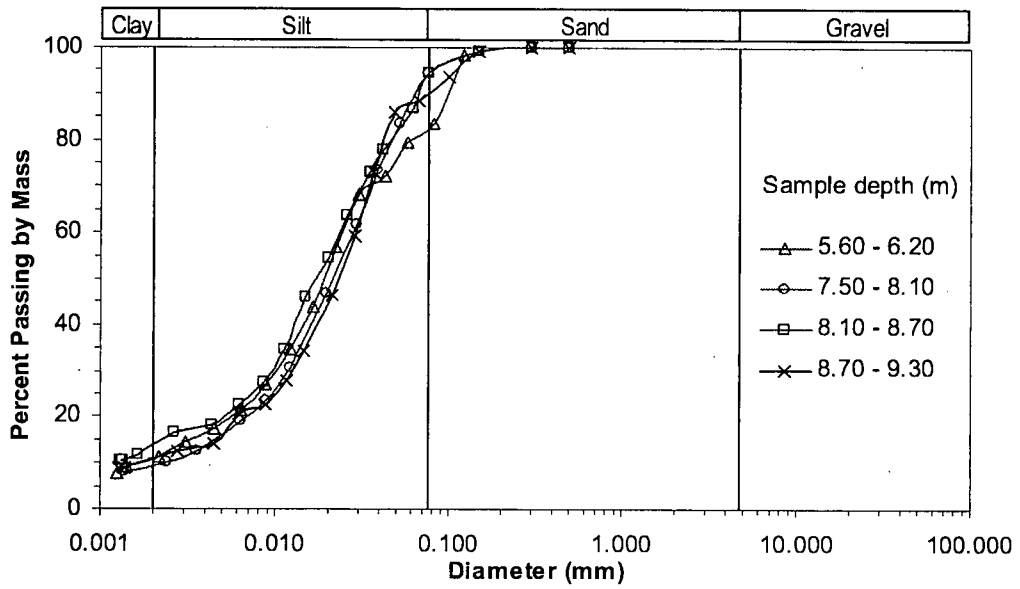


Figure 3.2. Grain size analysis of different samples of Fraser River silt

3.2 DIRECT SIMPLE SHEAR (DSS) TESTING

3.2.1 UBC Direct Simple Shear Test Device

Cyclic triaxial (CTX) and cyclic direct simple shear (CDSS) tests have been used by many researchers for the study of cyclic shear response of soils. While the CTX has been widely used because of its simplicity and common availability, the CDSS loading is considered to effectively mimic the anticipated stress conditions under seismic loading (Finn et al., 1978). This can be more readily explained with respect to Figure 3.3, where typical field stress conditions under seismic loading, and Figure 3.4 where the difference between the CTX and CDSS loading modes, are presented. In addition, the UBC DSS apparatus allows for constant volume tests, which avoids the errors associated to compliance and make the testing procedure simpler and eliminates the saturation requirements (Finn and Vaid, 1977; Finn et al., 1978). Considering the above, the cyclic direct simple shear apparatus at the University of British Columbia (UBC) was selected for the characterization of the cyclic loading response of Fraser River Delta silt.

The UBC simple shear apparatus is of the NGI type (Bjerrum and Landva, 1966). A schematic diagram of the apparatus is given in Figure 3.5. The cylindrical soil specimen, 70 mm in nominal diameter and approximately 20 mm height, is placed in a reinforced rubber membrane. The reinforced rubber membrane would constrain the specimen from deforming laterally; as such, the soil specimen would be in a state of zero lateral strain during consolidation and cyclic loading, which is considered to simulate the anticipated field stress conditions. Simple shear

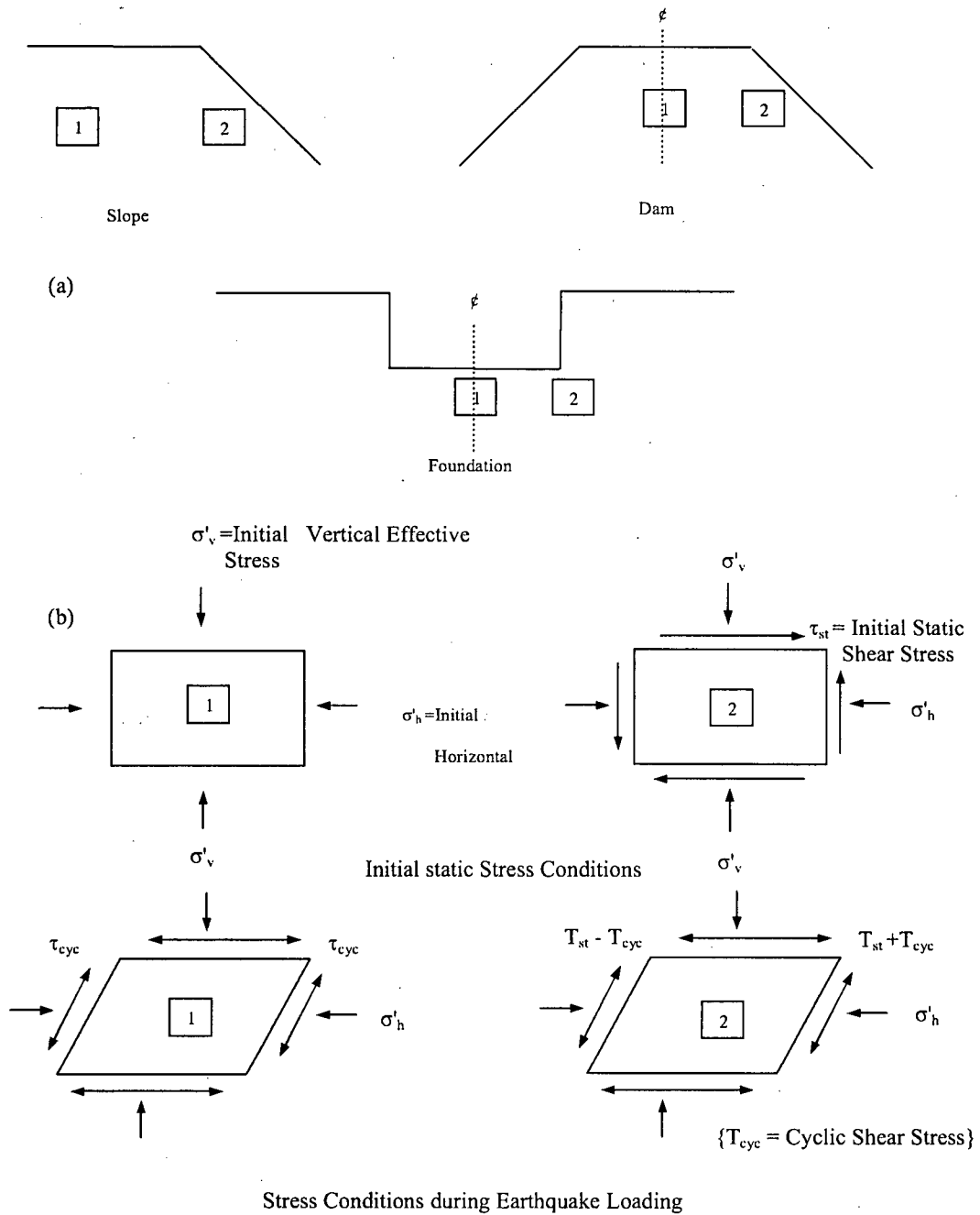


Figure 3.3. Stress conditions under seismic loading (a) Field and laboratory model cases and (b) stress conditions for an element of soil.

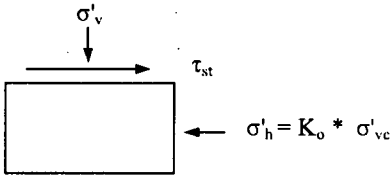
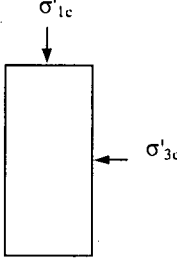
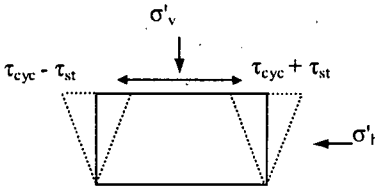
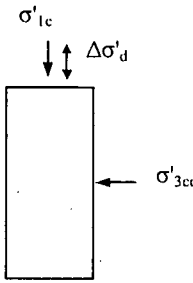
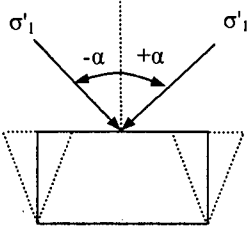
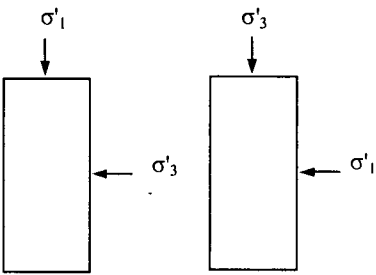
(a) DSS	(b) CTX	Stress status
		Initial (static) condition
		Cyclic loading condition
		Principal stress direction during cyclic loading

Figure 3.4. Comparison of stress conditions in (a) Simple Shear testing – DSS and (b) Triaxial testing – CTX (After Sriskandakumer, 2004).

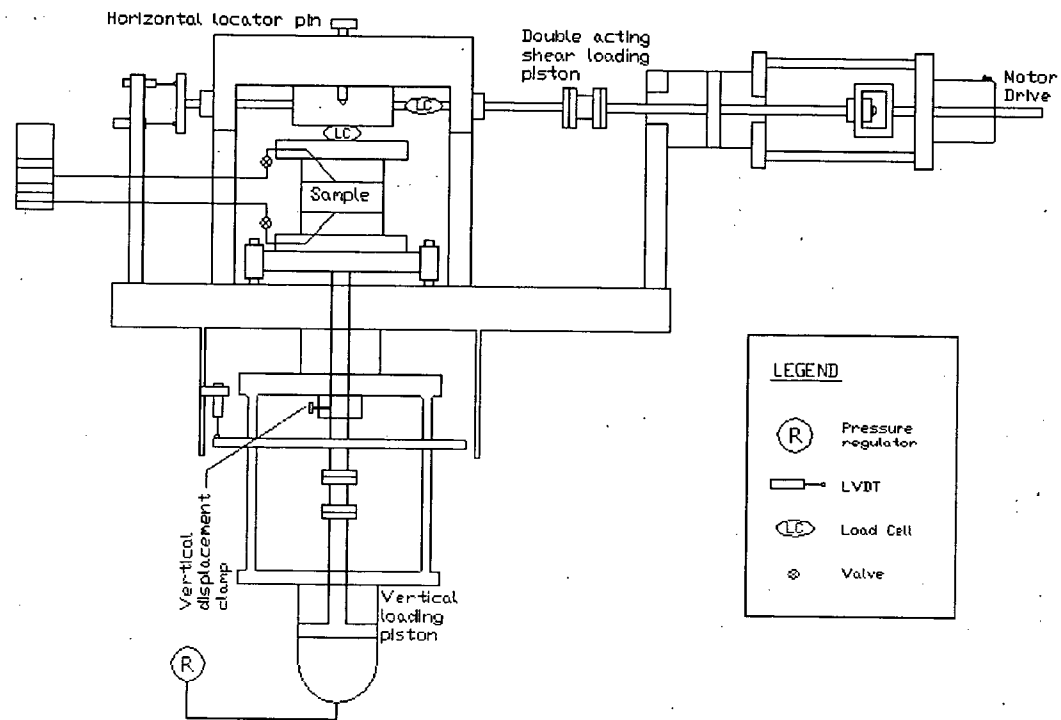


Figure 3.5. Schematic diagram of UBC simple shear test device (Modified from Sriskandakumar, 2004)

tests can be performed in undrained, or constant volume condition. The latter constant volume DSS test is an alternative to the former where all drainage in a saturated sample would be suspended. In a constant volume test, the specimen diameter is constrained by the reinforced membrane, and any vertical deformation is restricted by clamping the top and bottom loading caps against vertical movement. It has been shown that the decrease (or increase) of vertical stress in a constant volume DSS test is essentially equivalent to the increase (or decrease) of excess pore water pressures in an undrained test (Finn et al., 1978; Dyvik et al., 1987) where the near constant volume condition is sustained by keeping the mass of water unchanged. As such, the direct measurement of the vertical stress in a constant volume DSS test corresponds to the equivalent excess pore water pressure change.

3.2.2 DSS Loading System

The UBC-DSS apparatus consists of horizontal and vertical loading systems as shown in Figure 3.5. The vertical loading system, located at the bottom of the apparatus, consists of a simple single-active air piston controlled manually by an external pressure regulator. Horizontal load is applied by a double-acting frictionless air piston coupled in series with a constant speed motor drive. This horizontal loading system allows a smooth transition from stress-controlled to strain-controlled loading and vice versa, as required.

Stress-controlled cyclic loading is applied by changing the pressure on one side of the double acting piston with an electro-pneumatic regulator and maintaining the pressure on the other side constant. The electro-pneumatic regulator enables applying any prescribed form of cyclic loading by the coupling with a data acquisition system and computer. A sinusoidal wave form

is generally chosen for the cyclic loading, and the magnitude and duration of the wave can be changed during the test if required.

In strain-controlled monotonic or cyclic loading, since the loading arm is coupled to a constant speed motor, the direction and speed can be changed manually as required.

3.2.3 Data Acquisition, Control System and Measurement Resolution

The UBC DSS apparatus is equipped with a high speed data acquisition and control system. A 12-bit "PCL718" high speed data acquisition card is used for signal input and output. This card consists of five A/D input channels and a D/A output channel.

Two load cells and three linear variable displacement transducers (LVDTs) are monitored by the input channels. One of the load cells is dedicated to measure the vertical load, and the second one is for the horizontal load. One LVDT measures the vertical displacement and the other two are assigned to monitor the horizontal displacements. The use of two LVDTs allows measuring both small and large displacements. All transducers are excited with a 5V d.c voltage supply. Input signals from load cells are amplified by a factor of 1000. The measurements are further refined by averaging 60 readings for each data channel. The high speed data acquisition system is able to gather about 500 sets of data per second.

The D/A channel is used to control the electro-pneumatic transducer that regulates the air pressure to one of the chambers of the horizontal loading double acting air piston. The electro-pneumatic transducer is "SMC IT2051-N33" type, and it is capable of delivering 90 kPa full scale pressure output for a 1000 kPa input pressure. A high resolution of measurements is

obtained by the above carefully selected measurement devices (transducers) and a sophisticated data acquisition system. Shaft friction on the horizontal loading ram, stiffness of reinforced membrane, and spring forces arising from the LVDTs are also accounted for in the data reduction program.

Table 3.2 presents the resolution of each measurement for a typical 70 mm diameter and 20 mm height sample.

Table 3.2. Measurement resolution of UBC-DSS device

Measurement		Resolution
Vertical/Normal stress		± 0.25 kPa
Horizontal/Shear stress		± 0.25 kPa
Horizontal/Shear strain	Small range (<13%)	± 0.01 %
	Large range (>13%)	± 0.05 %
Vertical strain		± 0.01 %

3.2.4 DSS Test Procedure

3.2.4.1 Specimen Extrusion and Setup

The DSS test device was setup in advance to prepare for receiving the silt specimen upon completion of extrusion and trimming. A saturated porous stone was initially placed in the bottom pedestal of the DSS device. The reinforced rubber membrane was placed in position and the bottom of the membrane was sealed with the bottom pedestal using an o-ring (see

Figure 3.5). The split mould was then kept in position and vacuum was subsequently applied to stretch the membrane and create a cavity in the DSS device to receive the specimen.

Specimens for DSS testing were carefully extruded from the tube samples retrieved from the field (as per Section **Error! Reference source not found.**). For a given specimen, silt material of approximately 40 mm in thickness was extruded from the sampling tube. A stainless steel ring with a sharp cutting-edge and essentially having a diameter minutely smaller than the tube sample was gently pushed into the extruded specimen. The sharp edge of the stainless steel ring, while “trimming” the specimen to a 70-mm size, allowed securing silt material against disturbance during the next steps in sample setup. The specimen secured as per above, was then trimmed at the top and bottom using a wire saw to obtain a specimen height of approximately 20 mm. Trimmings obtained from the top, bottom and sides were collected for water content measurements.

Upon completion of the above process, the stainless steel ring that contains the specimen was placed over the cavity of the DSS device and then set into the cavity by applying a slight uniform pressure with a plastic plunger. Once the sample was in position in the DSS device, the top cap was placed and a pressure of ~10kPa was applied using the vertical loading system. The rubber membrane was sealed with the top cap using an o-ring.

All the transducers were properly positioned and initial outputs are set to zero values prior to commencement of testing. The split mould was removed while all transducer readings were monitored to assess that no undesirable movements or loads were imparted during this process.

3.2.4.2 Consolidation Phase

After completion of specimen setup, the vertical confining stress was increased to the target value corresponding to the test to be performed. The change in height of the specimen (equivalent to the volume change) with respect to the elapsed time was recorded using the data acquisition system. The samples were kept at the stress condition for 10,000 seconds. This time duration was adequate to obtain essentially unchanging vertical deformation of the specimen (i.e., adequate time allowed for completion of primary consolidation of Fraser River silt specimen).

The specimens that required overconsolidation prior to cyclic shearing were initially consolidated to a target stress level as per above, and then unloaded to another target stress level to achieve the desired overconsolidation effect. The specimens were kept under this final stress level for 30 minutes. It was noted that the Fraser River silt specimens experienced a moderate amount of swelling, (i.e., $\epsilon_v < 0.4\%$), with the deformations occurring almost instantaneously.

3.2.4.3 Shear Loading Phase

After completion of the consolidation phase, the specimen was constrained against vertical strains by clamping the vertical loading ram (see Figure 3.5). This ensured constant volume conditions during cyclic loading. The horizontal shear loading was applied either using double acting piston or a constant speed motor depending on whether the test was stress-controlled or strain-controlled, respectively. For cyclic stress-controlled tests, the shear load was applied in the form of a sinusoidal wave with a frequency of 0.1 Hz at the desired amplitude. Despite

frequency is greater than most of the frequencies encountered in typical earthquake loading, it allows a better control of loading as well as data acquisition. Zergoun and Vaid (1994) noted that the behaviour of clay in undrained cyclic triaxial shear loading cannot be confidently interpreted in fast loading tests because of unreliable measured pore water pressures (due to inadequate time for pore water pressure equalization in fast tests). In the DSS tests performed for this study, the constant volume condition is achieved by controlling the external boundaries, and pore water does not participate in volume control. Hence, there is no need for measurement of pore water pressure as the vertical effective stress on the sample at any given time is directly obtained from the measured load at the vertical stress boundary. With this consideration together with the need to obtain accurate control of applied stresses, the chosen loading frequency of 0.1 Hz is determined suitable, and this approach has been in use for constant volume cyclic DSS testing of silty and sandy soils at UBC over the last 20 years.

In monotonic strain-controlled loading, the tests were performed at a rate of 10% strain per hour. In cyclic tests, loading was conducted until a shear strain of approximately 15% was reached. Monotonic shear tests were terminated after reaching shear strains of approximately 20%.

3.2.4.4 Post-cyclic Reconsolidation and Repeated Cyclic Loading

Most tests were carried out to study the effects of repeated cyclic loading. After completion of the first constant volume cyclic loading stage as per above, specimens were re-consolidated to the initial confining stresses to assess potential post-cyclic volumetric deformations. Since the specimens generally had a residual shear strain at the end of cyclic loading, the specimen top

cap position was manually reset to reach an approximate shear strain of zero prior to reconsolidation.

Upon completion of the reconsolidation, the specimens were subject to a second cyclic phase with the applied loading parameters identical to those used for the first cyclic loading (i.e., same applied cyclic stress ratio final cyclic shear strain levels of approximately 15%). After completion of the second cyclic loading the specimens were reconsolidated to the original consolidation pressures and the resulting strains were, again, monitored.

3.3 TRIAXIAL TESTING

A limited number of conventional triaxial shear tests were performed in order to characterize the monotonic stress-strain response of the Fraser River Delta silt. The tests were conducted using the stress-path triaxial testing apparatus at UBC. Since the device has been in extensive use, and detailed description of the mechanical and testing aspects are given in Gananathan (2002), they are not repeated herein.

The specimens for triaxial testing were obtained directly from the undisturbed tube samples (see Section **Error! Reference source not found.** for details on field sampling). The silt specimens were secured against disturbance after extrusion and during setup using a new specimen holder, and these details are presented in Section 3.5.

Triaxial specimens were 72 mm in diameter (identical to the size of the tube sample) and ~150 mm long. The specimens were placed on smooth, hard anodized aluminium end plates of the test device with centrally located 44-mm diameter porous discs. Axial load, confining

pressure, pore pressure, and volume change are measured using electronic transducers coupled into a data acquisition system interfaced with a computer. All the tests were performed under strain-controlled conditions. Table 3.3 presents the resolution of measurements during testing for a typical triaxial specimen.

Table 3.3. Measurement resolution of triaxial device

Measurement	Resolution
Vertical stress	± 0.03 kPa
Cell pressure and pore pressure	± 0.1 kPa
Axial strain	$\pm 0.001\%$
Volumetric strain	$\pm 0.001\%$

3.4 OTHER TESTING

3.4.1 Consolidation Tests

Several one-dimensional consolidation tests were performed in order to investigate the compressibility characteristics of the silt. A conventional incremental consolidation tests was performed using a conventional oedometer and another using the UBC-DSS apparatus. In addition, a constant rate of strain consolidation test was also performed as described in Wissa et al. (1971). The applied load, vertical strain, and pore pressure were monitored during the consolidation process, as appropriate.

3.4.2 Index Tests

In order to obtain basic index properties, a number of Atterberg limits, grain size analysis and specific gravity of solids tests were performed in accordance to the ASTM standards ASTM D-4318-00, ASTM D-422-63 and ASTM D-854-02 respectively.

3.5 UNDISTURBED SOIL SPECIMEN HOLDER FOR PREPARATION OF TRIAXIAL SPECIMENS¹

Natural soils are generally micro-structured, heterogeneous, anisotropic, and their mechanical response is inelastic, non-linear, time-dependent, and complex. A thorough understanding of the mechanical response of soils under field loading conditions is of critical importance in the design and construction of geotechnical engineering works, and data acquired from geotechnical laboratory testing of element soil samples obtained from the field plays a major role in developing this understanding. This need for data from laboratory element tests simulating anticipated field-loading conditions has been well accepted since the introduction of the Stress Path Method by Lambe (1967).

While laboratory testing allows the determination of mechanical response based on the measurements made on a sample of soil subjected to a given loading, it is known that

¹ A version of this section has been submitted for publication as an article to the Geotechnical Testing Journal. Wijewickreme, D. and Sanin, M. V. New sample holder for the preparation of undisturbed fine-grained soil specimens for laboratory element testing. Geotechnical Testing Journal. ASTM; Paper No. GTJ12699, 2005 (subject to revisions).

disturbance to a sample from the time of field sampling to the point of testing in a laboratory device can have a profound effect on the parameters derived from laboratory testing. As Hight and Leroueil (2003) and Ladd and DeGroot (2003) have highlighted in their recent state-of-the-art papers, changes to the particle structure and in situ stress state are the key elements of sample disturbance. Since the mechanical performance of soils is intimately governed by its particle structure and stress state, it is imperative that any disturbance of the soil during field sampling as well as during laboratory testing is minimized. A stress path diagram hypothetically expressing the potential changes in the stress state during field sampling and laboratory specimen preparation for a lightly overconsolidated clay (based on the past work by Ladd and Lambe, 1963; and Baligh et al., 1987) extracted from Ladd and DeGroot (2003) is reproduced in Figure 3.6. Conceptually, several physical steps (i.e. stress state Points No. 1 through 8, Figure 3.6) where sample disturbance could take place have been identified. The movement of stress state from Points No. 1 through 7 corresponds to activities that take place during field sampling, transportation and storage. The activities of sample extrusion and final preparation have been suggested to result in further changes to the stress state from Points No. 7 through 9. Hight et al. (1992) also presents a detailed assessment of sample disturbance prior to testing based on extensive research work on Bothkennar clay. These works clearly highlight the strong need to pay attention to all the steps associated with bringing a sample from the field to laboratory to minimize potential sample disturbance and achieve high quality samples that have experienced minimal deviation from the original in situ condition.

In spite of extensive evaluation of the sources of sample disturbance, another consideration that has received very little attention is the disturbance due to potential deformations that take place in relatively soft samples after extrusion. Immediately after extrusion, and prior to placement,

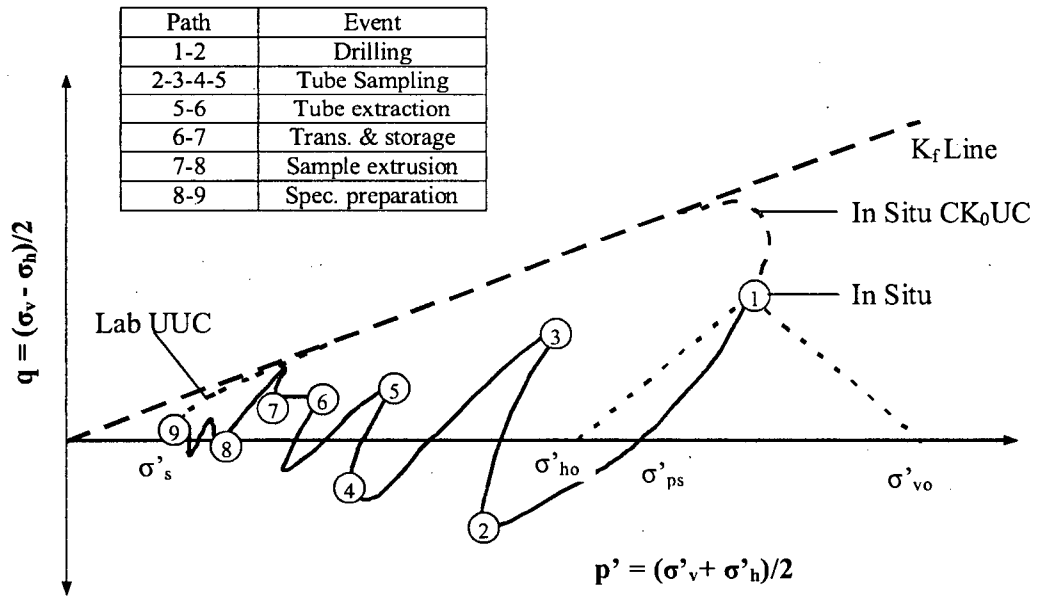


Figure 3.6. Hypothetical stress path during tube sampling and specimen preparation of fine-grained soils for laboratory element testing (After Ladd and DeGroot 2003)

and securing on a given test device (e.g. triaxial), the extruded field samples typically require to be held in an upright freestanding position to facilitate sample assembly. This freestanding time is variable, and a time range from 5 to 15 minutes is not unusual. During this freestanding period, some soils (e.g. relatively soft fine-grained silts) might experience significant deformations merely due to its self-weight, and, as a result, suffer unacceptable levels of sample disturbance. Figure 3.7 presents photographs that were taken during the extrusion of 76-mm (3 in.) diameter tube samples of relatively soft silty soils to illustrate this aspect. As may be noted, the development of undesirable sample disturbance in the form of vertical and lateral strains (i.e. shortening and bulging, Figure 3.7a) and/or tilting (Figure 3.7b) can take place during the freestanding period over a relatively short period of time (less than 2 to 5 minutes), and this is unavoidable in the case of most soft soils.

Based on the available information, at present, there is no accepted procedure to minimize the freestanding period and potential disturbance during sample preparation. In recognition of this, a new undisturbed soil sample holder (USSH) was developed for the preparation of soft-soil samples for geotechnical laboratory element testing (Wijewickreme and Sanin, 2005). Herein, the main features of the sample holder with detailed procedures for sample preparation are described. The effectiveness of the new sample holder in minimizing sample disturbance is demonstrated by comparing experimental observations between samples that were prepared “with” and “without” the use of the USSH.

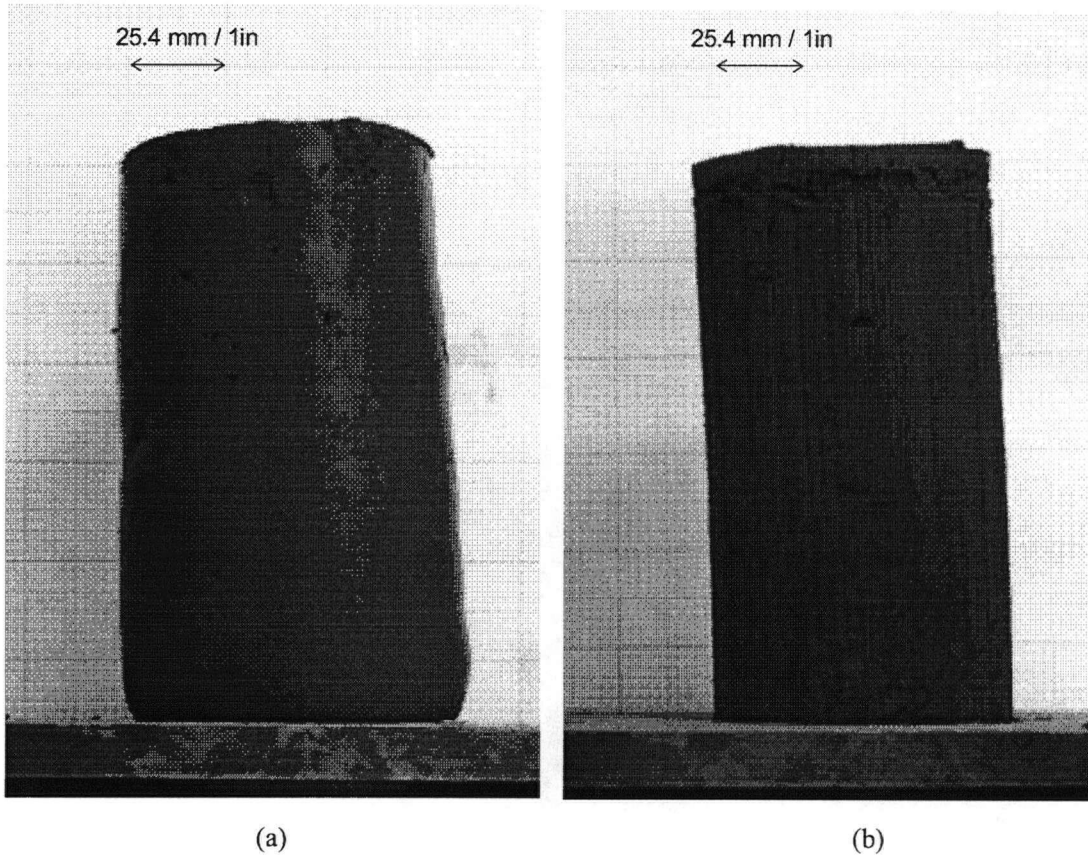
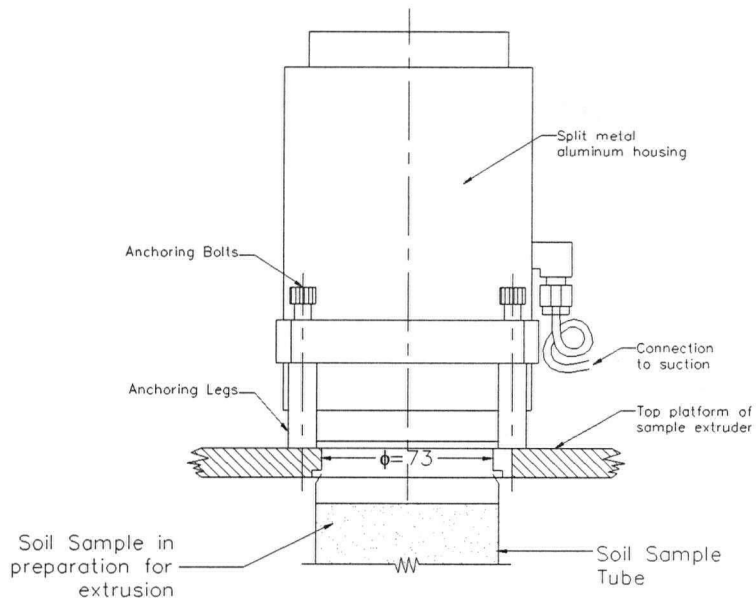


Figure 3.7. Typical mechanisms of sample disturbance in soft fine-grained soils due to self-weight during the free-standing period. (a) vertical deformation and lateral bulging; (b) tilting. [Samples extruded from a 76-mm diameter sample tube]

3.5.1 Description of the Undisturbed Soil Sample Holder

Elimination of potential deformations due to self-weight is the key to minimizing the disturbance of a relatively soft fine-grained cylindrical soil sample during the freestanding period. This would require providing a suitable external lateral confinement to a sample immediately upon extrusion. In this regard, it is important to ensure that the applied lateral confinement uniform over the cylindrical surface of the sample to avoid any potential “ovalization” effects. The new undisturbed soil sample holder (USSH) by Wijewickreme and Sanin (2005) was developed with these considerations in mind. The USSH comprises: (a) a metal (aluminum) housing, with a cylindrical cavity, that could be split in two for assembly/disassembly (see Figures 3.8 and 3.9); (b) a synthetic flexible foam material of uniform thickness lining the recessed zone in the housing (see Figure 3.10); (c) a thin cylindrical rubber membrane that is stretched over the inner cylindrical cavity and held by two o-rings (the “as-stretched” membrane conforms to the inner cavity defined by the foam material and it would also jacket the sample during subsequent mechanical testing in a shear test device); and (d) ports to apply a regulated vacuum to control the air pressure in the recessed zone where the foam material is secured. The dimensions of the key elements are also indicated in Figure 3.9 and 3.10. The present USSH was developed specifically for the confinement of samples extruded from a standard 76-mm nominal diameter tube samples and for vertical extrusion systems; however, it is noted that concept is equally applicable for samples of other diameters.

(a)



(b)

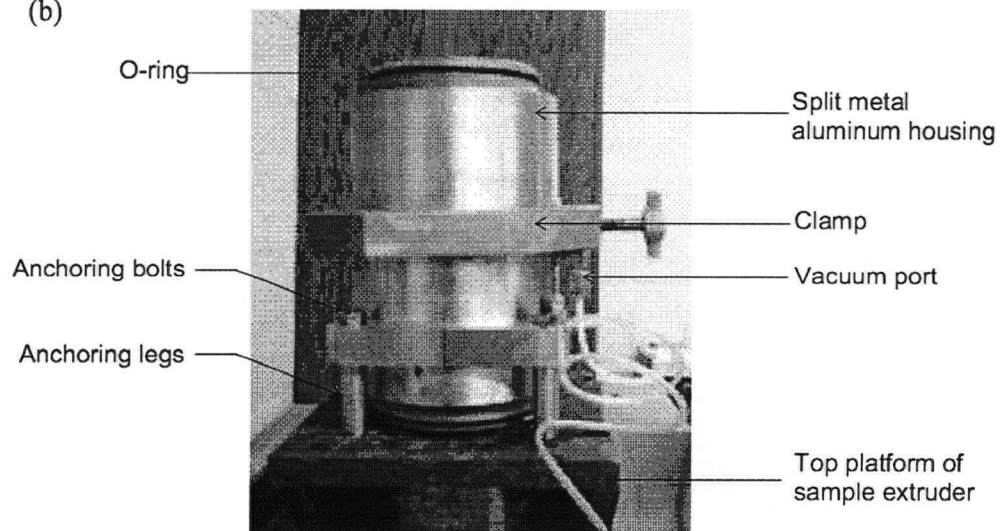
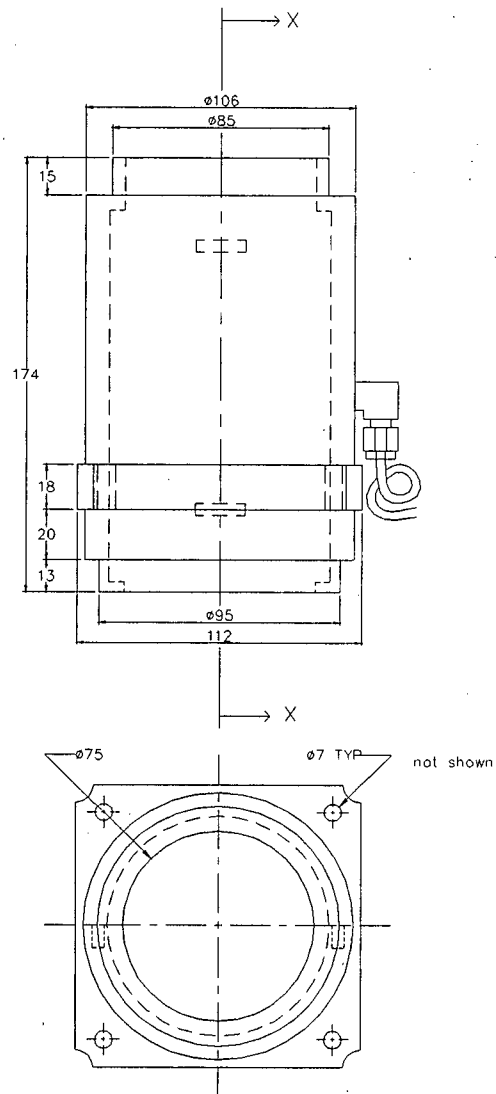
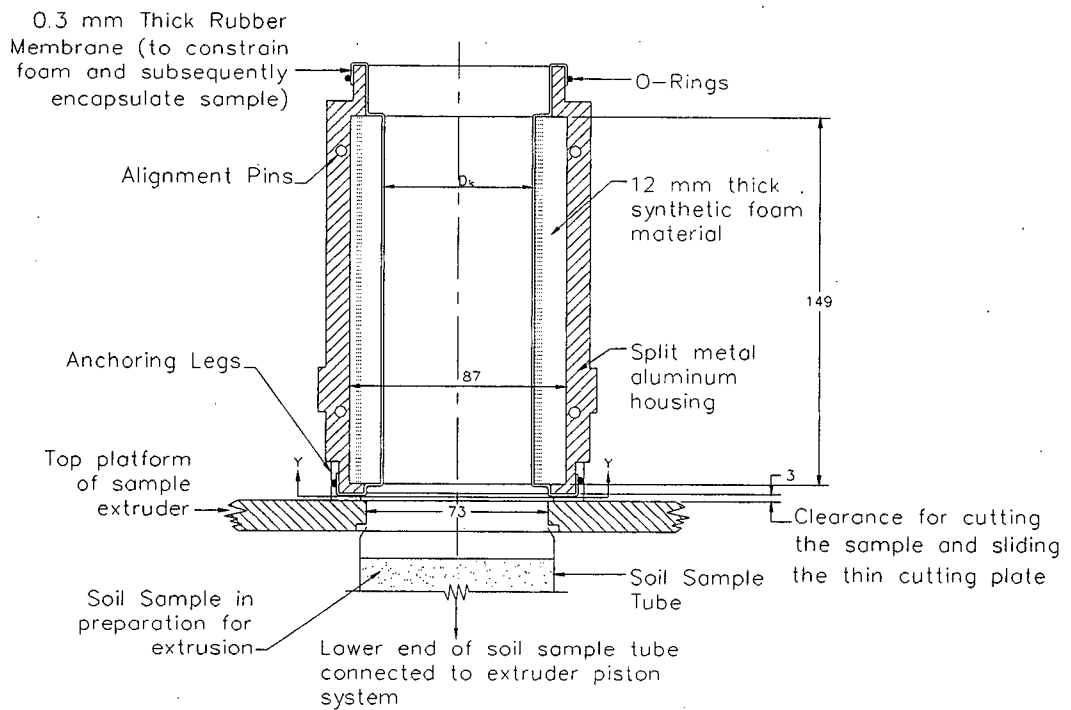


Figure 3.8. The Undisturbed Soil Sample Holder (USSH) - Assembly for tube sample extrusion.



Note: Membrane, o-ring and foam not shown.
 Some hidden details may not appear.
 Scale: as shown

Figure 3.9. The Undisturbed Soil Sample Holder (USSH) - Side view and dimensions. (see 3.10 for Section X-X details).



Note: $62.4 \text{ mm} < D < 75 \text{ mm}$ when vacuum is applied;
 $D = 62.4 \text{ mm}$ under no vacuum

Figure 3.10. The Undisturbed Soil Sample Holder (USSH) - Section X-X (see Figure 3.9 for location of section X-X).

One of the key and unique features of the USSH is that it provides a variable-diameter cylindrical cavity that has the ability to: (i) adjust to a diameter that is slightly larger than the diameter of the soil sample at the time of receiving a sample that is being extruded from a tube; (ii) expand to match the diameter of the soil sample and provide a lateral confinement immediate upon the completion of sample extrusion (see Figure 3.10).

3.5.1.1 Principle of Operation of the USSH

When a known regulated negative pressure of $-p$ kPa (with respect to atmospheric pressure) is applied through the vacuum application port (see Figures 3.8 and 3.9), the resulting differential air pressure across the rubber membrane would exert a uniform pressure (p kPa) on the foam layer in the recessed zone. The foam material would compress under this pressure p and, in turn, increase the internal diameter of the cylindrical cavity of the device (D_{ic}). Since the foam material is of constant thickness, the geometric shape of the cavity would remain essentially cylindrical under a given applied value of p . A calibration for these diametrical changes was obtained by subjecting the foam material to load/unload cycles where the value of p was varied between 0 and 30 kPa. In this exercise, for given change in p , the corresponding change in D_{ic} was calculated by measuring the change in mass of water required to fill the inner of cavity. The variation of applied vacuum (p) vs D_{ic} derived from this process is presented in Figure 3.11.

As may be noted, “virgin” foam material exhibited a somewhat stiff response during initial pressure application (see curve titled 1st (virgin) loading in Figure 3.11). However, after about three pressure cycles, the foam material seemed to have been “broken in”, and the p vs D_{ic}

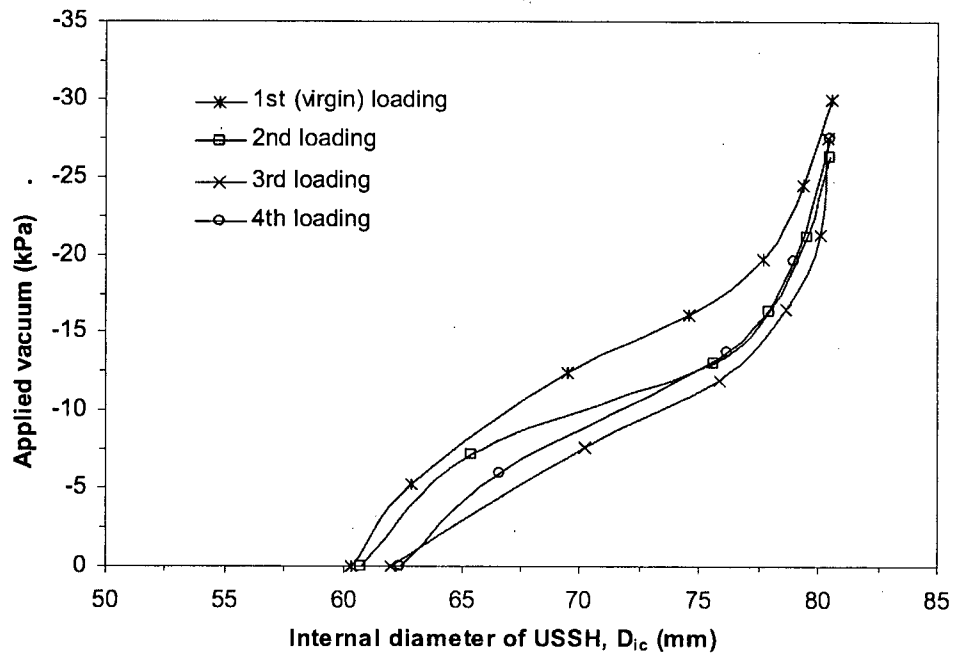


Figure 3.11. Variation of internal diameter of the USSH in response to applied vacuum (p) through suction port.

response basically remained unchanged under further cyclic loading (see curves titled 2nd, 3rd and 4th loading in Figure 3.11). Figure 3.11 also shows that when $|p| = 0$, D_{ic} is about 62.5 mm; a value of $|p| \approx 12$ kPa is required to bring D_{ic} to 72 mm, at which point the internal diameter of the cavity is essentially the size of the extruded tube sample considered herein.

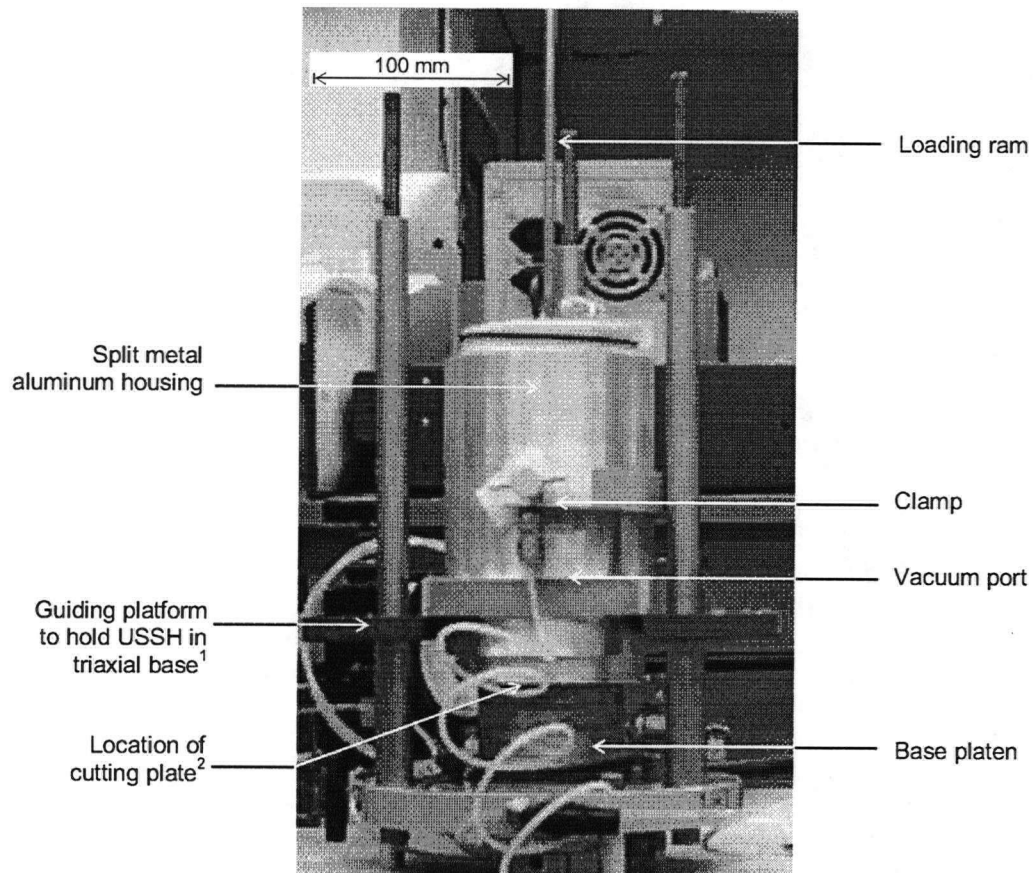
3.5.1.2 Basic Steps in Sample Preparation

The basic steps to be carried out in the use of the USSH in the preparation of a soil sample for testing are described below. It is noted that, except for those required for clarity, well-established steps commonly used in the preparation of cylindrical soil specimens are not repeated herein:

1. Mount the field tube sample on the sample extruder; after extruding and removing the potentially disturbed end zone, extrude and cut another small (e.g. ~1 cm) slice of soil using a wire saw (immediately above the soil specimen to be tested) to obtain a sample for determination of moisture content;
2. Mount the USSH on the top platform of the sample extruder that already has the tube sample readied for extrusion as per above. The USSH has been fabricated so that, when mounted on the top platform, the centerline of the USSH is in alignment with the centerline of the sample tube (see Figure 3.8);
3. Apply a sufficient level of vacuum to the recessed zone of the USSH so that the foam material would compress to result in a cylindrical cavity having an inner diameter, D_{ic} ,

that is slightly larger than the actual sample size of 72 mm (e.g. apply p slightly > 12 kPa);

4. Extrude the soil sample from the tube into the cylindrical cavity of the USSH;
5. Once the desired sample length has been extruded into the sample holder, adjust the vacuum to give rise to a cavity having a diameter of about 72 mm, which also would match with the sample diameter (see Figure 3.11 for p vs D_{ic} relationship). At this point, the specimen is laterally confined by the foam material. (Note: If the soil is very soft, a lower vacuum level may be considered; for example, if no vacuum is applied, the foam material will exert a lateral confining pressure of about 12 kPa on a 72 mm sample).
6. Make a cut on the extruded soil along line Y-Y (at the base of the USSH, see Figure 3.10) using a thin wire, and then slide a thin cutting plate to separate the pre-cut specimen from the remaining tube sample below. At this point, in addition to the lateral confinement by the foam material, the specimen is vertically supported by the thin smooth cutting plate; it is ready for removal from the extrusion platform.
7. Remove the bolts connecting to the top platform of the extruder, and lift off the USSH (with the specimen confined in the cavity by the foam material laterally and held by the thin cutting plate from the bottom) for transferring to the test device.
8. Secure the USSH on the triaxial test device (or any similar test device that is designated for testing the cylindrical sample), using a guiding platform as shown in Figure 3.12. The guiding platform (which essentially is a U-shaped plate of 12-mm thickness) and



- ¹ Guide-pins to align the sample with the base platen of the testing device are located in the back of the guiding platform (cannot be seen in the picture).
² Thin cutting plate removed at the time of taking the photograph.

Figure 3.12. The USSH assembled in the triaxial pedestal during specimen preparation.

two guide-pins make the test specimen in this configuration to be directly aligned with the base platen of the test device.

9. At this stage, the specimen is separated from the base pedestal only by the thin cutting plate. Remove the cutting plate carefully to make the sample sit on the base platen.
10. Place the top loading cap on the sample followed by unfolding of the rubber membrane from the USSH. The rubber membrane would now jacket the sample between the top cap and base platen. Seal the sample by securing the rubber membrane placing o-rings at the top and bottom end caps as per usual practice.
11. Apply a small (~15 to 20 kPa) vacuum through the drainage lines as per usual sample preparation procedures. The sample will now be secured due to the vacuum applied through drainage lines, and, at this stage, the external confinement from the USSH is no longer necessary. Split and remove the two parts of the USSH, and proceed with other testing procedures as usual.
12. From this point onwards, follow the standard procedures that are undertaken for device set up for testing

In addition to the technical capability, the following unique features of the USSH are noteworthy: (a) Other than for the changes in the applied vacuum, no external mechanical adjustments to the USSH-housing are necessary to change the sample diameter after initial set up; (b) By appropriate selection of foam material, as necessary, it is possible to provide constraining mechanisms of different stiffness. A foam material of suitable stiffness may be selected based on the type of soil materials to be secured; (c) The device can be readily used by

qualified geotechnical laboratory testing personnel after a relatively quick training session; and (d) the device can be easily operated by one person without compromising the time required for proper securing of the sample.

3.5.2 Assessment of the Effectiveness of the USSH

A number of indicators can be used to assess the degree of disturbance to a soil sample during specimen preparation. They include: (a) geometric deformations (strains) experienced by a sample in the form sample shortening (axial strains)/bulging (radial strains); (b) amount of volumetric strain experienced during reconsolidation of the sample to a stress level equal to or below the previous geostatic stress level; and (c) the stress-strain-pore water pressure response during shear loading. The level of geometric deformations [Item (a) above] suffered by a sample is a direct indicator of disturbance. The volumetric strain experienced during reconsolidation of the sample [Item (b)] has also been noted as a very good indicator of sample quality by many researchers (Mesri et al. 1994; Jamiolkowski et al. 1985; Lunne et al. 1997). Similarly, the mechanical response under shear loading [Item (c)] has also been used widely as a tool to assess sample disturbance (Hight and Leroueil 2003).

Using the above indicators as the basis, laboratory testing was undertaken to assess the effectiveness of the new sample holder in minimizing sample disturbance in Fraser River Delta silt (see Section **Error! Reference source not found.** for description of the material). The following section presents a comparison of the experimental observations made on the above indicators “with” and “without” the use of the USSH.

3.5.2.1 Specimen Deformations Immediately After Extrusion through Sample Set up

Figure 3.13 shows a plan view photograph of the USSH with a Fraser River silt sample secured upon extrusion. In contrast to the deformations that can take place in the freestanding position (as per Figure 3.7), the photograph clearly presents the ability of the USSH to laterally confine a sample while maintaining its circular configuration.

In order to obtain a quantitative assessment of deformations, it was decided to monitor the vertical (axial) deformations that take place during the preparation of the two triaxial Specimens A and B (see previous section for sample details) of Fraser River silt that were prepared with and without the use of the USSH, respectively. As shown in Figure 3.14, a timeline of axial strains (ϵ_a) experienced by the specimen from the time of placement on the bottom pedestal of test device until completion of the triaxial cell assembly was obtained using a dial gauge arrangement. Prior to application of vacuum through the drainage ports to confine the specimens using pore water pressure control, a time span of about 15 minutes (see Figure 3.14) was required to complete the following activities: (i) careful jacketing of specimen using the rubber membrane over the sample, (ii) measuring of sample dimensions (radii and height), (iii) securing of o-rings at top and bottom caps, and (iv) making appropriate "air-free" drainage connections. During this period, the freestanding Specimen B suffered $\epsilon_a = 0.48\%$ whereas Specimen A that was secured with the USSH experienced only a modest 1/4th of the above strain. As may also be noted from Figure 3.14, measurements taken after completion of the assembly indicated that the freestanding specimen had accumulated $\epsilon_a = 0.64\%$ that is about twice ϵ_a sustained by the USSH-supported specimen. Although radial deformations were not measured, clearly, the confined Specimen A with the USSH would have had very little, or no, opportunity to "bulge" [i.e. experience outward radial strains (ϵ_r)] in comparison to a

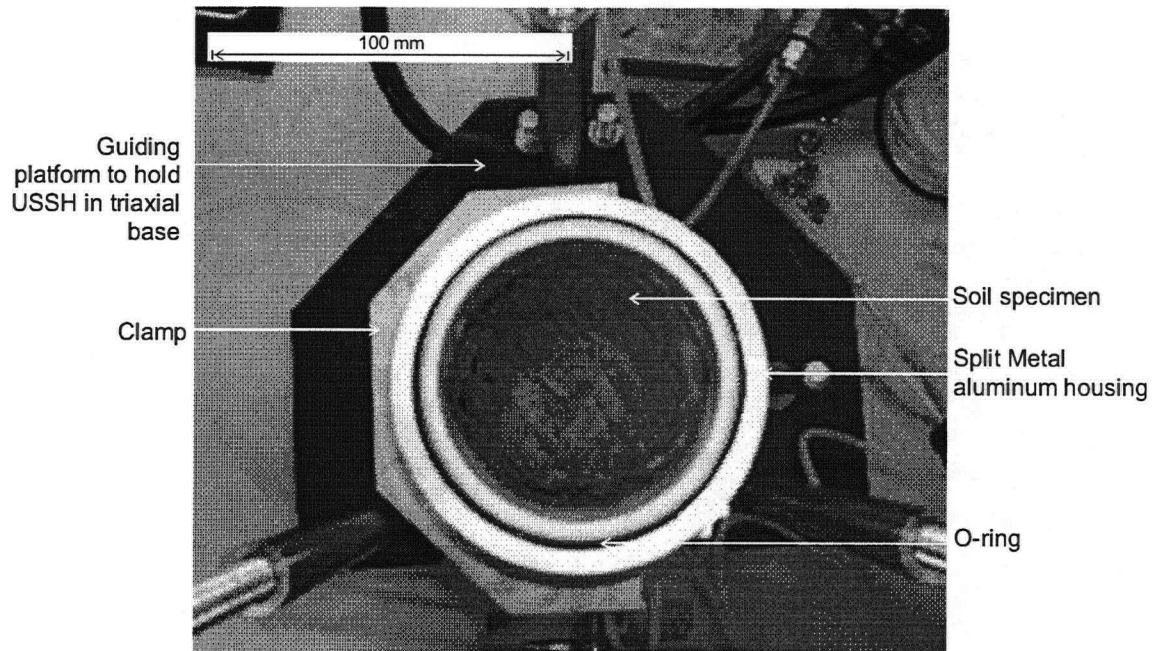


Figure 3.13. Plan view of lateral confinement provided by the USSH immediately after extrusion of a soil specimen.

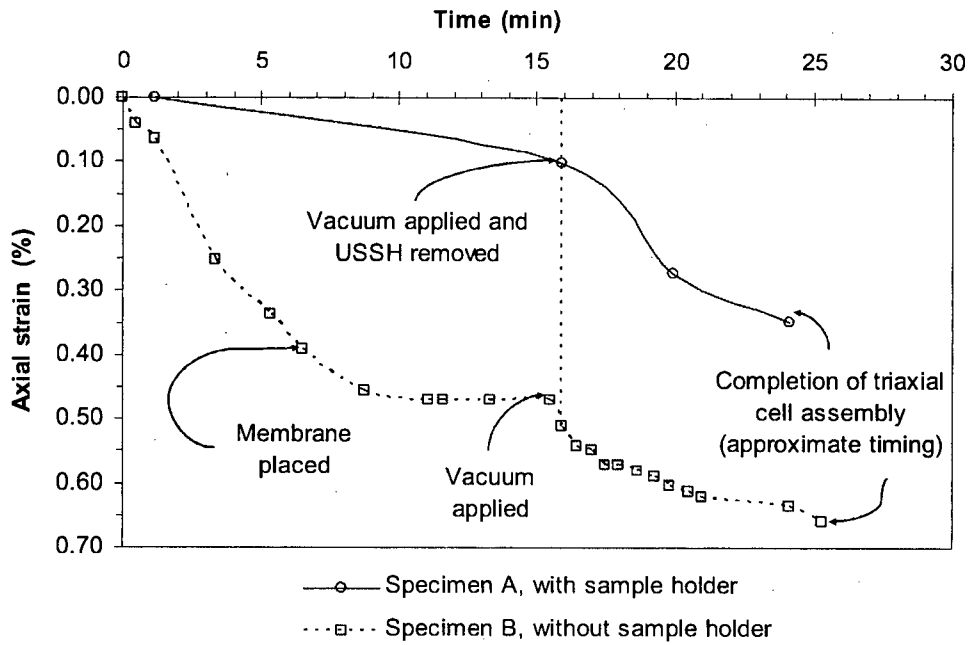


Figure 3.14. Timeline of axial strains during sample preparation - with and without the use of USSH.

freestanding sample. In light of the above, and knowing that the maximum shear strain γ can be expressed as $(\epsilon_a - \epsilon_r)$, and it can be deduced that the Specimen B would have experienced significantly higher shear strains than Specimen A during the specimen preparation process.

3.5.2.2 Volumetric Strains Experienced During Reconsolidation

The Specimens A and B of Fraser River silt prepared as above were subject to isotropic reconsolidation to a stress level of 40 kPa which is about 35% of the estimated effective vertical geostatic stress. Figure 3.15 presents the volumetric strains experienced by the two samples. Sample B that was prepared in a freestanding position experienced a volumetric strain (ϵ_v) of 1.4% during hydrostatic consolidation. In contrast, Sample A that was confined using the USSH developed only $\epsilon_v = 0.61\%$. This significantly reduced volumetric deformation observed in Sample A, again, suggests that the USSH has played a significant role in minimizing sample disturbance.

3.5.2.3 Undrained Response to Monotonic Shear Loading

After hydrostatic consolidation as per above, the Specimens A and B were subjected to monotonic undrained triaxial compression shear loading (i.e. CU testing). An axial shear strain rate of 5.5% per hour was selected for shearing the samples based on the degree of consolidation noted during hydrostatic consolidation. The deviator stress (σ_d) versus axial strain (ϵ_a), excess pore water pressure (Δu) versus ϵ_a , and stress path plots obtained for the Specimens A and B are presented in Figure 3.16. Again, a significant difference in behaviour between the two specimens is clearly evident. At a given strain level, Sample B exhibited a

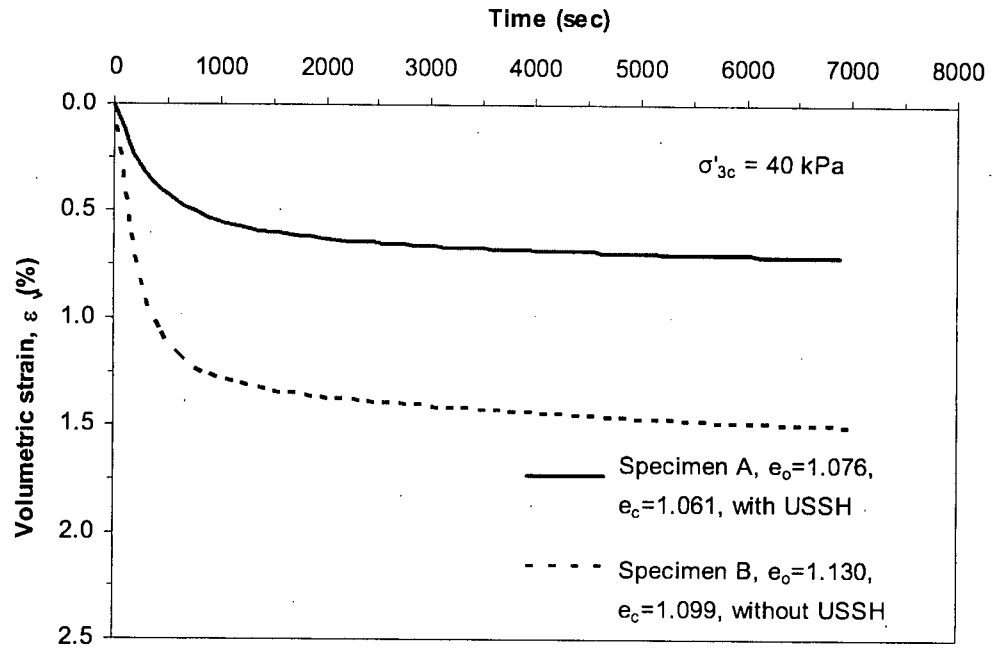


Figure 3.15. Volumetric strains during isotropic consolidation - with and without the use of USSH.

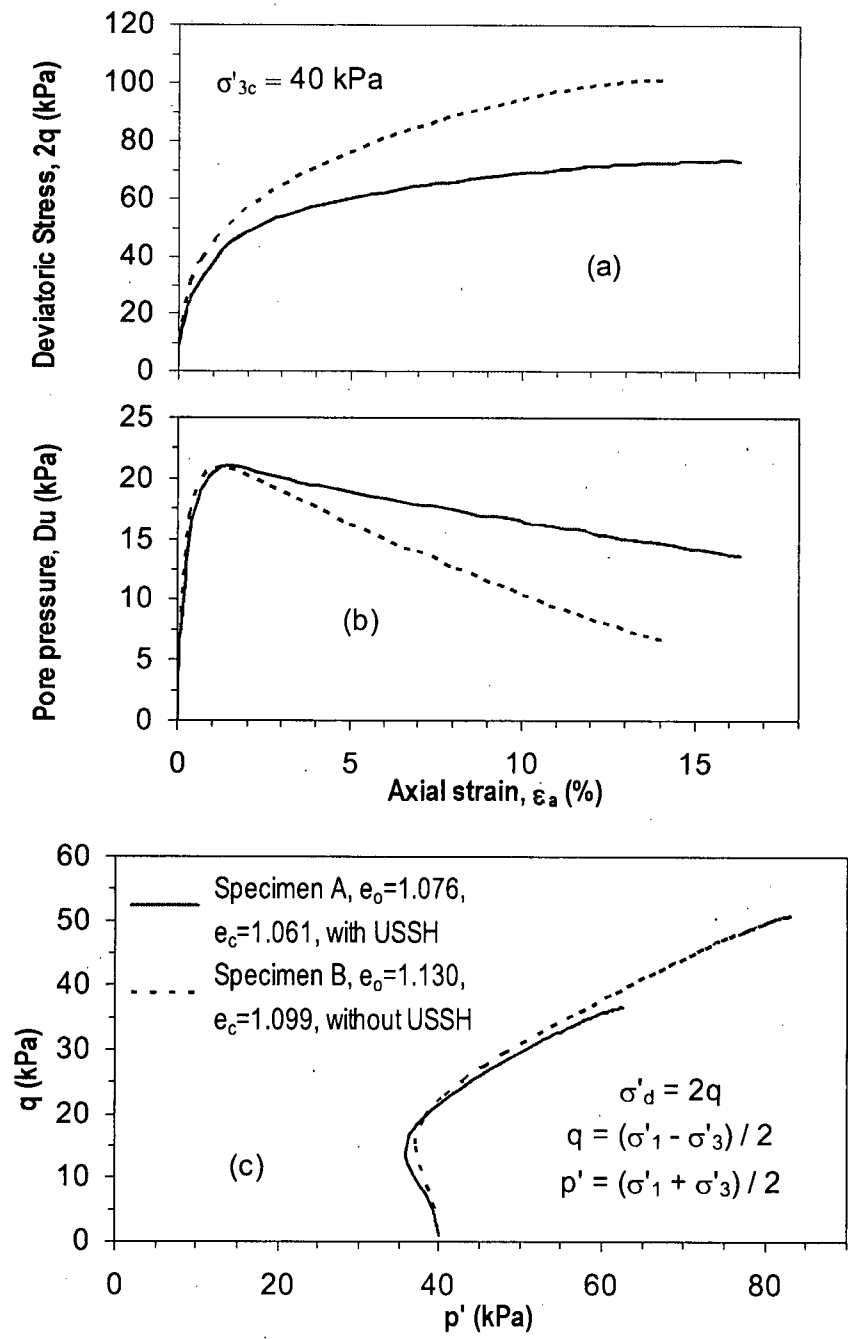


Figure 3.16. Mechanical response during consolidated-undrained triaxial compression testing - with and without the use of USSH. - a) Stress-strain response, b) Excess pore water pressure response and c) Stress path

significantly higher mobilized shear strength (σ_d) than that displayed by Sample A. Initially both the specimens experienced contractive response (see Figure 3.16b); however, upon reaching the point of maximum contraction, a markedly dilative response is exhibited by Sample B in spite of having a similar consolidation void ratio compared to Sample A. Again, in a similar manner to the conclusions drawn by others in their studies on disturbance due to field sampling (Long 2003; Hight and Leroueil 2003), the above variations in the stress-strain-pore water pressure response can be directly attributed to the differences in the changes to the particle structure during specimen preparation with and without the USSH.

3.6 TEST PROGRAM

A systematic testing program was undertaken with the main objective of characterizing the fundamental cyclic loading response of a natural channel-fill silt obtained from the Fraser River Delta, British Columbia, Canada. Undisturbed samples of this silt material were tested at different stress conditions and loading parameters, and the main components investigated in this test program are outlined below:

- One-dimensional consolidation characteristics;
- undrained monotonic response of normally consolidated and overconsolidated silt in the triaxial testing apparatus;
- undrained monotonic response of normally consolidated silt in the DSS device;
- undrained cyclic loading response of normally consolidated silt in the DSS device; and

- undrained cyclic loading response of overconsolidated silt.

The silt specimens tested in the DSS were selected from tube samples retrieved from depths between 5.6 m and 7.4 m. Samples tested in the triaxial apparatus were retrieved from depths between 8.1 m and 9.3 m. Table 3.4 shows the summary of consolidation tests performed and Table 3.5 and Table 3.6 present further details related to the test program with particular information on the loading parameters.

Table 3.4. Summary of consolidation tests

Test Type	Test ID	Range of σ'_v (kPa)
Incremental	CON-01	7.0 – 400.0
	CON-02	10.0 – 200.0
Constant Rate of Strain	CRS-01	0.0 – 700.0

Table 3.5. Summary of undrained triaxial and constant volume DSS tests

Test Type	Consolidation History	OCR	σ'_{vc} / σ'_3 (kPa)
DSS	NC Tests	1	100, 200
	OC Tests	~1.5	100
Triaxial	NC Tests	1	100, 200
	OC Tests	~2	40

Table 3.6. Summary of constant volume cyclic DSS tests

Consolidation History	OCR	σ'_{vo} (kPa)	~CSR	Test Series
NC Tests	1	100	0.10, 0.15, 0.20, 0.30	NC-1
		85*	0.10, 0.15, 0.20, 0.30	NC-2
		200	0.10, 0.15, 0.20	NC-3
OC Tests	~1.25, 1.50, 1.70, 2.00	100	0.15	OC-1
			0.20	OC-2
			0.30	OC-3

* Approximate in-situ vertical effective stress

4 CYCLIC LOADING RESPONSE OF CHANNEL-FILL FRASER RIVER SILT

This chapter presents a detailed examination of the results obtained from the test program outlined in Chapter 3. The presentation includes observations with respect to the following behavioural characteristics of the tested channel-fill Fraser River silt: a) consolidation response, along with a discussion on sample disturbance; b) monotonic response in the DSS and triaxial loading modes; and c) cyclic loading response of normally consolidated and overconsolidated silt under different vertical effective stress conditions.

4.1 CONSOLIDATION CHARACTERISTICS

Figure 4.1 presents the results obtained from consolidation tests performed on three specimens of the natural channel-fill Fraser River silt. Table 4.1 summarizes pertinent details including the field depths and initial water content of the specimens. Unlike the response typically observed for natural clays, the consolidation curves do not exhibit a particular sharp change during transition from reload to the virgin side of the consolidation curve (i.e., from normally consolidated state to overconsolidated state). Because of this, a combination of methods

(Casagrande, 1936b; Janbu et al., 1981; and Becker et al., 1987) was considered in the evaluation of the preconsolidation pressure, σ'_c . The estimated preconsolidation pressures (σ'_c) along with the estimated field in-situ overburden stress ($\sigma'_{v-in-situ}$) for the specimens are also shown in Table 4.1. As may be noted, the applicability of Janbu et al. (1981) and Becker et al. (1987) did not allow estimation of σ'_c with any clarity for some tests; hence, they are not reported in Table 4.1.

Table 4.1. Summary of results from consolidation tests performed in Fraser River silt

Test ID	Depth (m)	$\sigma'_{v-in-situ}$ (kPa)	e_o	σ'_c (kPa)		
				Casagrande (1936b)	Janbu et al. (1981)	Becker et al. (1987)
CON-01	5.9	78.6	0.965	80	79	88
CON-02	6.5	83.5	0.985	80	N/A	N/A
CRS-01	7.1	88.3	1.067	100	N/A	105

The preconsolidation pressures (σ'_c) of ~80 kPa derived from incremental consolidation testing compare well with the estimated $\sigma'_{v-in-situ}$. This agreement between σ'_c and $\sigma'_{v-in-situ}$ suggests that the in situ silt deposit at the sampled location is in a normally consolidated state with no apparent significant aging effects. This observation is not unexpected considering that the tested silt material originates from a relatively recent channel deposit in the Fraser River Delta. The results for constant rate of strain test (CRS), however, show a higher estimated σ'_c pressure than the estimated $\sigma'_{v-in-situ}$. In CRS tests, the estimation of σ'_c for the e vs. $\log(\sigma'_v)$ plot is obtained based on the measured pore water pressure at the base of the sample. This measured pore water pressure can be subject to under-estimation if the sample is not fully saturated or the measuring system has low compliance.

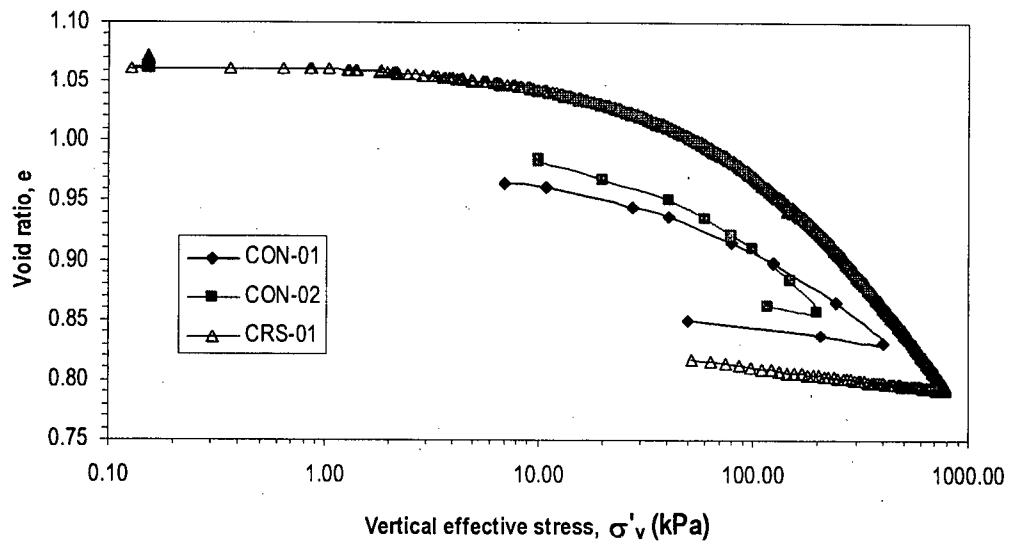


Figure 4.1. Consolidation tests performed on Fraser River delta silt

4.2 ASSESSMENT OF SAMPLE DISTURBANCE

As indicated in Section 3.5, it is known that disturbance to a sample from the time of field sampling to the point of testing in a laboratory device can have a profound effect on the parameters derived from laboratory testing. Changes in the particle structure and stress state would introduce changes in the mechanical performance of soils, and the parameters measured in the laboratory may not be entirely representative of the in-situ conditions. Any disturbance of the soil during field sampling, as well as during laboratory testing, should be minimized in order to obtain meaningful parameters of the soil. While particular care was exercised during sampling, transportation, storage and sample extrusion for this research program (see Section **Error! Reference source not found.** for details), some disturbance to the samples is inevitable. With this background, it was considered prudent to make an assessment of the quality of sampling of the silt used in the present study.

The void ratio change during reconsolidation up to apparent preconsolidation stress has been noted as a good indicator of sample quality (Mesri et al. 1994; Jamiolkowski et al. 1985; Lunne et al. 1997). For example, based on research on uniform marine clays, Lunne et al. (1997) proposed that the normalized void ratio change ($\Delta e/e_0$) can be used as an index of describing sample quality with respect to disturbance, where Δe = change in void ratio of a laboratory sample during reconsolidation to in situ effective stress, and e_0 = in situ void ratio. Table 4.2 presents the $\Delta e/e_0$ obtained from one-dimensional consolidation tests and those derived from the initial consolidation phase of DSS specimens used in test series NC-2 that were consolidated to a vertical stress very similar to the in situ stress. Lunne et al. (1997) criteria

suggests that samples could be considered “good to fair” in terms of sample disturbance if $\Delta e/e_0 < 0.07$, and the specimens are to be classified as “poor” if $\Delta e/e_0 \leq 0.09$. As may be noted from Table 4.2, five out of the seven samples would classify below or in the immediate vicinity of the $\Delta e/e_0$ limit of 0.07.

Table 4.2. Sample quality classification according to Lunne et al. (1997) for channel-fill Fraser River silt samples of this study

Test ID	e_0	$\Delta e/e_0$
CON-01	0.965	0.051
CON-02	0.985	0.064
CSR-01	1.067	0.090
NC-2-1	1.036	0.093
NC-2-2	1.017	0.071
NC-2-3	1.027	0.041
NC-2-4	1.052	0.067

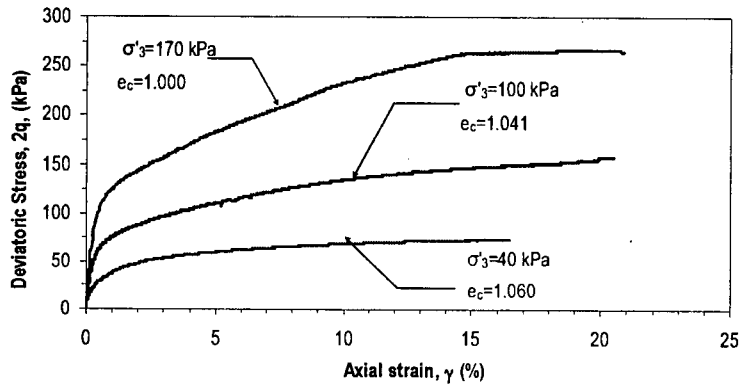
It is also of relevance to examine the above $\Delta e/e_0$ values in relation to the observations made by Long (2003) based on his investigations on sample disturbance effects on Bothkennar laminated facies that has significant presence of layered silt. In this work, Long observed $\Delta e/e_0$ values above 0.08 for 3 out of 4 samples obtained using tubes with 5° cutting-edge, and $\Delta e/e_0$ values above 0.10 for 6 out of 7 samples obtained using tubes with 25°-30° cutting-edge. He pointed out that obtaining “good to fair” specimens (as per Lunne et al., 1997 criteria) is a difficult task because of the inherent difficulties associated in the sampling of soils having silt zones; in spite of this difficulty, it was suggested that the use of thin-walled sampling tubes with a sharp cutting edge would still provide a suitable approach to obtain samples for testing. Mostly “good to fair” classifications obtained for channel-fill Fraser River silt as in Table 4.2, when reviewed in the context of the above observations for Bothkennar laminated facies,

suggests that the sampling and specimen preparation methods used in the present study are effective and suitable for the intended laboratory research work.

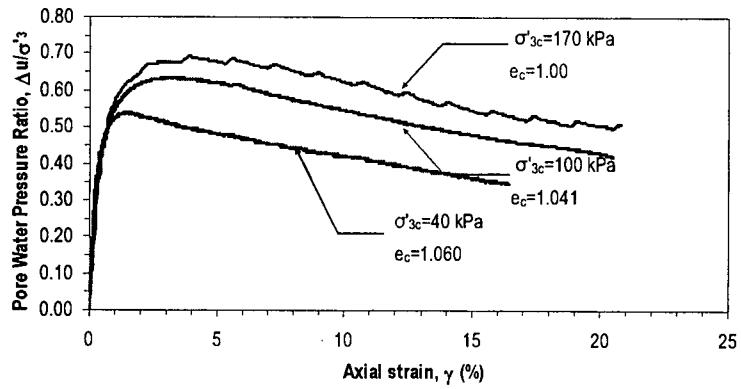
4.3 UNDRAINED RESPONSE OF FRASER RIVER DELTA SILT

4.3.1 Monotonic Shear Response

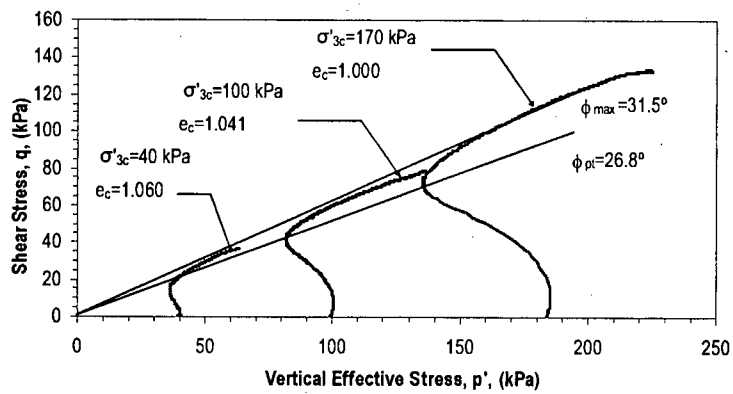
Figure 4.2 presents the stress-path and stress-strain response from consolidated undrained (CU) tests performed on specimens of channel-fill Fraser River silt consolidated to $\sigma'_{3c} = 100$ kPa, $\sigma'_{3c} = 170$ kPa (NC conditions) and $\sigma'_{3c} = 40$ kPa (OC condition). The undisturbed soil sample holder described in Section 3.5 was used in the preparation of the specimens. Although tested at different confining stresses, the void ratio after consolidation is very similar (e_c ranging from 1.000 to 1.061) in the specimens, which is a reflection of the natural variability of the soil. All specimens initially showed a contractive response followed by a dilative response after reaching the point of phase transformation. Nevertheless, specimens consolidated to higher σ'_{3c} values (NC) exhibited a relatively more contractive response than the specimen that was tested at $\sigma'_{3c} = 40$ kPa. This difference is in accord with the expected response between a slightly OC and an NC samples. The mobilized angles of friction at maximum obliquity (ϕ_{max}) and phase transformation (ϕ_{pt}) are also identified in Figure 4.2 (c). As may be noted, a common ϕ_{pt} value can be observed for all tests; a similar observation is also noted for (ϕ_{max}). This behaviour is essentially similar to the response observed for water pluviated medium loose sand by Vaid and Chern (1985) and Negussey et al. (1988) from undrained tests.



a)



b)



c)

Figure 4.2. Results of consolidated undrained tests performed on Fraser River silt. a) Stress-strain, b) pore water pressure development, c) stress-path

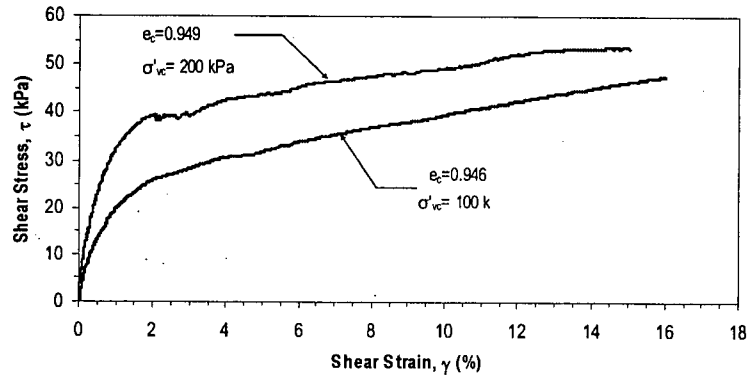
Figure 4.3 shows the stress-strain and stress-path response of normally consolidated samples of channel-fill Fraser River delta silt tested under different vertical confining stress (σ'_{vo}) levels in the DSS. Similar to the observations from triaxial tests, both samples initially deformed in a contractive manner followed by a dilative response. In terms of the stress-strain characteristics, the samples clearly exhibited a strain-hardening behaviour.

The response of the specimen tested at an initial $\sigma'_{vo} \sim 100$ kPa is compared in Figure 4.4 with the results for another specimen that was previously loaded to $\sigma'_{vo} \sim 150$ kPa and then unloaded to $\sigma'_{vo} \sim 106$ kPa (i.e., OCR = 1.4). While the stress-strain relation appears to be similar, clearly the OC specimen exhibits a small dilative response at the very early stages of shearing, and then followed by contractive and dilative responses in sequence. Similar observations of small initial dilative response followed by contraction and dilation, have also been noted on aged Fraser River sand by Lam (2003). In addition to the difference simply in terms of OCR values, it is important to note that the OC specimen had been subject to more destructuration of its natural microstructure during initial consolidation to 150 kPa in comparison to the counterpart specimen that was consolidated to 100 kPa, which is only slightly above the overburden stress.

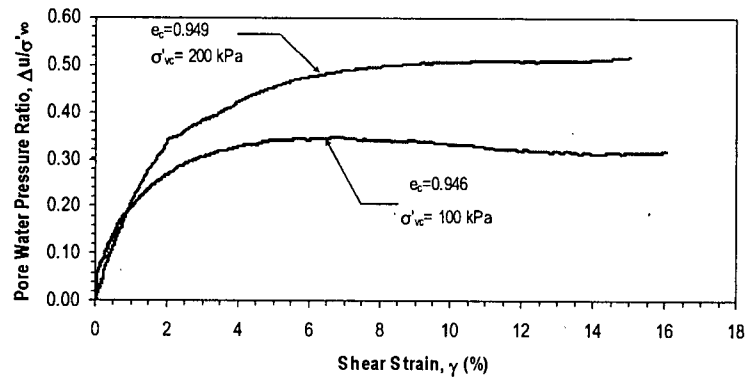
4.3.2 Cyclic Shear Response of Normally Consolidated Silt

4.3.2.1 Definition of Liquefaction in Laboratory Specimens Subject to Cyclic Shear Loading

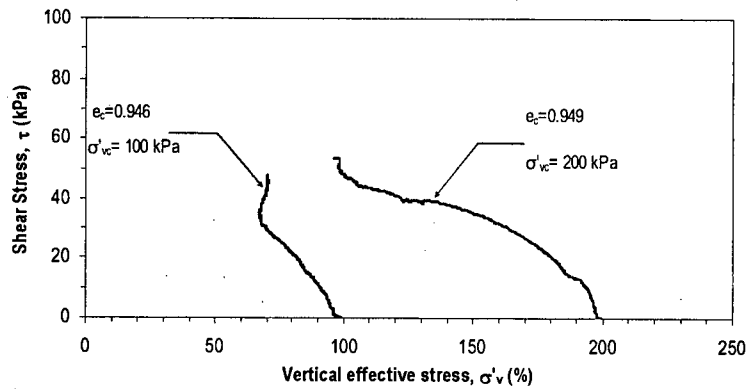
Reduction of effective stress (or raise in equivalent excess pore water pressures) is the cause of the large shear deformations and low strength under cyclic loading. With the need to reduce



a)

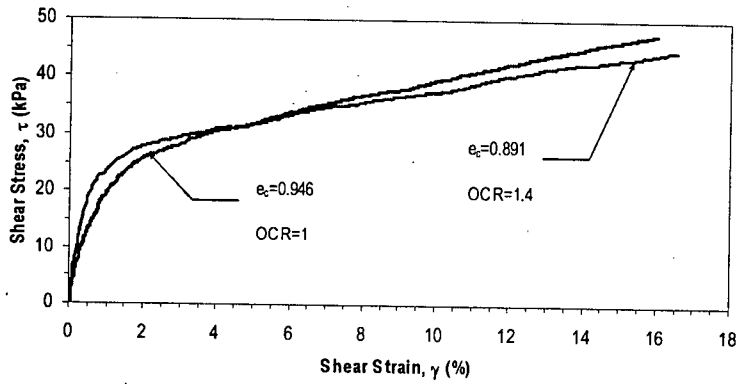


b)

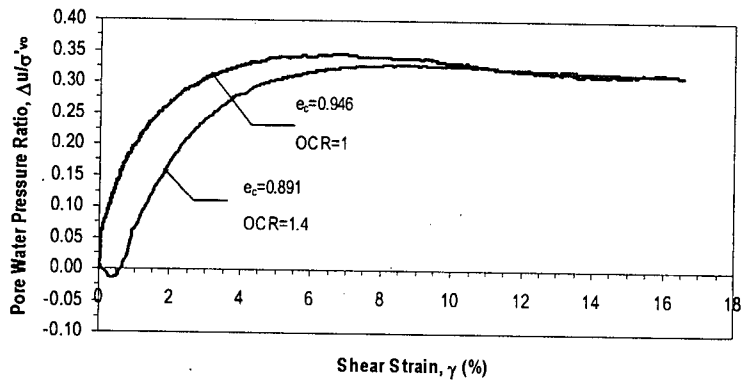


c)

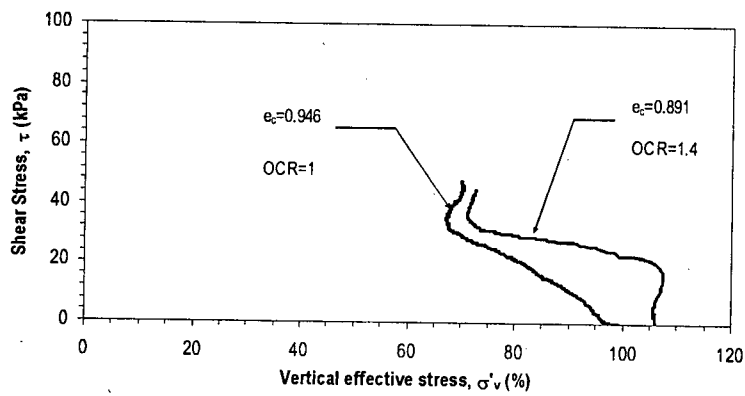
Figure 4.3. Results of constant volume monotonic direct simple shear tests performed on Fraser River silt. a) Stress-strain, b) pore water pressure development, c) stress-path



a)



b)



c)

Figure 4.4. Results of constant volume monotonic direct simple shear tests performed on Fraser River silt. on normally and overconsolidated samples a) Stress-strain, b) pore water pressure development, c) stress-path

shear displacements to improve the performance of structures, laboratory shear strain-based criteria have been used as one of the approaches to delineate liquefaction triggering (e.g., NRC, 1985; Wu et al., 2004). Strain criteria to define triggering of liquefaction have been developed mainly on the basis of the response observed for loose sands, and the approach has been effective because: a) there is a clear contrast between the shear stiffness prior to and after the onset of liquefaction in loose sand; and b) the development of high pore water pressure ratio, r_u , and large strain are essentially synonymous for such sands (except for some cases of sloping ground conditions). A typical contractive response observed for loose Fraser River sand by Wijewickreme et al. (*In print*) is reproduced in Figure 4.5 to illustrate this aspect of sand behaviour.

In contrast to the response of loose sands, for soils exhibiting dilative response such as Fraser River silt as discussed later in Figures 4.6 through 4.10, the degradation of shear stiffness (and generation of equivalent excess pore water pressure) during cyclic loading is a relatively gradual process; hence, separating the shear response into distinct pre-liquefaction and post-liquefaction zones for such materials using strain criterion is only arbitrary, and it does not have fundamental basis. In spite of this drawback, recent findings by Bray et al. (2004a) from field observations in Adapazari following the 1999 Kocaeli (Turkey) earthquake suggest that the use of laboratory strain criteria to assess liquefaction of silts still has merit. Bray et al. (2004a) observed that buildings founded on soil deposits that display cyclic mobility in the laboratory can settle/tilt excessively; they also noted that surface expressions such as sediment ejecta may also be evident under conditions of cyclic mobility. In addition, the use of strain criterion to define the onset of liquefaction becomes useful due to the following reasons: a) a strain criteria would serve as an “index” of comparison to examine the response between different tests; and

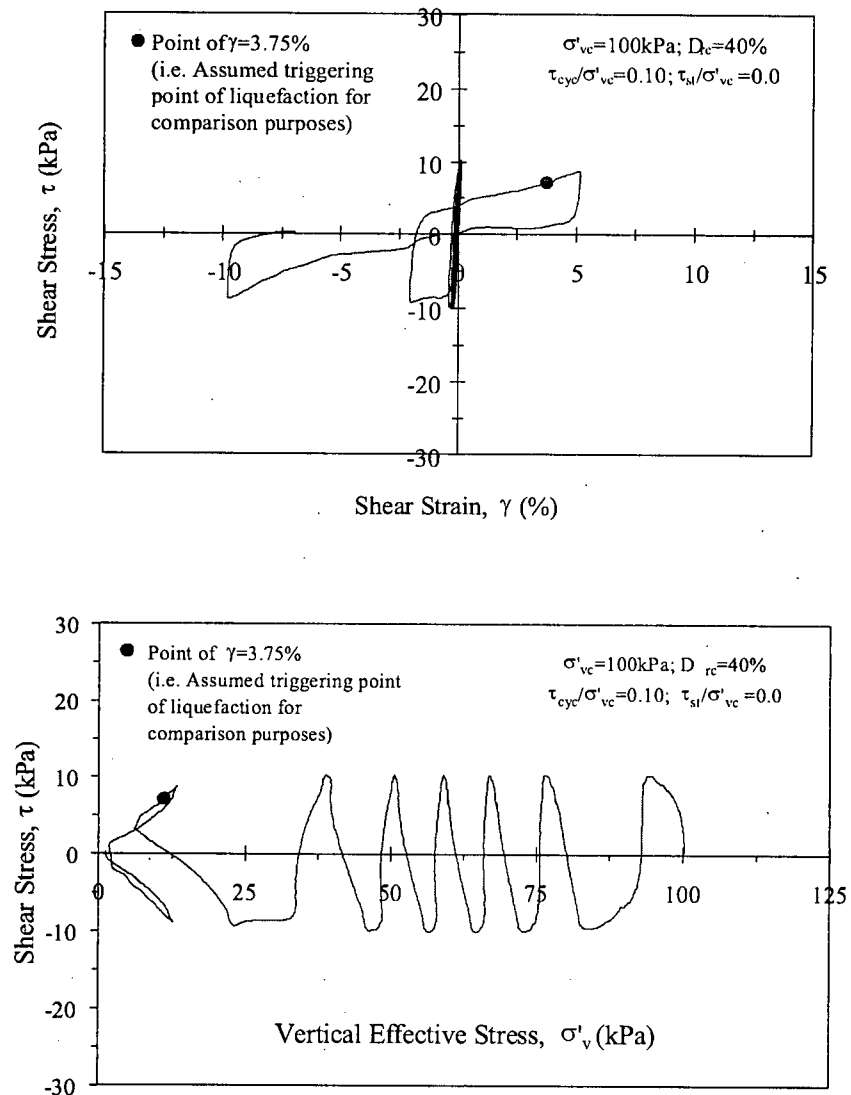
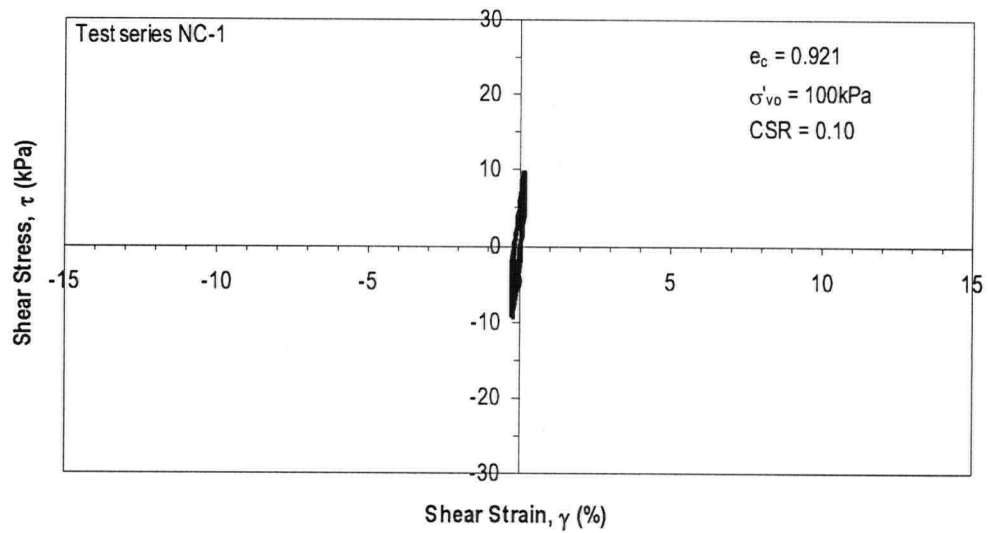


Figure 4.5. Typical contractive response observed for loose Fraser River sand (after Wijewickreme et al., *In print*)

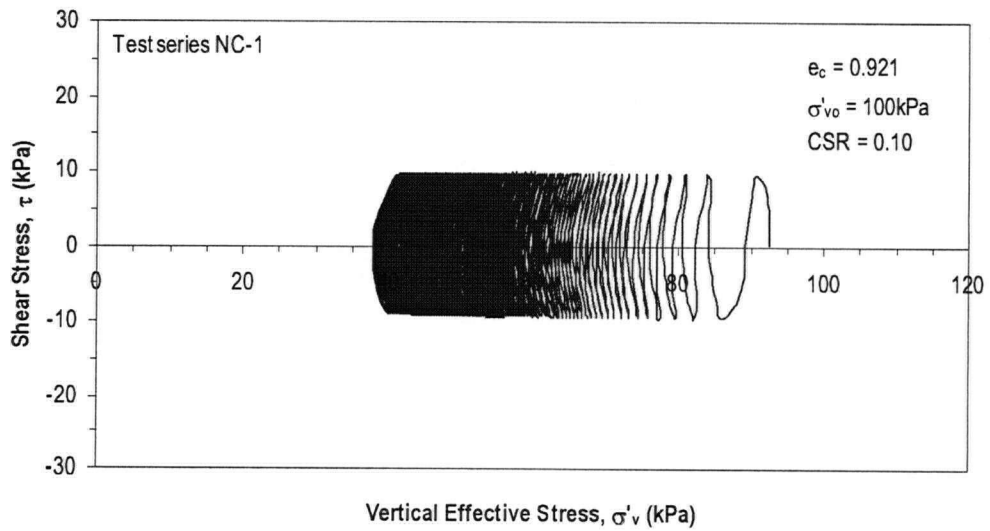
b) it also allows to examine silt behaviour in the context of the existing approaches for sands that have been mainly developed based on strain criteria. With this background, for the present study, liquefaction is considered to have occurred when the single amplitude horizontal shear strain reached 3.75% in a DSS specimen. This criterion for the DSS test is essentially equivalent to reaching a 2.5% single-amplitude axial strain in a triaxial sample, which is a definition for liquefaction previously suggested by the NRC (1985), and it has been used in many previous liquefaction studies at UBC.

4.3.2.2 General Stress-Strain and Pore Water Pressure Response

Laboratory observed cyclic shear response of normally consolidated channel-fill Fraser River silt is presented in Figures 4.6 through 4.10. All specimens were subject to cyclic loading after consolidation to an initial vertical effective stress $\sigma'_{vo} = 100$ kPa. The applied cyclic stress ($CSR = \tau_{cy}/\sigma'_{vc}$) in these tests series ranged from $CSR = 0.10$ to $CSR = 0.30$ (test series NC-1). At the lowest applied cyclic stress ratio ($CSR=0.10$), the specimen did not liquefy as per the definition given in Section 4.3.2.1, even after application of 150 cycles as shown in Figure 4.6. Although the specimen exhibited contractive behaviour in the first cycle and gradual reduction of σ'_v , with further cyclic loading there was a significant reduction in shear stiffness. As may be noted from Figure 4.11, the equivalent excess pore water pressure ratio, $r_u = \Delta u/\sigma'_{vo}$, almost reached a plateau (i.e., $r_u \sim 50\%$) for this test [Note: as indicated in Section 3.2.1, the decrease (or increase) in vertical stress in a constant volume DSS test is equivalent to a rise (or drop) in excess pore water pressure]. The specimen that was subject to a $CSR = 0.15$ (Figure 4.7) also exhibited gradual increase in equivalent excess pore water pressure (decrease in vertical effective stress) with increasing number of cycles. Unlike the case with $CSR = 0.10$ the r_u of the

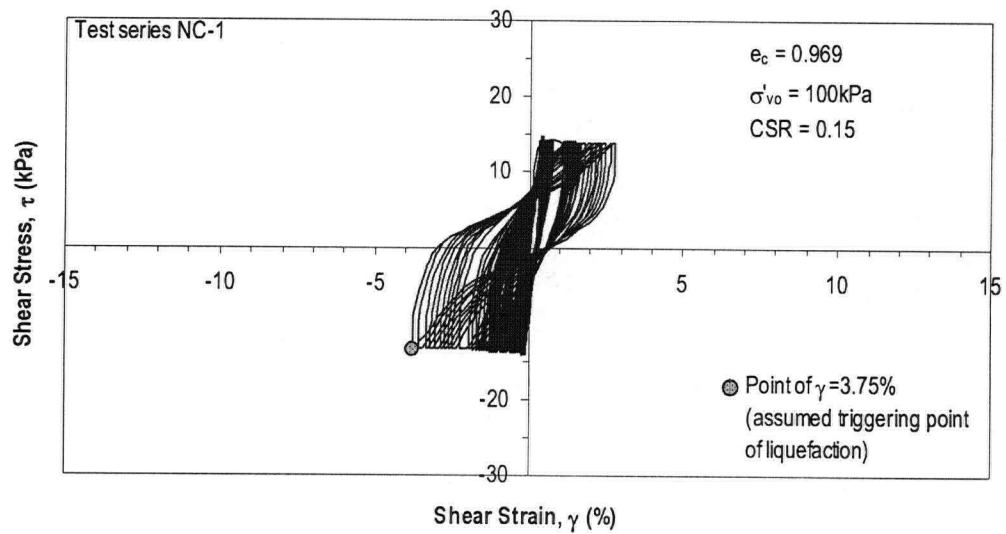


a)

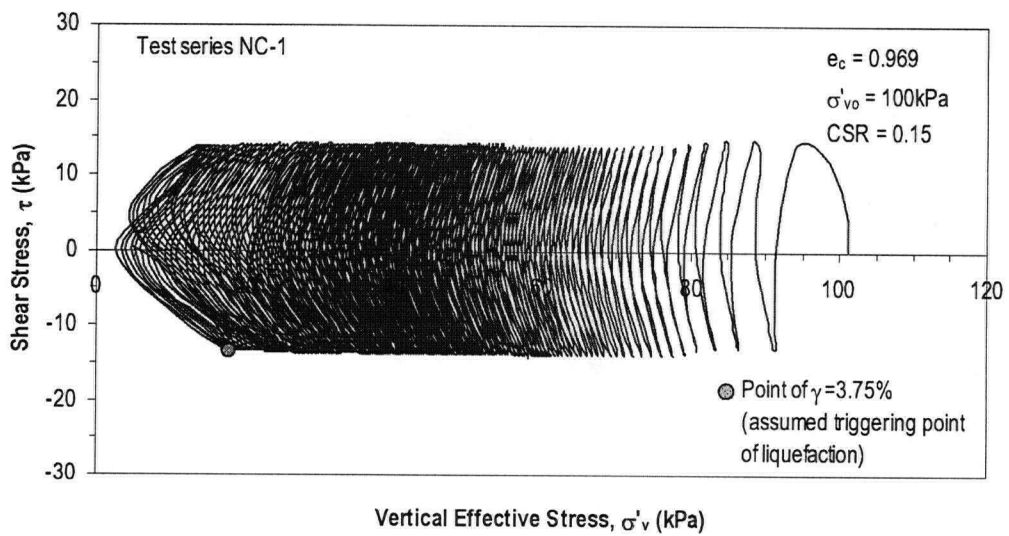


b)

Figure 4.6. Constant volume DSS test results on normally consolidated sample – Tests series NC-1 (CSR = 0.10, $\sigma'_{v0} = 100$ kPa). a) Stress-strain response. b) Stress-path.

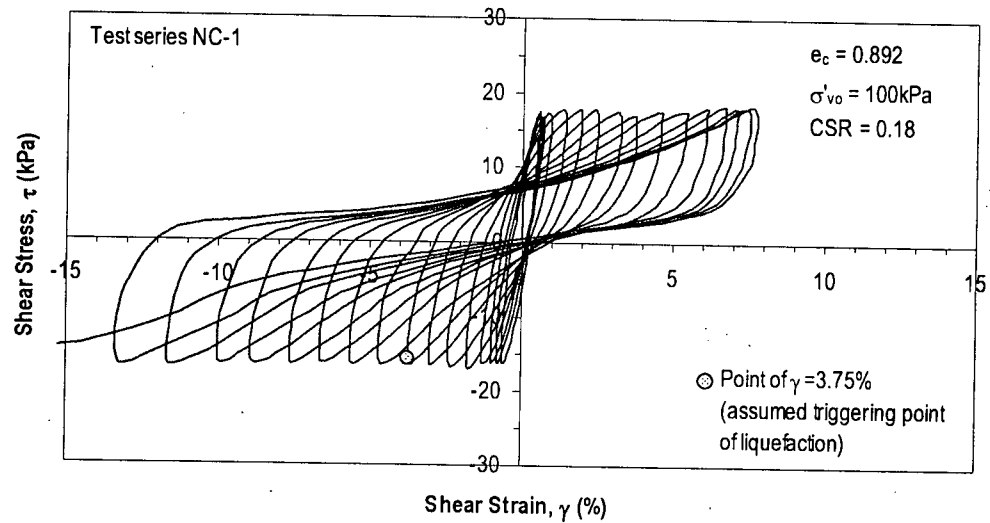


a)

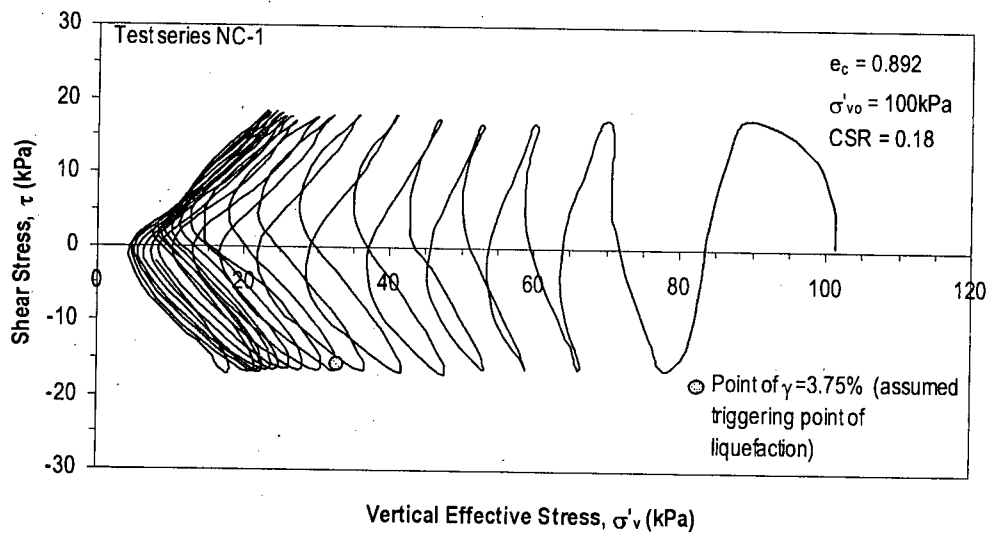


b)

Figure 4.7. Constant volume DSS test results on normally consolidated sample – Tests series NC-1 (CSR = 0.15, σ'_{vo} = 100 kPa). a) Stress-strain response. b) Stress-path.

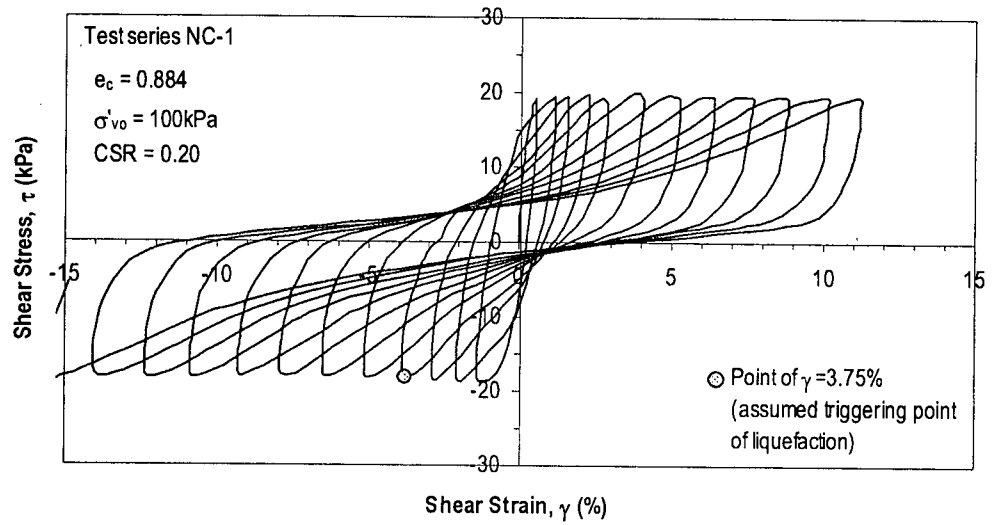


a)

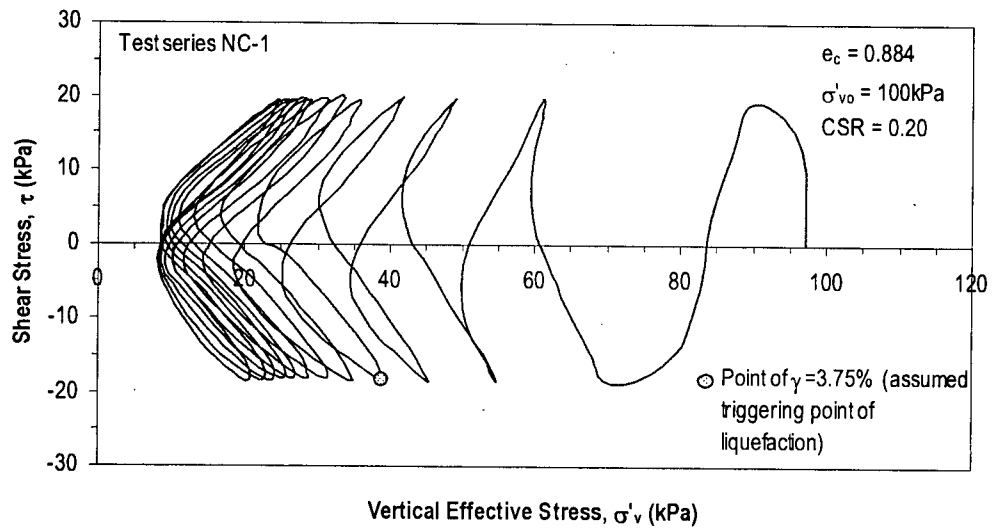


b)

Figure 4.8. Constant volume DSS test results on normally consolidated sample – Tests series NC-1 (CSR = 0.18, σ'_{vo} = 100 kPa). a) Stress-strain response. b) Stress-path.

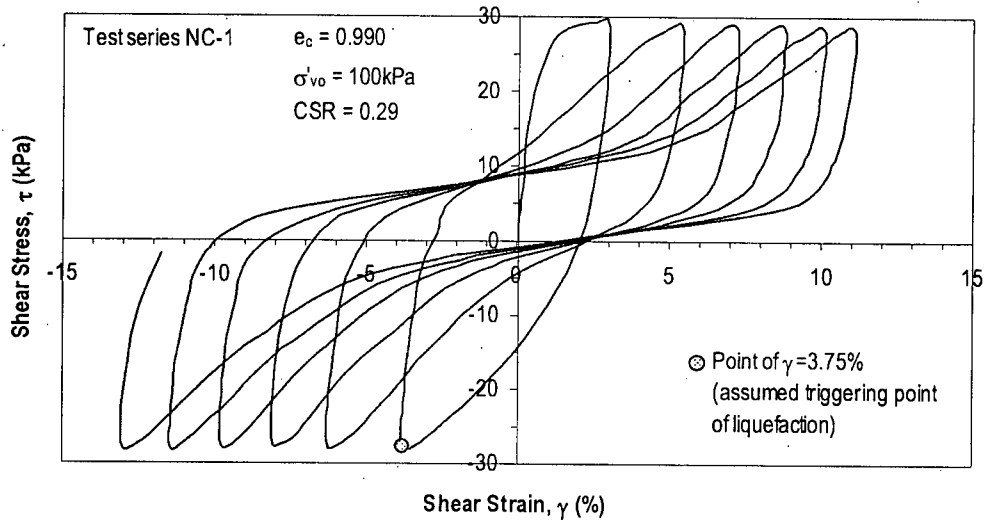


a)

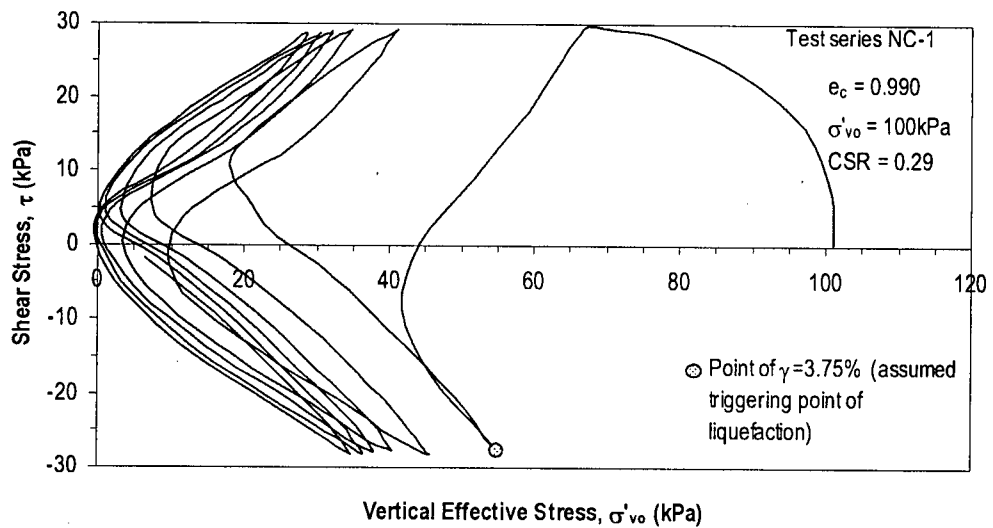


b)

Figure 4.9. Constant volume DSS test results on normally consolidated sample – Tests series NC-1 (CSR = 0.20, σ'_{vo} = 100 kPa). a) Stress-strain response. b) Stress-path.



a)



b)

Figure 4.10. Constant volume DSS test results on normally consolidated sample – Tests series NC-1 (CSR = 0.30, σ'_{vo} = 100 kPa). a) Stress-strain response. b) Stress-path.

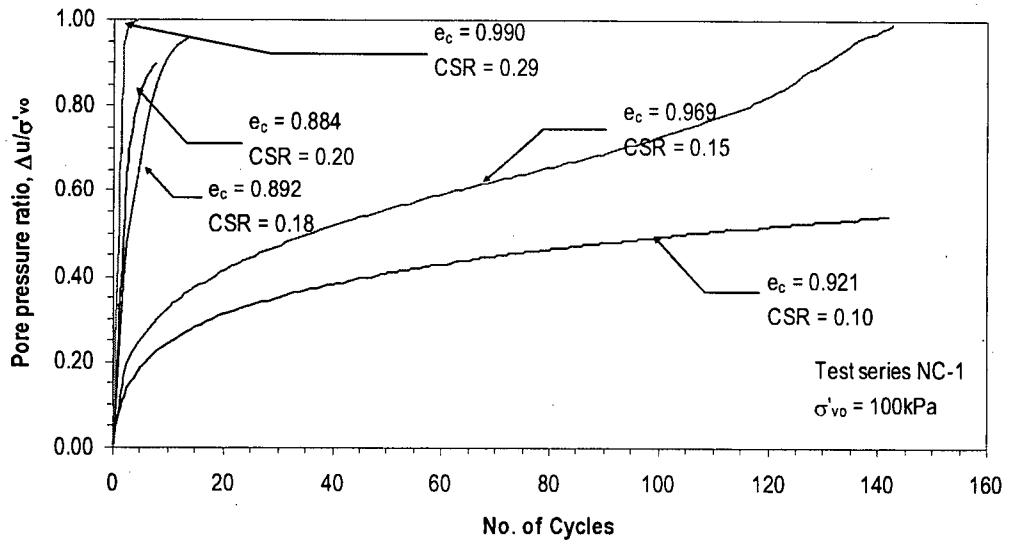


Figure 4.11. Cumulative pore water pressure during constant volume DSS test on normally consolidated sample – Tests series NC-1 ($\sigma'_{vo} = 100\text{ kPa}$).

specimens reached relatively larger values ($r_u \sim 100\%$) with a clear degradation of shear stiffness with increasing load cycles. As noted from Figure 4.7, the specimen reached liquefaction ($\gamma=3.75\%$) after 141 cycles of loading. With increasing CSR, the rate of generation of r_u increased (Figures 4.8 and 4.9). The contractive behaviour in the first cycle followed by the alternating dilative/contractive response noted for lower CSR values is still prevalent under CSR = 0.18 and 0.20. The specimen tested with CSR=0.30 (see Figure 4.10) reached liquefaction in one cycle. It showed contractive response during the first half cycle, followed by dilative response in the loading part of the next half cycle. This implies an early manifestation of phase transformation under more severe CSR levels. The specimens subjected to relatively large values of CSR reached $r_u \sim 100\%$ in a lesser number of cycles than those subjected to low CSR values. The key results obtained from these constant volume cyclic DSS test are summarized in Table 4.3.

Cumulative equivalent excess pore water pressure with number of cycles for the specimens tested in test series NC-1 are presented in Figure 4.11. The samples that liquefied experienced generally large pore water pressure ratios (or low vertical effective stress) during cyclic loading. It is important to note that the curves presented in Figure 4.11 are only the envelope of maximum pore water pressure developed during the cyclic loading. Typically, the curve would show spikes for cycles that involve dilation/contraction. The build-up of cumulative equivalent excess pore water pressure with the increasing number of cycles appear to result in large cyclic shear strains even at moderate magnitudes of cyclic loading; For example, for CSR values in the order of 0.20, shear strains of the order of 15% were reached in between 7 to 12 cycles. However, this data should be extended to engineering practice with caution since this many cycles of high CSR loading may not materialize under most level ground conditions.

Table 4.3. Summary of results of constant volume cyclic DSS tests performed on channel-fill Fraser River silt.

Test series	e_i^*	σ'_{vc} (kPa)	$\epsilon_v^{\#}$ (%)	OCR	e_c^{\dagger}	First cyclic loading					Second cyclic loading				
						CSR	N_L^{\ddagger}	$N_{cy}^{\ }$ ($\gamma=15\%$)	$r_u^{\ \ }$ (%)	ϵ_{vcyc}^{\S} (%)	CSR	N_L^{\ddagger}	$N_{cy}^{\ }$ ($\gamma=15\%$)	$r_u^{\ \ }$ (%)	ϵ_{vcyc}^{\S} (%)
NC-1	0.991	95.0	3.54%	1.00	0.921	0.10	N_{Liq}	N/A	60.5	0.5%	N/A	N/A	N/A	N/A	
	1.041	101.3	3.53%		0.969	0.15	142	N/A	101.5	3.3%	0.15	115	N/A	100.5	1.5%
	0.990	101.2	4.92%		0.892	0.18	8	17	97.1	2.4%	0.18	1	24	88.5	0.7%
	0.974	97.2	4.55%		0.884	0.21	4	12	91.8	4.2%	0.20	3	41	90.5	1.3%
	1.041	101.1	2.48%		0.99	0.29	1	8	103.5	3.5%	0.29	1	21	104.1	2.8%
NC-2	1.036	86.9	4.75%	1.00	0.939	0.10	N_{Liq}	N/A	53.1	0.5%	0.10	NL	NL	30.7	0.4%
	1.017	84.9	3.56%		0.945	0.15	39	81	97.6	4.1%	0.14	6	105	98.8	2.4%
	1.027	85.0	2.09%		0.985	0.25	2	7	93.9	4.3%	0.25	1	18	98.3	2.7%
	1.052	87.2	3.45%		0.981	0.29	1	4	91.1	3.6%	0.30	1	6	92.1	2.4%
NC-3	0.997	198.6	5.72%	1.00	0.882	0.11	164	180	96.9	5.1%					
	1.047	199.3	7.16%		0.900	0.15	13	20	94.4	1.7%					
	0.989	199.8	6.74%		0.854	0.20	3	7	94.4	4.5%					
OC-1	1.016	104.1	4.89%	1.21	0.918	0.15	78	94	97.8	2.9%					
	1.065	98.7	4.69%	1.52	0.970	0.15	180	NA	83.3	1.3%					
OC-2	0.990	95.5	3.97%	1.32	0.912	0.21	6	17	90.0	3.7%					
	0.936	109.4	4.40%	1.37	0.853	0.21	14	27	95.7	4.1%					
	1.009	98.0	5.51%	1.53	0.900	0.21	18	32	91.7	2.6%					
	1.006	104.5	5.79%	1.68	0.894	0.21	37	53	97.6	3.2%					
	1.046	104.5	7.01%	1.91	0.908	0.20	136	160	95.7	3.7%					
	0.952	106.0	4.93%	2.13	0.863	0.21	N_{Liq}	N/A	55.0	0.2%					

Table 4.3. Summary of results of constant volume cyclic DSS tests performed on channel-fill Fraser River silt (contd.).

Test series	e_i^*	σ'_{vc} (kPa)	$\varepsilon_v^\#$ (%)	OCR	e_c^\dagger	First cyclic loading					Second cyclic loading							
						CSR	N_L^\ddagger	$N_{cy}^ $ ($\gamma=15\%$)	$r_u^{ }$ (%)	$\varepsilon_{v_{cyc}}^\S$ (%)	CSR	N_L^\ddagger	$N_{cy}^ $ ($\gamma=15\%$)	$r_u^{ }$ (%)	$\varepsilon_{v_{cyc}}^\S$ (%)			
OC-3	1.036	106.5	5.01%	1.18	0.9357	0.30	1	3	86.0	3.3%								
	0.980	105.5	4.46%	1.43	0.894	0.30	2	6	90.1	3.2%								
	1.032	111.0	5.23%	1.58	0.929	0.30	3	8	88.7	3.6%								
	0.985	104.9	7.21%	1.91	0.846	0.31	7	14	89.2	3.5%								

Table 4.3. Summary of results of constant volume cyclic DSS tests performed on channel-fill Fraser River silt (contd.) - Notes.

- *: Initial void ratio, computed as $e_i = w_c \cdot G_s$.
- ** : Initial vertical effective confining stress (previous to cyclic loading)
- # : Volumetric strain after application of initial load, σ'_{vc} for NC specimens and σ'_{vp} (pre-load) for OC specimens.
- † : Void ratio previous to cyclic loading.
- ‡ : Number of cycles to liquefaction (i.e., $\gamma = 3.75\%$).
- || : Number of cycles to reach shear strain, $\gamma \sim 15\%$.
- ||| : Pore water pressure ratio, $r_u = \Delta u / \sigma'_{vc}$.
- § : Volumetric strain due to re-consolidation after application of indicated cyclic loading.
- N_{liq} : Specimen not liquefied
- N/A: Not available

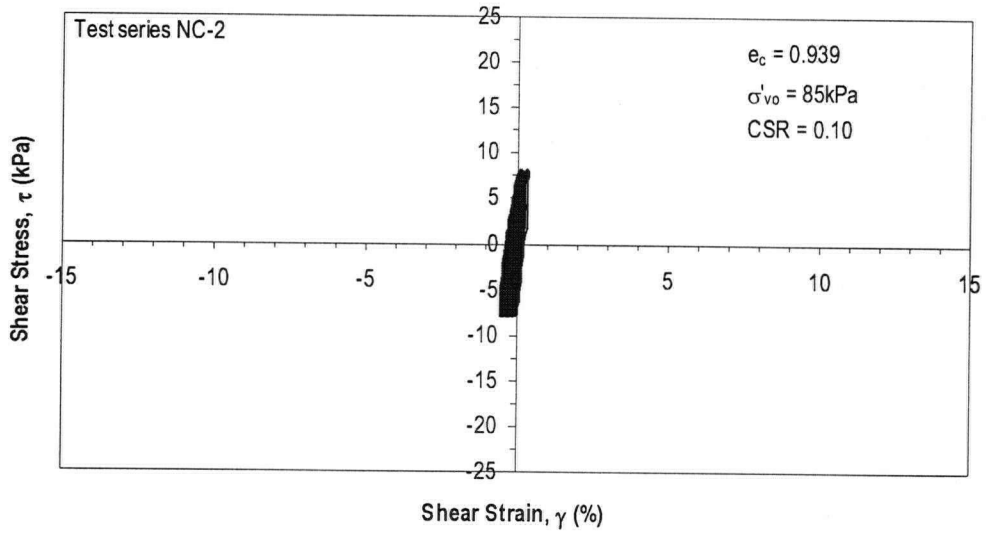
The observed progressive increase in r_u associated with degradation of shear modulus is common to all the test results presented in Figures 4.6 through 4.10. This observed response is essentially the “cyclic mobility” type mechanism observed by Siskandakumar (2004) and Kammerer et al. (2002) for dense (i.e., dilative) sands.

4.3.2.3 General Stress-Strain and Pore Water Pressure Response at Other Stress Levels

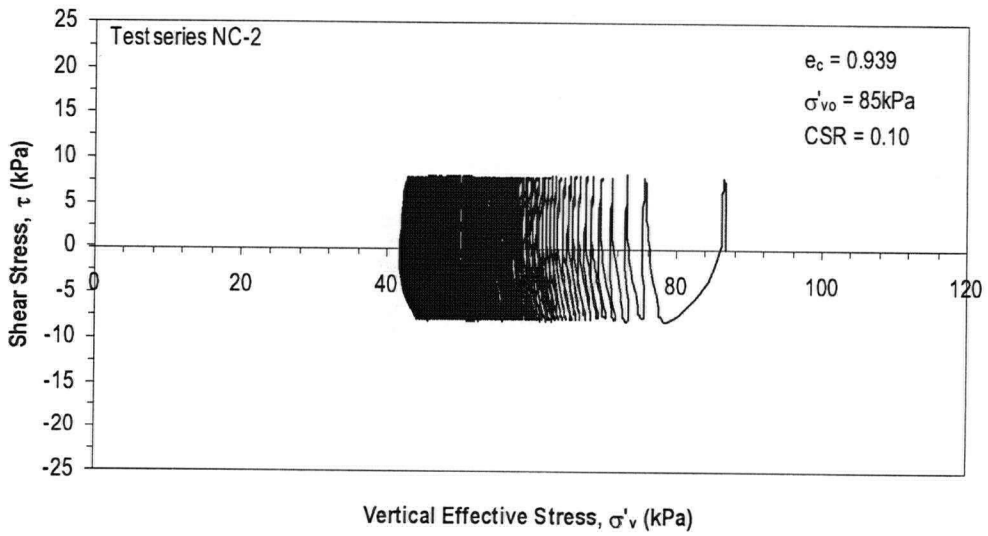
This section presents the results from constant volume DSS tests conducted on specimens initially consolidated to $\sigma'_{vo} = 85$ kPa (test series NC-2) and $\sigma'_{vo} = 200$ kPa (test series NC-3). The vertical stress level of test series NC-2 is approximately equal to the in-situ stress level $\sigma'_{v, in-situ}$; as such it is reasonable to state that microstructure and fabric of the specimens used in this test series would be closer to the in-situ conditions than those tested under higher σ'_{vo} values. The tests were conducted to cover a CSR range between 0.10 and 0.30, and the observed stress-strain and stress-path response is presented in Figures 4.12 to 4.15. Figure 4.16 depicts the generation of equivalent excess pore water pressure with the number of cycles for the 4 tests.

Since the tests series NC-3 were conducted at $\sigma'_{vo} = 200$ kPa, it is likely that the specimens would have experienced destructuration of the in-situ fabric and microstructure. The results from this series of tests (CSR 0.11 through 0.20) are presented in Figures 4.17 through 4.20, in a similar format to the results displayed for test series NC-1 and NC-2.

In a general context, the patterns and trends of stress-strain and equivalent excess pore water pressure development observed for test series NC-2 and NC-3 are very similar to those noted for tests series NC-1 (see Section 4.3.2.2). However, careful examination would indicate that the response in the first cycle of loading of the tests in series NC-2 is less contractive than the

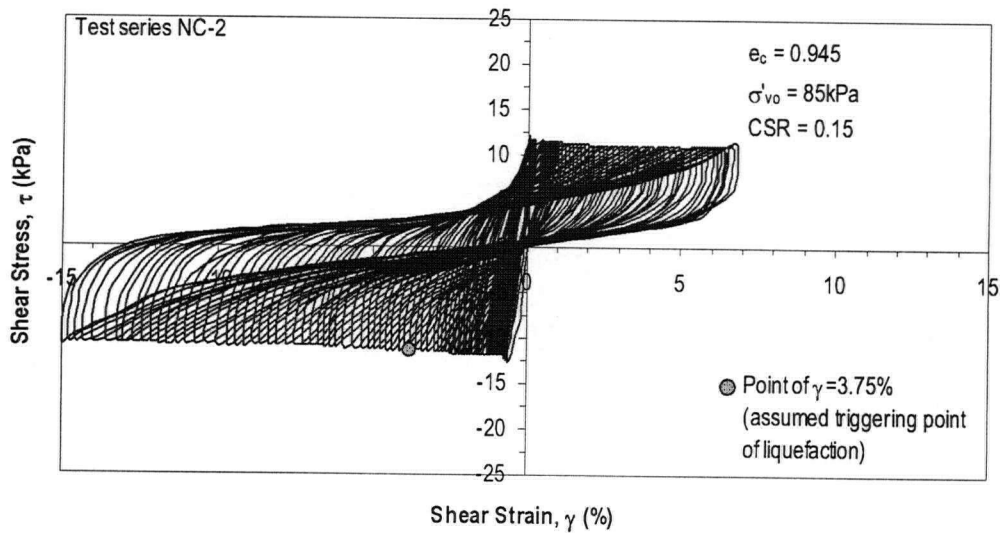


a)

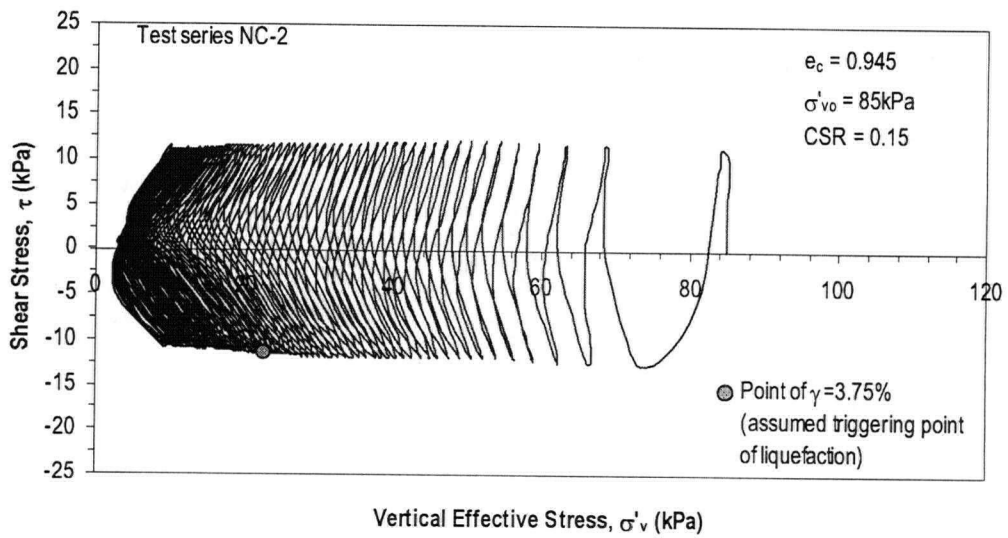


b)

Figure 4.12. Constant volume DSS test results on normally consolidated sample – Tests series NC-2 ($\text{CSR} = 0.10$, $\sigma'_{vo} = 85 \text{ kPa}$). a) Stress-strain response. b) Stress-path.

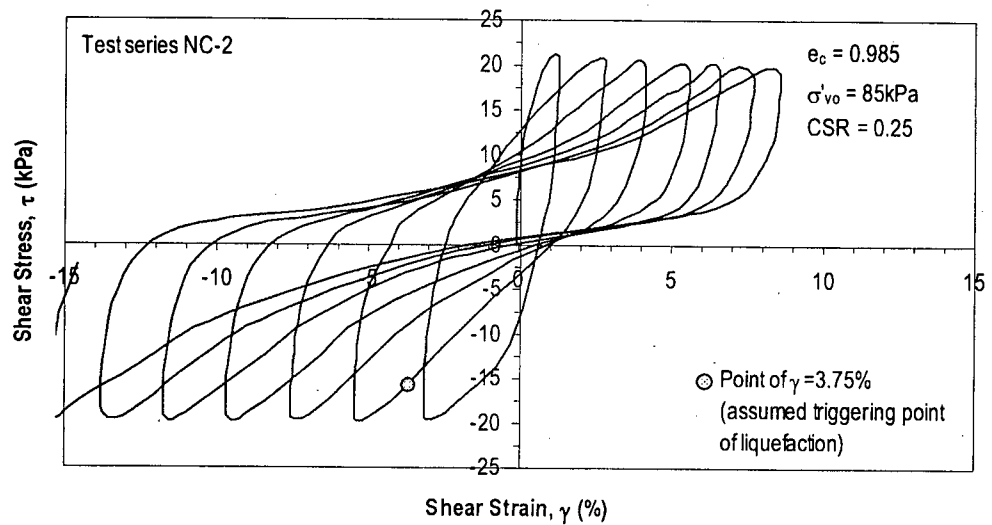


a)

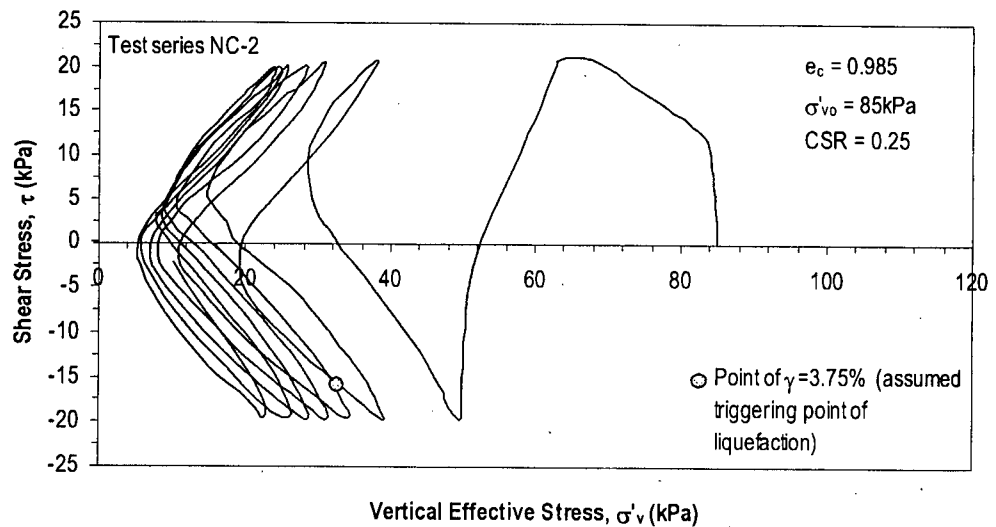


b)

Figure 4.13. Constant volume DSS test results on normally consolidated sample – Tests series NC-2 (CSR = 0.15, $\sigma'_{vo} = 85$ kPa). a) Stress-strain response. b) Stress-path.

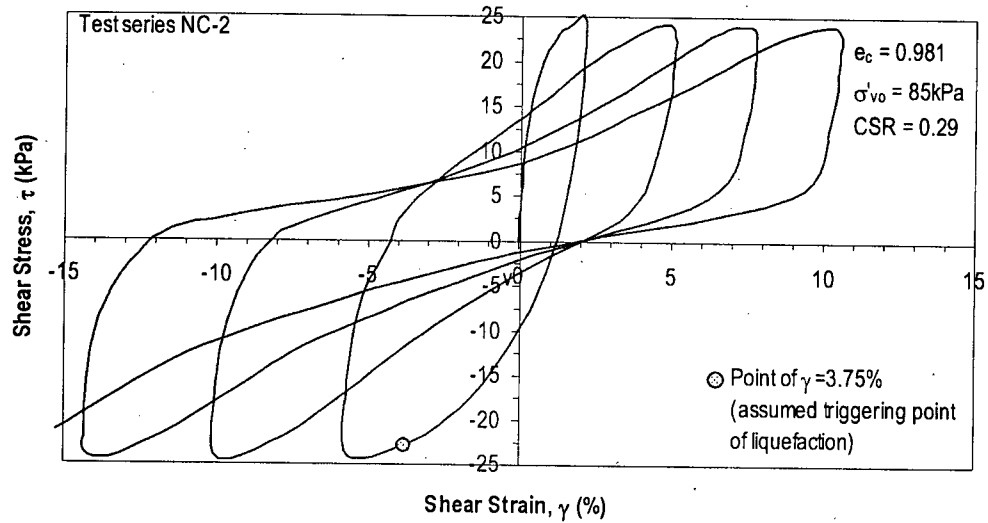


a)

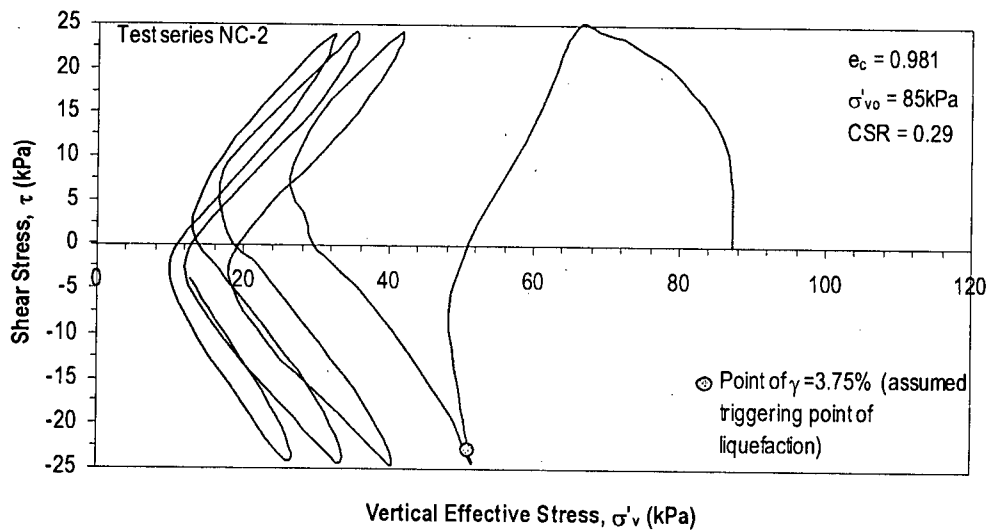


b)

Figure 4.14. Constant volume DSS test results on normally consolidated sample – Tests series NC-2 (CSR = 0.25, σ'_{vo} = 85 kPa). a) Stress-strain response. b) Stress-path.



a)



b)

Figure 4.15. Constant volume DSS test results on normally consolidated sample – Tests series NC-2 (CSR = 0.30, $\sigma'_{vo} = 85$ kPa). a) Stress-strain response. b) Stress-path.

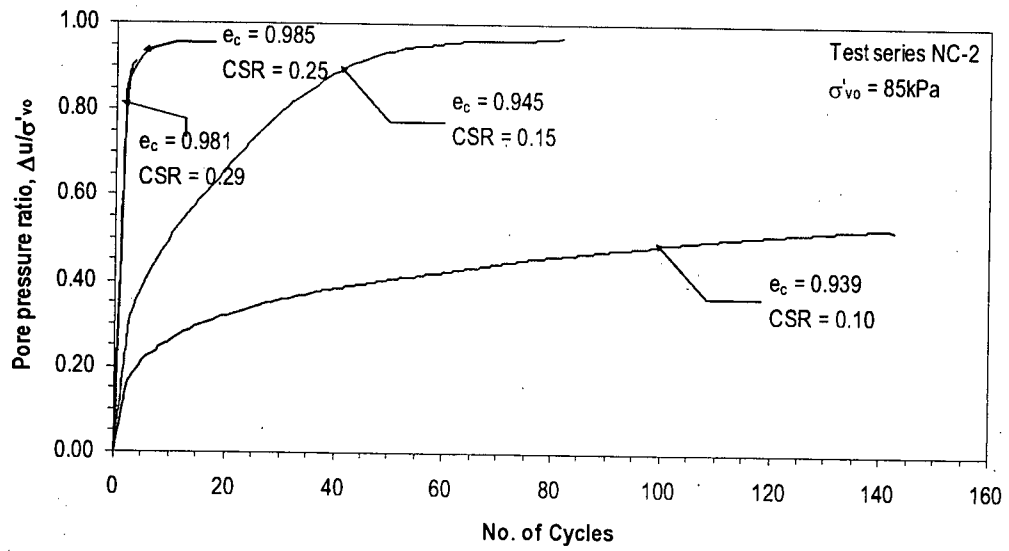
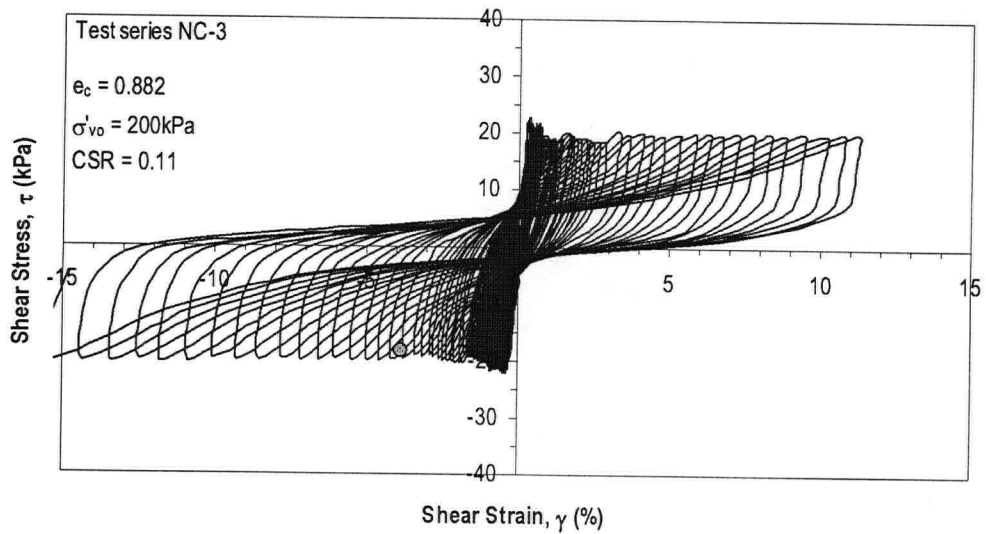
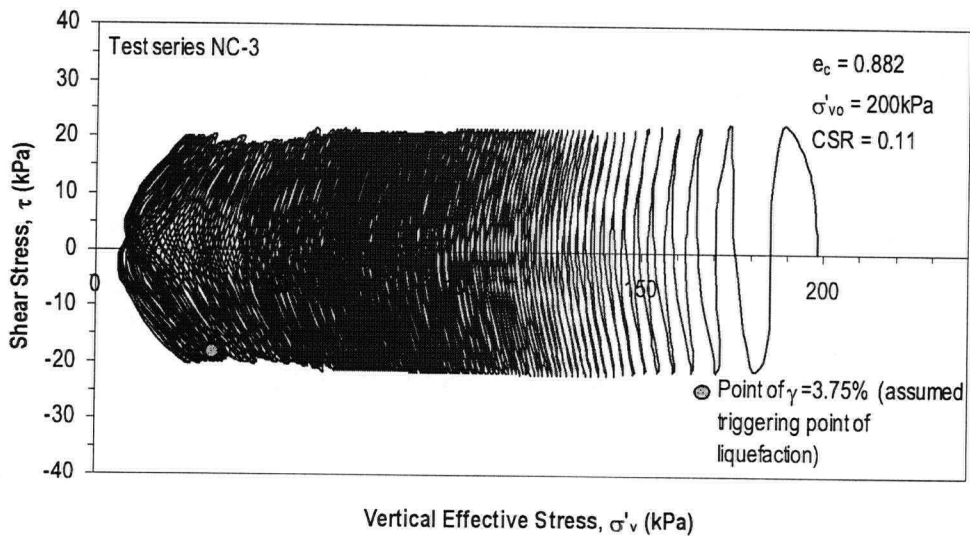


Figure 4.16. Cumulative pore water pressure during constant volume DSS test on normally consolidated sample – Tests series NC-2 ($\sigma'_{vo} = 85$ kPa).

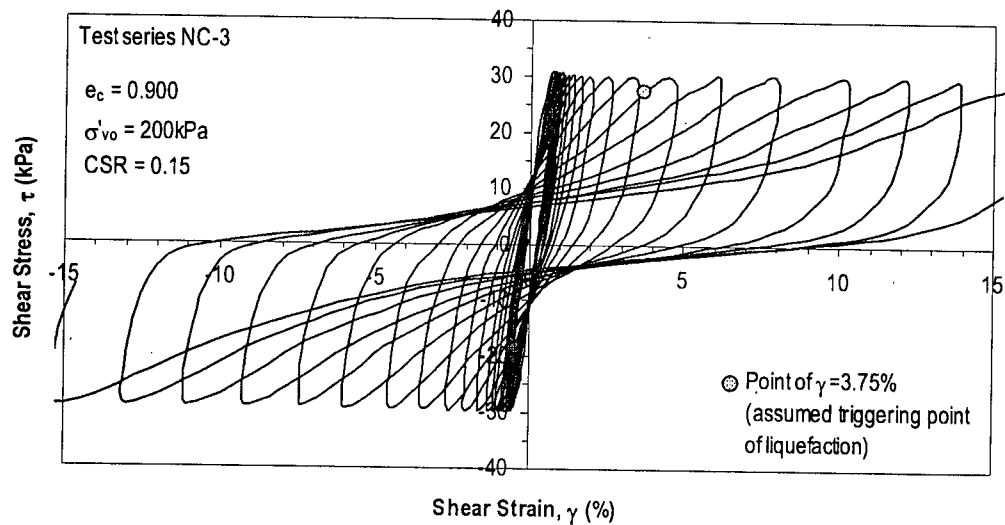


a)

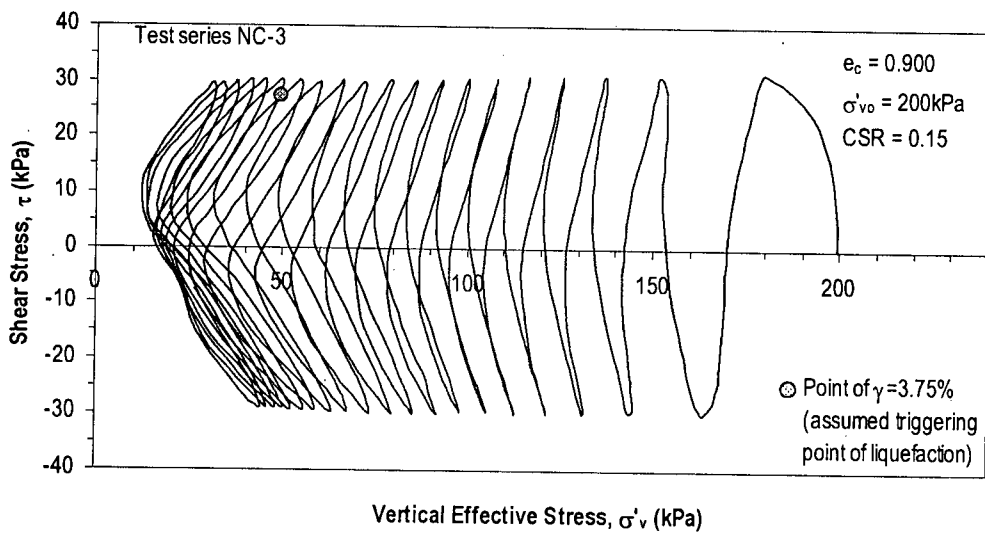


b)

Figure 4.17. Constant volume DSS test results on normally consolidated sample – Tests series NC-3 (CSR = 0.11, σ'_{vo} = 200 kPa). a) Stress-strain response. b) Stress-path.

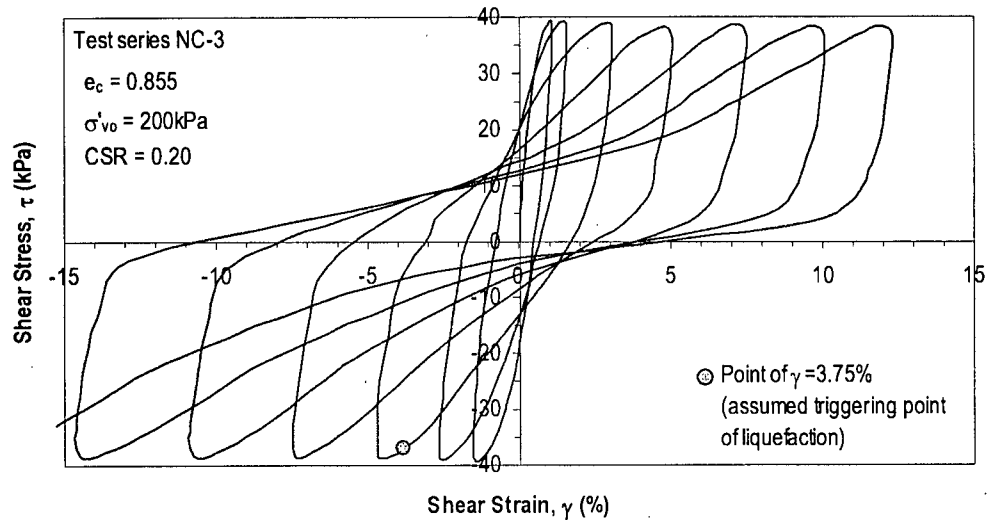


a)

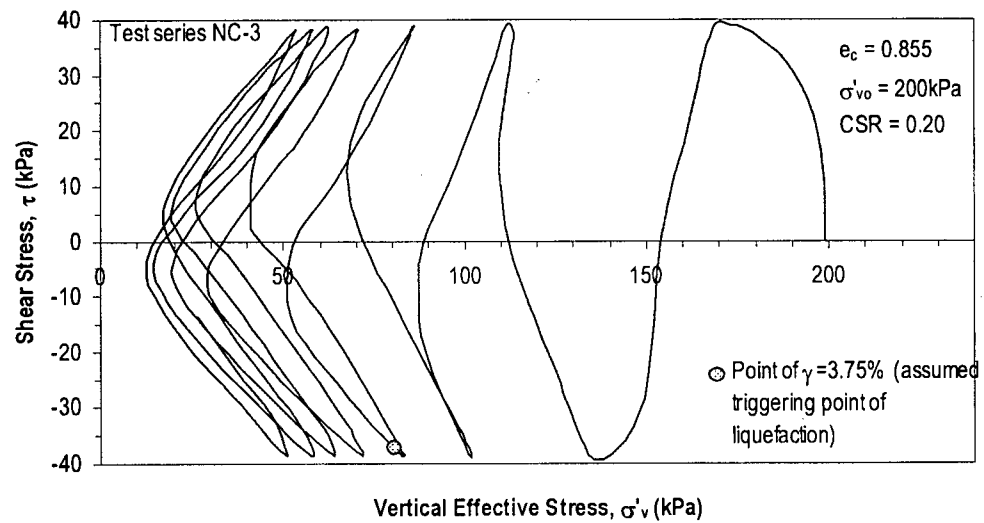


b)

Figure 4.18. Constant volume DSS test results on normally consolidated sample – Tests series NC-3 ($CSR = 0.15$, $\sigma'_{vo} = 200$ kPa). a) Stress-strain response. b) Stress-path.



a)



b)

Figure 4.19. Constant volume DSS test results on normally consolidated sample – Tests series NC-3 (CSR = 0.20, σ'_{v0} = 200 kPa). a) Stress-strain response. b) Stress-path.

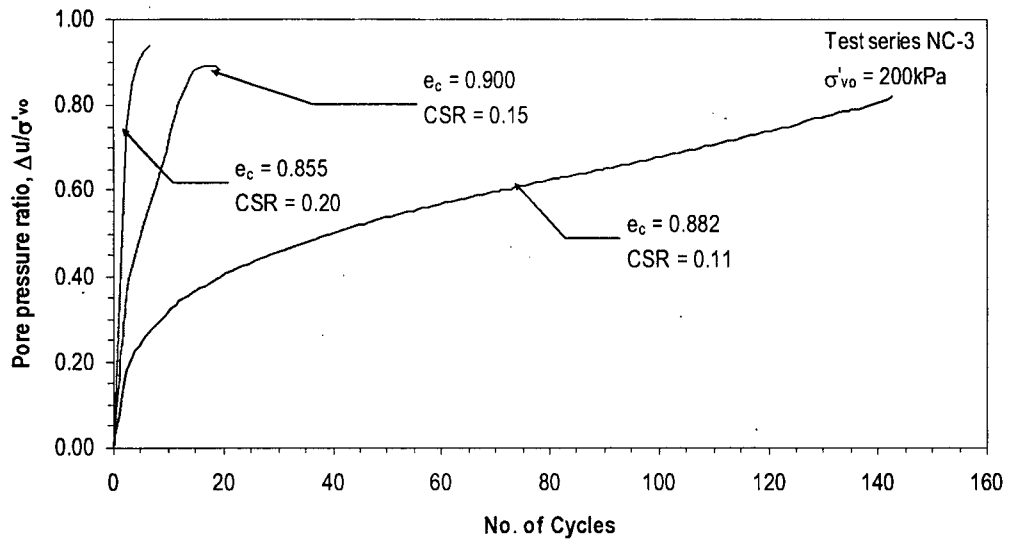


Figure 4.20. Cumulative pore water pressure during constant volume DSS test on normally consolidated sample – Tests series NC-3 ($\sigma'_{vo} = 200$ kPa).

counterpart response in series NC-1 and NC-3. It appears that the relatively preserved in-situ microstructure and possible aging effects in the specimens of test series NC-2 (tested at $\sigma'_{vo} = 85 \text{ kPa} \sim \sigma'_{v-in-situ}$) deliver a more dilative response in comparison to the specimens in test series NC-1 and NC-3 that would have been destructured to a higher degree during consolidation to σ'_{vo} levels above $\sigma'_{v-in-situ}$.

4.3.2.4 Degradation of Shear Stiffness During Cyclic Loading

The progressive strain development described above can also be examined in terms of the shear stiffness (G_{secant}) computed at peak stress amplitude points schematically presented in Figure 4.21. As may be noted, in addition to the peak stress amplitude points, G_{secant} was also computed at several points within the first-quarter cycle, starting at a $\gamma \sim 0.05\%$, to show the degradation of the shear stiffness commencing from relatively small-strain values (see inset of Figure 4.21). It is not possible to obtain the shear stiffness at very small strain (i.e., maximum shear modulus G_{max}) due to practical limitations in the measurement of very small strains in the DSS device. Figure 4.22 shows the shear stiffness degradation for the specimens tested with normally consolidated initial conditions that suffered shear stiffness degradation (i.e., reached liquefaction). The value of G_{secant} drops significantly in the first part of strain accumulation ($\gamma < 1\%$); almost a 20-fold reduction in the shear stiffness can be noted with strain accumulation up to 3.75%.

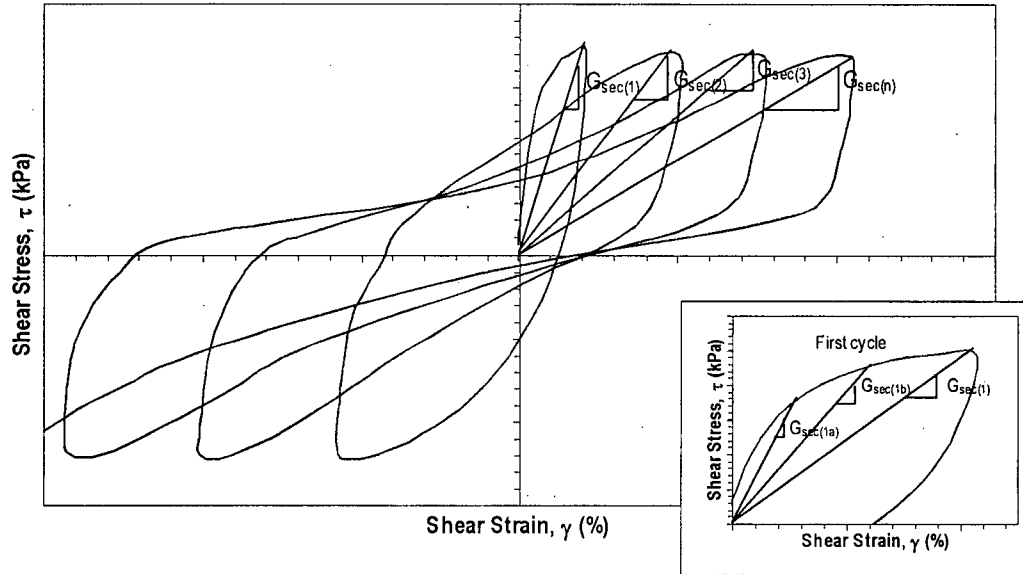


Figure 4.21. Schematic representation of degradation of shear stiffness during cyclic loading.

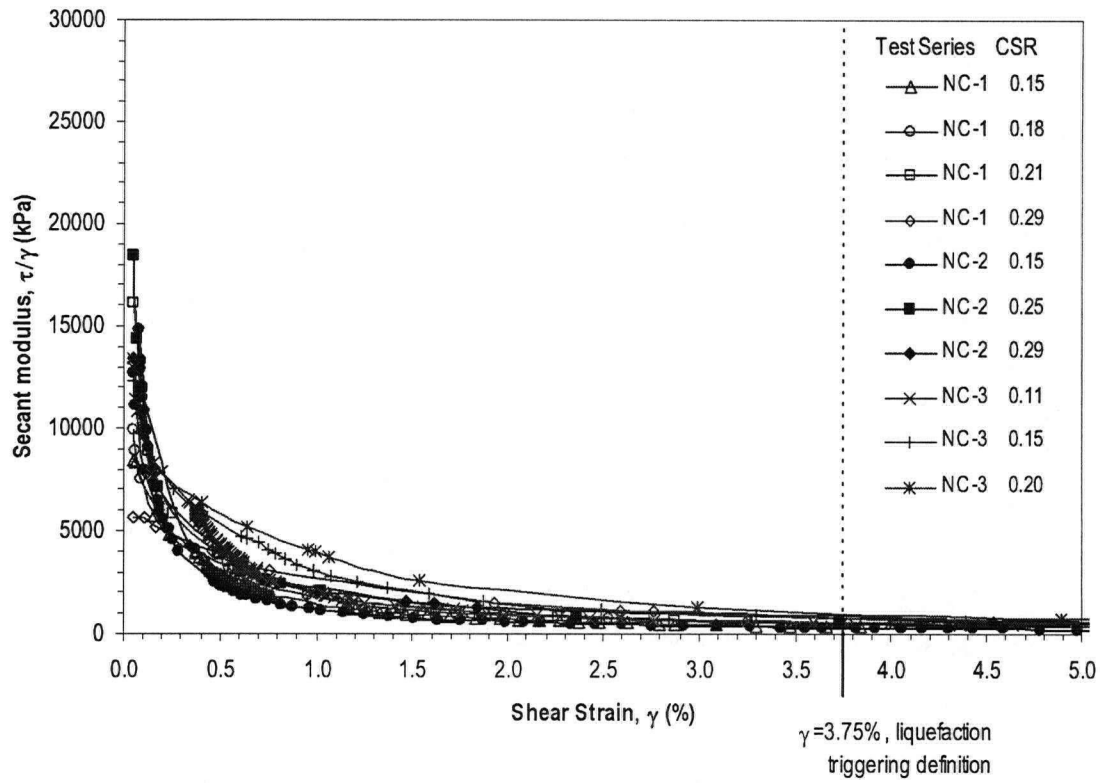


Figure 4.22. Modulus degradation for samples tested in the DSS on normally consolidated state.

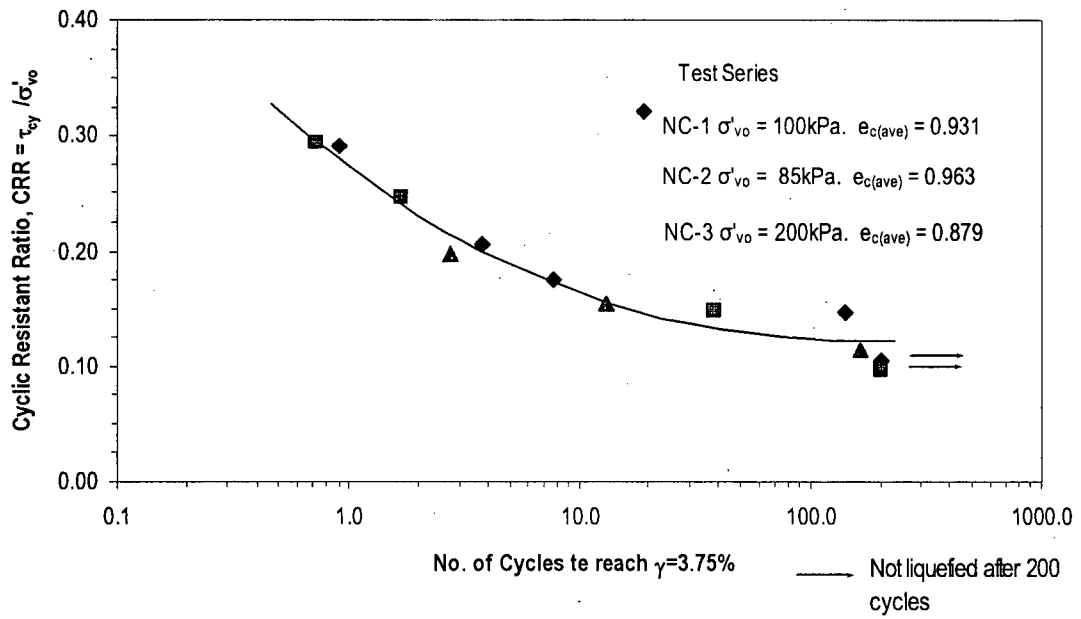


Figure 4.23. Cyclic resistant ratio versus number of cycles to reach liquefaction for specimens tested on the DSS on normally consolidated conditions.

4.3.2.5 *Cyclic Resistance Ratio*

Figure 4.23 shows the cyclic resistance ratio versus number of cycles required to reach liquefaction (as previously defined by the strain criteria $\gamma = 3.75\%$) for all test series of normally consolidated samples (NC-1, NC-2 and NC-3). Samples that did not reach the established liquefaction criteria are also plotted, but identified with an arrow.

The test results suggest that the cyclic resistance ratio (CRR) versus N_L relationship for channel-fill Fraser River silt has no significant sensitivity to the confining pressures up to 200 kPa. Although a small reduction in the CRR for the sample tested $\sigma'_{vo} = 200$ kPa can be observed, it is not judged a significant reduction considering the natural variability of the silt deposit. This implies that the generation of shear strains during undrained cyclic loading is governed only by the mobilized shear stress ratio. A similar behaviour pattern has been observed by Zergoun and Vaid (1994) for normally consolidated clay in cyclic triaxial tests, and it is in accord with the typical shear behavioural frameworks noted for normally consolidated clay (Atkinson and Bransby, 1978). Ishihara et al. (1981) have found a similar trend for undisturbed samples of tailings from zinc-lead mines and gold-silver mines.

In case of sands, the CRR for a given relative density has been noted to decrease with increasing confining stress, which is accounted for using the parameter K_σ in commonly used liquefaction evaluation procedures (Youd et al., 2001; Seed and Harder, 1990). The low prominence of the K_σ -effect in the observed response in Figure 4.23 with respect to the cyclic resistance ratio, seem to suggest that channel-fill Fraser River silt exhibits a more “clay-like” response.

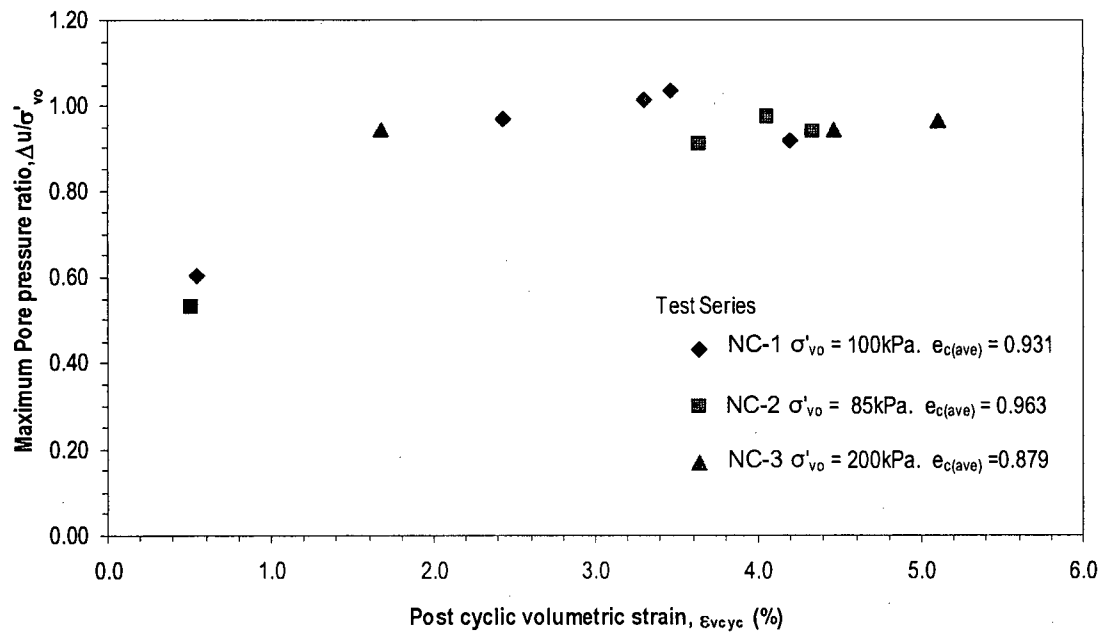


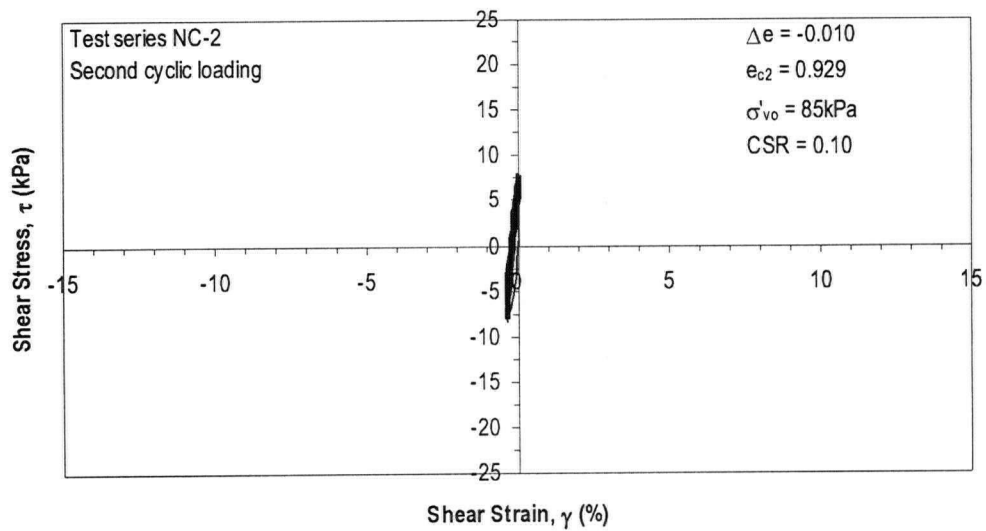
Figure 4.24. Post-cyclic volumetric strain vs. maximum pore water pressure ratio developed during cyclic loading. Test series NC-1, NC-2 and NC-3

4.3.2.6 Post-cyclic Re-consolidation Response

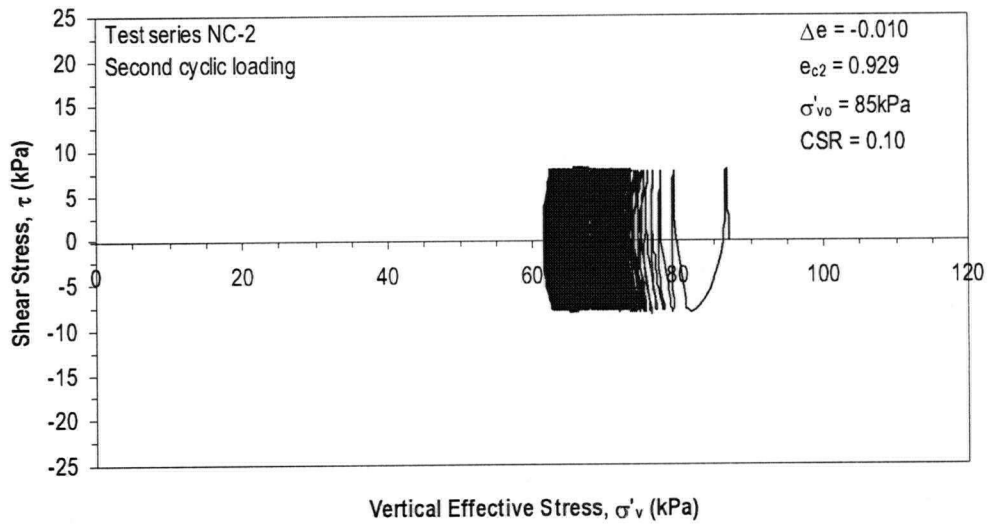
The specimens in test series NC-1 through NC-3 were subject to post-cyclic re-consolidation to the original σ'_{vo} value after completion of the first cyclic loading. Figure 4.24 shows the variation of volumetric strain during re-consolidation with the maximum pore water pressure ratio developed during the previous cyclic loading. The specimens that experienced high pore water pressure ratios ($r_u \sim 100\%$), suffered significant post-cyclic consolidation strains (in the order of 2% to 5%), while the samples that just reached r_u values in the order of 50% developed relatively smaller post-cyclic consolidation strains. The observed volumetric strains in the case of silt specimens that developed high r_u values seem to be higher than those typically observed by others from post-cyclic consolidation of sands (Tokimatsu and Seed, 1987; Cetin et al., 2004). The observed considerable volume changes are likely a reflection of the significant changes in the particle structure experienced by the specimens due to cyclic loading.

4.3.2.7 Effects of Repeated Cyclic Loading (Re-liquefaction)

Normally consolidated samples of test series NC-1 and NC-2 were subject to a second cyclic loading after the post-cyclic consolidation. Figures 4.25 to 4.28 show the stress-strain and stress-path response of the second cyclic loading for the samples tested at $\sigma'_{vo} = 85$ kPa (test series NC-2). Corresponding results obtained during first cyclic loading of these tests are shown in Figures 4.12 to 4.15. The specimen tested at $CSR=0.10$ did not liquefy and experienced similar cyclic response to the first cyclic loading. Nevertheless, this specimen experienced lesser increase in the pore water pressure (decrease in σ'_v) than the first cyclic loading for the same number of cycles (Figure 4.29). The samples tested at higher CSR values

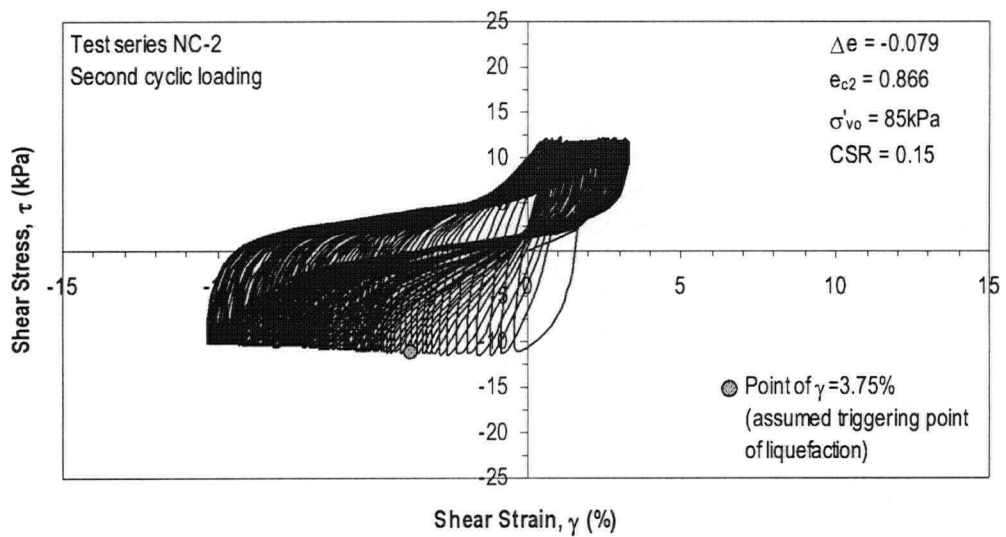


a)

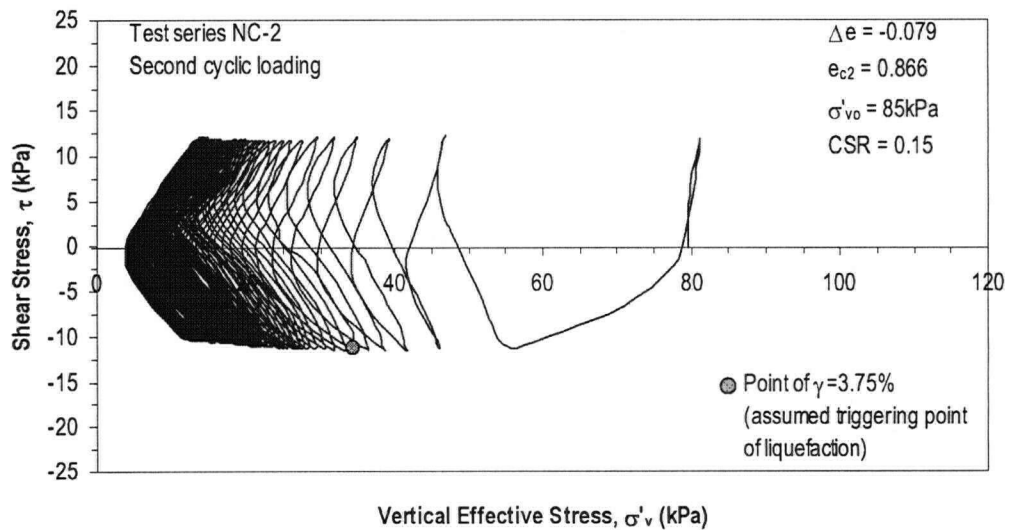


b)

Figure 4.25. Constant volume DSS test results on normally consolidated sample – Tests series NC-2 ($\text{CSR} = 0.10$, $\sigma'_{v0} = 85 \text{ kPa}$) – Second cyclic loading. a) Stress-strain response. b) Stress-path.

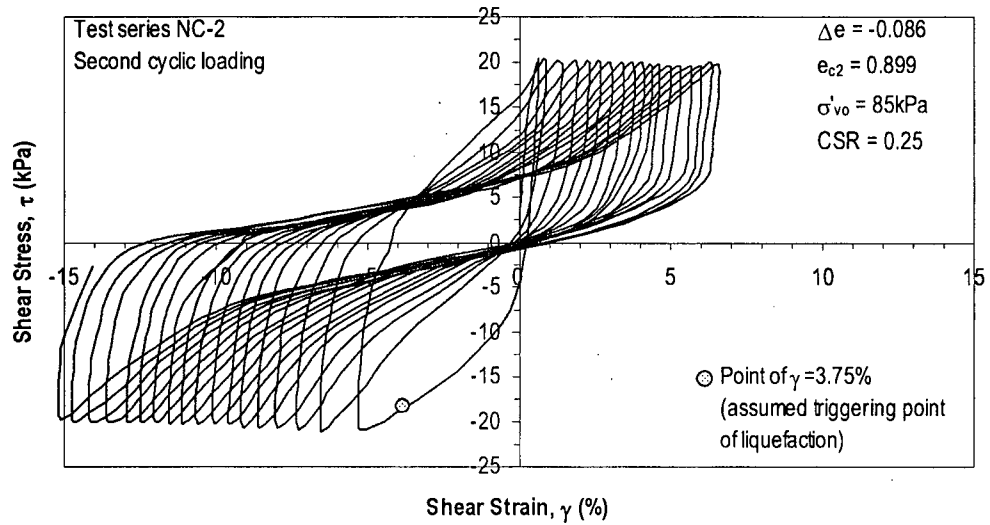


a)

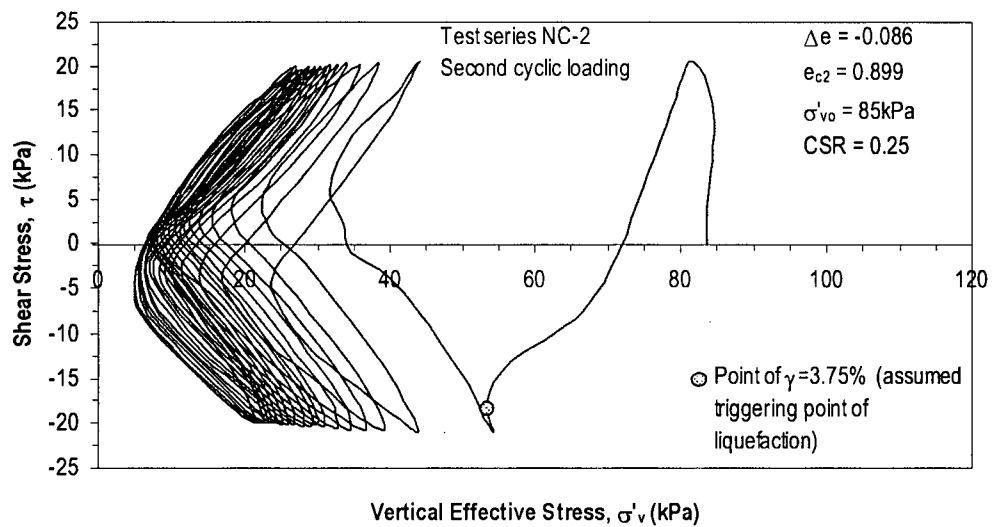


b)

Figure 4.26. Constant volume DSS test results on normally consolidated sample – Tests series NC-2 (CSR = 0.15, $\sigma'_{v0} = 85$ kPa) – Second cyclic loading. a) Stress-strain response. b) Stress-path.

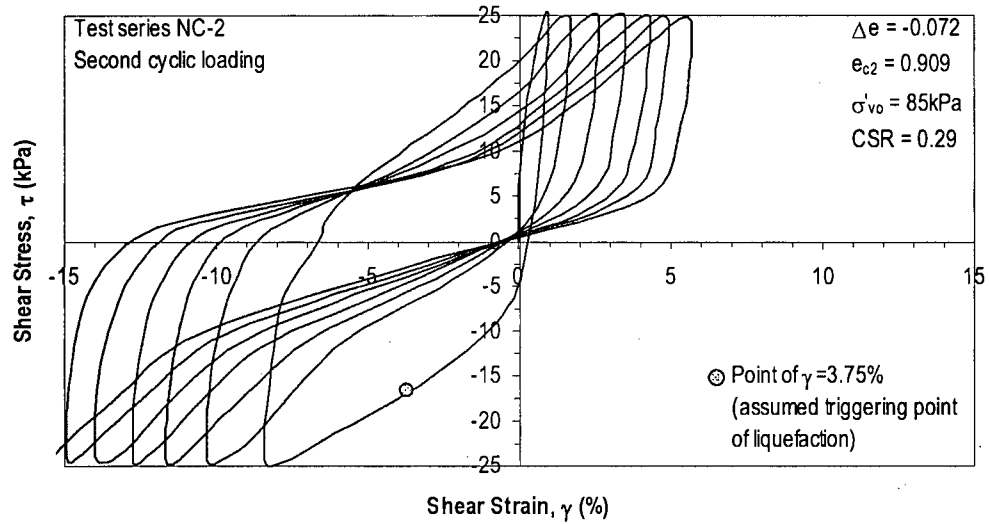


a)

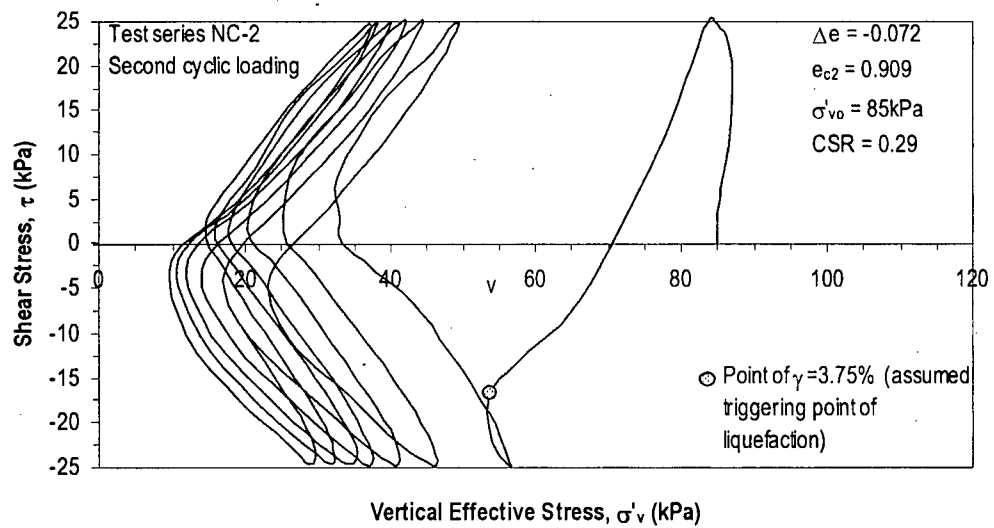


b)

Figure 4.27. Constant volume DSS test results on normally consolidated sample – Tests series NC-2 (CSR = 0.25, $\sigma'_{v0} = 85$ kPa) – Second cyclic loading. a) Stress-strain response. b) Stress-path.



a)



b)

Figure 4.28. Constant volume DSS test results on normally consolidated sample – Tests series NC-2 ($CSR = 0.29$, $\sigma'_{vo} = 85$ kPa) – Second cyclic loading. a) Stress-strain response. b) Stress-path.

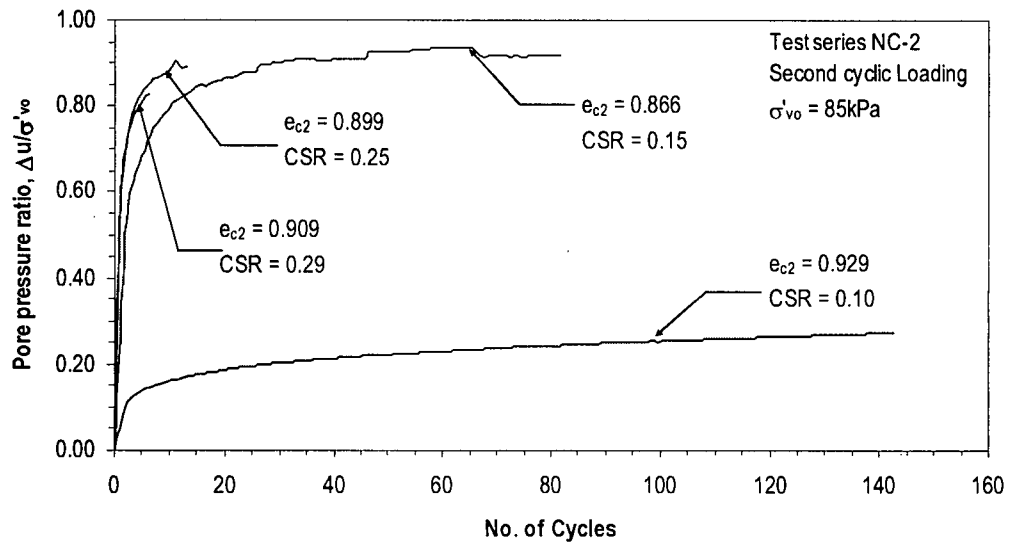


Figure 4.29. Cumulative pore water pressure during constant volume DSS test on normally consolidated sample – Tests series NC-1 ($\sigma'_{vo} = 85\text{ kPa}$) – Second cyclic loading.

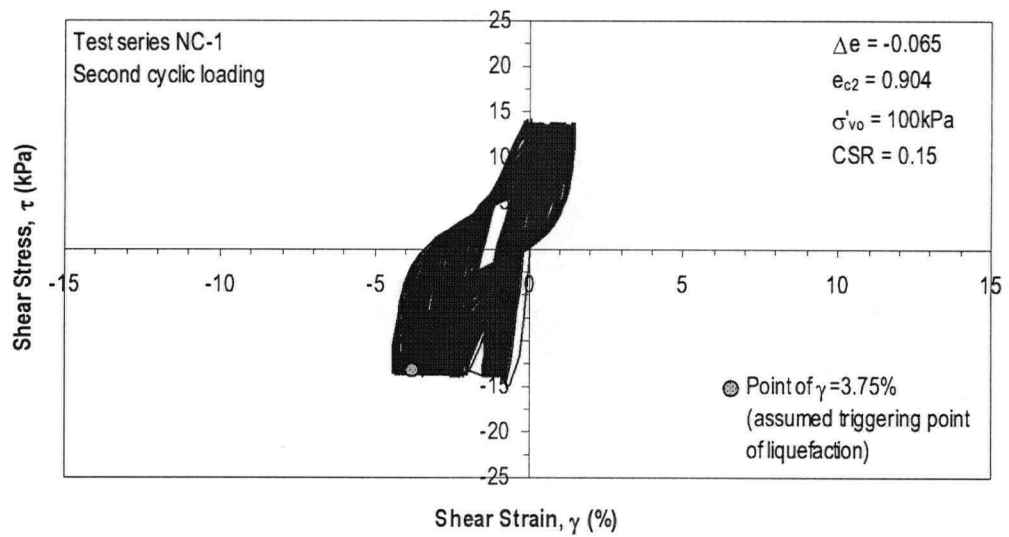
experienced a slight dilative response during the “loading” part of the 1st cycle (i.e., 1st quarter cycle); however a very significant contractive response (pore water pressure development) was noted during the immediately followed cyclic loading. It appears that the resulting rapid drop in effective stress caused the sample to perform softer in comparison to the corresponding loading point in the first phase of cyclic loading. This effect caused the specimen to reach the pre-defined liquefaction triggering strain ($\gamma = 3.75\%$) in fewer cycles in the second cyclic phase than in the first cyclic loading phase. It is notable that this observed response is despite the void ratio reduction due to consolidation at the end of first cyclic phase. It is also interesting to note that with increasing the number of cycles, the specimens began to behave in a stiffer manner, and they all required more cycles to reach larger cyclic strain levels. For example, the sample tested at $CSR=0.25$ required one and a half cycle to reach $\gamma = 3.75\%$ and 7 cycles to reach $\gamma = 15\%$ in the first cyclic loading phase (see Figure 4.14). The same sample, during the second cyclic loading phase required less than one cycle to reach $\gamma = 3.75\%$ and 18 cycles to reach $\gamma = 15\%$ (Figure 4.27).

Cumulative equivalent excess pore water pressure during the second cyclic loading of the specimens of test series NC-2 is presented in Figure 4.29. The response is similar to the observed during the first cyclic loading phase, with a “cyclic mobility” type of response. The samples tested at high values of CSR reached high r_u values; however, this r_u values reached during the second cyclic loading are smaller than those observed during the first phase of cyclic loading.

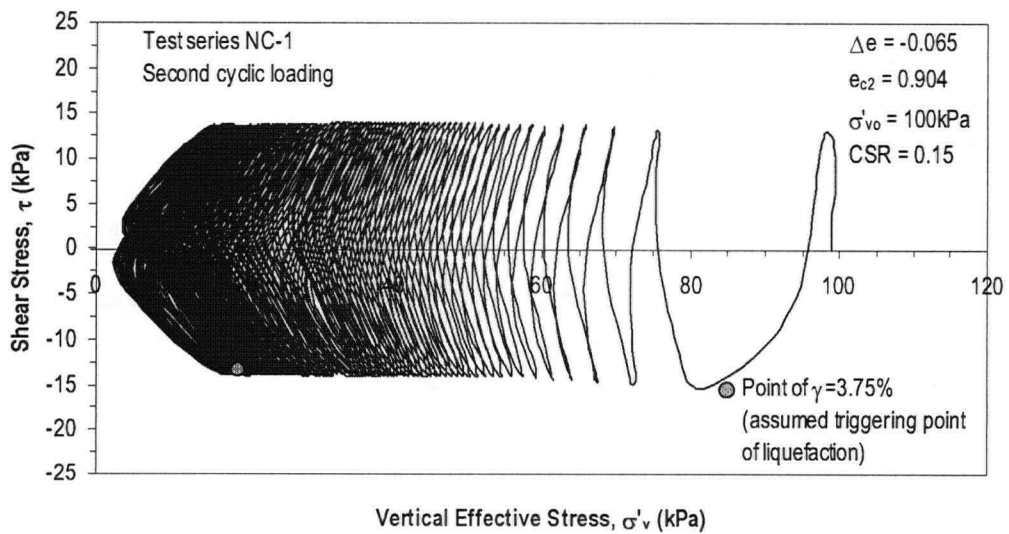
Figures 4.30 to 4.33 present the stress-strain and stress path for the second cyclic loading phase of test series NC-1. Similar to the observations on test series NC-2, the samples exhibit slight dilation in the first quarter cycle and significant contraction in the unloading part of the cycle.

Again, the specimens reached liquefaction ($\gamma = 3.75\%$) in lesser number of cycles than during the first cyclic loading and more cycles to reach higher values of cyclic shear strain (see Table 4.3). Pore water pressure accumulated during the second cyclic loading of test series NC-2 is presented in Figure 4.34.

Figure 4.35 presents the cyclic resistance ratio with the number of cycles to reach shear strain $\gamma = 3.75\%$ for the first cyclic loading phase (closed symbols) and second cyclic loading phase (open symbols). Clearly, the number of cycles of loading required to achieve $\gamma = 3.75\%$ during the second cyclic phase is consistently less than first cyclic phase, despite the densification that took place during re-consolidation. It appears that the decrease in cyclic shear resistance (CRR) due to degradation of particle fabric as a result of previous shearing has overshadowed any gain in CRR that would have taken place due to reduction of void ratio during consolidation. The observed behaviour is in accord with the previous findings by others on the response of water-pluviated samples of sand subjected to large pre-shearing (Finn et al., 1970; Ishihara and Okada, 1982; Vaid et al., 1989, Sriskandakumar, 2004). Nevertheless, with large shear strains, it appears that some strengthening in the soil fabric takes place during latter part of second cyclic phase.

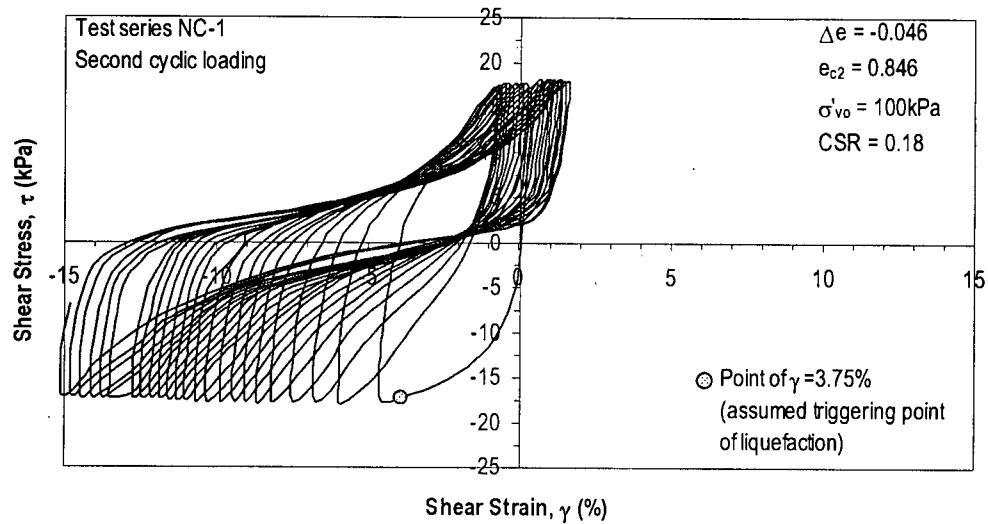


a)

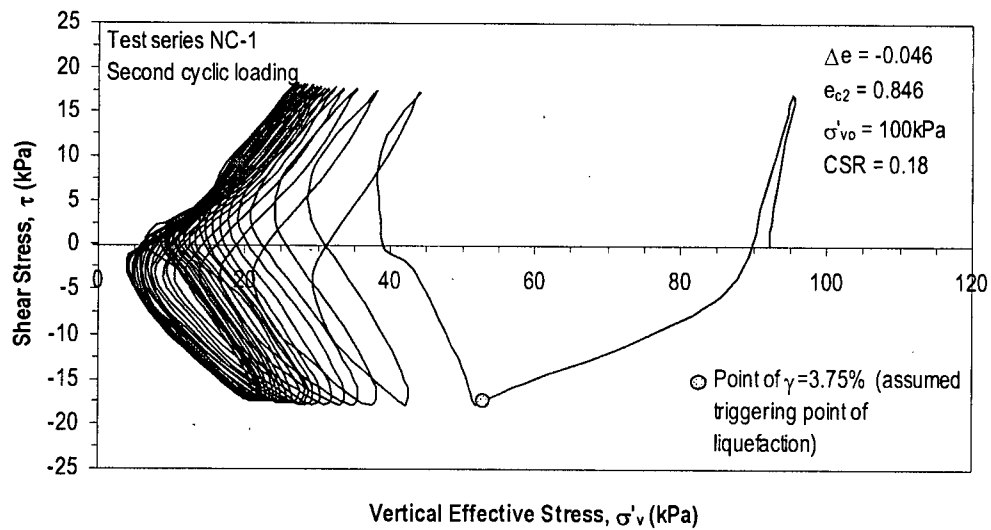


b)

Figure 4.30. Constant volume DSS test results on normally consolidated sample – Tests series NC-1 ($\text{CSR} = 0.15$, $\sigma'_{vo} = 100 \text{ kPa}$) – Second cyclic loading. a) Stress-strain response. b) Stress-path.

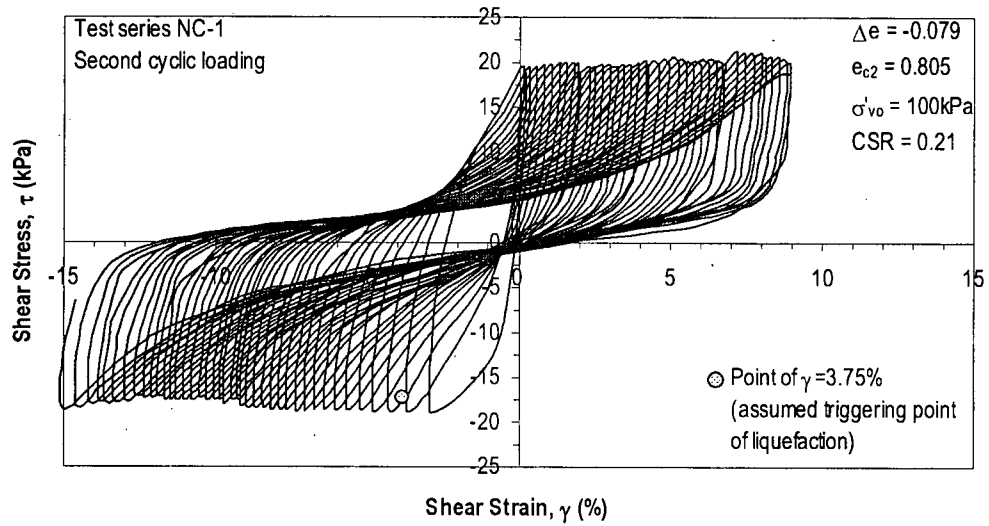


a)

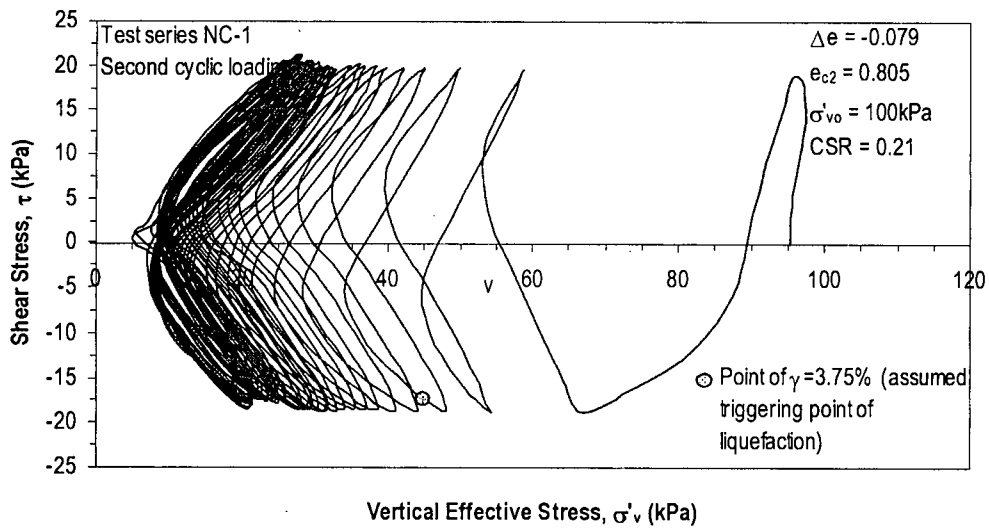


b)

Figure 4.31. Constant volume DSS test results on normally consolidated sample – Tests series NC-1 (CSR = 0.18, $\sigma'_{v0} = 100$ kPa) – Second cyclic loading. a) Stress-strain response. b) Stress-path.

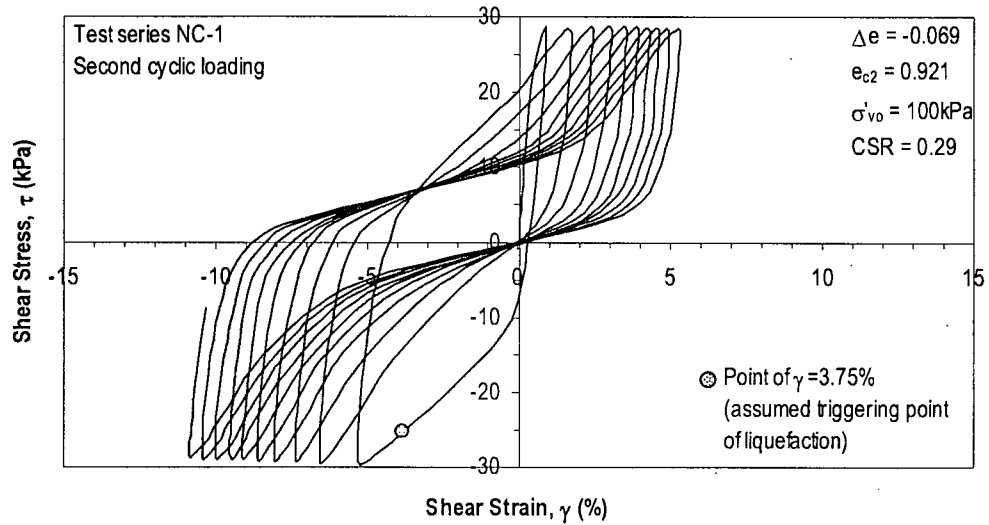


a)

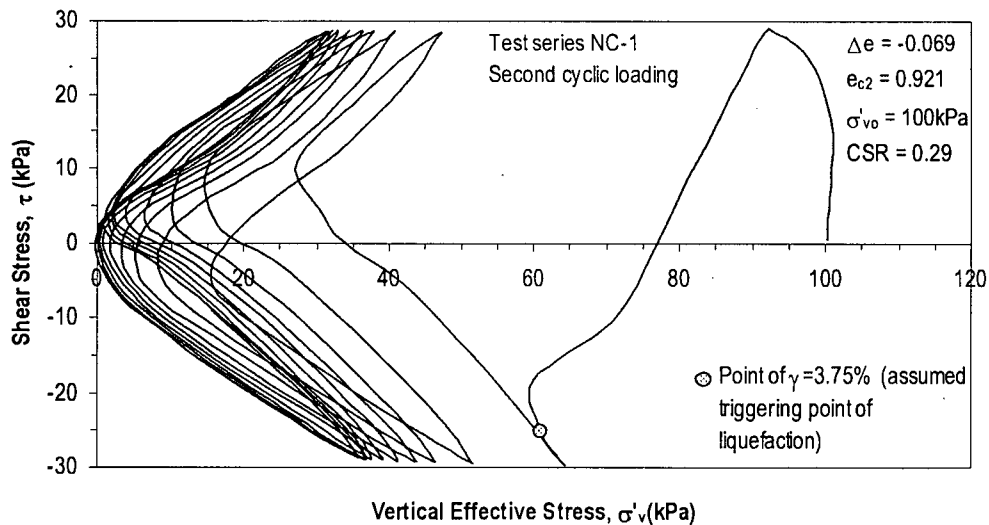


b)

Figure 4.32. Constant volume DSS test results on normally consolidated sample – Tests series NC-1 (CSR = 0.21, $\sigma'_{v0} = 100$ kPa) – Second cyclic loading. a) Stress-strain response. b) Stress-path.



a)



b)

Figure 4.33. Constant volume DSS test results on normally consolidated sample – Tests series NC-1 (CSR = 0.29, σ'_{v0} = 100 kPa) – Second cyclic loading. a) Stress-strain response. b) Stress-path.

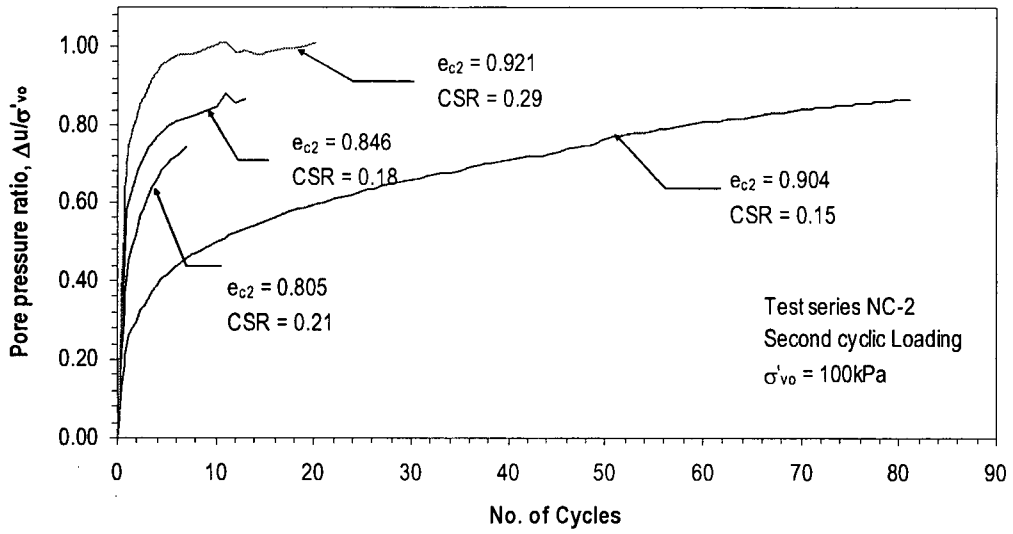
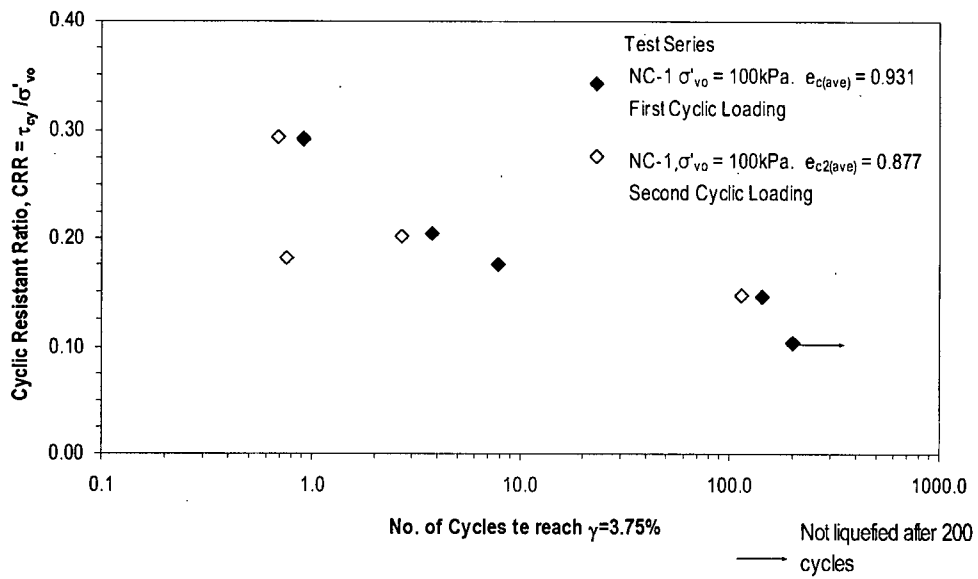
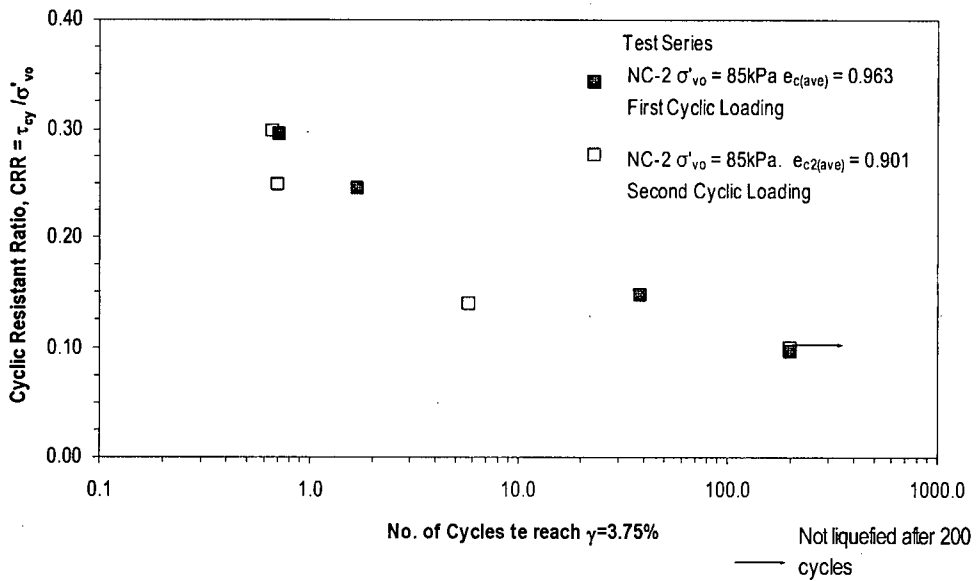


Figure 4.34. Cumulative pore water pressure during constant volume DSS test on normally consolidated sample – Tests series NC-1 ($\sigma'_{vo} = 100 \text{ kPa}$) – Second cyclic loading.



a)



b)

Figure 4.35. Cyclic resistant ratio versus number of cycles to reach liquefaction for samples tested on the DSS on normally consolidated state. Effects of repeated cyclic loading. a) Test Series NC-1. b) Test Series NC-2.

4.3.2.8 Post-cyclic Consolidation Response after Re-Liquefaction

Figure 4.36 shows the variation of post-cyclic volumetric strains during re-consolidation with respect to the maximum pore water pressure generated during the second cyclic loading (open symbols), and compared to the generated during the first cyclic loading phase (closed symbols). It may be noted that the specimens have suffered further settlements after the second cyclic loading (i.e., post-cyclic consolidation strains ~ 0.12 to 2.8%). Although less than those observed in the 1st cyclic loading, it is clear that the potential for this additional settlement was generated purely by the cyclic shearing action imparted during the second cyclic phase. This can be considered as a reflection of extensive particle rearrangement suffered by the silt specimens during cyclic loading.

4.3.3 Cyclic Loading Response of Overconsolidated Specimens

Three constant volume cyclic DSS tests series (OC-1, OC-2 and OC-3) were conducted on overconsolidated specimen of channel-fill Fraser River silt. The specimens in all the test series were at a condition of $\sigma'_{vo} = 100$ kPa prior to the commencement of cyclic loading. In a given test series, the specimens consolidated to achieve different OCR levels were subjected to an identical CSR level during the cyclic loading phase.

Figures 4.37 and 4.38 show the stress-strain and stress-path response obtained from tests series OC-1 (i.e., CSR = 0.15 applied on specimens consolidated to OCR ~ 1.2 and 1.5). The results from counterpart tests with CSR = 0.15 and OCR = 1 are available for comparison in Figure 4.7. The corresponding development of r_u with number of cycles is given in Figure 4.39.

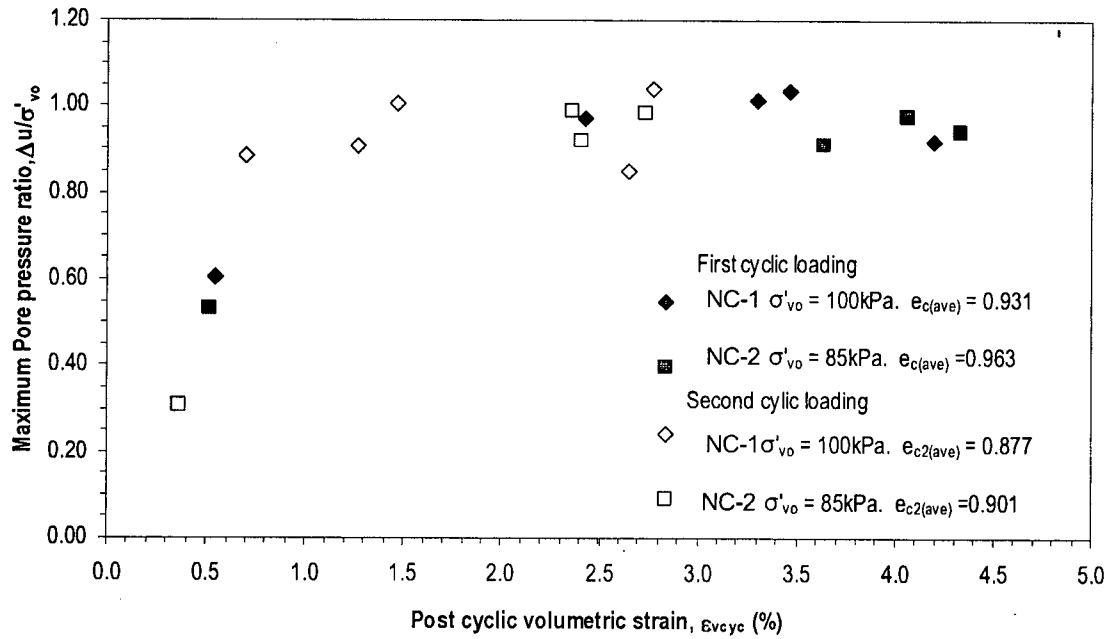
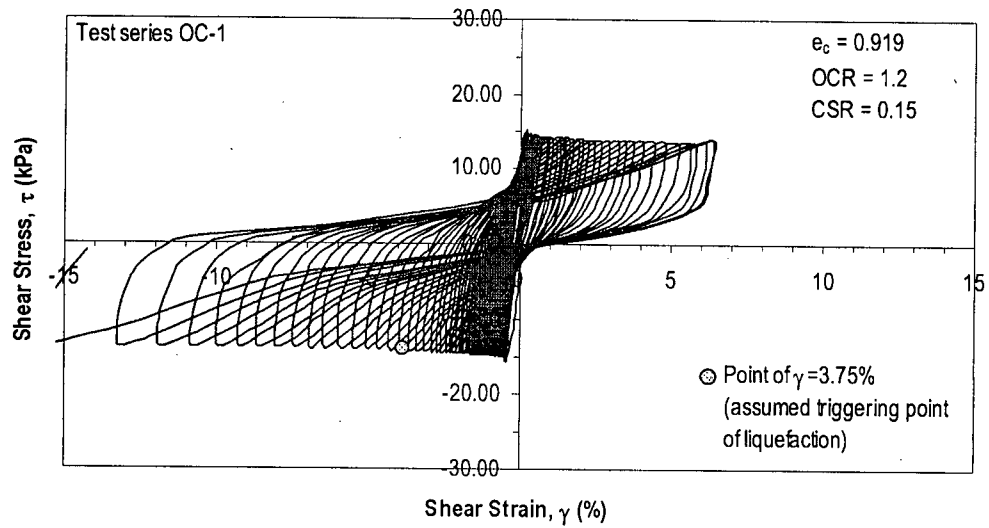
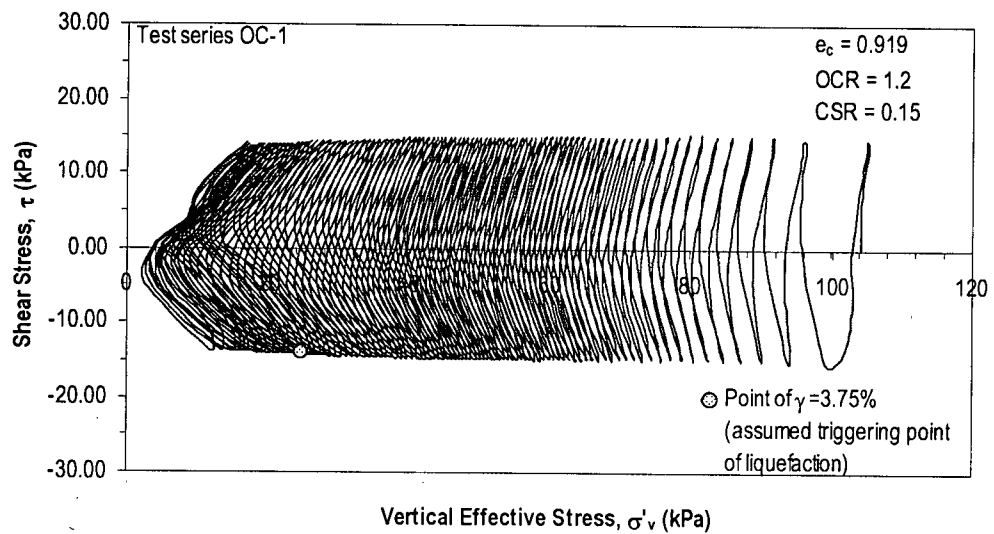


Figure 4.36. Post-cyclic volumetric strain vs. maximum pore water pressure ratio developed during first and second cyclic loading. Test series NC-1 and NC-2.

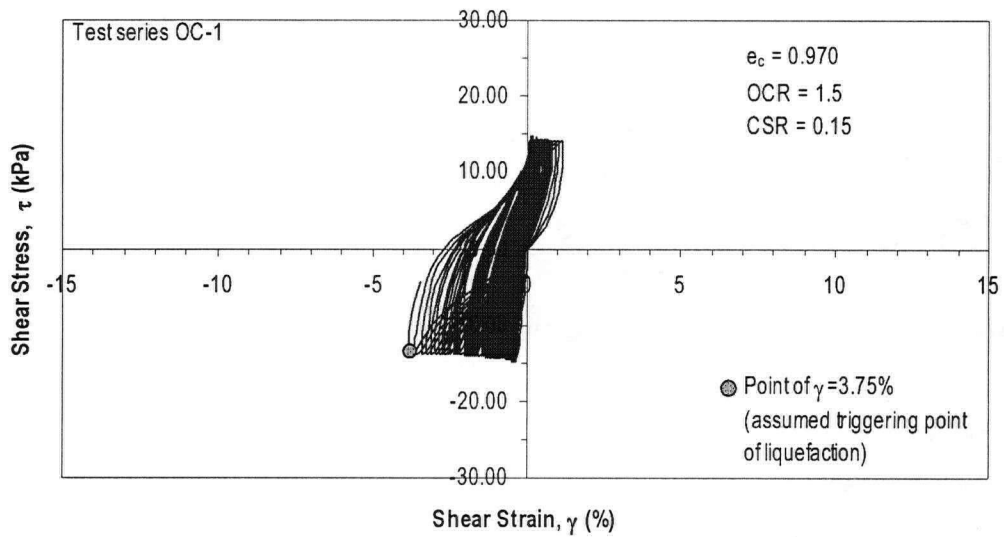


a)

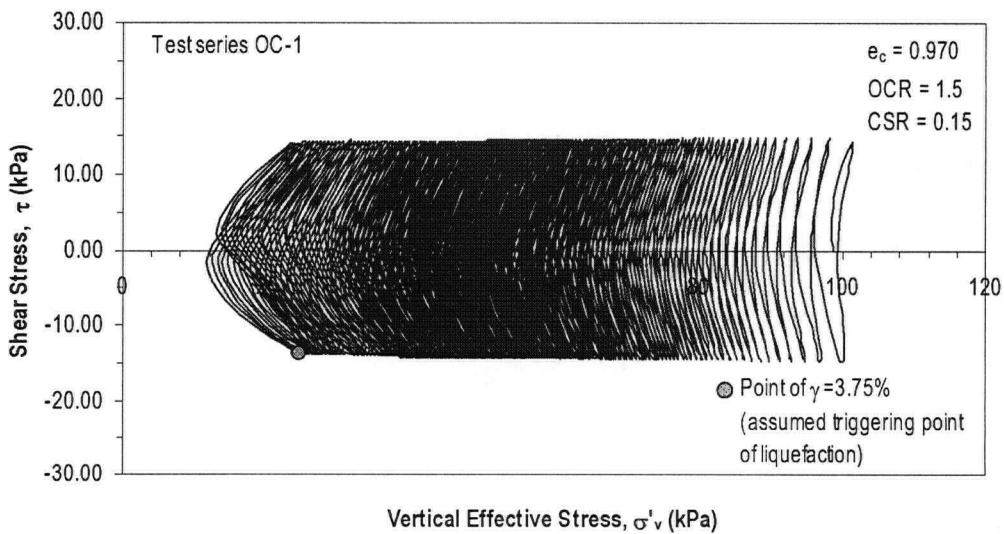


b)

Figure 4.37. Constant volume DSS test results on overconsolidated sample – Tests series OC-1 (OCR = 1.2). a) Stress-strain response. b) Stress-path.



a)



b)

Figure 4.38. Constant volume DSS test results on overconsolidated sample – Tests series OC-1 (OCR = 1.5). a) Stress-strain response. b) Stress-path.

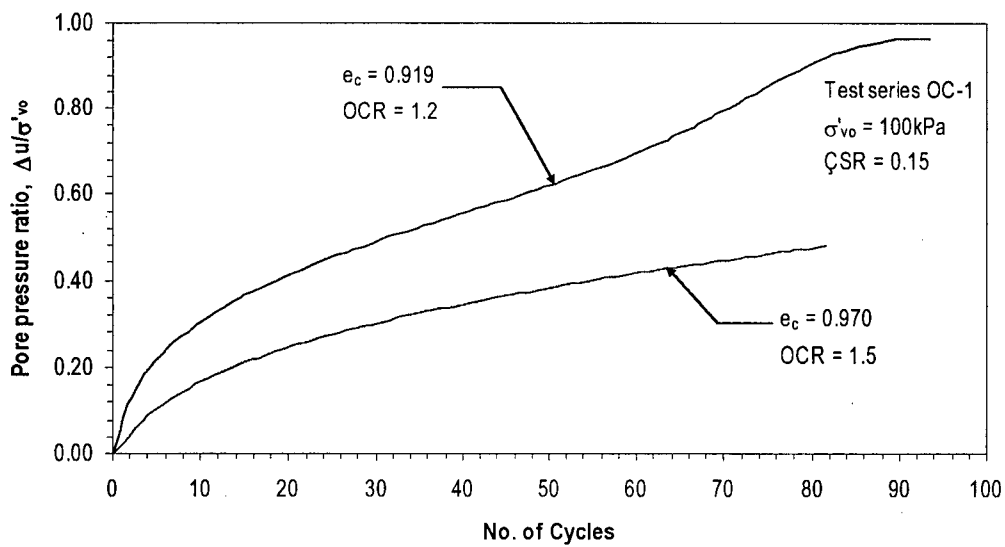
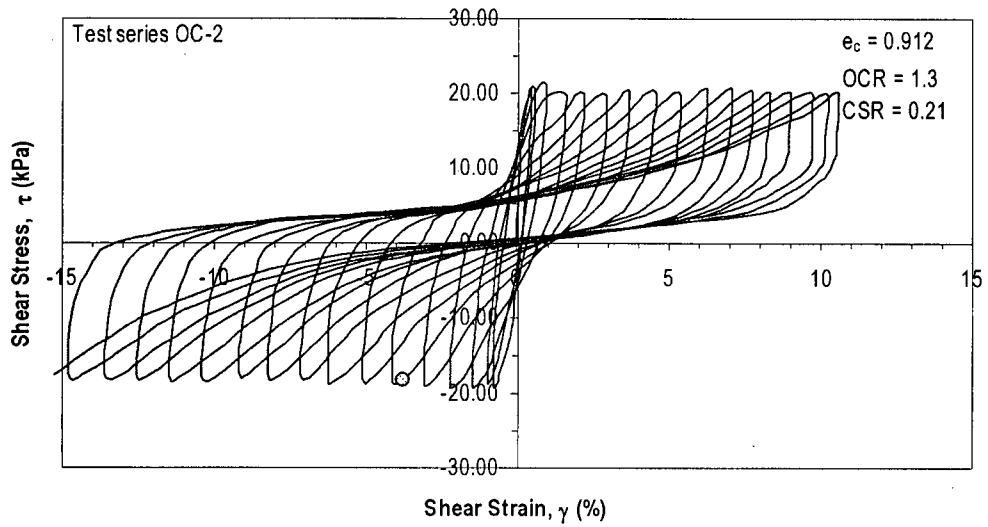


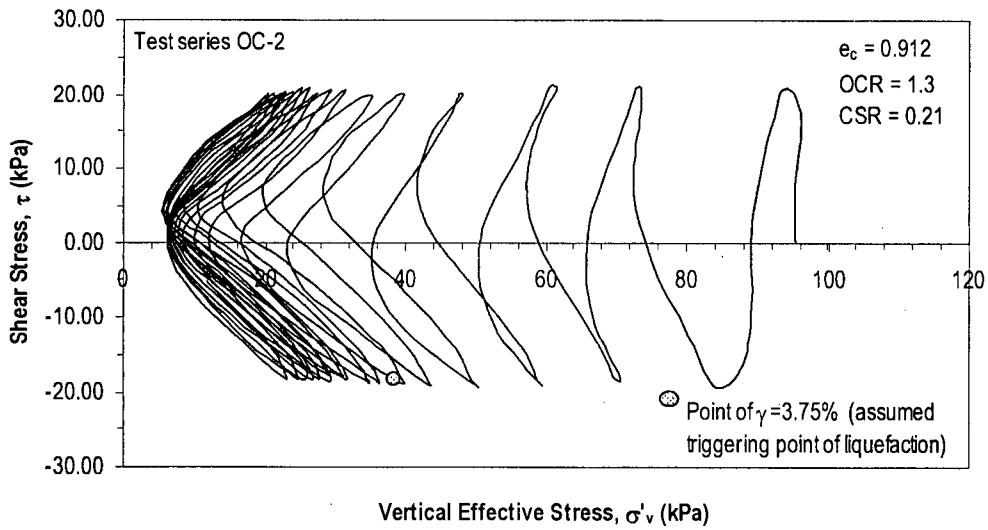
Figure 4.39. Cumulative pore water pressure during constant volume DSS test on overconsolidated samples – Tests series OC-1 (CSR = 0.15).

It can be noted that the OC specimens also display the “cyclic mobility” type of response similar to those observed for the NC specimen. The stress-paths of both OC specimens show dilative response in the first half cycle followed by contractive response in the second half cycle. This is notably different from the observed behaviour for the NC specimen where the first cycle showed a predominantly contractive response in both loading and unloading parts of the first half cycle (see Figure 4.7). The specimen tested with an OCR = 1.2 (Figure 4.37) reached the pre-established strain criteria for liquefaction in 77 cycles, and with additional loading in the order of 90 cycles, the shear strains accumulated up to a value close 15%; the associated increase in pore water pressure caused the r_u to reach a value close to 100%. In contrast, the sample tested at a higher OCR value (Figure 4.38), required 180 cycles to achieve shear strain $\gamma = 3.75\%$. This specimen also exhibited gradual build-up of excess pore water pressure, in this, however, only an $r_u \sim 85\%$ was reached even after subjecting the specimen to 180 cycles (see Figure 4.39).

Results for the test series OC-2 (with CSR ~ 0.20) are shown in Figures 4.40 to 4.45. Again, all samples, tested at CSR ~ 0.20 , show a more dilative response, commencing from the first cyclic loading, compared to those observed for the counterpart normally consolidated specimens (see Figure 4.9). Clearly, the dilatancy becomes more evident for higher values of OCR. Samples tested at OCR values between 1.3 and 1.9 (Figures 4.40 to 4.44) experienced liquefaction (i.e., reached $\gamma = 3.75\%$) with number of cycles to liquefaction N_L ranging between 6 and 136. However, the specimen with an OCR = 2.1 (Figure 4.45), did not develop shear strains more than 0.9% even after the application of 200 cycles. For this specimen, r_u did not reach high values compared to the samples tested with lower values of OCR in the same test series.

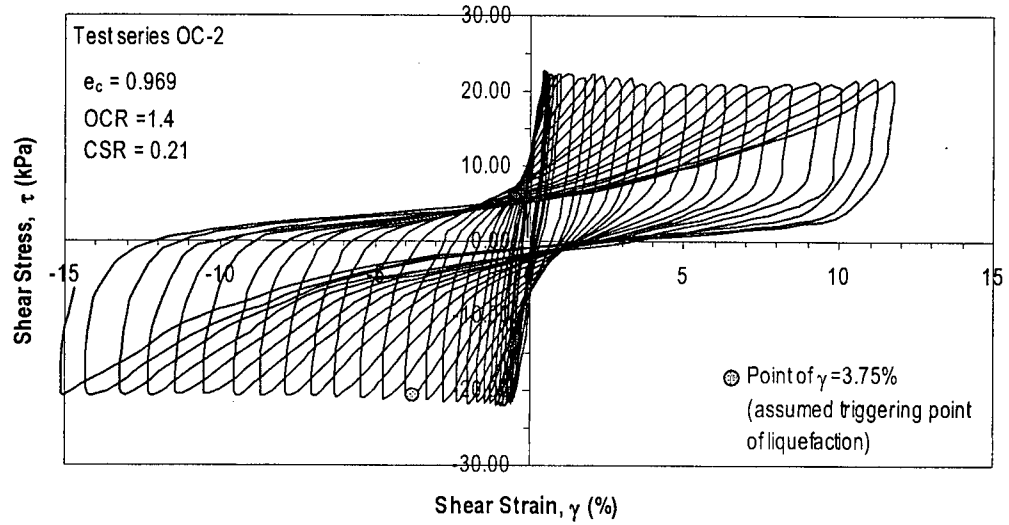


a)

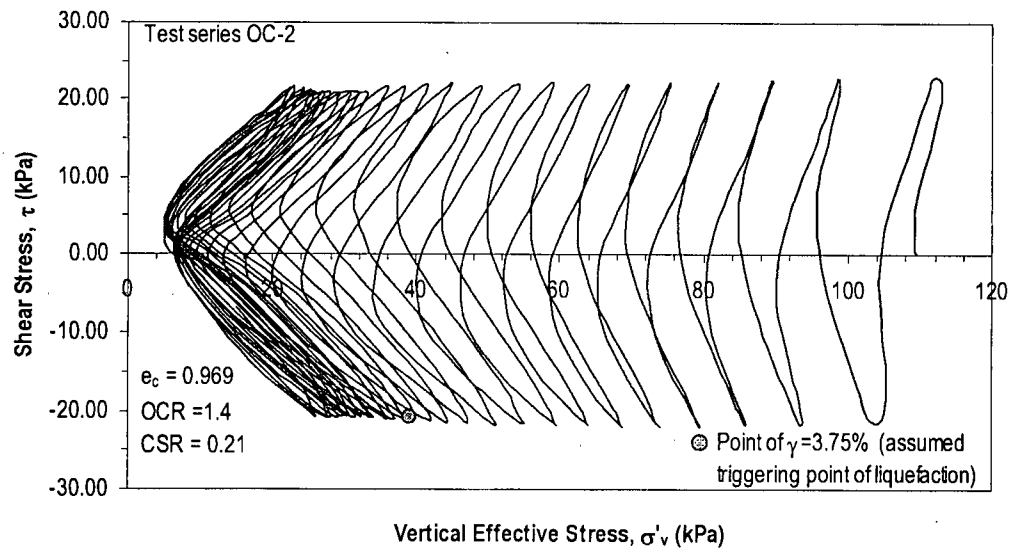


b)

Figure 4.40. Constant volume DSS test results on overconsolidated sample – Tests series OC-2 (OCR = 1.3). a) Stress-strain response. b) Stress-path.

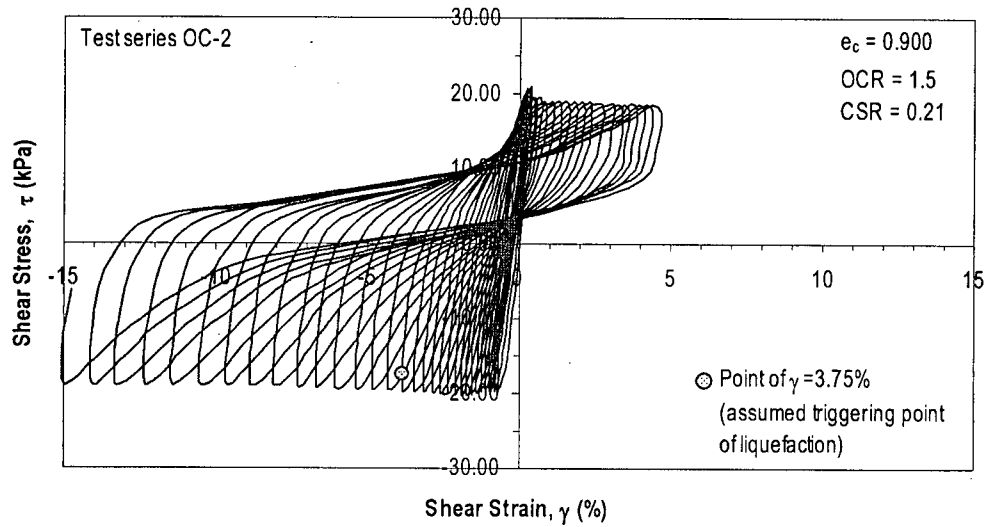


a)

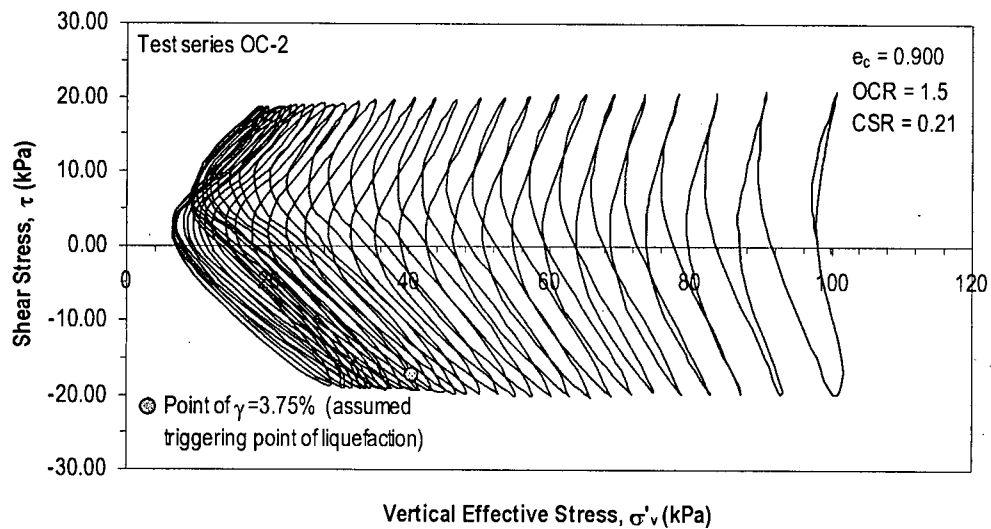


b)

Figure 4.41. Constant volume DSS test results on overconsolidated sample – Tests series OC-2 (OCR = 1.4). a) Stress-strain response. b) Stress-path.

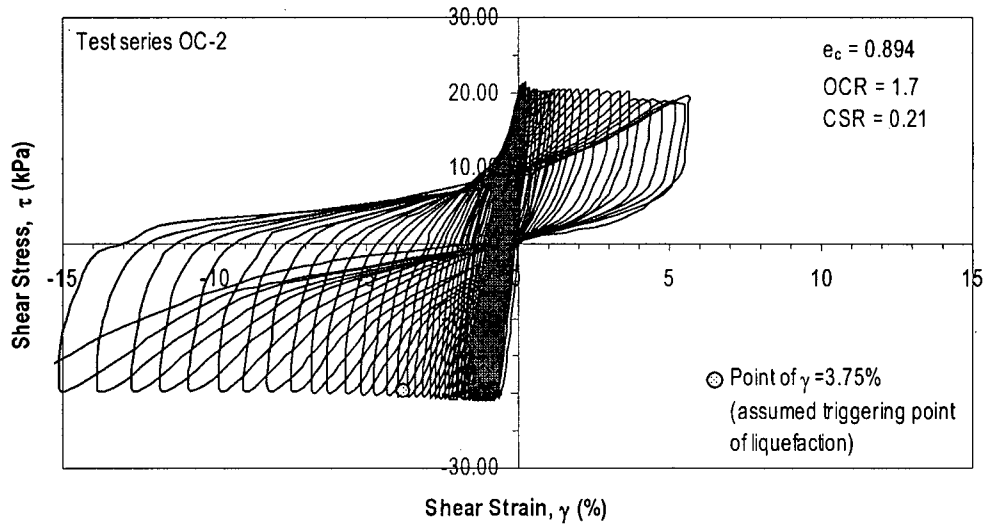


a)

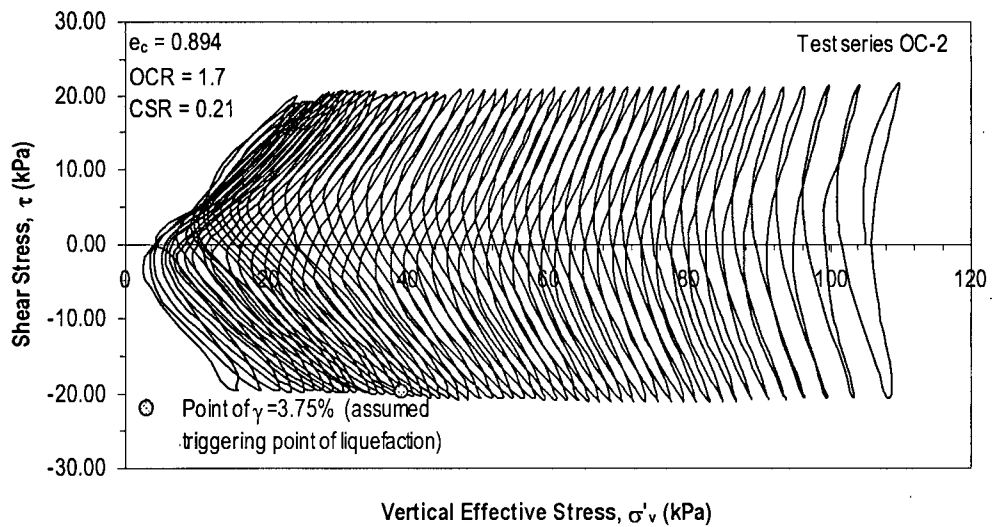


b)

Figure 4.42. Constant volume DSS test results on overconsolidated sample – Tests series OC-2 (OCR = 1.5). a) Stress-strain response. b) Stress-path.

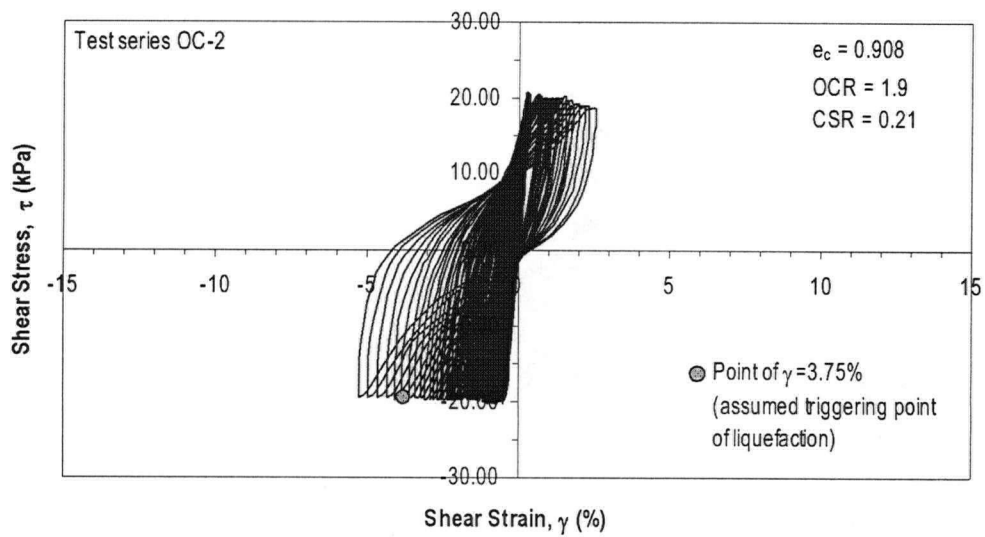


a)

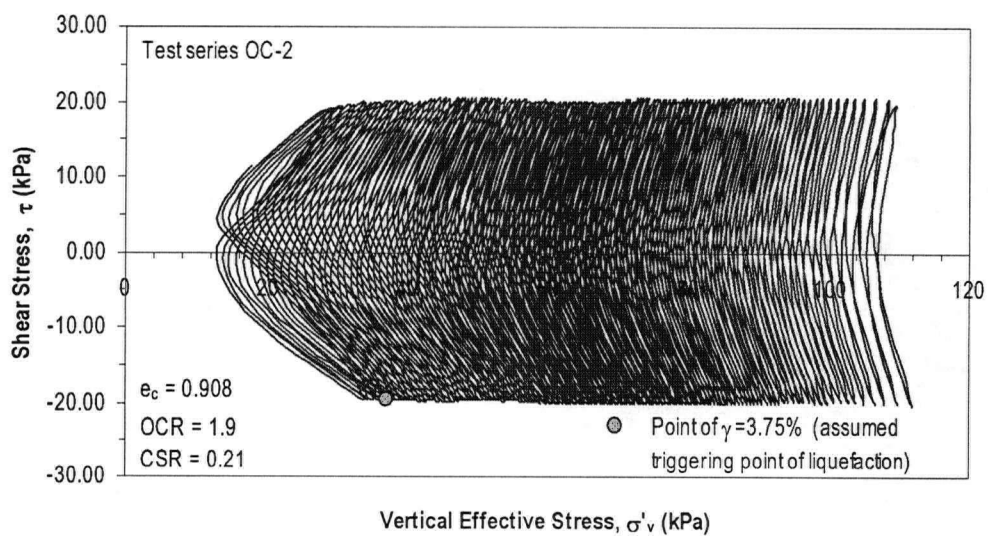


b)

Figure 4.43. Constant volume DSS test results on overconsolidated sample – Tests series OC-2 (OCR = 1.7). a) Stress-strain response. b) Stress-path.

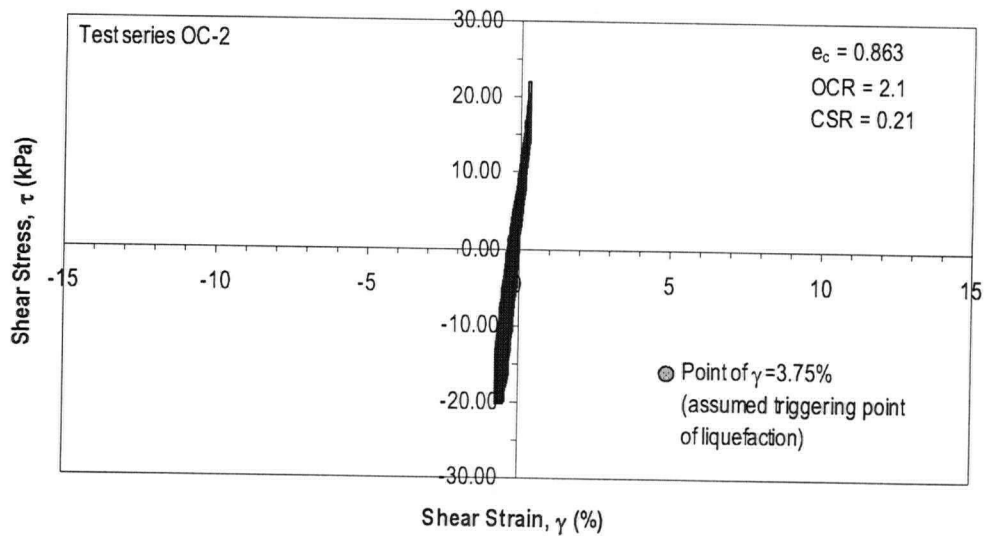


a)

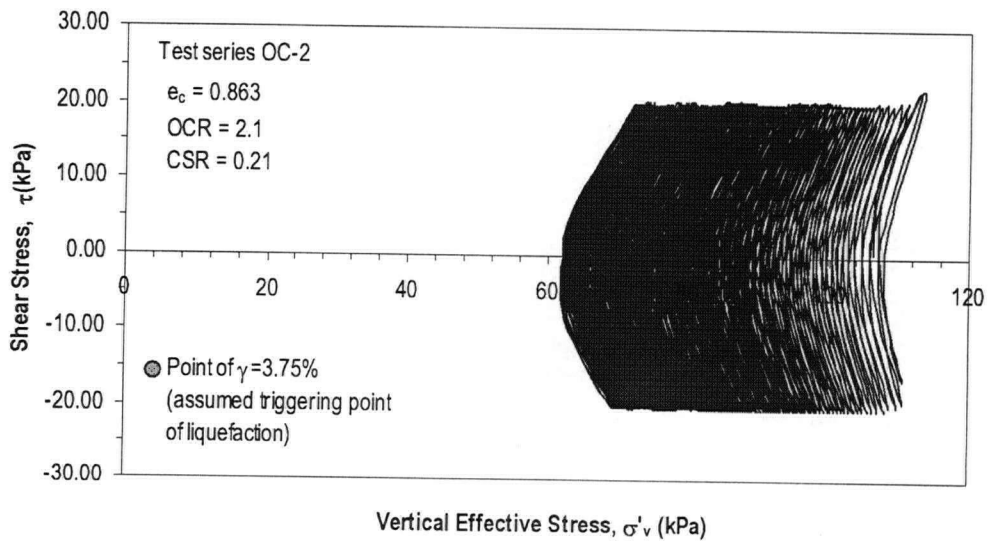


b)

Figure 4.44. Constant volume DSS test results on overconsolidated sample – Tests series OC-2 (OCR = 1.9). a) Stress-strain response. b) Stress-path.



a)



b)

Figure 4.45. Constant volume DSS test results on overconsolidated sample – Tests series OC-2 (OCR = 2.1). a) Stress-strain response. b) Stress-path.

Figure 4.46 shows the cumulative pore water pressure ratio with number of cycles for specimens of test series OC-2.

The observed response from the test series OC-3 are presented in Figures 4.47 to 4.50. All specimens herein were tested at a CSR = 0.30. Pore water pressure development with number of cycles are shown in Figure 4.51. The specimen tested at OCR = 1.20 (Figure 4.47) displayed a response similar to that tested under normally consolidated conditions (Figure 4.10). Specimens tested at higher OCR values show a more dilative response starting from the first cycle, and with increasing OCR the samples require more cycles to liquefy (Figures 4.48 to 4.50).

Again, in a general sense, the mechanism of strain development in the overconsolidated specimens is via “cyclic mobility”, and similar to those observed for NC silt. The OC specimens seem to manifest phase transformation from contractive to dilative almost in the first loading cycle itself.

4.3.3.1 Degradation of Shear Stiffness During Cyclic Loading

In a similar manner to the examination of results for NC specimens, the gradual degradation of the secant shear stiffness (G_{secant}) with increasing number of cycles for the OC specimens from all tests in series OC-1 through OC-3 are shown in Figure 4.52 (see Figure 4.21 for schematic representation of the definition of G_{secant}). The envelope of shear stiffness degradation observed for NC samples in Figure 4.22 are also superimposed in Figure 4.52 for comparison. The rate of shear stiffness degradation with respect to shear strain that takes place in overconsolidated samples is basically similar to that observed for normally consolidated specimens.

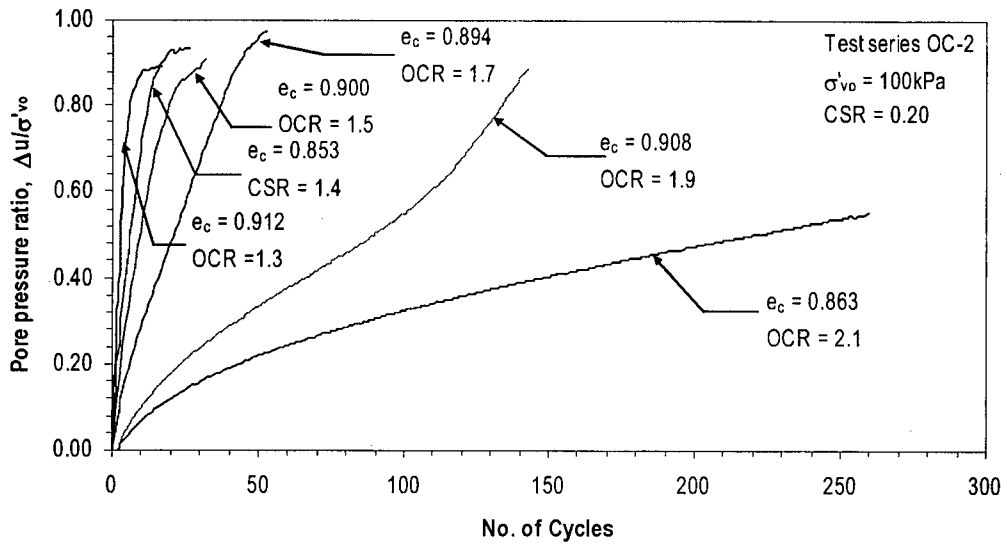
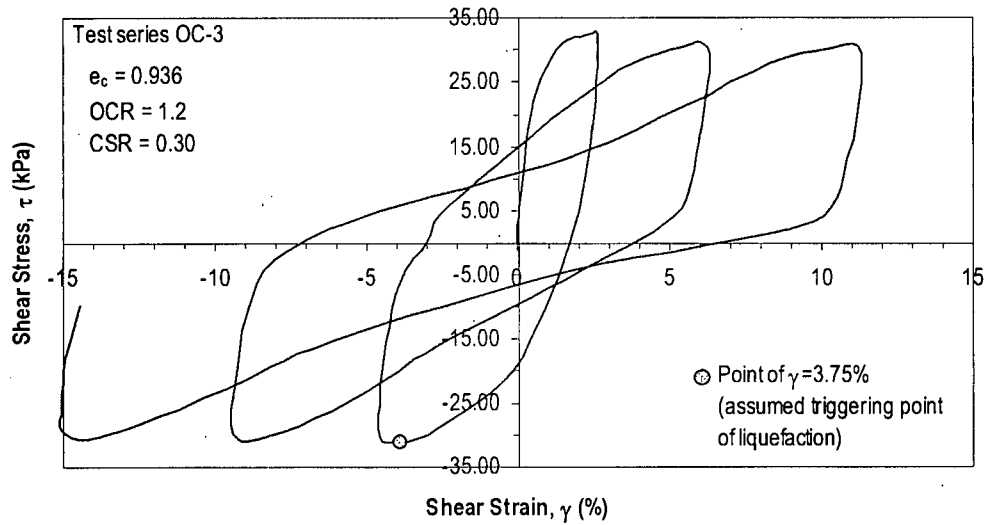
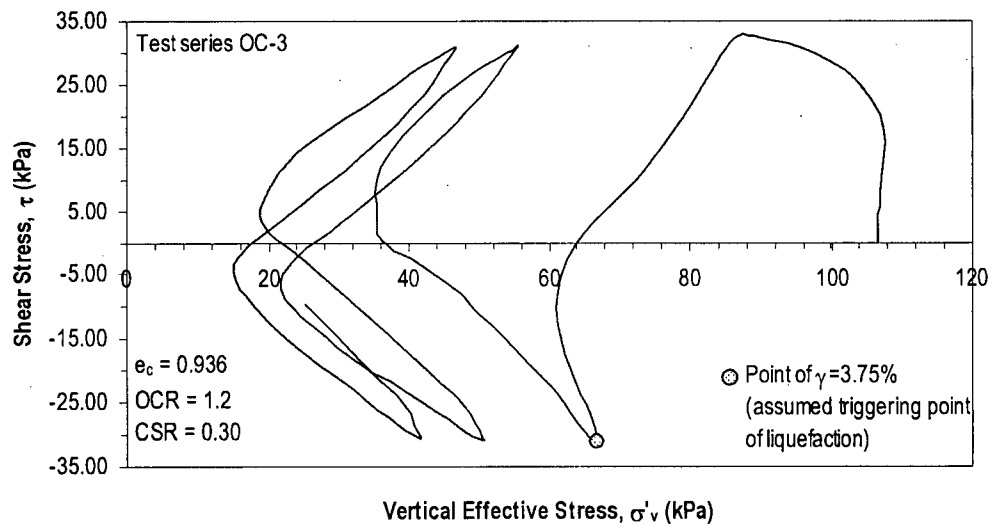


Figure 4.46. Cumulative pore water pressure during constant volume DSS test on overconsolidated samples – Tests series OC-2 ($\text{CSR} = 0.20$).

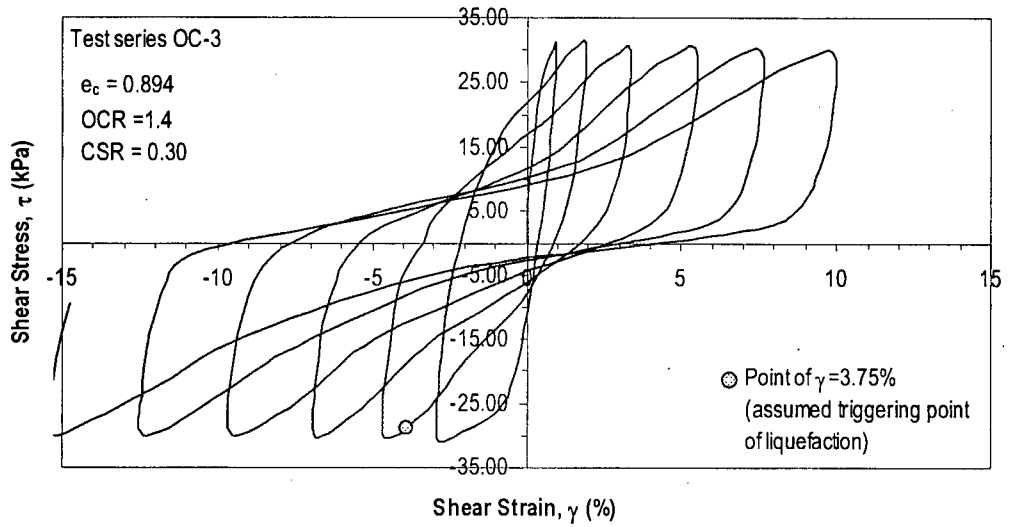


a)

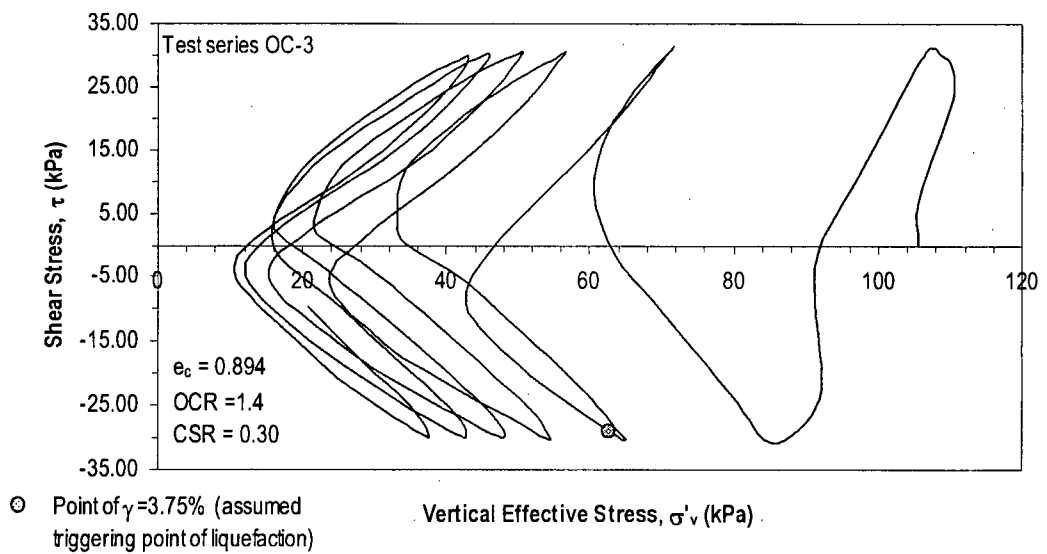


b)

Figure 4.47. Constant volume DSS test results on overconsolidated sample – Tests series OC-3 (OCR = 1.2). a) Stress-strain response. b) Stress-path.

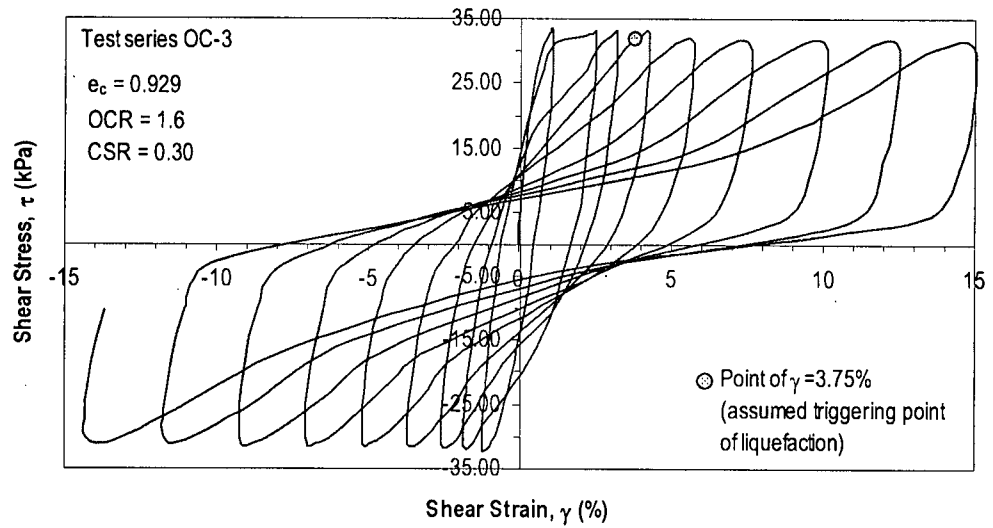


a)

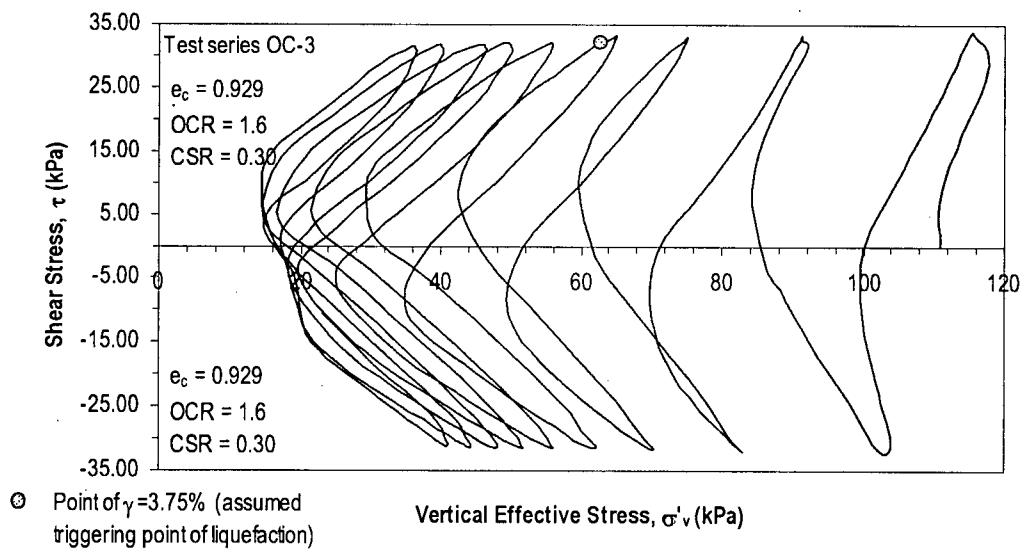


b)

Figure 4.48. Constant volume DSS test results on overconsolidated sample – Tests series OC-3 (OCR = 1.4). a) Stress-strain response. b) Stress-path.

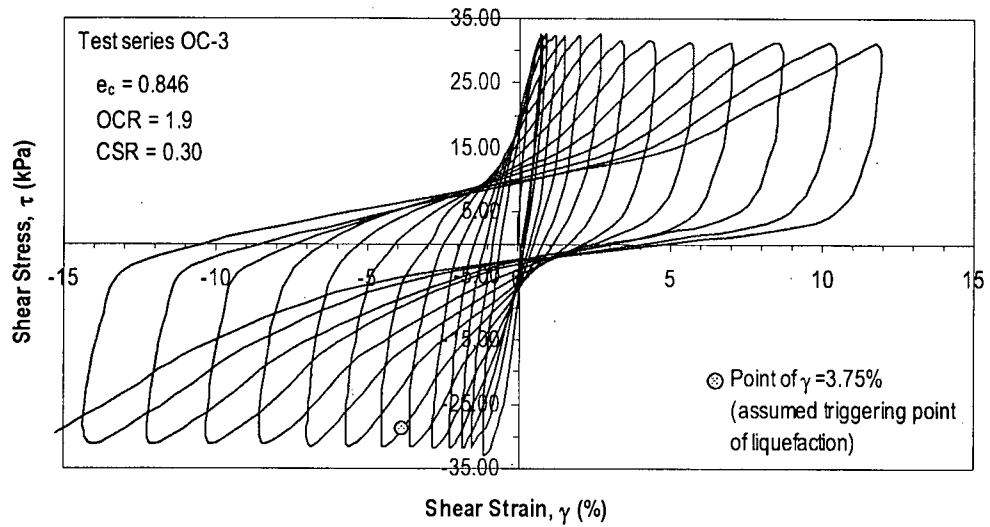


a)

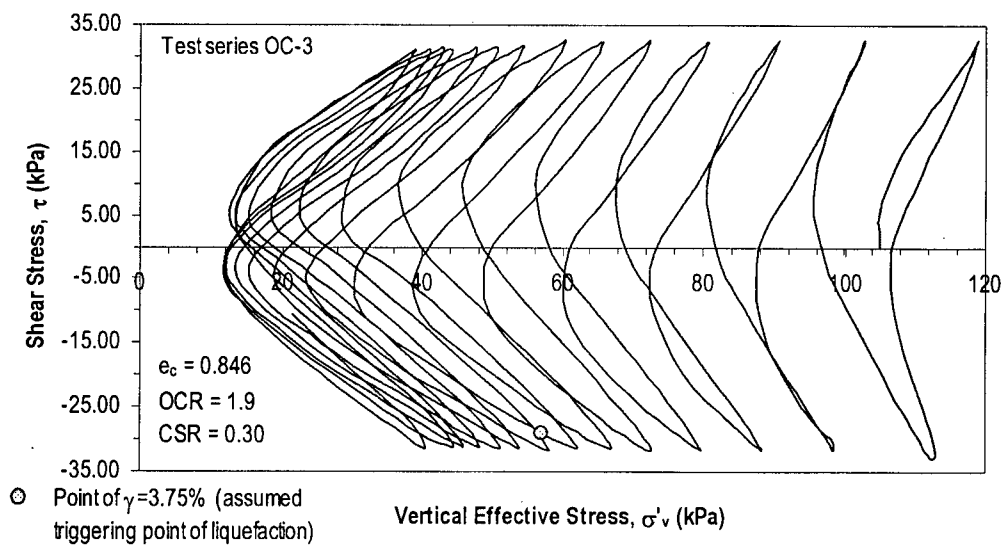


b)

Figure 4.49. Constant volume DSS test results on overconsolidated sample – Tests series OC-3 (OCR = 1.6). a) Stress-strain response. b) Stress-path.



a)



b)

Figure 4.50. Constant volume DSS test results on overconsolidated sample – Tests series OC-3 (OCR = 1.9). a) Stress-strain response. b) Stress-path.

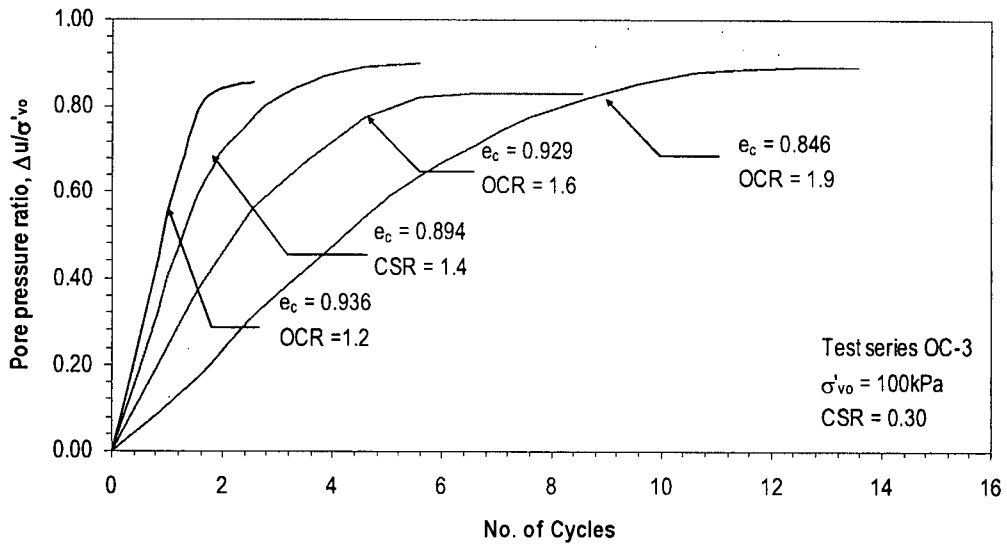


Figure 4.51. Cumulative pore water pressure during constant volume DSS test on overconsolidated samples – Tests series OC-2 (CSR = 0.20).

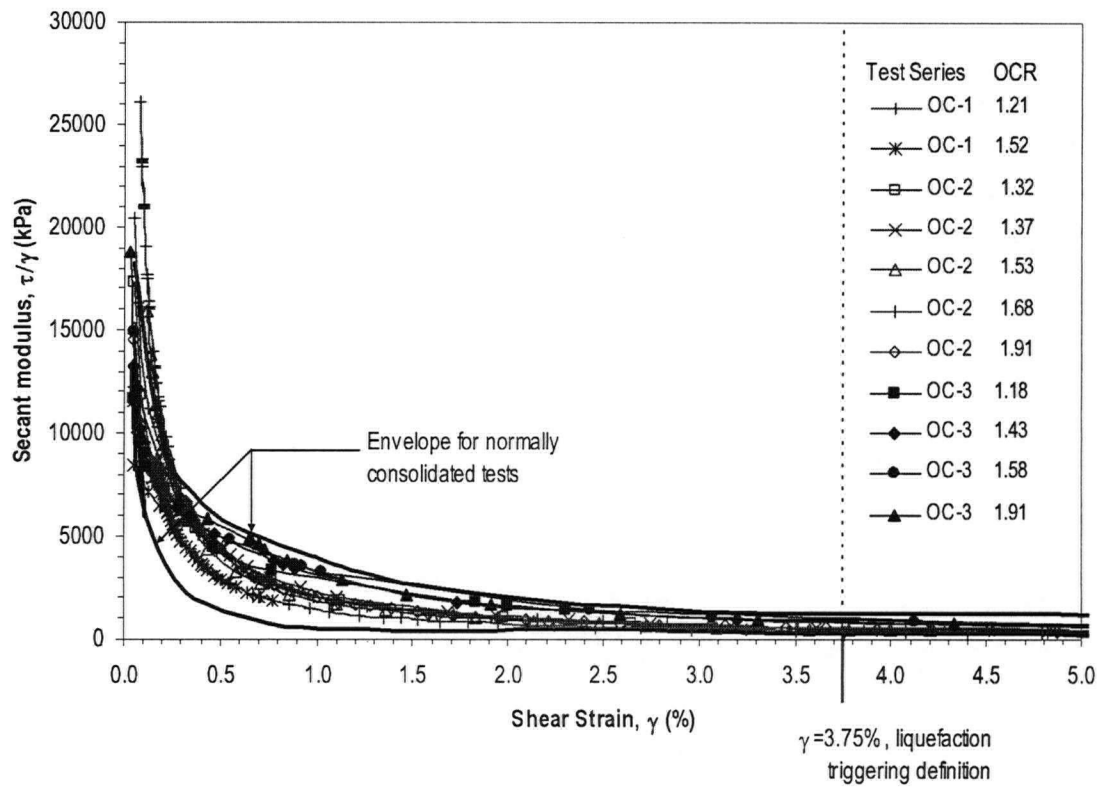


Figure 4.52. Modulus degradation for samples tested in the DSS on overconsolidated state.

4.3.3.2 Cyclic Resistance Ratio (CRR)

Figure 4.53 shows the variation of cyclic resistant ratio with the number of cycles to reach liquefaction ($\gamma = 3.75\%$) for the specimens tested in overconsolidated conditions together with the counterpart results for $OCR = 1$ (or NC condition) from test series NC-1. Clearly the cyclic resistance ratio (CRR) increases with increasing OCR. Figure 4.54 shows the same data but plotted in a different format. The data shows that for values of OCR up to about 1.3 there is no significant improvement in terms of liquefaction resistance (no change in the number of cycles to reach $\gamma = 3.75\%$). In other words, it appears that the silt has to be overconsolidated to a level above $OCR > 1.3$ to yield to any noticeably improvement in terms of liquefaction resistance.

4.3.3.3 Post-cyclic Consolidation Response

Figure 4.55 presents the observed volumetric strains for the test series OC-1, OC-2 and OC-3 during post-cyclic consolidation. The samples that experienced excess pore water pressure ratios (r_u) close to 100% suffered significantly high post-cyclic consolidation strains (1.5 to 4.0%) in comparison to the sample that developed relatively small r_u (<50%). The magnitude of post-cyclic volumetric strains in the specimens that had high pore water pressures are still significant and only slightly smaller than those observed for the counterpart NC specimens (see Figure 4.24). Again, this can be considered as a reflection of extensive particle rearrangement suffered by the silt specimens during cyclic loading.

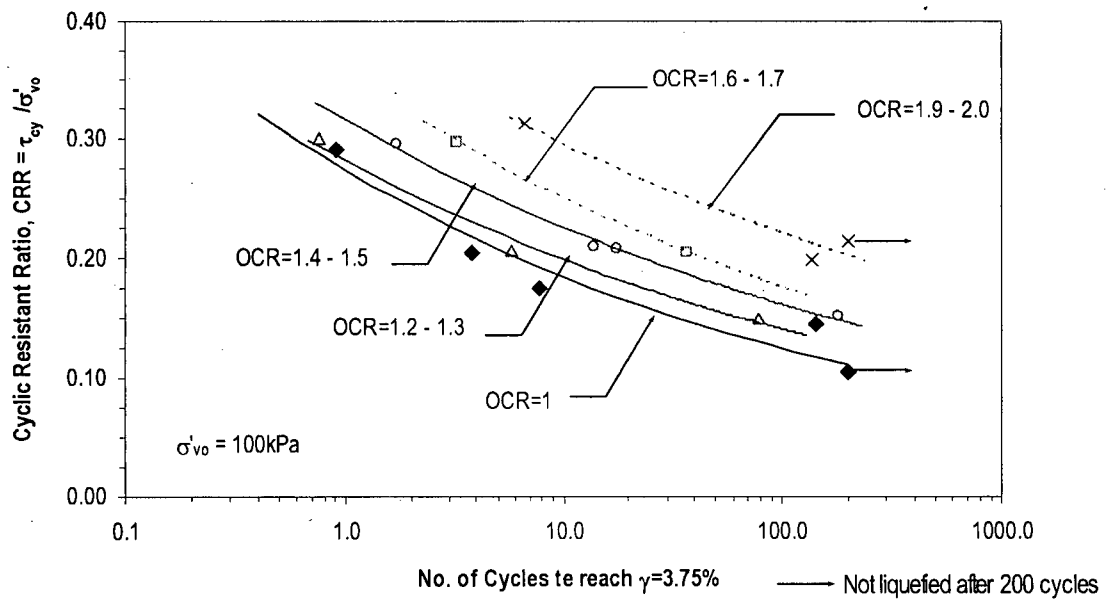


Figure 4.53. Cyclic resistant ratio versus number of cycles to reach liquefaction for samples tested on the DSS: influence of overconsolidation ratio.

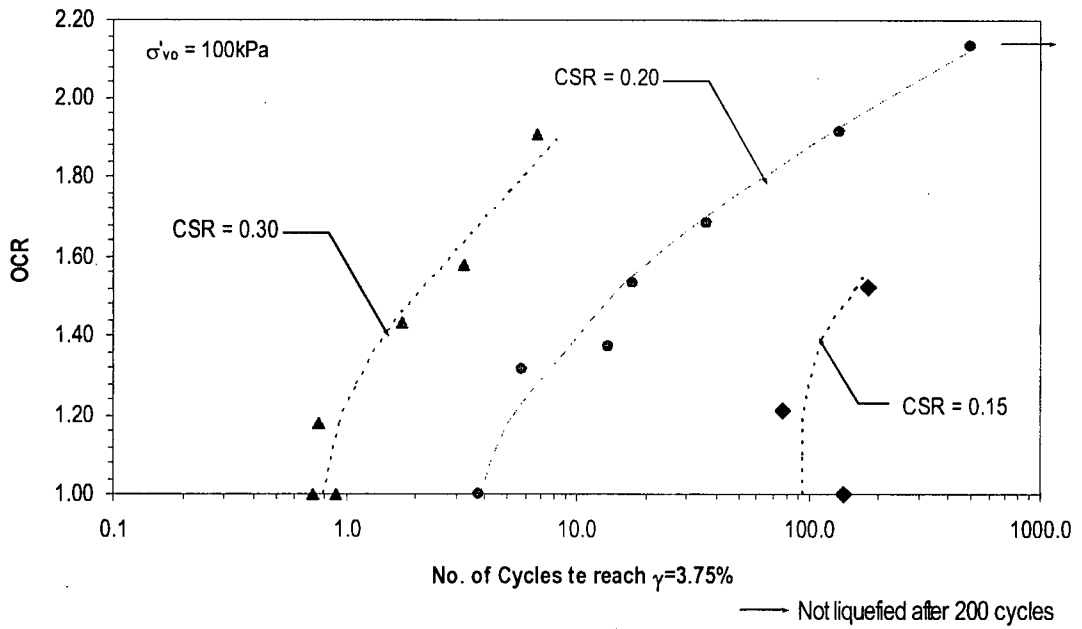


Figure 4.54. Variation of OCR with No. of cycles to reach $\gamma = 3.75\%$ for constant cyclic stress ratio.

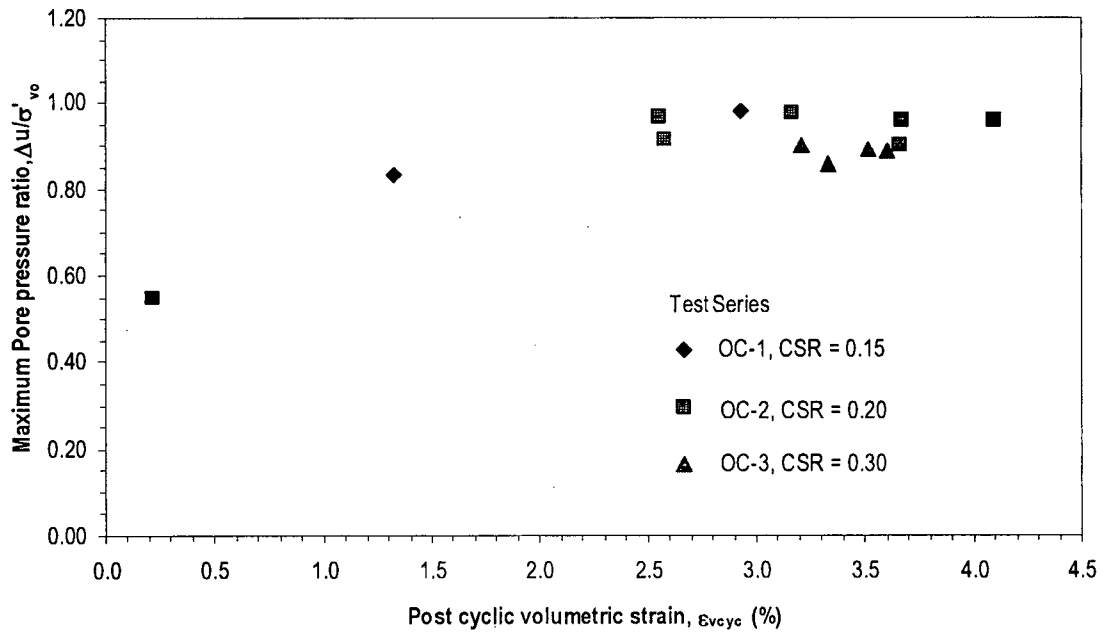


Figure 4.55. Post-cyclic volumetric strain for overconsolidated samples.

4.4 APPLICABILITY OF EMPIRICALLY BASED CRITERIA FOR LIQUEFACTION ASSESSMENT

The data from DSS testing provides an opportunity to check the validity of the empirically based criteria in the evaluation of liquefaction susceptibility of Fraser River silt as described below. Figure 4.56 shows the Chinese Criteria (Wang, 1979) as presented by Seed et al. (1983), and graphically represented by Marcuson et al. (1990). The index parameters for the tested Fraser River silt are also plotted in the same Figure along with the suggested modifications proposed by Finn et al. (1994) and Koester (1992). With an LL of 30.5, and percent finer than 0.005 mm of 16%, with respect to the criteria presented by Wang (1979), the Fraser River silt plots essentially close to the boundary that defines susceptibility to liquefaction. The modified criterion of fine contents proposed by Finn et al (1994) and Koester et al. (1992), would also classify the silt as susceptible to liquefaction.

Figure 4.57 shows a graphical representation of the index parameters of channel-fill Fraser River silt with respect to Andrews and Martin (2000) criteria. Given that the criterion of $LL = 32$ is very close to the Fraser River silt $LL = 30.5$, the sample plots in the boundary between “susceptible to liquefaction” and “further studies required”.

As per Polito (2001) criteria for liquefaction assessment, the index properties would place the Fraser River silt on the “potentially liquefiable” zone as shown in Figure 4.58. Polito’s approach allows the plasticity chart to give an indication of the likelihood of liquefaction, regardless the in-situ state of water content. He has noted that Chinese criteria (Wang 1979, Finn et al. 1994 and Koester et al. 1992) criteria for water content were applicable to the tests

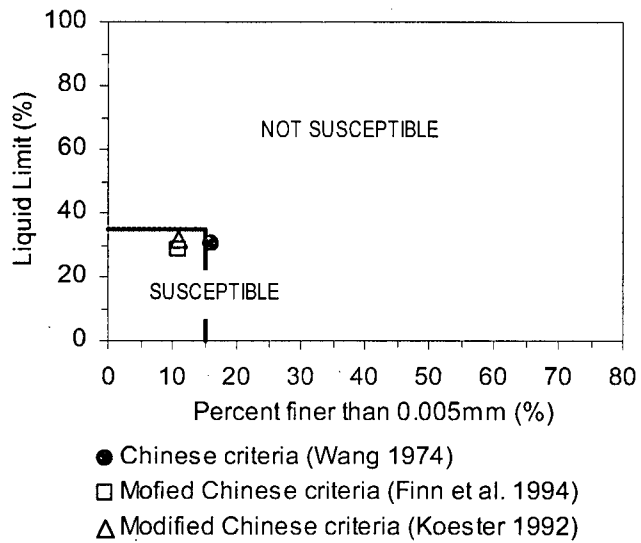
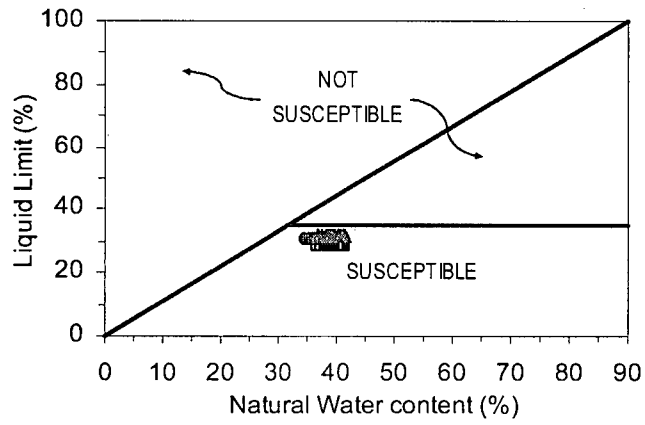


Figure 4.56. Applicability of the Chinese criteria for liquefaction assessment for Fraser River silt.

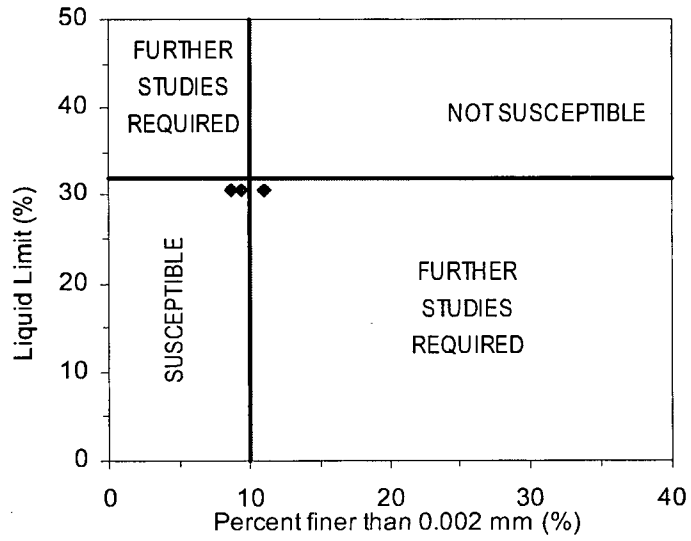


Figure 4.57. Applicability of Andrews and Martin (2000) criteria for liquefaction assessment on Fraser River silt.

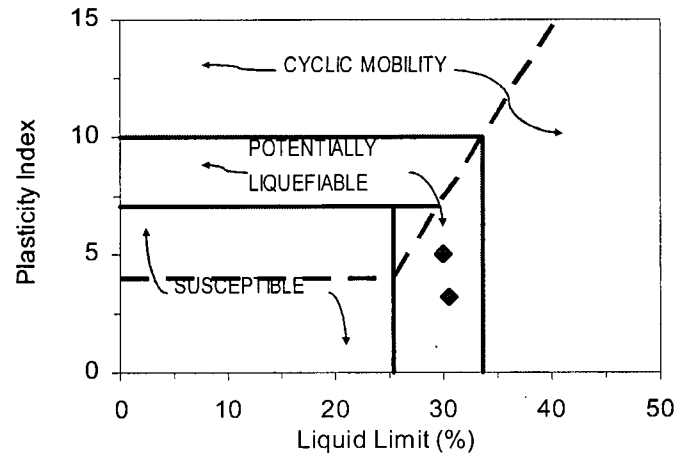


Figure 4.58. Applicability of Polito (2001) criteria for liquefaction assessment on Fraser River silt.

performed on his study; nevertheless, the water content was not included in the recommended parameters to assess liquefaction.

Bray et al (2004a) criteria, presented in Figure 4.59 along with the Fraser River Delta silt index parameters, clearly classify Fraser River silt in the zone for the soils susceptible to liquefaction. Bray et al. criteria determine the liquefaction susceptibility based on plasticity and in-situ moisture content (i.e. void ratio)

As an alternative to the above empirical criteria, Boulanger and Idriss (2004) have recently recommended that fine-grained soils be classified as “sand-like” (susceptible to liquefaction) if $PI < 7$ and “clay-like” if $PI \geq 7$. They also indicate that this criterion may be adjusted on a site specific basis if justified by the results of detailed in-situ and laboratory testing. In accordance with the delineation by Boulanger and Idriss (2004), with PI between 3 and 5, channel-fill Fraser River silt of the present study would classify as “sand-like”. On one hand, the laboratory results of the present study indicate that the strain development mechanism for Fraser River silt is “dense sand-like” (as per discussed for the test results on Section 4.3.2); on the other hand, the absence of the K_σ -effect in the cyclic resistance ratio (CRR) for the silt may be interpreted more as a “clay-like” behaviour. Again, the laboratory results clearly portray the difficulties associated in predicting the cyclic response using criteria solely based around index properties.

As noted in Section 4.3.2.1, Bray et al. (2004a) observed that fine-grained soils that would classify as liquefiable based on laboratory strain criteria suffered damage under real-life earthquake loading conditions. In this context, it is appropriate to review the observations made in Figures 4.46 through 4.59 in relation to the laboratory test findings presented in Sections 4.3.2 and 4.3.3. In particular, the CRR vs. N_L relationships presented in Figures 4.23

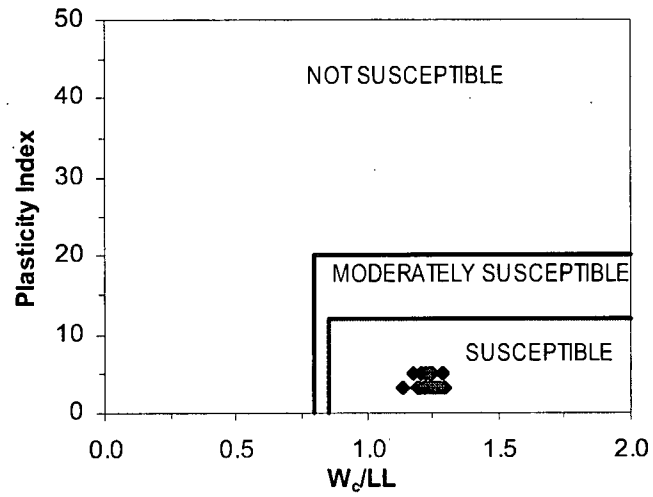


Figure 4.59. Applicability of Bray et al. (2004b) criteria for liquefaction assessment on Fraser River silt.

and 4.53 confirm that the occurrence of liquefaction of this silt would be determined by many parameters such as applied cyclic stress ratio, stress level, overconsolidation ratio, etc., in addition to the simple index parameters. For example, some samples required large number of load cycles to reach $\gamma = 3.75\%$ simply due to the low intensity of cyclic loading (CSR) or due to relatively high initial overconsolidation levels.

In a general context, as shown in Table 4.4, the current empirical criteria do not consider many of the above parameters that critically govern the liquefaction susceptibility. The satisfaction of certain conditions with regard to soil parameters selected for empirical criteria can be argued to be *necessary*; however, it is apparent that this accordance alone may not be *sufficient* to describe the undrained response of a given fine-grained soil. While use of a "yes/no" classification as suggested in the use of empirical criteria is simple and practically attractive, the laboratory observations such as above, confirm that the use of empirical criteria may not provide the liquefaction susceptibility with the level of certainty needed for engineering practice.

In addition to the above, it is also important to note that the accuracy of the measured index parameters (such as liquid limit, plastic limit, and moisture content) becomes a critically important factor especially when the parameters lie close to classification boundaries in empirical criteria. For example, in-situ water content may be affected during sample retrieval, handling, and preparation of test specimens. During the testing of Fraser River silt, it was noted that changes in moisture content in the order of 4% can easily take place during handling and exposure to atmosphere. Moreover, the liquid limit and plastic limit measurements can be subject to errors arising due to operator dependency. Laboratory element testing that allows

capturing the effect of most controlling parameters seems to still remain as the prudent approach for estimating liquefaction susceptibility.

Table 4.4. Factors controlling the response of soils to cyclic loading and their consideration by different empirical criteria for liquefaction assessment

Criteria	Chinese criteria ¹	Andrews and Martin (2000)	Polito (2001)	Bray (2004b)
Mineralogy / plasticity	Yes	Yes	Yes	Yes
Grain size	Yes	Yes	No	No
Packing density	Yes ²	No	No	Yes ²
Microstructure	No	No	No	No
Fabric	No	No	No	No
Age	No	No	No	No
Confining stress level	No	No	No	No
Level of cyclic loading	No	No	No	No
Initial static shear bias	No	No	No	No

¹ Wang (1976), Seed et al. (1983), Finn et al (1994), Koester (1992)

² In terms of water content.

5 CYCLIC LOADING RESPONSE OF FINE-GRAINED MINE TAILINGS²

5.1 INTRODUCTION

As mentioned earlier, in addition to studying the response of Fraser River silt, a detailed review of already available data on the cyclic response of fine-grained mine tailings from three mine sites was undertaken as part of this study. This chapter presents the key experimental observations from this database and discussion on the cyclic and post-cyclic shear behaviour. The applicability of the commonly used empirical approaches for the assessment of liquefaction susceptibility of silty tailings is also examined.

² A version of this chapter has been accepted for publication as an article in the Canadian Geotechnical Journal. Wijewickreme, D. Sanin, M. V. Greenaway, G. R. Cyclic shear response of fine-grained mine tailings. Canadian Geotechnical Journal. *In print*, 2005.

5.2 MINE TAILINGS MATERIALS OF THE DATABASE

The primary database used herein comprises the results obtained from a series of constant volume direct simple shear (DSS) tests conducted on fine-grained tailings at the UBC geotechnical research laboratory over the last 10 years. The DSS tests had been performed on undisturbed and/or reconstituted samples of laterite tailings and two other tailings resulting from the extraction of copper-gold and copper-gold-zinc. The number of DSS tests for each tailings type and material parameters derived from index testing and grain size analyses for the individual samples are summarized in Table 5.1.

The laterite tailings are obtained from the processing of limonite ore by a pressure acid leach process. This process involves the solution of nickel and cobalt by sulphuric acid at high temperature and pressure, as described by Chalkley and Toirac (1997). As may be noted from Table 5.1, the fine-grained laterite tailings typically consist of silts and clayey silts with a relatively high specific gravity (i.e., $G_s = 4.1$). The copper-gold tailings and copper-gold-zinc tailings are both obtained using traditional ore processing methods. The copper-gold tailings are essentially non-plastic. Plasticity of the copper-gold-zinc tailings has been noted as very low ($PI < 2.0$) from a limited number of index tests. The specific gravity of the copper-gold-zinc tailings is also high.

For all three tailings types, the field samples for DSS testing were obtained with standard stainless steel Shelby tubes. Ideally, a method that imparts minimal changes to the particle structure and in situ stress state would be the most suitable for soil sampling (Hight and Leroueil 2003; Ladd and DeGroot 2003). The ability of samplers such as Sherbrooke sampler (Lefebvre and Poulin 1979) and Laval sampler (La Rochelle et al. 1981) to retrieve high quality

Table 5.1. Characteristics and properties of the tailings included in this study

Sample ID	Depth (m)	Gradation			Gs*	ei†	ec‡	LL§	PI	$\sigma'_{v-in-situ}$ ¶ (kPa)	σ'_{vo} # (kPa)	Cyclic Tests		Post Cyclic Tests	
		% Sand	% Silt	% Clay								τ_{cy}/σ'_{vc} a	NL b	γ_{peak} c (%)	S_{u-PC}/σ'_{vc} d
Laterite tailings															
L-100-01	5.3	0.0	65.0	35.0		1.509	1.390			66.2	100.0	0.245	4	12.0	0.480
L-100-02	5.3	0.0	65.0	35.0		1.460	1.324			66.2	100.0	0.225	7	20.0	0.550
L-100-03	5.3	0.0	65.0	35.0	4.10 ^e	1.587	1.451	34 ^e	12 ^e	66.2	100.0	0.193	8	14.0	0.410
L-100-04	5.3	0.0	65.0	35.0		1.554	1.374			66.2	100.0	0.153	22	15.0	0.470
L-100-05	5.3	0.0	65.0	35.0		1.570	1.427			66.2	100.0	0.112	76	16.0	0.470
L-200-01	8.0	7.0	91.0	2.0		1.179	1.116			99.4	200.0	0.150	41	15.8	0.52
L-200-02	8.0	7.0	91.0	2.0	4.10 ^e	1.219	1.166	N/A	N/A	99.4	200.0	0.200	26	13.9	0.60
L-200-03	8.0	7.0	91.0	2.0		1.477	1.391			99.4	200.0	0.250	7	13.3	0.44
L-200-04	8.0	7.0	91.0	2.0		1.421	1.338			99.4	200.0	0.220	14	14.3	0.46
Copper-Gold															
CG-01	9.0	3.0	90.7	6.3		N/A	0.556			99.3	100.0	0.130	43	23.0	0.640
CG-02	9.0	1.5	90.5	8.0	2.78 ^c	N/A	0.556	27 ^e	NP ^e	99.3	100.0	0.155	50	20.0	0.610
CG-03	9.0	0.4	87.9	11.7		N/A	0.556			99.3	100.0	0.190	29	17.0	0.420
CG-04	9.0	3.0	83.4	13.6		N/A	0.556			99.3	100.0	0.250	5	17.0	0.480
Copper-Gold-Zinc															
CGZ-01	14.9	3.1	96.9	N/A	3.62	1.130	0.980			177.2	347.0	0.124	20	20.0	0.179
CGZ-02	7.9	6.4	93.6	N/A	3.62	1.320	1.180			85.9	181.0	0.125	16	16.0	0.144
CGZ-03	11.9	0.0	100.0	N/A	3.54	1.310	1.170			125.9	265.0	0.128	13	18.0	0.132
CGZ-04	12.2	0.0	100.0	N/A	3.72	1.220	1.080			144.5	253.0	0.128	13	19.0	0.170
CGZ-05	15.2	0.0	100.0	N/A	3.60	1.210	1.040	19 ^e	2 ^e	172.8	338.0	0.127	13	18.0	0.157
CGZ-06	6.4	0.0	100.0	N/A	3.93	0.840	0.730			98.7	144.0	0.110	13	25.0	0.375
CGZ-07	9.8	2.4	97.6	N/A	3.63	1.250	1.090			110.5	223.0	0.130	14	19.0	0.157
CGZ-08	6.1	0.0	100.0	N/A	4.42	0.720	0.640			117.8	147.0	0.107	9	19.0	0.401
CGZ-09	18.9	16.0	84.0	N/A	3.42	0.740	0.690			254.5	461.0	0.117	15	15.0	0.130
CGZ-10	8.2	43.1	56.9	N/A	3.36	0.590	0.540			117.7	209.0	0.112	12	20.0	0.287

Table 5.1. Characteristics and properties of the tailings included in this study (contd.)

Sample ID	Depth (m)	Gradation			Gs*	ei†	ec‡	LL§	PI	$\sigma'_{v-in-situ}$ ¶ (kPa)	σ'_{vo} # (kPa)	Cyclic Tests		Post Cyclic Tests	
		% Sand	% Silt	% Clay								τ_{cy}/σ'_{vc} a	NL b	γ_{peak} c (%)	S_{u-PC}/σ'_{vc}
Copper-Gold-Zinc (contd.)															
CGZ-11	14.9	3.1	96.9	N/A	3.69	0.915	0.867			202.5	352.0	0.121	14	15.0	0.205
CGZ-12	11.9	0.9	99.1	N/A	3.54	1.289	1.129			127.3	248.0	0.126	21	15.0	0.198
CGZ-13	6.4	11.4	88.6	N/A	3.94	0.640	0.580			111.4	149.0	0.110	29	15.0	0.940
CGZ-14	18.9	37.3	62.7	N/A	3.79	0.716	0.493			297.8	452.0	0.120	24	9.3	0.367
CGZ-15	15.5	0.6	99.4	N/A	3.65	1.318	1.004	19 ^c	2 ^e	170.9	357.0	0.121	18	15.0	0.171
CGZ-16	8.8	0.0	100.0	N/A	4.17	0.976	0.890			163.0	183.0	0.128	9	22.0	0.339
CGZ-17	11.6	0.0	100.0	N/A	3.78	1.719	1.432			100.4	236.0	0.137	11	18.0	0.169
CGZ-18	13.7	3.3	96.7	N/A	3.57	1.380	1.107			129.7	295.0	0.137	9	20.0	0.203
CGZ-19	5.9	9.3	90.7	N/A	3.75	0.904	0.770			76.9	115.0	0.125	13	18.0	1.070
Copper-Gold-Zinc (Reconstituted samples)															
CGZ-21	N/A	2.4	89.5	8.1		N/A	0.862			N/A	100.0	0.190	13	16.0	0.330
CGZ-22	N/A	2.4	89.5	8.1	3.67 ^c	N/A	0.870	21 ^e	1 ^e	N/A	100.0	0.115	23	20.0	0.320
CGZ-23	N/A	2.4	89.5	8.1		N/A	0.840			N/A	250.0	0.125	15	20.0	0.272

Notes:

* Specific gravity of solids

† Initial void ratio

‡ Void ratio after consolidation

§ Liquid limit

|| Plasticity index

¶ Estimated in-situ vertical effective stress

Vertical effective stress used for testing

a Cyclic stress ratio from cyclic DSS tests

b Number of cycles to reach shear strain $\gamma = 3.75\%$

c Shear strain at maximum shear stress S_{u-PC} in post-cyclic shear tests

d Ratio of maximum shear stress over initial vertical effective stress reached in post-cyclic shear tests

e Based on tests conducted on samples obtained from the same horizon

N/A Not available

NP Non plastic

“undisturbed” samples of fine-grained soil, in comparison to those from conventional tube sampling is well known. However, the use of these samplers is not practical and cost-effective in the sampling of tailings soils. Thin-walled tubes with no inside clearance and cutting edge angle of less than 6° is also increasingly used as a means of obtaining good quality samples in fine-grained soils (Hight and Leroueil 2003). However, this method has a tendency for poor sample recovery in non-plastic fine-grained soils, and there is also a risk of damage to the sharp cutting-edge if the tube is pushed through compact sandy zones. Such limitations have made this method less attractive since good recovery is an important factor particularly considering the high costs associated with sampling in geographically distant mine site locations. Shelby tube sampling, in spite of its potential for a relatively higher degree of sample disturbance, is still used as the common sampling tool.

Another source of sample disturbance is potential vibrations and shaking during transportation. The samples used in the tests reported herein had been shipped after securing in light-weight packing (foam-based) material and in boxes labelled with instructions as to minimize imparting disturbance; however, it is recognized that the level of disturbance imparted on the samples during transportation is not known.

5.3 TEST PROGRAM

The constant volume cyclic shear test data used herein was obtained using the UBC-DSS test apparatus. A description of the UBC-DSS device was presented in Section 3.2. The test specimens were initially consolidated to a desired vertical effective stress (σ'_{vo}) prior to cyclic

loading as indicated in Table 5.1. As may be noted, for a given specimen, the value of σ'_{vo} specified for testing is larger than the estimated in situ overburden effective stress $\sigma'_{v-in-situ}$ experienced by the specimen at the time of sampling. The tests were undertaken to analyze the stability of future configurations of the tailings structure with increased heights, and, hence the higher specified values of σ'_{vo} for testing.

During the cyclic loading phase, symmetrical sinusoidal shear pulses were applied at constant cyclic stress ratio τ_{cy}/σ'_{vo} amplitudes, at a frequency of 0.1 Hz, which has been considered suitable for this type of tests (see Section 3.2.4.3). The cyclic loading phase was continued until the single-amplitude horizontal shear strain (γ) of the specimen reached a value of 3.75%. Upon completion of the cyclic loading phase, the specimens were subject to post-cyclic undrained monotonic shear using a shear strain rate of about 10% per hour.

For the laterite and copper-gold tailings, the DSS tests conducted at a given stress level corresponded to specimens obtained from the same Shelby tube sample. This was not the case for the copper-gold-zinc tailings where the DSS tests had been performed on samples obtained from different (plan and depth) locations within the tailings deposit, although the tailings material was otherwise similar in terms of its characteristics. In essence, this implied that the tests on undisturbed samples of copper-gold-zinc tailings corresponded to a much broader range of initial void ratios and stress levels in comparison to the laterite and copper-gold tailings. In addition, the results from two other DSS tests conducted on reconstituted (slurry-consolidated) samples of the same material provided an opportunity to examine the cyclic shear response of copper-gold-zinc tailings under similar initial void ratios.

5.4 CYCLIC SHEAR RESISTANCE OF FINE-GRAINED MINE TAILINGS

Figures 5.1 to 5.3 show typical stress-strain relationships and stress path for the 3 types of tailings considered in this study. All the samples exhibit predominantly contractive response during the 1st quarter-cycle of loading. With increasing number of load cycles, the samples experience cumulative increase in excess pore water pressure with associated progressive degradation of shear stiffness. In a given cycle, the shear stiffness experiences its transient minimum when the applied shear stress is close to zero. The observed cyclic mobility type stress-strain response is similar in form to the undrained (constant volume) cyclic shear responses observed from cyclic shear tests on Fraser River silt presented in Chapter 4 as well as those observed for dense sands (Kammerer et al., 2002; Sriskandakumar, 2004). Similar response has been observed by Zergoun and Vaid (1994) during their tests on a natural clay.

5.4.1 Cyclic Stress Ratio

The variation of applied cyclic stress ratio (CSR) versus number of cycles required to liquefaction (N_L) in cyclic shear tests (i.e., $\gamma = 3.75\%$) on laterite tailings samples consolidated to vertical effective stresses of $\sigma'_{vo} = 100$ kPa and 200 kPa are shown in Figure 5.4. Under a given applied CSR, the number of cycles to liquefaction (N_L) under $\sigma'_{vo} = 100$ kPa is consistently lower than N_L obtained under $\sigma'_{vo} = 200$ kPa. This suggests that, in laterite tailings, the dilative tendency arising due to stress densification seems to have overcome the possible contractive tendency due to the increase in confining stress. Park and Byrne (2004) and Wijewickreme et al. (In press) have noted similar effects due to stress densification in their tests on sands. As seen in Table 5.1, the average void ratio after consolidation, and prior to

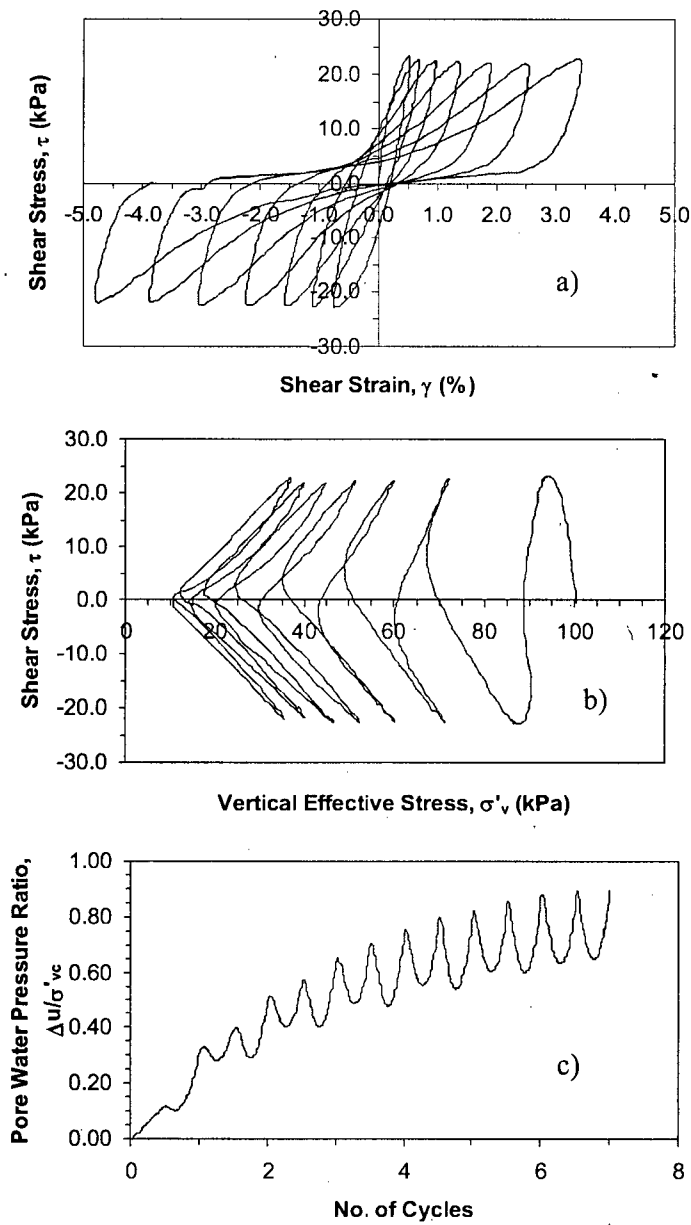


Figure 5.1. Typical response of laterite tailings in constant volume cyclic DSS loading (sample L-100-02: $\sigma'_{vo} = 100$ kPa, CSR = 0.225). a) Stress strain, b) stress path response, and c) pore water pressure ratio versus number of cycles.

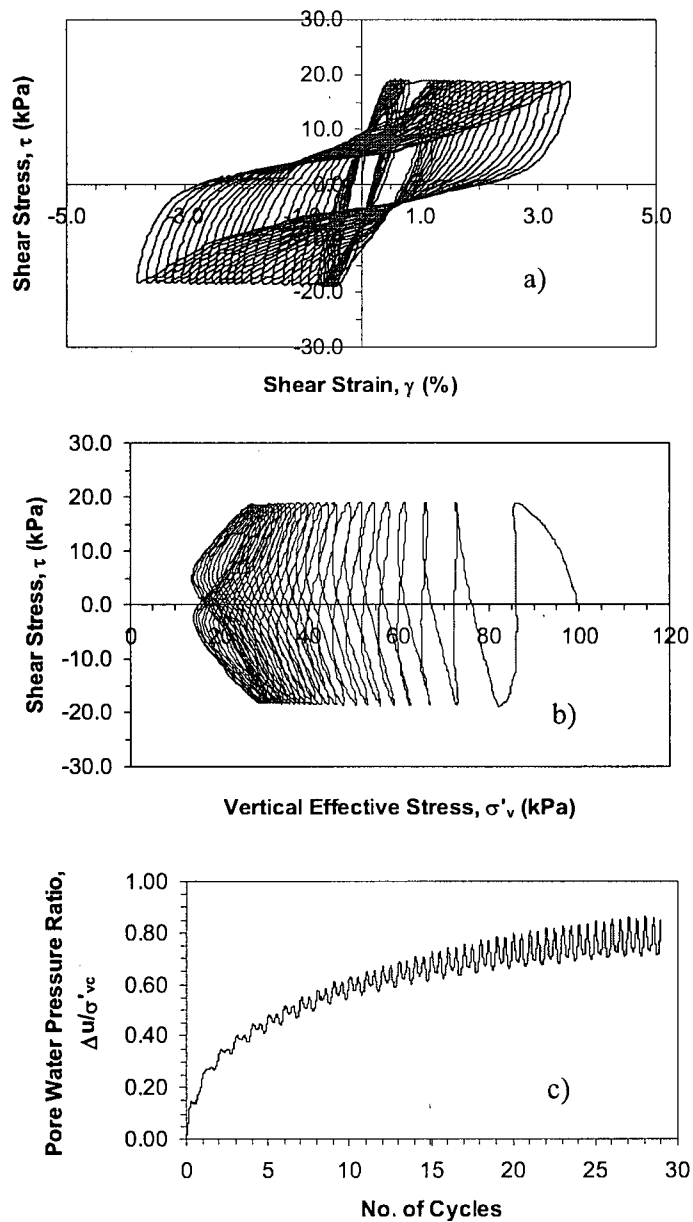


Figure 5.2. Typical response of copper-gold tailings in constant volume cyclic DSS loading (sample CG-03: $\sigma'_{vo} = 100$ kPa, CSR = 0.190). a) Stress strain, b) stress path response, and c) pore water pressure ratio versus number of cycles.

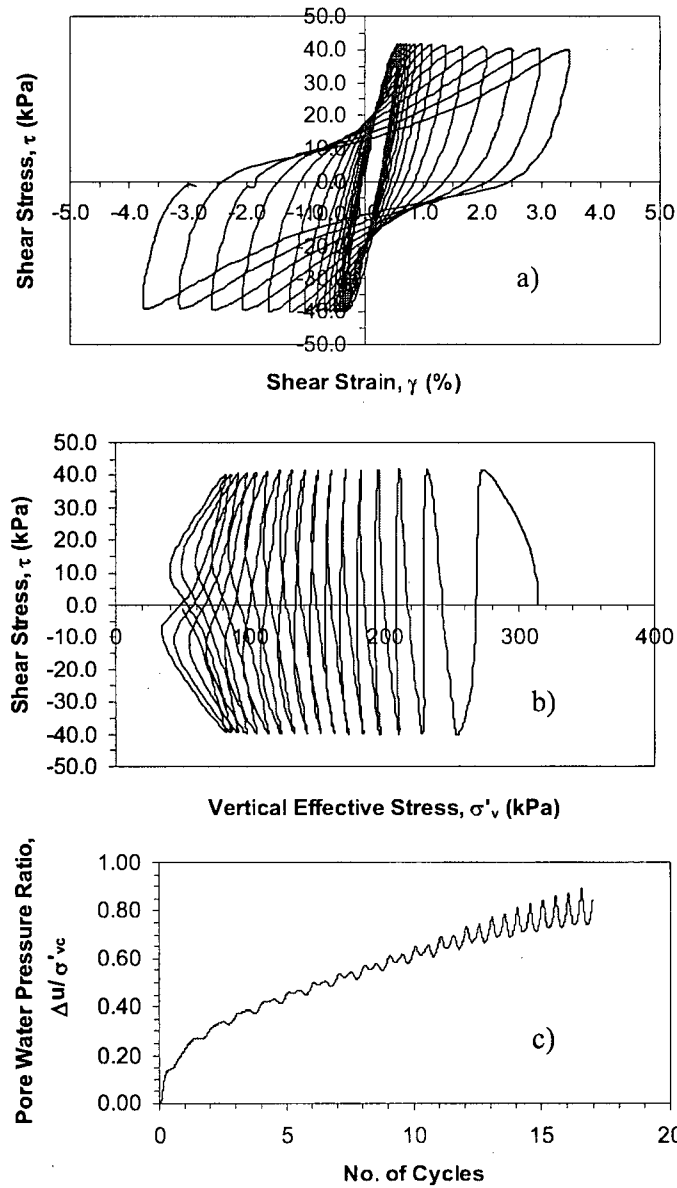


Figure 5.3. Typical response of copper-gold-zinc tailings in constant volume cyclic DSS loading (sample CGZ-20: $\sigma'_{vo} = 314$ kPa, $CSR = 0.129$). a) Stress strain, b) stress path response, and c) pore water pressure ratio versus number of cycles.

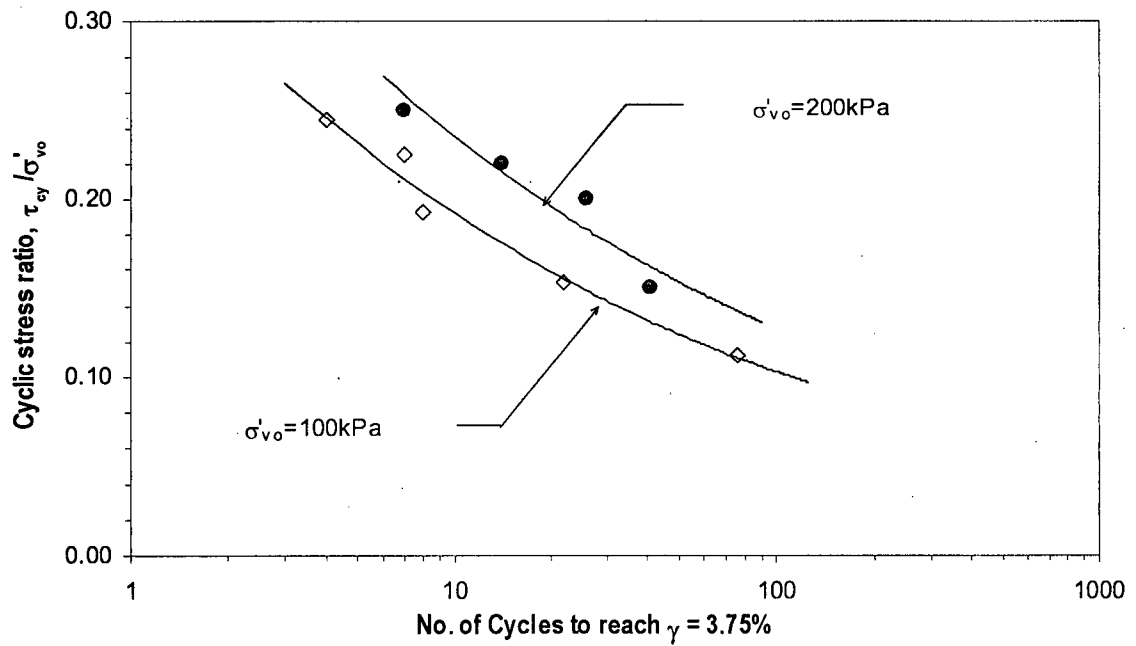


Figure 5.4. Cyclic stress ratio versus number of cycles to trigger liquefaction for samples of laterite tailings tested at two confining stress levels.

cyclic loading, e_c , varies from 1.393 for samples tested at $\sigma'_{vo} = 100$ kPa to 1.253 for samples tested at $\sigma'_{vo} = 200$ kPa.

The observed experimental relationship between CSR vs. N_L from the tests on copper-gold-zinc tailings is shown in Figure 5.5. In contrast to the effects of confining pressure observed above for the laterite tailings, the cyclic resistance ratio appears to be relatively insensitive to the initial density condition and confining pressure. This essentially implies that the generation of shear strains during undrained cyclic loading is governed by the mobilized shear stress ratio. Similar behaviour has been observed by Zergoun and Vaid (1994) for normally consolidated clay in cyclic triaxial tests, and it is in accord with the typical behavioural frameworks noted for normally consolidated clay (e.g., Atkinson and Bransby 1978). Ishihara et al. (1981) have found a similar trend for undisturbed samples of tailings from zinc-lead mines and gold-silver mines; however, when reconstituted samples from a wide variety of tailings were tested, the CRR was noted to decrease with increasing void ratio (Ishihara et al. 1980). With regard to copper-gold-zinc data examined herein, it is important to note that the observations are based on test specimens obtained from a range of test locations and depths (i.e., corresponding to a wide range of void ratio and stress levels); as such, additional tests conducted on specimens obtained from similar depths would be required prior to arriving at definitive conclusions.

The cyclic shear resistance values from three reconstituted tailings samples of copper-gold-zinc tailings, prepared using the slurry-deposition method, are also overlain in Figure 5.5. Except for one test result that appears to be anomalous, results for the remaining two tests are in good agreement with those obtained from the testing of field samples. It is possible that potential destructuring of particle fabric due to sample disturbance, and due to subsequent consolidation

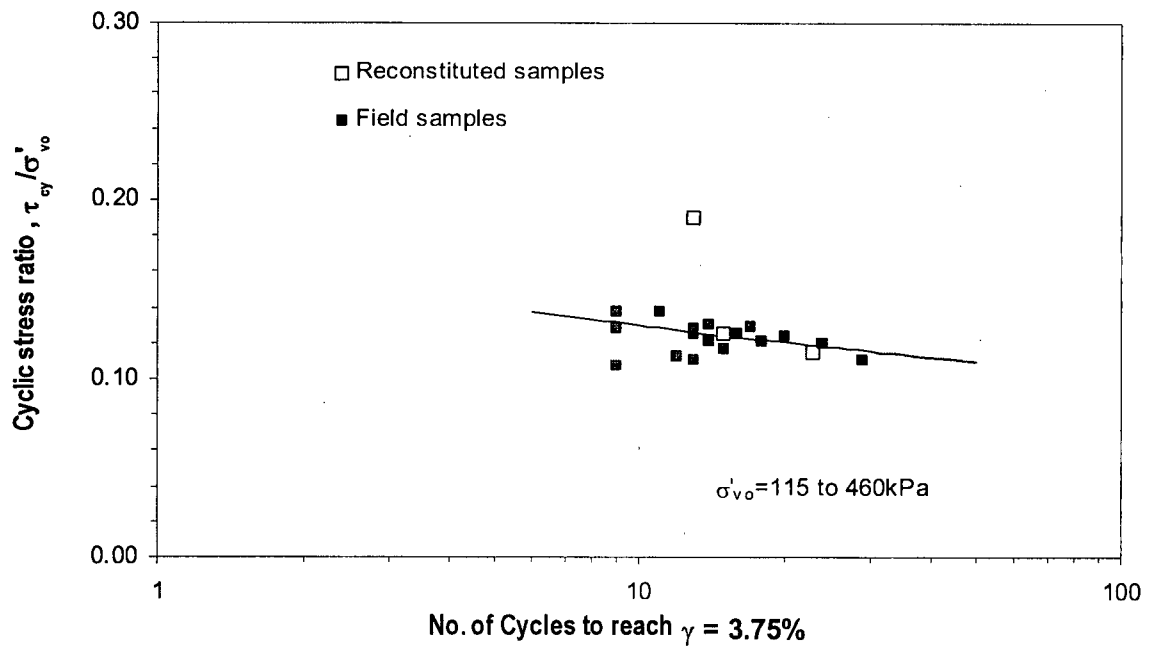


Figure 5.5. Cyclic stress ratio versus number of cycles to trigger liquefaction for samples of copper-gold-zinc tailings tested at different confining stress levels.

to stress levels in excess of the in situ overburden stresses, may have caused the field samples to yield CRR values similar to those obtained for re-constituted samples.

The value of CRR versus number of cycles to trigger liquefaction obtained from the cyclic DSS tests on copper-gold tailings conducted with $\sigma'_{vo} = 100$ kPa are plotted in Figure 5.6 together with the results of laterite tailings tested at $\sigma'_{vo} = 100$ kPa and copper-gold-zinc tailings. Although similar in terms of the observed low plasticity, the cyclic resistance of copper-gold tailings is noted to be significantly higher than those observed for copper-gold-zinc tailings. It is also of interest to note that the laterite tailings with a relatively high plasticity exhibited a cyclic resistance somewhat lower than that for the copper-gold tailings. This difference is likely due to the higher void ratio of the former in comparison to the latter, along with the contributions from experimental scatter. It is also known that laterite tailings are subjected to high temperatures and pressures combined with exposure to sulphuric acid imparted during the acid leach process. Using microscopic examination techniques, Azam et al. (2000) have noted that acid leach process could introduce profound changes to the mineralogy of laterite tailings. Further study would be required to determine whether there is any specific effect of acid leaching on the cyclic shear response.

In addition to the above data presented herein, previously published data on the cyclic resistance of several other types of tailings, arising from both cyclic triaxial (CTX) and DSS tests (See Section 2.3.4 and Figure 2.6), is presented in Figure 5.7 together with the data examined in this study.

The results from Moriwaki et al. (1982), shown in Figure 5.7, indicate that the cyclic resistance ratio (CRR) values derived from DSS tests on undisturbed samples of copper slimes (fine

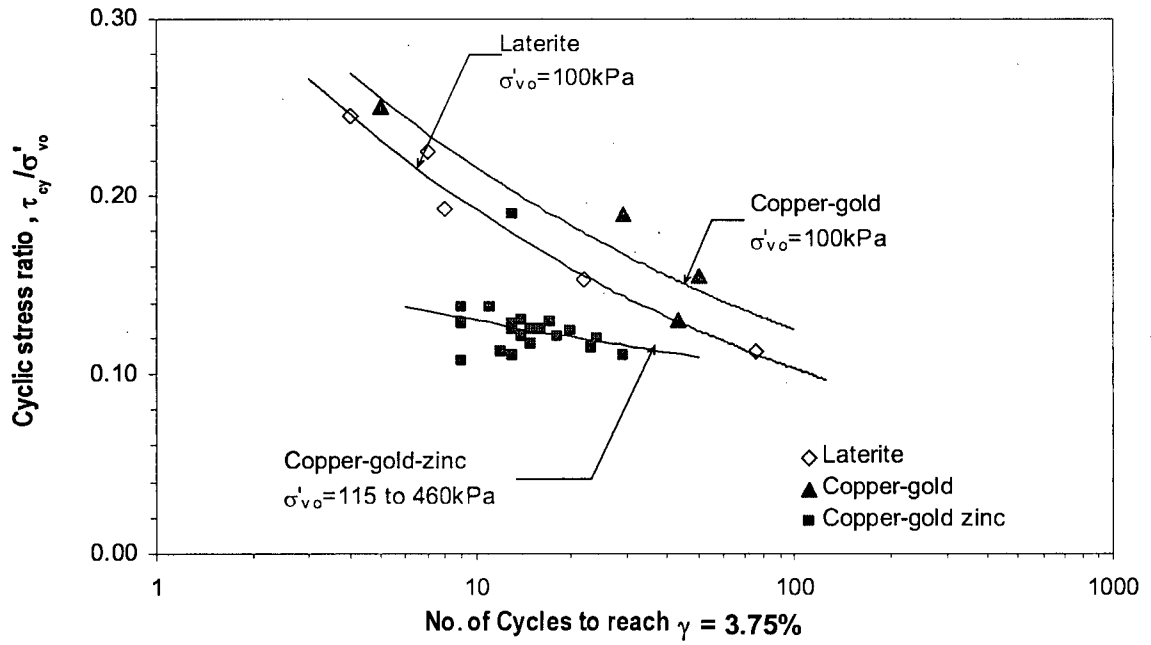


Figure 5.6. Comparison of cyclic stress ratio versus number of cycles to trigger liquefaction for laterite, copper-gold, and copper-gold-zinc tailings.

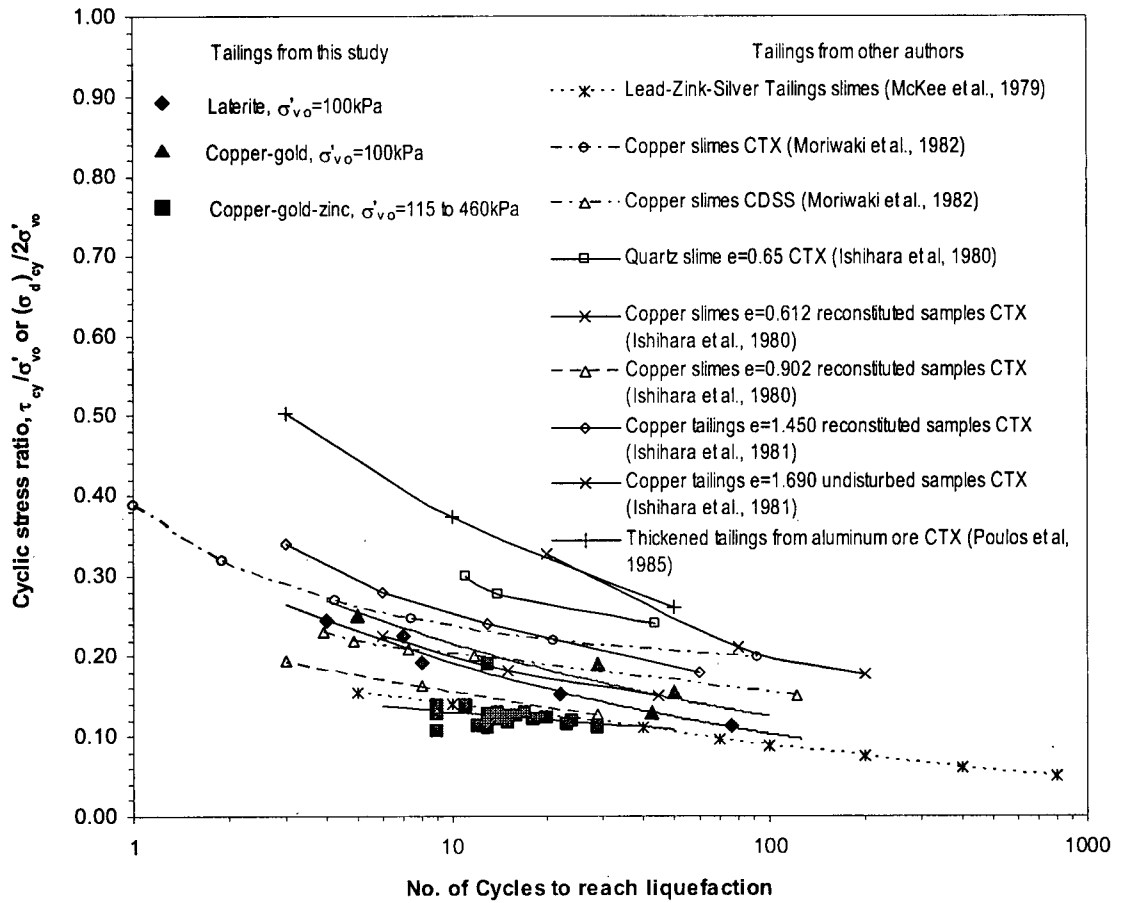


Figure 5.7. Cyclic shear resistance to liquefaction of samples included in this study compared with data from literature.

tailings) are significantly less than those derived from cyclic triaxial tests for the same tailings. The data compiled for this study from cyclic DSS tests also fall in the lower part of the plot in comparison to those reported by others, mainly based on data from cyclic triaxial tests. While this difference could be considered mainly a result of the difference in the mode of loading between DSS and triaxial tests (Roscoe 1970; Seed and Peacock 1971; Finn et al. 1978; Donaghe and Gilbert 1983), it may also be attributable to the manner in which τ_{cy} in DSS tests, and $(\sigma_d)_{cy}/2$ in triaxial tests, are normalized (i.e., the use of σ'_{vo} for normalizing both test types). For example, based on hollow cylinder tests on sands, Ishihara (1996) has observed that there is no significant difference in the cyclic resistance obtained for varying K_c conditions if the cyclic resistance ratio (CRR) is examined in terms of τ_{cy}/σ'_{mc} instead of using τ_{cy}/σ'_{vc} [Note: σ'_{mc} = initial effective mean normal stress (σ'_{mc}); $K_c = \sigma'_{ho} / \sigma'_{vo}$; σ'_{ho} = consolidation horizontal effective stress σ'_{vo} prior to cyclic loading]. Since the horizontal stress is not measured in the DSS tests presented herein, the value of σ'_{mc} could not be computed for the data presented; therefore, a comparison between the results from triaxial vs. DSS tests using σ'_{mc} as a normalizing parameter was not attempted with the present database.

5.4.2 Post-Cyclic Shear Resistance

Figure 5.8 presents typical post-cyclic response observed in monotonic constant volume DSS tests conducted on specimens of laterite, copper-gold, and copper-gold-zinc tailings that had reached $\gamma = 3.75\%$ strain criteria during cyclic loading. As may be noted, post-cyclic shear stress-strain response has a very low initial shear stiffness that is typical of liquefied soils in comparison to non-liquefied soils where the initial shear stiffness is generally larger than the

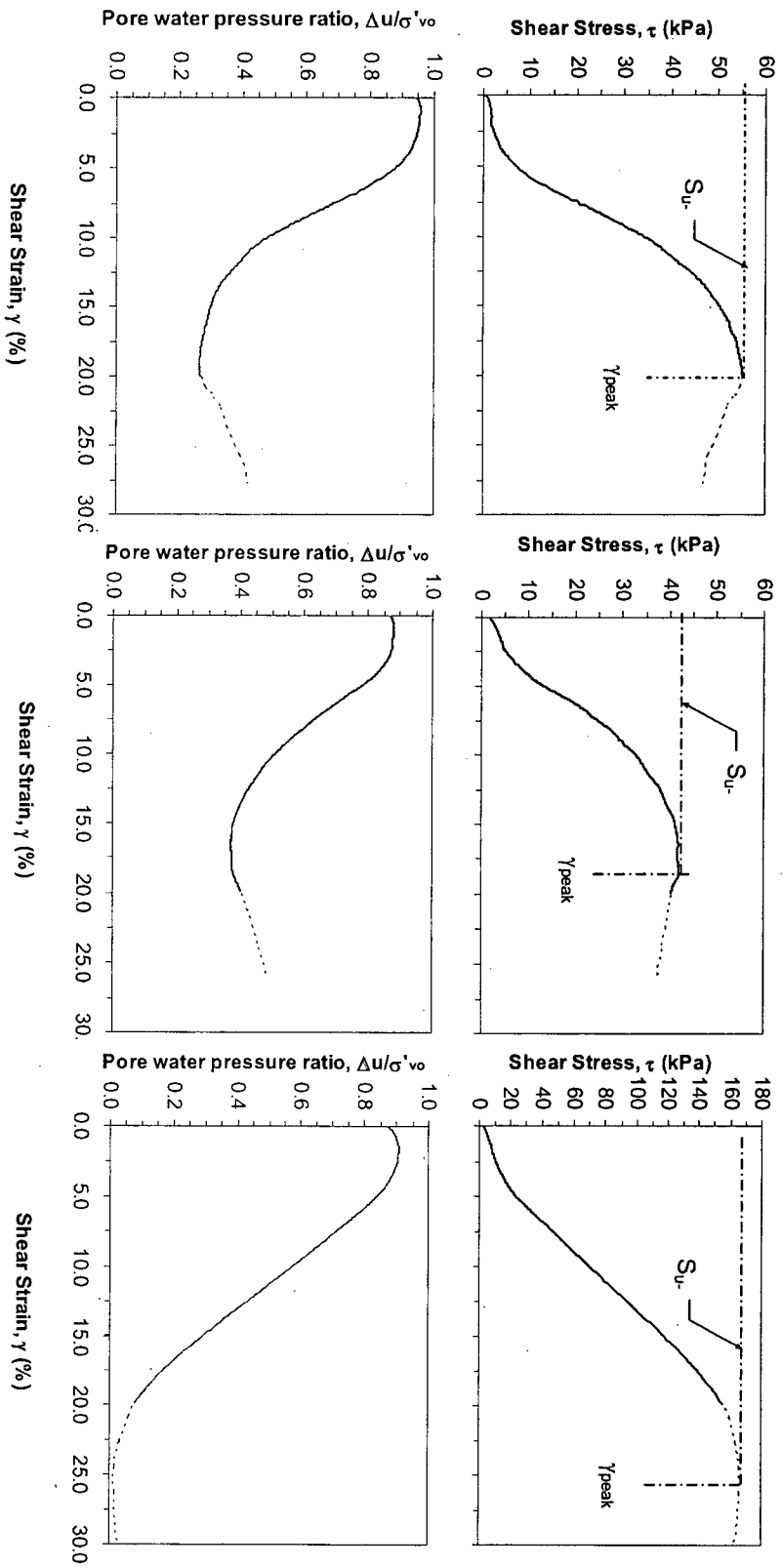


Figure 5.8. Post cyclic monotonic DSS tests on samples of a) laterite – sample L-100-02, b) copper-gold – sample CG-03 and c) copper-gold zinc – sample CGZ-20. Definition of post-cyclic maximum undrained shear strength (S_{u-PC}) is also shown.

stiffness generated with increasing strain level. With increasing shear strain level, the samples clearly exhibited dilative response along with increasing shear stiffness; with further shearing, the shear stiffness drops until shear strength seems to reach a peak (or a plateau) at relatively large strains (i.e., $\gamma = 15\%$ to 20%). It is noted that test data at large strains, shown in dashed lines in Figure 5.8, may be subject to error due to potential high stress and strain non-uniformities within DSS specimens. Hence, caution should be exercised in interpreting the data at these strain levels. The early part of the post-cyclic stress strain response, with initially very low and subsequent build up of shear stiffness, is also similar to those reported by Vaid and Sivathayalan (1997) from their simple shear tests on water-pluviated sands under simple shear loading.

The post-cyclic maximum undrained shear strength (S_{u-PC}) was estimated from the available post-cyclic monotonic DSS test data for the three fine-grained tailings. The definition of S_{u-PC} is schematically illustrated in Figure 5.8. The S_{u-PC} thus obtained for all the DSS tests were then normalized with respect to the initial vertical effective consolidation stress (σ'_{vc}) to obtain the post-cyclic maximum shear strength ratio (S_{u-PC}/σ'_{vc}). Figure 5.9 presents a plot of S_{u-PC}/σ'_{vc} vs. the corresponding consolidation void ratio (e_c) for the laterite and copper-gold-zinc tailings samples. It is noted that the two points of $S_{u-PC}/\sigma'_{vc} > 0.6$, for copper-gold-zinc tailings, in Figure 5.9 were considered anomalous and not included for developing the trend lines. A clear trend of increasing post-cyclic shear strength ratio with decreasing void ratio (or increasing density) can be noted for the laterite and copper-gold-zinc tailings. The results also indicate that, for a given void ratio, the value of S_{u-PC}/σ'_{vc} for laterite tailings is larger than that for copper-gold-zinc tailings, similar to the observations with regard to the relative difference in the observed CRR between the two tailings. Since the copper-gold samples were tested at

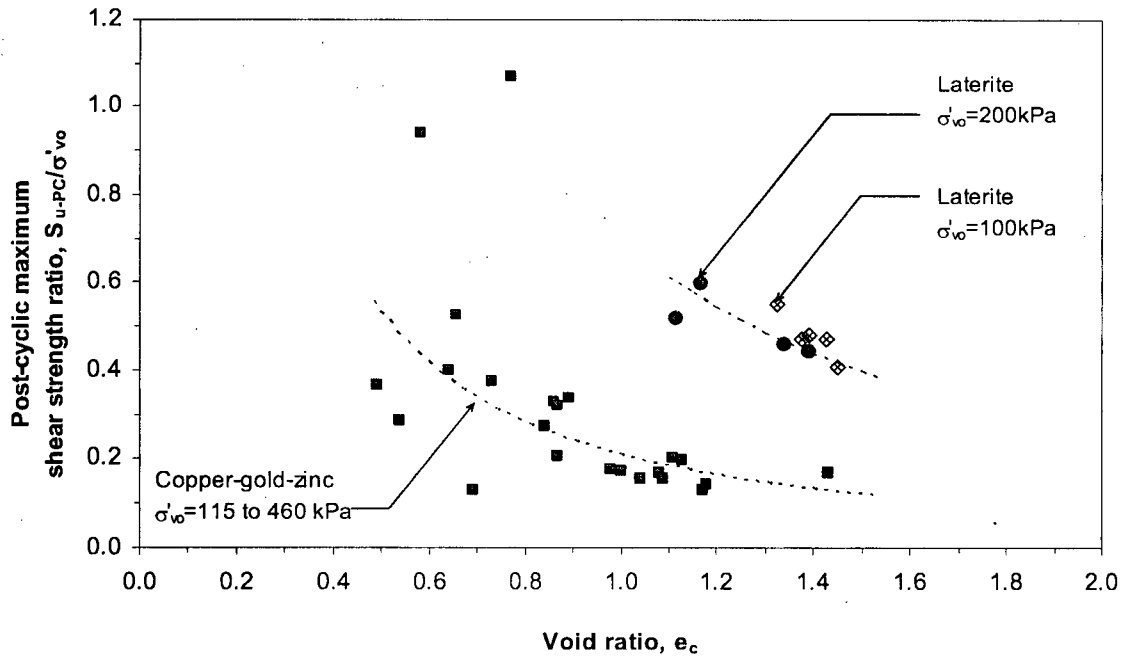


Figure 5.9. Variation of post-cyclic maximum shear strength ratio with void ratio.

essentially the same starting void ratio (e_c), the data for that material did not provide an opportunity to observe the effect of void ratio on liquefied strength ratio for these tailings.

The trend noted in Figure 5.9 is conceptually in accord with liquefied strength ratio (S_u -LIQ) vs. normalized penetration resistance (i.e., packing density) correlations suggested by Olson and Stark (2002), based on back analysis of 33 case histories. The S_{u-PC}/σ'_{vc} observed in the laboratory for the laterite and copper-gold-zinc tailings (i.e., ranging between 0.41 to 0.60 and 0.13 to 0.53, respectively) are larger than the liquefied strength ratio of $0.02 < S_{u(min)}/\sigma'_{vc} < 0.20$ assessed by Olson and Stark (2003) from triaxial compression test data for loose sandy soils. The S_{u-PC}/σ'_{vc} values are also different from the values of $0.10 < S_{PT}/\sigma'_{vc} < 0.26$ observed by Vaid and Sivathayalan (1996) for Fraser River sand in simple shear. Olson and Stark (2003) used the minimum strength observed in monotonic triaxial undrained testing as the liquefied shear strength $S_{u(min)}$; Vaid and Sivathayalan (1996) have defined S_{PT} as the mobilized shear strength at phase transformation (i.e. minimum strength) in constant volume monotonic loading DSS tests.

Castro (2003), based on triaxial tests conducted on a natural fine-grained soil of low plasticity, has also observed differences in liquefied strength ratios similar to those noted above; in this study, he noted that the post-cyclic S_{u-PC}/σ'_{vc} is significantly higher than the observed undrained steady state strength ratio (S_{u-SS}/σ'_{vc}).

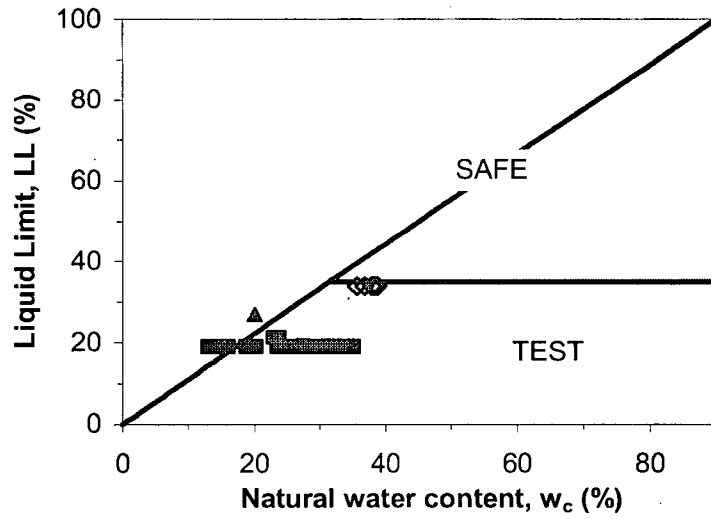
The post-cyclic monotonic DSS tests on fine-tailings used for the computation of (S_{u-PC}/σ'_{vc}) commence from an initial state that has a stress-strain history (and particle fabric) significantly different from the initial states of the static (monotonic) tests considered for computing $S_{u(min)}/\sigma'_{vc}$ (Olson and Stark 2003) as well as S_{PT}/σ'_{vc} (Vaid and Sivathayalan 1996). As

such, in addition to the contrast in particle size distributions between the material types tested (sandy soils vs. fine-grained tailings), the above disparity in initial state with regard to strain history would have contributed to the observed differences between S_{u-PC}/σ'_{vc} of this study and the other two liquefied strength ratio values reported by Olson and Stark (2003) and Vaid and Sivathayalan (1996). Clearly, in addition to the distinction between the field and laboratory, the above differences among the laboratory testing approaches is another important consideration in the interpretation and usage of derived shear strengths for seismic stability evaluation.

5.4.3 Applicability of Empirically Based Liquefaction Criteria

The results from DSS tests on the three tailings materials considered herein were initially evaluated with respect to the commonly used empirical Chinese criteria, stated by Seed and Idriss (1982) based on an original proposal by Wang (1979), described in Section 2.3.2 of this thesis. As proposed by Marcuson et al. (1990), the above liquid limit and water content criteria can be graphically presented as shown in Figure 5.10, and any soils that would classify into the zone denoted as “safe” are considered not susceptible to liquefaction. It has been recommended that the samples of any soils that would classify outside the “safe” zone should be tested in cyclic shear (or “further investigated”) to determine the liquefaction susceptibility.

The index data for the three tailings types considered for this study were also plotted in Figure 5.10 to review the suitability of these criteria. It can be noted that the liquid limit and water contents for the copper-gold tailings classify within the “safe” or no-liquefaction zone. Nevertheless, the available results from cyclic laboratory DSS testing suggest that the copper-gold tailings would reach a shear strain (γ) of 3.75% in 15 cycles, or considered to have



Tailing	Clay content: (% finer 0.002 mm)
◇ Laterite	35%
▲ Copper-gold	9.9%*
■ Copper-gold-zinc	N/A

* Average value

Figure 5.10. Applicability of Chinese criteria for the tailings considered in this study (modified from Marcuson et al. 1990).

liquefied, if the samples are subjected to a cyclic stress ratio of 0.17. This indicates that this material has the potential to liquefy (or develop significant strains and pore water pressure) under a level of shaking commonly encountered in seismically active areas. The liquid limit and water contents of most of the copper-gold-zinc tailings samples were classified within the zone of "further testing required". Yet, the results from DSS tests for two copper-gold-zinc tailings samples that were classified as "safe" using Chinese criteria clearly, again, indicate potential liquefaction under certain levels of cyclic loading. It is also noted that the laterite tailings with a percent of fines smaller than 0.002 mm of 35% are not considered susceptible to liquefaction according to the Chinese criteria. Andrews and Martin (2000) suggest that soils are liquefiable if they have less than 10% clay-size particles and a liquid limit of less than 32. The soils are considered not susceptible to liquefaction if the above criteria are not met. Soils that classify between these criteria should be tested to assess the liquefaction potential.

Andrews and Martin (2000) emphasize that the clay content alone does not properly address the cases involving non-plastic clay-size particles such as mine tailings. Since there is an exception to the materials with clay particles from mine tailings, Andrews and Martin (2000) criteria are not directly applicable herein.

Bray et al. (2004a) proposed new criteria for the evaluation of liquefaction susceptibility of fine-grained soils based on observations and laboratory testing after the 1999 Kocaeli earthquake. The criteria are based on the ratio of water content to liquid limit (w_c/LL) and the plastic index (PI). Data from the three fine-grained tailings of this study are plotted in Figure 5.11 to compare with the proposed criteria. The Bray et al. empirical criterion is in good agreement with the assessments from cyclic DSS tests for laterite tailings and most of copper-

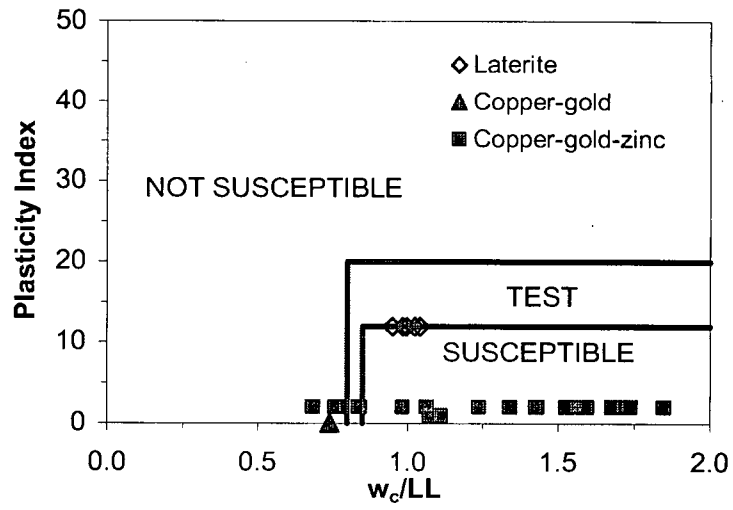


Figure 5.11. Applicability of the liquefaction susceptibility criteria proposed by Bray et al. (2004b) for the tailings considered in this study.

gold-zinc tailings. However, similar to the observations for Chinese criteria, the samples of copper-gold tailings and two samples of the copper-gold zinc tailings are considered not susceptible to liquefaction, contrary to the results derived from the DSS tests.

6 SUMMARY AND CONCLUSIONS

A detailed laboratory element testing research program was undertaken to investigate the undrained cyclic loading response of a natural channel-fill silt obtained from the Fraser River Delta of British Columbia, Canada. Undisturbed samples were used in the testing program, the main focus of which was on constant volume direct simple shear (DSS) tests. A limited number of conventional triaxial and consolidation tests were also undertaken. Available data from constant volume cyclic DSS tests from fine-grained mine tailings was also reviewed.

6.1 Undrained Monotonic Response of Channel-Fill Fraser River silt

Normally consolidated specimens tested in the triaxial apparatus and in the DSS device showed that channel-fill Fraser River silt initially behaves in a contractive manner followed by a dilative response. In terms of stress-strain response, all specimens showed a strain-hardening behaviour that is typical of material undergoing shear-induced dilative response.

6.2 Undrained Cyclic Loading Response of Normally Consolidated Silt

Under cyclic loading, normally consolidated specimens of channel-fill Fraser River silt exhibited progressive increase in equivalent excess pore water pressure ratio (r_u) with degradation of shear modulus in all tests conducted at different cyclic stress ratios (CSR). This is essentially the “cyclic-mobility” type of response that has been observed previously in dense sands. The specimens generally exhibited initially contractive response followed by dilative response. Specimens tested under more severe CSR levels manifested phase transformation at early stages of cyclic loading, and reached r_u of approximately 100% in a lesser number of cycles than those subjected to low CSR values. The cyclic resistance ratio versus number of cycles to liquefaction relationship for the tested channel-fill silt is not sensitive to the initial confining stress, for stress levels below 200 kPa.

6.3 Undrained Cyclic Loading Response of Overconsolidated Silt

Overconsolidated specimens of channel-fill Fraser River silt exhibit “cyclic mobility” type stress-strain response similar to that observed for normally consolidated specimens. However, for moderate levels of cyclic loading, specimens of overconsolidated Fraser River silt exhibit a more pronounced dilative response in comparison to the normally consolidated counterparts. This effect becomes more evident for higher values of OCR.

The cyclic resistance ratio (CRR) of Fraser River silt increases with increasing OCR when the overconsolidation ratio is above 1.3. For example, the specimen of silt initially consolidated to $OCR = 2$ exhibited CRR values about 60% higher than those observed for the counterpart NC

specimens. No significant improvement in CRR was noted for lightly consolidated silt ($OCR < 1.3$).

6.4 Repeated Cyclic Loading Response of Silt

Undrained cyclic shear tests conducted on silt specimens that had been previously subjected to cyclic loading display a "cyclic mobility" type of response, again, similar to that observed during the first cyclic loading. The number of cycles to reach the pre-defined strain liquefaction criteria, however, is consistently less than those noted during the first cyclic loading. The decrease in cyclic shear resistance (CRR) due to degradation of particle fabric as a result of previous shearing appears to have overshadowed any gain in CRR that would have taken place due to reduction of void ratio during re-consolidation. Nevertheless, some strengthening in the soil fabric seems to take place after reaching larger strain levels.

6.5 Post-cyclic Consolidation Response of Channel-fill Fraser River Silt

The silt specimens that experienced large equivalent excess pore water pressure ratios (r_u values) during cyclic loading suffered significant post-cyclic consolidation strains. On the other hand, the specimens that developed small r_u levels during cyclic loading resulted in relatively smaller post-cyclic consolidation strains. The observed considerable volume changes are likely a reflection of the significant changes in the particle structure experienced by the specimen due to cyclic loading. In general, the observed volumetric strains in the case of silt

specimens that developed high r_u values are higher than those typically observed by others from post-cyclic consolidation of sands.

Extensive particle rearrangement appears to occur in the silt after repeated cyclic loading. It is observed that specimens subjected to repeated cyclic loading and subsequent re-consolidation also show considerable settlement, although smaller than those observed during re-consolidation following the first cyclic loading.

6.6 Applicability of Empirically Based Criteria for Liquefaction Assessment

On the basis of strain development, Fraser River silt is liquefiable when subjected to a certain threshold number of cycles of a given cyclic shear stress. Bray et al. (2004b) criteria that determine the liquefaction susceptibility based on plasticity and in-situ moisture content (i.e., void ratio) clearly classify Fraser River silt as liquefiable. Polito (2001) criteria, which are based only on plasticity and without including moisture content, place Fraser River silt in the “potentially liquefiable” zone. The original Chinese criteria (which use plasticity characteristics, fraction of clay size particles, and moisture content as parameters) provide borderline classifications for the liquefaction susceptibility of Fraser River silt. The present study confirms that the liquefaction susceptibility assessed using empirical criteria sometimes lead non-conclusive determinations. The occurrence of liquefaction is determined by many parameters such as applied cyclic stress ratio, overconsolidation ratio, etc., in addition to the simple index parameters. The current empirical criteria do not consider many of the above parameters that critically govern the liquefaction susceptibility, and as a result, they may not

provide the liquefaction susceptibility with the level of certainty needed for engineering practice. Laboratory element testing that allows capturing the effect of most controlling parameters seems to still remain as the more reliable approach for estimating liquefaction susceptibility of a given silt.

6.7 Cyclic Loading Response of Fine-grained Mine Tailings

Fine-grained mine tailings typically exhibit "cyclic mobility" type of response, similar to the behavioural trend observed for natural Fraser River silt and compact to dense reconstituted sand. In contrast to the effects of confining pressure observed for channel-fill Fraser River silt and for the copper-gold fine-grained tailings, where the cyclic resistance ratio appears to be insensitive to the initial density condition and confining pressure, cyclic shear tests on laterite tailings indicate that the resistance to liquefaction increases with the increasing confining pressure. This suggests that, for this material, any dilative tendency arising due to stress densification seems to have overcome the possible contractive tendency due to the increase in confining stress.

A clear trend of increasing post-cyclic maximum shear strength ratio with decreasing void ratio (or increasing density) has been noted for the laterite and copper-gold-zinc tailings. This trend is conceptually in accord with liquefied strength ratio vs. normalized standard penetration resistance correlations derived based on back-analysis of field case histories. However, it is noted that larger measured liquefied strengths arising in the laboratory samples do not necessarily represent the in-situ conditions; in particular, the undrained tests on laboratory

samples are not capable of representing the void redistributions, and associated changes in pore water pressure, that take place under field conditions. Therefore, it is important that direct use of laboratory derived post-cyclic strength data should be used with caution in the seismic stability analyses of tailings structures with due recognition of the differences between the field and the laboratory.

For the fine-grained tailings considered in the study, the liquefaction susceptibility predicted using commonly used empirical criteria is not always in agreement with the liquefaction triggering determined from cyclic DSS tests.

6.8 Sample Disturbance

In addition to investigating the fundamental characteristics of cyclic loading response of channel-fill Fraser River silt, this research work also included the developing and assessment of effectiveness of an undisturbed soil sample holder (USSH) for preparation of triaxial specimens. The purpose of this device is to minimize disturbance of specimens during the preparation of relatively soft fine-grained cylindrical soil samples. The USSH is capable of receiving a specimen of soil upon extrusion from a field sampling tube and, immediately thereafter, providing suitable external, uniform lateral confinement to the extruded specimen.

7 REFERENCES

- Andrews, D.C. and Martin, G.R., 2000. Criteria for liquefaction of silty soils. Proceedings of the 12th World Conference on Earthquake Engineering, Auckland, New Zealand, Paper No. 0312, pp. 1-8.
- ASTM-D 422-63. Standard test method for particle-size analysis of soils. ASMT International.
- ASTM-D 4318-00. Standard test methods for liquid limit, plastic limit and plasticity index if soils. ASTM International.
- ASTM-D 854-02. Standard test methods for specific gravity of soil solids by water picnimeter. ASTM International.
- Atkinson, J.H., and Bransby, P.L. 1978. The mechanics of soils: An introduction to critical state soil mechanics. McGraw-Hill Book Co., London and New York.
- Atukorala, U.D., Wijewickreme, D., and McCammon, N.R. 2000. Some observations related to liquefaction susceptibility of silty soils. In Proceedings of the 12th World Conference on Earthquake Engineering, Auckland, New Zealand. Paper No. 1324.
- Azam, S., Chalaturnyk, R.J., Scott, J.D., and Stiksmas, J. 2000. Characteristics of laterite slurry tailings from acid leach metal extraction process. In Proceedings of the 53rd Annual Conference of the Canadian Geotechnical Society, Montreal. 4-9 September 2000. Canadian Geotechnical Society, pp. 657-664.
- Baligh, M.M., Azzouz, A.S., and Chin, C.T., 1987, Disturbances due to ideal tube sampling, Journal of the Geotechnical Engineering Division, ASCE, Vol. 113, No. GT7, pp. 739-757.
- Becker, D. E., Crooks, J. H. A., Been, K. and Jefferies, M. G. 1987. Works as a criterion for determining insitu and yield stresses in clay. Canadian Geotechnical Journal. 24:549-564.
- Bjerrum, L., and Landva, A. 1966. Direct simple shear tests on a Norwegian quick clay. Geotechnique, 16(1): 1-20.
- Boulanger, R. W. and Idriss, I. M. 2004. Evaluating the potential for liquefaction or cyclic failure of silts and clays. Report No. UCD/CGM-04/01. Center for Geotechnical Modeling,

- Department of Civil and Environmental Engineering, University of California, Davis, California.
- Boulanger, R. W., Meyers, M. W., Mejia, L. H., Idriss, I. M. 1998. Behavior of a fine-grained soil during the Loma Prieta earthquake. *Canadian Geotechnical Journal*; 35: 146-158.
- Bray, J.D., Sancio, R.D., Durgunoglu, T., Onalp, A., Youd, T.L., Stewart, J. P., Seed, R.B., Cetin O. K., Bol, E., Baturay, M. B., Christensen, C., and Karadayilar, T. 2004a. Subsurface Characterization at Ground Failure Sites in Adapazari, Turkey. *Journal of Geotechnical and Geoenvironmental Engineering*. ASCE, 130(7):673-685.
- Bray, J.D., Sancio, R.B., Riemer, M.F. and Durgunoglu, T. 2004b. Liquefaction Susceptibility of Fine-Grained Soils, Proceedings of the 11th International Conf. On Soil Dynamics and Earthquake Engineering and 3rd International Conf. On Earthquake Geotechnical Engineering, Berkeley, CA, Jan. 7-9, 2004; pp. 655-662.
- Byrne, P.M., Park, S.S., Beaty, M., Sharp, M., Gonzalez, L., and Abdoun, T. 2004. Numerical modeling of liquefaction and comparison with centrifuge tests. *Canadian Geotechnical Journal*, 41(2):193-211.
- Campanella, R. G. and Lim, B.S. 1981. Liquefaction characteristics of undisturbed soils. In Proceedings of International Conference on Recent Advances in Geotechnical Earthquake Engineering and Soil Dynamics, University of Missouri-Rolla, St. Louis, MO. Vol.1, pp. 227 - 230.
- Casagrande, A. 1936a. Characteristics of cohesionless soils affecting the stability of slopes and earth fills. *Journal of the Boston Society of Civil Engineers*, pp. 257-276.
- Casagrande, A. 1936b. The determination of the preconsolidation load and its practical significance. In Proceedings of the 1st International Conference on Soils Mechanics and Foundation Engineering. Cambridge, Mass., 3:60-64.
- Casagrande, A. 1975. Liquefaction and cyclic deformation of sands: A critical review. In Proceedings of the 5th American Conference on Soil Mechanics and Foundations Engineering, Buenos Aires, Argentina, Vol 5, pp. 79-133.
- Castro, G. 1969. Liquefaction of sands. Ph.D. thesis, Harvard University, Cambridge, Mass.
- Castro, G. 2003. Evaluation of seismic stability of tailings dams. In Proceedings of the 12th Panamerican Conference on Soil Mechanics and Geotechnical Engineering. Soil Rock America 2003, Massachusetts Institute of Technology, Cambridge Mass. 22-26 June 2003. Edited by P.J. Culligan, H.N. Einstein, and A.J. Whittle. Vol.2, pp. 2229-2234.
- Castro, G. Poulos, S. J., France, J. W., And Enos, J.L. 1982. Liquefaction induced by cyclic mobility. Report by Geotechnical engineering Inc., Winchester, Mass., to the National science Foundation, Washington, D.C., Department of Commerce, Access number PB 82-235508.

- Cetin, K.O., Seed, R.B., Kiureghian, A.D., Tokimatsu, K., Harder, L.F. Jr., Kayen, R.E., and Moss, R.E.S. 2004. Standard Penetration Test-Based Probabilistic and Deterministic Assessment of Seismic Soil Liquefaction Potential, *Journal of Geotechnical and Geoenvironmental Engineering*, ASCE, 130(12): 1314-1340.
- Chalkley, M.E., and Toirac, I.L. 1997. The acid pressure leach process for nickel and cobalt laterite. Part I: Review of operation at Moa. In *Proceedings of the 27th Annual Hydrometallurgical Meeting*, Sudbury, Ontario. 17-20 August 1997. The Metallurgical Society of CIM, pp. 341-347.
- Chern, J.C. 1985. Undrained response of saturated sands with emphasis on liquefaction and cyclic mobility. Ph.D Thesis, Department of Civil Engineering, University of British Columbia, Vancouver, BC, Canada.
- Clague, J.J., Bobrowsky, P. T., Guilbault, J. P., Linden, R. H., Mathewes, R. W., Naesgaard, E., Shilts, W. W., and Sy, A. 1996. Paleoseismology and Seismic Hazards, Southwestern British Columbia. Geological Survey of Canada, Bulletin 494: 1-88.
- Crawford, C. B. and Morrison, K. I. 1996. Case histories illustrate the importance of secondary-type consolidation settlements in the Fraser River Delta. *Canadian Geotechnical Journal*, 33: 866-878.
- Davies, M.P. 2002. Tailings impoundment failures: Are geotechnical engineers listening? *Geotechnical News*, 20(3): 31-36.
- Donaghe, R.T., and Gilbert, P.A. 1983. Cyclic rotation of principal planes to investigate liquefaction of sands. Miscellaneous Paper GL-83-24. US Army Engineer Waterways Experiment Station, Vicksburg, MS.
- Dyvik, R., Berre, T., Lacasse, S., and Raadim, B. 1987. Comparison of truly undrained and constant volume direct simple shear tests. *Geotechnique*, 37(1): 3-10.
- Finn, W.D.L., and Vaid, Y.P. 1977. Liquefaction potential from drained constant volume cyclic simple shear tests. In *Proceedings of the 6th World Conference on Earthquake Engineering*. Sarita Prakashan Publishers, Meerut, India. Vol III, pp. 2157-2162.
- Finn, W.D.L., and Yogendrakumar, M. 1989. TARA-3FL: Program for analysis of liquefaction-induced flow deformations. Department of Civil Engineering, The University of British Columbia, Vancouver, B.C., Canada.
- Finn, W.D.L., Bransby, P.L., and Pickering, D.J. 1970. Effect of strain history on liquefaction of sand. *Journal of the Soil Mechanics and Foundations Division*, 96(SM6): 1917-1934.
- Finn, W.D.L., Vaid, Y.P., and Bhatia, S.K. 1978. Constant volume simple shear testing. In *Proceedings of the 2nd International Conference on Microzonation for Safer Construction-Research and Application*, San Francisco, U.S.A. Vol.II, pp. 839-851.

- Finn, W.D.L., Ledbetter, R.H., and Wu, G. 1994. Liquefaction in silty soils: design and analysis. In *Ground failures under seismic conditions*. Edited by S. Prakash and P. Dakoulas. American Society of Civil Engineers. Geotechnical Special Publication 44, pp. 51-76.
- Gananathan, N. 2002. Partially drained response of sands. M.A.Sc. thesis, Department of Civil Engineering, The University of British Columbia, Vancouver, B.C., Canada.
- Hight, D.W., and Leroueil, S. 2003. Characterisation of soils for engineering purposes. In *Characterisation and Engineering Properties of Natural Soils*. Edited by Tan et al. Vol. 1, pp. 255-360.
- Hight, D.W., Boese, R., and Butcher, A.P., Clayton, C.R.I., and Smith, P.R., 1992, Disturbance of the Bothkennar Clay prior to laboratory testing, *Geotechnique*, Vol. 42, No. 2, pp. 199-217.
- Høeg, K., Dyvik, R and Sandbækken, G. 2000. Strength of undisturbed versus reconstituted silt and silty sand specimens. *Journal of Geotechnical and Geoenvironmental Engineering*, ASCE, 126(7):606-617.
- Ishihara, K. 1996. *Soil behaviour in earthquake Geotechnics*. Clarendon Press, Oxford.
- Ishihara, K. and Okada, S. 1982. Effects of large pre-shearing on cyclic behaviour of sand. *Soils and Foundations*, 22(3): 109-125.
- Ishihara, K. Tatsuoka, F. and Yasuda, S. 1975. Undrained deformation and liquefaction under cyclic stresses. *Soil and Foundations*, 15(1): 29-44.
- Ishihara, K. Sodekawa, M. and Tanaka, Y. 1977. Effects of overconsolidation on liquefaction characteristics of sands containing fines. *Dynamic Geotechnical Testing*. ASTM Special Technical Publication 654. Denver, Col., 28 June 1977. pp. 247 – 264.
- Ishihara, K., Troncoso, J., Kawase, Y., and Takahashi, Y. 1980. Cyclic strength characteristics of tailings materials. *Soils and Foundations*, Japanese Society of Soil Mechanics and Foundations Engineering, 20(4): 127-142.
- Ishihara, K., Yasuda, S., and Yokota, K. 1981. Cyclic strength of undisturbed mine tailings. In *Proceedings of International Conference on Recent Advances in Geotechnical Earthquake Engineering and Soil Dynamics*, University of Missouri-Rolla, St. Louis, MO. Vol.1, pp. 53-58.
- Jamiolkowski, M., Ladd, C.C., Germaine, J.T., and Lancellotta, R., 1985, New developments in field and laboratory testing of soils, Theme Lecture, *Proceedings of the 11th International Conference on Soil Mechanics and Foundation Engineering*, San Francisco, Ca., pp: 57-153.
- Janbu, N., Tokheim, O. and Senneset, K. 1981. Consolidation test with continuous loading. *Proceedings of the 10th International Conference in Soil Mechanics and Foundation Engineering*, Stockholm. 1:645-654.
- Kammerer, A., Wu, J., Pestana, J., Riemer, M., and Seed, R. 2002. Undrained response of Monterey 0/30 sand under multidirectional cyclic simple shear loading conditions:

Electronic Data Files. Geotechnical Engineering Research Report No. UCB/GT/02-02. University of California, Berkeley.

- Koester, J.P. 1992. The influence of test procedure on correlation of Atterberg limits with liquefaction in fine-grained soils. *Geotechnical Testing Journal*, 15 (4): pp. 352 – 361.
- Kokusho, T. 2003. Current state of research on flow failure considering void redistribution in liquefied deposits. *Soil Dynamics and Earthquake Engineering*, 23: 585-603.
- Kuerbis, R., Negussey, D. and Vaid, Y. P. 1988. Effect of gradation and fines content on the undrained response of sand. In *Hydraulic Fill Structures*. Edited by D.J.A. Van Zyl and S.G. Vick. Geotechnical Special Publication 21. ASCE. New York. pp: 330-345.
- La Rochelle, P., Sarraith, J., Tavenas, F., Roy, M., and Leroueil, S. 1981. Causes of sampling disturbance and design of a new sampler for sensitive soils. *Canadian Geotechnical Journal*, 18(1): 52-66.
- Ladd, C.C., and DeGroot, D.J. 2003. Arthur Casagrande Lecture: Recommended practice for soft ground characterization. In *Proceedings of the 12th Panamerican Conference on Soil Mechanics and Geotechnical Engineering*, Cambridge, Mass. Vol.1, pp. 3-58.
- Ladd, C.C., and Lambe, T.W., 1963, The strength of undisturbed clay determined from undrained tests, *Symposium on Laboratory Shear Testing of Soils*, ASTM, STP 361, pp. 342-371.
- Lade, P. V. and Yamamuro, J. A. 1997. Effect of non-plastic fines on static liquefaction of sands. *Canadian Geotechnical Journal*, 34(6):918-928.
- Lam, C. K. K. 2003. Effects of aging duration, stress ratio during aging and stress path on stress-strain behaviour of loose Fraser River sand. M.A.Sc. thesis, Department of Civil Engineering, University of British Columbia, Vancouver, BC, Canada.
- Lambe, T.W., 1967, Stress Path Method, *Journal of the Soil Mechanics and Foundation Division*, ASCE, Vol. 93, No. SM6, pp. 309-331.
- Lee, K. L., and Seed, H. B. 1967. dynamic strength of anisotropically consolidated sand. *Journal of the Soil Mechanics and Foundation Division*, ASCE, 93(SM5): 169-190.
- Lefebvre, G., and Poulin, C. 1979. A new method of sampling in sensitive clay. *Canadian Geotechnical Journal*, 16(1), 226-233.
- Leroueil, S., and Hight, D.W. 2003. Behaviour and properties of natural soils and soft rocks. In *Characterisation and Engineering Properties of Natural Soils*. Edited by Tan et al. Vol. 1, pp. 29-254.
- Long, M., 2003, Sampling disturbance effects in soft laminated clays, *Geotechnical Engineering*, Vol. 156, No. GE4, pp. 213-224.

- Lunne, T., Berre, T., and Strandvik, S., 1997, Sample disturbance effects in soft low plastic Norwegian clay, Almeida (Ed.), *Recent Developments in Soil and Pavement Mechanics*, Rotterdam: Balkema, pp. 81-102.
- Marcuson, W.F., Hynes, M.E., and Franklin, A.G. 1990. Evaluation and use of residual strength in seismic safety analysis of embankments. *Earthquake Spectra*, EERI, 6(3): 529-572.
- McKee, B.E., Robinson, K.E., and Ulrich, C.M. 1978. Upstream design for extension of an abandoned tailings pond. In *Proceedings of the 2nd International Tailings Symposium*, Denver, CO. May 1978, pp. 210-233.
- Mesri, G., Lo, D.O.K., and Feng, T.W., 1994, Settlement of Embankments on Soft Clays, Keynote Lecture, Settlement '94, Texas A&M University, College Station, Texas, Geotechnical Special Publication No. 40, Vol. 1, June 1994, 8-56.
- Monahan, P. A., Luthernauer, J. L., Barrie, J. V. 1997. The Topset and upper Foreset of the modern Fraser River Delta, British Columbia, Canada. In *Core Conference, June 5-6, 1997, CSPG-SEPM Joint Convention June 1-6, 1997*. Compiled by J. Wood and W. Martindale. Canadian Society of Petroleum Geologists, pp. 491-517.
- Monahan, P. A., Byrne, P. M., Watts, B. D and Naesgaard, E. 2000. Engineering Geology and Natural Hazards of the Fraser River Delta. Guidebook for geological field trips in Southwestern British Columbia and Northern Washington. Annual Meeting of the Cordilleran Section of the Geological Society of America. Vancouver, April 2000. pp. 27-47.
- Moriwaki, Y., Akky, M.R., Ebeling, A.M., Idriss, I.M., and Ladd, R.S. 1982. Cyclic strength and properties of tailings slimes. *Dynamic Stability of Tailings Dams*, Preprint 82-539 ASCE.
- NBCC 1995. National Building Code of Canada (NBCC), Eleventh Edition 1995, National Research Council of Canada, Ottawa, Canada
- Neguessy, D., Wijewickreme, D., and Vaid, Y.P. 1988. Constant volume friction angle of granular materials. *Canadian Geotechnical Journal*, 25(1):50-55.
- NRC. Liquefaction of soils during earthquakes. National Research Council Report CETS-EE-001, National Academic Press, Washington, D.C, 1985.
- Olson, S.M., and Stark, T.D. 2002. Liquefied strength ratio from liquefaction flow failure case histories. *Canadian Geotechnical Journal*, 39(3): 629-647.
- Olson, S.M., and Stark, T.D. 2003. Use of laboratory data to confirm yield and liquefied strength ratio concepts. *Canadian Geotechnical Journal*, 40(6): 1164-1184.
- Park, S.S., and Byrne, P.M. 2004. Stress densification and its evaluation. *Canadian Geotechnical Journal*, 41(1): 181-186.
- Peters, G., and Verdugo, R. 2003. Seismic design considerations of tailings dams (In Spanish). In *Proceedings of the 12th Panamerican Conference on Soil Mechanics and Geotechnical*

- Engineering. Soil Rock America 2003, Massachusetts Institute of Technology, Cambridge Mass. 22-26 June 2003. Edited by P.J. Culligan, H.N. Einstein, and A.J. Whittle. Vol.2, pp. 2241-2246.
- Polito, C. 2001. Plasticity based liquefaction criteria. In Proceedings of the Fourth international Conference on Recent Advances in Geotechnical Earthquake Engineering and Soil dynamics and Symposium in Honour of Professor W.D.L. Finn. San Diego, California, March 26-31, 2001; paper No. 1.33.
- Polito, C.P., and Martin, J.R. 2001. Effect on non-plastic fines on the liquefaction resistance of sands. *Journal of Geotechnical and Geoenvironmental Engineering*, ASCE, 127(5): 408-415.
- Poulos, S.J., Robinsky, E.I., and Keller, T.O. 1985. Liquefaction resistance of thickened tailings. *Journal of Geotechnical Engineering*, ASCE, 111(12): 1380-1394.
- Roscoe, K.H. 1970. 10th Rankine Lecture: The influence of strains in soil mechanics. *Geotechnique*, 20(2): 129-170.
- Roscoe, K.H., Schofield, A.N., and Thurairajah, A. 1963. An evaluation of test data for selectinf a yield criterion for soils. ASTM Special Technical Publication, No. 361, PP. 111-128.
- Schofield, A. and Wroth, P. 1968. *Critical state soil mechanics*. McGraw-Hill
- Seed, H.B. 1979. Soil liquefaction and cyclic mobility evaluation for level ground during earthquakes. *Journal of the Geotechnical Engineering Division*, ASCE, 105(GT2): 201-255.
- Seed, H.B., and Idriss, I.M. 1982. *Ground motions and soil liquefaction during earthquakes*. Earthquake Engineering Research Institute (EERI) Monograph, Berkeley, CA, USA.
- Seed, H. B. and Peacock, W. H. 1971. Test procedures for measurement soil liquefaction characteristics. *Journal of the Soil Mechanics and Foundations Division*. ASCE; 97 (SM8): 8330-1119.
- Seed, H.B. Mori, K., and Chan, C. D. 1975. Influence of seismic history on the liquefaction characteristics of sands. Report EERC 75-25, Earthquake Engineering Research Center, university of California, Berkeley, Calif.
- Seed, H.B. Mori, K., and Chan, C. D. 1977. Influence of seismic history on liquefaction of sands. *Journal of the Geotechnical Engineering Division*, ASCE, 103(GT4): 257-270.
- Seed, H. B., Idriss, I.M. and Arango, I. 1983. Evaluation of liquefaction potential using field performance data. *Journal of Geotechnical Engineering* ASCE; 109 (3): pp. 458-482.
- Seed, R.B., and Harder, L.F. 1990. SPT based analysis of cyclic pore pressure generation and undrained residual strength. In Proceedings of the Seed Memorial Symposium, Vancouver, B.C., Canada. Edited by J.M. Duncan. BiTech Publishers, pp. 351-376.
- Seed, R.B., Cetin, K.O. Moss, R.E.S., Kammerer, A.M., Wu, J., Pestana, J.M., Riemer, M. F. 2001. Recent Advances in Soil Liquefaction Engineering and Seismic Site Response

- Evaluation. Proceedings of the Fourth International Conference and Symposium On Recent Advances In Geotechnical Earthquake Engineering And Soil Dynamics, Paper SPL-2, March 26, San Diego, CA USA.
- Sriskandakumar, S. 2004. Cyclic loading response of Fraser River sand for validation of numerical models simulating centrifuge tests. M.A.Sc. thesis, Department of Civil Engineering, The University of British Columbia, Vancouver, B.C., Canada.
- Stamatopoulos, C; Stamatopoulos, A; Kotzias, P. 1995. Effect of pre-stress on the liquefaction potential of silty sands. In Proceedings of the 7th International Conference on Soil Dynamics and Earthquake Engineering. Computational Mechanics Publications. Southampton, Boston, pp: 181-188.
- Stark, T.D., and Mesri, G. 1992. Undrained shear strength of liquefied sands for stability analysis. *Journal of the Geotechnical Engineering, ASCE*, 118(11): 1727-1747.
- Suzuki, T., and Toki, S. 1984. Effect of pre-shearing on liquefaction characteristics of saturated sand subject to cyclic loading. *Soils and Foundations*, 24(2):16-28.
- Thevanayagam, S., Shenthan, T., Mohan, S., and Liang, J. 2002. Undrained fragility of clean sands, silty sands, and sandy silts. *Journal of Geotechnical and Geoenvironmental Engineering, ASCE*, 128(10):849-859.
- Tohno, I and Yashuda, S. 1981. Liquefaction of the ground during the 1978 Miyagiken-Oki earthquake. *Soils and Foundations*, 21(3):18-34.
- Tokimatsu, K., and Seed, H. B. 1987. Evaluation of settlements in sands due to earthquake shaking. *Journal of Geotechnical Engineering, ASCE*, 113(8): 861-878.
- Vaid, Y. P. and Chern, J. C. 1985. Cyclic and monotonic undrained response of sands. In *Advances on the art of Testing Soils Under Cyclic Loading Conditions, Proceedings of the ASCE Convention, Detroit*, pp. 171-176.
- Vaid, Y.P., and Chung, E.K.F., and Kuerbis, R.H. 1989. Pre-shearing and undrained response of sand. *Soils and Foundations*, 29(4): 49-61.
- Vaid, Y.P., and Finn, W.D.L. 1979. Static shear and liquefaction potential. *Journal of the Geotechnical Engineering Division, ASCE*, 105(GT10): 1233-1246.
- Vaid, Y.P., and Sivathayalan, S. 1996. Static and cyclic liquefaction potential of Fraser Delta sand in simple shear and triaxial tests. *Canadian Geotechnical Journal*, 33(2): 281-289.
- Vaid, Y.P., and Sivathayalan, S. 1997. Post liquefaction behaviour of saturated sand under simple shear loading. In *Proceedings of the 14th International Conference on Soil Mechanics and Foundation Engineering, Hamburg, 6-12 September 1997. Vol. 1*, pp. 221-224.
- Vaid, Y. P., and Thomas, J. 1995. Liquefaction and post-liquefaction behaviour of sand. *Journal of Geotechnical Engineering, ASCE*, 121(2):163-173.

- Vaid, Y.P., Sivathayalan, S., and Stedman, J.D. 1999. Influence of specimen reconstitution method on the undrained response of sand. *Geotechnical Testing Journal*, GTJODJ, 22(3):187-195.
- Vaid, Y.P., Stedman, J.D., and Sivathayalan, S. 2001. Confining stress and static shear effects in cyclic liquefaction. *Canadian Geotechnical Journal*, 38(3):580-591.
- Vick, S.G. 1983. Planning, design and analysis of tailings dams. Wiley Series on Geotechnical Engineering. John Wiley & Sons, New York.
- Wang, W. 1979. Some findings in soil liquefaction. Water Conservation and Hydroelectric Power Science Research Institute, Beijing, China.
- Wijewickreme, D. and Sanin, M. 2005. New sample holder for the preparation of undisturbed fine-grained soil specimens for laboratory element testing, Submitted to ASTM Geotechnical Testing Journal for review.
- Wijewickreme, D. Sanin, M. V. Greenaway, G. R. 2005. Cyclic shear response of fine-grained mine tailings. *Canadian Geotechnical Journal*. *In print*, 2005.
- Wijewickreme, D., Sriskandakumar, S., and Byrne, P.M. 2005. Cyclic loading response of loose air-pluviated Fraser River sand for validation of numerical models simulating centrifuge tests. *Canadian Geotechnical Journal*. *In print*, 2005..
- Wissa, A. E. Z., Christian, J. T., Davis, E. H and Heiberg, S. 1971. Consolidation at constant rate of strain. *Journal of the Soil Mechanics and Foundations Division*. ASCE; 97 (SM10): 1393-1413.
- Wu, J., Kammerer, A.M., Riemer, M.F., Seed, R.B., and Pestana, J.M. 2004. Laboratory study of liquefaction triggering criteria. In *Proceedings of the 13th World Conference on Earthquake Engineering*, Vancouver, B.C., Canada. Paper No. 2580.
- Youd, T.L., Idriss, I.M., Andrus, R.D., Arango, I., Castro, G., Christian, J.T., Dobry, R., Finn, W.D.L., Harder Jr., L.F., Hynes, M.E., Ishihara, K., Koester, J.P., Liao, S.S.C., Marcuson III, W.F., Martin, G.R., Mitchell, J.K., Moriwaki, Y., Power, M.S., Robertson, P.K., Seed, R.B., and Stokoe II, K.H. 2001. Liquefaction resistance of soils: Summary report from the 1996 NCEER and 1998 NCEER/NSF Workshops on Evaluation of Liquefaction Resistance of Soils. *Journal of Geotechnical and Geoenvironmental Engineering*, ASCE, 127(10): 817-833.
- Zergoun, M., and Vaid, Y.P. 1994. Effective stress response of clay to undrained cyclic loading. *Canadian Geotechnical Journal*, 31(5): 714-727.